ELSEVIER

JOURNAL

of

CHROMATOGRAPHY

INCLUDING ELECTROPHORESIS AND OTHER SEPARATION METHODS

SPECIAL ISSUE

BIOCHEMICAL SEPARATION TECHNOLOGY

PAPERS PRESENTED AT THE HONORARY SYMPOSIUM ON THE OCCASION OF THE 70TH BIRTHDAY OF JERKER O. PORATH, UPPSALA, JUNE 16–19, 1991

Guest Editors

J.-C. JANSON
(Uppsala)

K. D. Caldwell
(Salt Lake City, UT)

I. Johansson
(Uppsala)

J. Carlsson
(Uppsala)

CONTENTS

Foreword

Developments in science often run parallel to developments in techniques and methodologies and these have been particularly obvious in the area of bioscience and biotechnology. Thus, the development of biochemical separation techniques have been crucial to an understanding of the composition and structures of proteins, peptides and polynucleotides, ever since the work by Sanger 45 years ago on the structure of insulin using paper chromatography for the separation and identification of dinitrophenyl-amino acids, right through to more recently developed sophisticated techniques and instrumentation for the analysis of microheterogeneities of recombinant proteins using highly resolving reversed-phase chromatography, capillary electrophoresis and mass spectrometry. Significant contributions to the now abundant variety of techniques and tools for protein separation and analysis have emerged from the "Uppsala School of Separation Science". This was established by The Svedberg and Arne Tiselius during the 1920s–1940s and the tradition was later on continued and strengthened by their pupils and successors Harry Svensson (Rilbe), Jerker Porath, Stellan Hjertén, Per Flodin, Per-Åke Albertsson and their descendants.

In 1991, Jerker Porath, the successor of Arne Tiselius to the Jacobsonian Chair of Biochemistry at Uppsala University, attained the age of 70 years, and to celebrate this fact, many of his pupils and friends gathered in Uppsala for a three-day's symposium on the subject of the principles and applications of biochemical separation technologies. Many of the contributions were variants or applications of themes within which the celebrity himself has made pioneering contributions, such as affinity chromatography technologies in general and immobilized metal ion affinity chromatography in particular. About 120 participants listened to the 40 oral presentations, studied the posters displayed and enjoyed the social programme and the beautiful June weather in the city of Uppsala.

Jan-Christer Janson

CHROM. 24 135

Jerker Porath: on the occasion of his 70th birthday

Jerker O. Porath was born in Sala, Sweden on October 23, 1921. In a celebration of his seventy years and his many significant contributions to separation science, a large number of his colleagues and friends from around the globe gathered for a symposium in Uppsala on June 16–19, 1991. As reflected by the broad interests of the honoree, presentations given at this meeting were not limited to separation science, but covered many additional topics of general biochemical nature. However, for the present issue of the *Journal of Chromatography* only those manuscripts were selected which discuss topics related to separation science.

Jerker's own scientific training began in a different field, namely synthetic organic chemistry, and his focus on separations did not come about until the day in 1950 when he walked into the laboratory of Arne Tiselius at the University of Uppsala to begin research for a Doctorate of Science. In a little over two decades, Tiselius and his teacher The Svedberg had managed to build a highly visible program aimed at developing methods for the separation and physical characterization of proteins. The spectacular results of these efforts, including ultracentrifugation, zone electrophoresis and isoelectric focusing had brought biochemists from around the world to Uppsala with their separation problems, and had caused a number of gifted graduate students like Jerker to join this active, international research group. The many techniques which he studied and published on in these early years include paper chromatography, column chromatography on ion-exchanging cellulose and displacement chromatography on beds of charcoal.

In addition, much effort was devoted to the development of preparative column electrophoresis for the fractionation of gram quantities of protein. Starch was frequently used as a support material at the time, and early on it was noted that proteins tended to separate on these preparative columns, even in the absence of an electric field. This appeared to be due, not to ion-exchange or other high-affinity interaction, but more to a sieving effect, where smaller molecules became segregated from large ones. The separation was crude and unpredictable, but it sowed a seed in Jerker's mind which led to another milestone in the field of macromolecular separation and characterization.

With the 1959 introduction of the epichlorohydrine cross-linked dextran gels, Jerker Porath and Per Flodin gave us a separation tool of unsurpassed usefulness. Furthermore, by explaining its principle of operation, they set the stage for production of a wide assortment of matrices with different pore size characteristics. There is a Swedish proverb which says that *a beloved child has many names*. This is very much applicable to the Porath–Flodin method which, under the names of gel filtration, gel permeation chromatography or size-exclusion chromatography, is arguably the most widely used separation technique today.

The inert dextran matrices were easily derivatized, and during the 1960s Jerker Porath came to spearhead a school of bioorganic chemists who learned to master the art of selectively modifying these gels, particularly with the intent of using them to immobilize proteins. When I joined the Department of Biochemistry in 1965, there were already advanced experiments under way to build stationary phases for biospecific affinity chromatography. In fact, the selected system was based on the avidin–biotin pair, which is the same as that developed and first described in the literature by Cuatrecasas, Wilchek and Anfinsen in their landmark 1968 article [*Proc. Natl. Acad. Sci. U.S.A.*, 61 (1968) 636].

The development of the cyanogen bromide-coupling method by Axén, Porath and Ernback was another leap forward which gave us a convenient and gentle way to immobilize enzymes, immunoglobulins and other amine-containing molecules. This greatly expanded the usefulness of the polysaccharide matrices to the protein chemist. Cross-linking of agarose and coupling of a wide assortment of groups to this matrix was also shown to convenient-

ly occur by means of either the divinylsulphone or bis-oxirane reagents.

In the two most recent decades, the ability to introduce a variety of reactive structures onto the polysaccharide matrices led to the exploration of three different types of affinity chromatography involving charge-transfer interaction, thiophilic adsorption and metal–chelate complex formation.

A theme underlying much of this work has been the ability to scale up the separation process for commercial use. This was true for the early preparative electrophoresis work as well as for the recent utilization of e.g. the thiophilic gels for easy group separations of immunoglobulins. The openness for commercial processing questions led to a close collaboration between the Porath group at the University of Uppsala and a number of industrial laboratories at a time when such collaborations were frowned upon by the academic community.

Jerker's dogged persistance in following his intuition has paid dividends to the extent that laboratories around the world today routinely use the tools he created to accomplish their various separation tasks. This contribution has certainly not gone unnoticed, as evidenced by his numerous awards and memberships in academies and scientific societies in Sweden and elsewhere. On the occasion of his seventieth birthday, there are many who wish to celebrate the significant scientific contributions made by Jerker Porath. In addition, those who have had the good fortune of knowing him personally wish to show their respect for a man whose outgoing and engaging personality over the years has transformed scores of students, collaborators, and casual scientific contacts into a set of close personal friends.

Karin Dahlgren Caldwell

Reactive carriers for the immobilization of copper ions

Maria Walenius and Per Flodin

Department of Polymer Technology, Chalmers University of Technology, S-412 96 Gothenborg (Sweden)

Jerker Porath

Department of Biochemistry, Uppsala University, Biomedical Center, S-751 23 Uppsala (Sweden)

ABSTRACT

Macroporous functionalized gels based on copolymers of trimethylolpropane trimethacrylate and glycidyl methacrylate were prepared for the adsorption of copper ions. The gels were functionalized with iminodiacetate, tris(2-aminoethyl)amine, tetraethylenepentamine (TEPA) and ammonia. The most favourable conditions for obtaining a high yield of TEPA were a high concentration of TEPA in the reaction mixture (at least 3 mol of TEPA per mole of epoxy), toluene as solvent, elevated temperature (70°C) and at least 4 h of reaction.

INTRODUCTION

Ligand-exchange chromatography was introduced in 1975 [1] and was later renamed immobilized metal ion affinity chromatography (IMAC) [2]. Recently, chromatographic methods for the purification of proteins and peptides were reviewed by Janson and Rydén [3]. The IMAC method takes advantage of transition metal interactions with biological molecules such as peptides and proteins [2,4–6]. The hydrophilic supports used for this affinity chromatographic method are usually based on cross-linked dextran or agarose [2,7,8]. However, functionalization of these gels usually involves at least two steps, activation and functionalization, which might cause losses of epoxy groups due to side-reactions. Hence it would be advantageous to omit the activation step.

The monomer glycidyl methacrylate (GMA) contains an epoxy group that has been successfully copolymerized with, *e.g.*, ethylene dimethacrylate to produce hydrophilic gels [9–11]. The reaction of the epoxy groups with various reagents and the chelation of the derivatized polymers were studied by Kalál and co-workers [12–15].

New materials based on trimethylolpropane trimethacrylate (TRIM) have been prepared [16–22]. They are mechanically stable and 40 mol% GMA can be incorporated without seriously affecting their mechanical properties [20]. As copolymerization is a random or close to random process, the epoxy groups will be located in both dense and open regions of the gels. Hence steric hindrance can affect the accessibility of the epoxy groups to solutes, which manifests itself in yields of product ligands lower than theoretically expected. High degrees of substitution of the epoxy groups have been achieved with dialkylamines and diamines [19].

This paper describes the synthesis and basic properties of functionalized poly(TRIM-co-GMA) gels. The gels were functionalized with iminodiacetate (IDA), tris(2-aminoethyl)amine (TREN), tetraethylenepentamine (TEPA) and ammonia. The reaction conditions necessary to obtain high yields of TEPA and the capacity of the amines mentioned above to chelate copper ions in distilled water and in

Correspondence to: Dr. P. Flodin, Department of Polymer Technology, Chalmers University of Technology, S-412 96 Gothenburg, Sweden.

buffers were investigated. The aim was to prepare functional gels that could be converted into metal complexes for IMAC of proteins and peptides.

EXPERIMENTAL

All chemicals were of analytical-reagent grade and used as received unless stated otherwise. The chromatographic columns were ordinary Pasteur pipettes (short form, 150 mm total length × 5 mm I.D.).

Materials

Trimethylolpropane trimethacrylate (TRIM) and glycidyl methacrylate (GMA) (technical quality, Merck and Fluka, respectively) were separately filtered through basic aluminium oxide (Fluka) before use. Ethylhydroxyethylcellulose (Bermocoll E 411 G, Batch 3537) was supplied by Berol Nobel (Sweden). Tetraethylenepentamine (TEPA) of technical quality and disodium iminodiacetate monohydrate (98% pure) was obtained from Fluka and [2-(N-morpholino)ethanesulphonic acid] (MES) from Sigma.

Synthesis of poly(TRIM-co-GMA)

The poly(TRIM-co-GMA) matrices were prepared by suspension polymerization as described

TABLE I

GMA TO TRIM RATIO AND MONOMER TO TOLUENE RATIO OF THE REACTION MIXTURE FOR THE PREPARATION OF poly(TRIM-co-GMA) GELS

Sample	Content of total monomer (%, v/v)	GMA (%, w/w)
TG8	50	21.6
TG10	30	19.6
TG20	30	20.1

elsewhere [21]. Details of the composition of the matrices are given in Table I. The polymer particles were allowed to sediment in distilled water at 50°C. The supernatant was decanted four times. The slurry was dried at 60°C and sieved (aperture 38 µm). Most of the particles were 20–30 µm in diameter, as measured by a Malvern Mastersizer.

Preparation of chelating polymers

Tetraethylenepentamine–poly(TRIM-co-GMA) gel. This ligand was chosen for reduced factorial design experiments as it was readily available and contained five nitrogens. The poly(TRIM-co-GMA) gel particles were washed with methanol and acetone

TABLE II

REACTION CONDITIONS FOR FUNCTIONALIZATION OF poly(TRIM-co-GMA) GEL PARTICLES (TG20) WITH TETRAETHYLENEPENTAMINE (TEPA)

The matrix for TEPA9 was TG8.

Sample	Monomer/toluene (%, v/v)	TEPA/epoxy (mol/mol)	Temperature (°C)[a]	Solvent	Time (h)
TEPA1	30	3.34	AT	Toluene	4
TEPA2a	30	6.63	AT	Toluene	8
TEPA2b	30	6.63	AT	Toluene	27
TEPA3	30	3.34	70	Toluene	8
TEPA4	30	6.63	70	Toluene	4
TEPA5	30	3.34	AT	Water	8
TEPA6a	30	6.63	AT	Water	4
TEPA6b	30	6.63	AT	Water	27
TEPA7	30	3.34	70	Water	4
TEPA8	30	6.63	70	Water	8
TEPA9	50	6.64	70	Toluene	4

[a] AT = Ambient temperature.

and 6.00 g of the suction-dried gel were weighed in (TG20 for samples TEPA1–TEPA8 and TG8 for TEPA9). Tetraethylenepentamine (TEPA) and 25 ml of distilled water or toluene were added. Details of the composition of the reaction mixtures are given in Table II. The Hypo-vials were sealed and placed in an agitating device (Tecam SB-4 shaking water-bath) at the desired temperature and time. Gels functionalized in distilled water (solvent) were washed with distilled water until pH 6 and then with methanol and acetone. Gels prepared in toluene were washed with methanol and mixtures of methanol and distilled water and of methanol and acetone. The levels of nitrogen atoms in the dry metal-free gels are given in Table III.

Three additional samples were prepared in a slightly different manner from that described above. A 3.85-g amount of ammonia (25% aqueous solution), 8.27 g of TREN and 10.88 g of TEPA (TEPA10) were separatively weighed into Hypo-vials together with 25 ml of toluene. Poly(TRIM-co-GMA) particles (6.00 g of TG20) were added to each Hypo-vial. The Hypo-vials were sealed and placed in the agitating device at 70°C. After 4 h, 5 ml of 50% acetone in distilled water were injected in each

Hypo-vial and after 1 h 5 ml of distilled water were added. The time of reaction was 8 h. The dry, metal-free gels contained 0.42, 3.75 and 4.01 wt.% N, respectively.

Iminodiacetate–poly(TRIM-co-GMA)gels. These were prepared according to a previously described procedure [2] with some minor modifications. A 200-ml volume of 2 M Na$_2$CO$_3$ solution and 20 g of disodium iminodiacetate monohydrate were added to 10 g of dry polymer (TG10, see Table I).

For IDA1, the suspension was kept at 60°C overnight with stirring. The gel was washed with distilled water until pH 6 was reached and then with ethanol and acetone. The dry gel contained 0.21% (w/w) N.

For IDA2, the suspension was stirred at 60°C for 40 h. Ethanol (5 ml) was added after 15 h of reaction. The washing procedure was performed as stated above. The dry gel contained 0.31% (w/w) N.

Hydrophilization of polymers. An amount of 4 mol of ethanolamine per mol of epoxy group in the poly(TRIM-co-GMA) gel and 9 ml of distilled water per gram of dry polymer were added to the dry polymer in a Hypo-vial (50 ml). The Hypo-vials were sealed and placed in the agitating device at

TABLE III

ELEMENTAL ANALYSIS OF NITROGEN IN poly(TRIM-co-GMA) GELS FUNCTIONALIZED WITH VARIOUS AMINES

The conversion of epoxy groups was calculated according to eqn. 1.

Sample	Content of nitrogen (%, w/w)	Amine (mmol ligand/g dry matrix)	Ratio[a], mol epoxy/mol ligand
TEPA1	0.59	0.09	16.5
TEPA2a	0.93	0.14	10.4
TEPA2b	3.59	0.58	2.5
TEPA3	4.00	0.64	2.2
TEPA4	3.99	0.64	2.2
TEPA5	1.75	0.26	5.4
TEPA6a	1.65	0.25	5.7
TEPA6b	2.98	0.46	3.1
TEPA7	2.65	0.41	3.5
TEPA8	2.80	0.43	3.3
TEPA9	4.04	0.65	2.3
Ammonia	0.42	0.32	4.7
TREN	3.75	0.74	1.9
TEPA10	4.01	0.64	2.2
IDA1	0.21	0.15	9.0
IDA2	0.31	0.23	6.1

[a] The molar ratio of epoxy groups in the starting material to amino groups in the product.

70°C for *ca.* 5 h. The gels were washed with distilled water until pH 6 was reached.

Metal adsorption experiments

Method 1. A stock solution of 0.5 M CuCl$_2$ containing 0.2 mol/l of NaCl was prepared. The solution was diluted tenfold with distilled water before use. The suction-dried gels were packed in Pasteur pipettes in distilled water (0.6–1.2 ml of gel). The pipettes were loaded with *ca.* 0.5 ml of the diluted copper solution containing sodium ions and then with distilled water. The amount of copper ion bound by the ligand was approximated from the volume of the migrated coloured front as

$$\frac{\text{mmol Cu}^{2+}}{\text{ml gel}} = \frac{cV}{\pi r^2 L} \qquad (1)$$

where c is the concentration of copper ions, V is the volume of added copper solution (containing sodium ions), r is the radius of the column (Pasteur pipette) and L is the length of the stabilized migrated coloured front.

Method 2. This method, described by Muszynska *et al.* [23], was used to determine the displacement of copper ions by some buffers as a function of the bed volume. The adsorbents, 0.6–1.2 ml, were packed in Pasteur pipettes in distilled water. Approximately 0.26 ml of the copper ion solution (A) per millilitre of bed volume was percolated through each pipette. The pipettes were thoroughly washed with 2–4 bed volumes of solutions B, C and D to remove unbound and loosely bound copper ions. Solutions E and F were intended for the elution of future proteins. The volume of the coloured front was calculated according to eqn. 1, subsequent to the percolation of each of the following solutions:

  (A) 50 mM CuCl$_2$ in 0.1 M sodium acetate containing 1 M NaCl, pH 4;
  (B) 0.1 M sodium acetate (pH 4) containing 1 M NaCl;
  (C) 0.1 M sodium acetate, pH 4;
  (D) 0.1 M glycine, pH 8;
  (E) equilibration buffer, 50 mM MES, pH 6;
  (F) 0.1 M imidazole in 50 mM MES, pH 6;
  (G) 20 mM EDTA solution;
  (H) 1 M NaCl, pH 7.2.

The copper ions were removed using solution G. Solutions H and B were subsequently used to condition the column for a re-run.

Characterization

Elemental analysis of nitrogen was performed on dried gel samples by the micro-Kjeldahl method with mercury as catalyst. The amine content was calculated as

$$\frac{\text{mmol ligand}}{\text{g dry matrix}} = \frac{p_N}{100 \cdot 14 n_N m_{\text{matrix}}} \qquad (2)$$

where p_N is the percentage of nitrogen atoms in the dry gel, n_N is the total number of nitrogen atoms in the ligand and m_{matrix} is the weight of the dry poly(TRIM-co-GMA).

Fourier transform infrared (FT-IR) spectra were recorded on a Perkin-Elmer Model 1720X spectrophotometer fitted with a diffuse reflectance device (DRIFT). The samples were dried under vacuum at 60°C for 24 h and then ground together with KBr (1:20, w/w) before analysis. The Kubelka–Munk equation [24] was applied to the data to obtain the spectra. The peak at 910 cm^{-1} (epoxy group) was divided by the reference peak at 1733 cm^{-1} (carbonyl group). The value thus obtained was used as an approximation of the yield of reacted ligand [21].

RESULTS AND DISCUSSION

Synthetic aspects

The optimum reaction conditions for obtaining 0.64 mmol of TEPA per gram of dry matrix were to add TEPA in excess (3 mol of TEPA per mol of epoxy group in the matrix), elevate the temperature (70°C), use toluene as solvent and let the reaction run for at least 4 h (Table III). It was important to have a good swelling agent for the matrix in combination with elevated temperature during the reaction. The yield of TEPA could be increased fourfold by prolonging the reaction time (27 h) if ambient temperature during the reaction was desirable (TEPA2a and TEPA2b in Table III). Distilled water was inferior as a solvent but the yield increased 1.8-fold after 27 h of reaction compared with 4 h of reaction at ambient temperature (TEPA6a and TEPA6b in Table III).

The ratio between the epoxy groups in the poly(TRIM-co-GMA) gel and TEPA was *ca.* 2 mol/mol for gels containing *ca.* 0.6 mmol of TEPA per gram of dry matrix (Table III). It can be assumed that the two primary amino groups of TEPA had reacted and formed "bridges", giving a 1:1 ratio between epoxy groups and primary amino groups.

TABLE IV

RESULTS OBTAINED BY FT-IR FOR THE CONVERSION OF EPOXY GROUPS ACCORDING TO THE KUBELKA–MUNK EQUATION [24]

Hydrophilized samples are designated by "-OH".

Sample	$A(910 \text{ cm}^{-1})/A(1733 \text{ cm}^{-1})$	Conversion of epoxy groups (%)	
		FT-IR	Elemental analysis
TG10	0.0190	0	0
Ammonia-OH	0.0038	80.0 ± 0.0030	21[a]
TEPA10-OH	0.0022	88.0 ± 0.0018	45[a]
TREN-OH	0.0024	87.4 ± 0.0015	52[a]
IDA1	0.0092	51.6 ± 0.0055	11
IDA1-OH	0.0043	77.4 ± 0.0035	–

[a] Calculated for non-hydrophilized samples.

The amount of incorporated TEPA (sample TEPA10) did not increase when a mixture of distilled water and acetone was introduced into the Hypo-vials after a few hours of reaction (Table III). The number of amino groups seemed to be important for the incorporation of the amine. A higher yield (0.74 mmol of ligand per gram of dry matrix) was obtained for TREN, containing three primary amino groups, than for TEPA (0.64 mmol of ligand per gram of dry matrix), containing two primary amino groups. The yield of ammonia was low owing to the unfavourable reaction conditions.

An elemental analysis of IDA1 showed that 11% of the epoxy groups had reacted with IDA molecules (Table IV). However, FT-IR measurements on the same sample showed that about 51.6% of the epoxy groups had reacted. The discrepancy could be due to side-reactions that are still not fully understood. Another explanation could be the difficulty in measuring the peak at 910 cm^{-1} (epoxy group) owing to partial coverage of another peak [21] (Fig. 1). Hydrophilization of the IDA1 gel increased the amount of reacted epoxy groups to 77.4% (IDA1-OH).
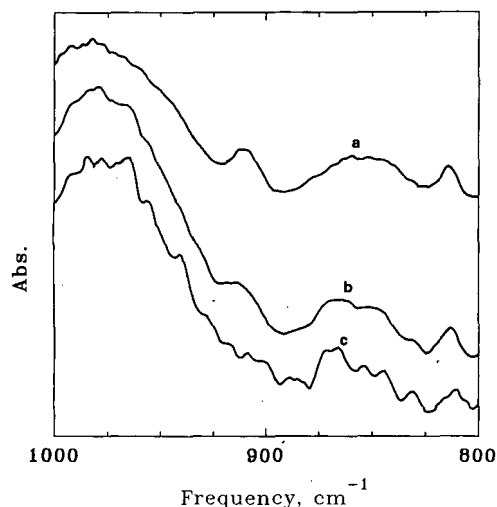
Fig. 1. FT-IR analyses of (a) poly(TRIM-co-GMA) gel, (b) poly(TRIM-co-GMA)–IDA gel (IDA1) and (c) hydrophilized poly(TRIM-co-GMA)–IDA gel (IDA1-OH). Abs. = Absorbance.

TABLE V

ADSORPTION OF COPPER IONS ON FUNCTIONALIZED GELS IN DISTILLED WATER CONTAINING SODIUM IONS (pH 4) ACCORDING TO METHOD 1

Hydrophilized samples are designated by "-OH".

Polymer	Adsorption of copper ions (mmol Cu^{2+}/ml wet gel)
TG10	0
Ammonia-OH	0.02
TREN-OH	0.13
TEPA3-OH	0.14
TEPA10-OH	0.13
IDA1	0.08
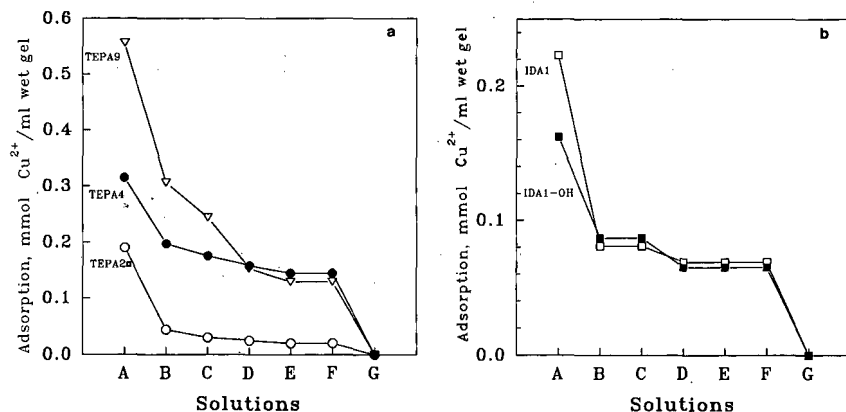
Fig. 2. Adsorption capacity of copper ions after percolation of a series of buffers according to method 2 for (a) some of the poly(TRIM-co-GMA)–TEPA gels and (b) the poly(TRIM-co-GMA)–IDA gel and the hydrophilized IDA gel (IDA1-OH).

Chelating properties of functional poly(TRIM-co-GMA) gels

The adsorption of copper ions in distilled water, according to the first chromatographic method, depended on the ligand concentration in the gel (Tables III and V). The copper ion complexes were more stable for the TREN and TEPA gels than for the IDA1 and ammonia gels. The TEPA and TREN gels adsorbed *ca.* 0.13 mmol of copper ions per millilitre of wet gel, although the ligand concentration was higher in the TREN than in the TEPA gel (Table III).

The second chromatographic method showed that the metal leakage was reduced almost to zero after the percolation of 0.1 M glycine (pH 8) (Fig. 2a and b). Despite the displacement of copper ions, it was shown that the more TEPA that was immobilized, the higher the copper ion adsorption capacity (Fig. 2a). The hydrophilization of the IDA1 gel did not alter the amount of copper ions adsorbed (Fig. 2b).

CONCLUSIONS

Optimum reaction conditions for the incorporation of TEPA were obtained when TEPA was added in excess (at least 3 mol of TEPA per mol of epoxy groups in the matrix), the temperature was elevated (70°C), toluene was used as the solvent and the time for reaction was at least 4 h. The yield could be increased by prolonging the reaction time if ambient temperature and aqueous diluents, such as distilled water, were desirable reaction parameters.

The highest yield of incorporated amine was obtained with TREN. The lowest yield was obtained with ammonia owing to the unfavourable reaction conditions.

The adsorption of copper ions was proportional to the amount of attached chelating ligand. The hydrophilization of the IDA gel with ethanolamine did not change the adsorption capacity of copper ions in various buffer solutions.

REFERENCES

1 J. Porath, J. Carlsson, I. Olsson and G. Belfrage, *Nature (London)*, 258 (1975) 598.
2 J. Porath and B. Olin, *Biochemistry*, 22 (1983) 1621.
3 J.-C. Janson and L. Rydén, *Protein Purification*, VCH, New York, 1989, Ch. 8.
4 J. Porath, *J. Chromatogr.*, 443 (1988) 3.
5 J. Porath, *Trends Anal. Chem.*, 7 (1988) 254.
6 M. C. Smith, T. C. Furman and C. Pidgeon, *Inorg. Chem.*, 26 (1987) 1965.
7 T. W. Hutchens, T. T. Yip and J. Porath, *Anal. Biochem.*, 170 (1988) 168.
8 P. Flodin, *Dextran Gels and Their Application in Gel Filtration*, Meijels Bokindustri, Halmstad, 1962.

9 F. Švec, J. Hradil, J. Coupek and J. Kalal, *Angew. Makromol. Chem.*, 48 (1975) 135.

10 F. Švec, H. Hrudková, D. Horak and J. Kalal, *Angew. Makromol. Chem.*, 63 (1977) 23.

11 D. Horak, F. Švec, M. Ilavsky, M. Bleha, J. Baldrian and J. Kalal, *Angew. Makromol. Chem.*, 95 (1981) 117.

12 E. Kalalová, J. Kalal and F. Švec, *Angew. Makromol. Chem.*, 54 (1976) 141.

13 E. Kalalová, Z. Radová, F. Švec and J. Kalal, *Eur. Polym. J.*, 13 (1977) 293.

14 Z. Radová, E. Kalalová, J. Kalal, Y. Kukushkin, S. A. Simanova, L. V. Konovalov and V. N. Pak, *Angew. Makromol. Chem.*, 81 (1979) 55.

15 F. Švec, D. Horák and J. Kálal, *Angew. Makromol. Chem.*, 63 (1977) 37.

16 J. E. Rosenberg and P. Flodin, *Macromolecules*, 20 (1987) 1522.

17 J. E. Rosenberg and P. Flodin, *Macromolecules*, 21 (1988) 2041.

18 J. E. Rosenberg and P. Flodin, *Macromolecules*, 22 (1989) 155.

19 M. Walenius and P. Flodin, *Br. Polym. J.*, 23 (1991) 67.

20 A. Schmid, M. Walenius and P. Flodin, *J. Appl. Polym. Sci.*, in press.

21 M. Walenius, L.-I. Kulin and P. Flodin, *React. Polym.*, in press.

22 P. D. Verweij and D. C. Sherrington, *J. Mater. Chem.*, 1 (1991) 371.

23 G. Muszynska, Y.-J. Zhao and J. Porath, *J. Inorg. Biochem.*, 26 (1986) 127.

24 P. Kubelka and F. Munk, *Z. Tech. Phys.*, 12 (1931) 593.

Short Communication

Evaluation of the interaction of protein α-amino groups with M(II) by immobilized metal ion affinity chromatography

Lennart Andersson and Eugene Sulkowski[*]

Biochemical Separation Centre, Biomedical Centre, University of Uppsala, Box 577, S-751 23 Uppsala (Sweden)

ABSTRACT

The adsorption properties of various peptides and proteins, lacking histidyl groups, on immobilized Cu(II), Ni(II), Zn(II) and Co(II) ions are described; at pH 6 and below they were little retarded. At higher pH the retention became pronounced for iminodiacetate (IDA)–Cu(II) gel. This effect seems to be related to the presence of a terminal α-amino group; in the absence of this group the retention of the protein was largely eliminated. At pH 8.5 a terminal α-amino group is adsorbed as strongly as a histidyl group. IDA–Ni(II), IDA–Zn(II) and IDA–Co(II) gels display little or no attraction for the terminal α-amino group of a protein.

INTRODUCTION

Immobilized metal ion affinity chromatography (IMAC) is a type of chromatography designed for the separation of biomolecules such as proteins and nucleic acids. It was introduced by Porath *et al.* in 1975 [1] and has since gained worldwide acceptance, as documented by many review articles.

Investigation into the interaction between immobilized iminodiacetate (IDA)–Cu(II) and IDA–Ni (II) ions and proteins has shown that, at neutral pH, accessible histidines are the primary adsorption sites [2]. One of the imidazole nitrogens is believed to form a coordination bond with the metal ion,

resulting in increased retention. This model is supported by the observation that the retention is highly dependent on the pH of the surrounding medium and on the pK_a of the imidazole [3].

The practical applications of IMAC are numerous. To a large extent this is because of the possibility of designing an advanced protocol for the purification if the structures of a peptide or protein are known. It is, for example, known that one single exposed histidine will be recognized by immobilized IDA–Cu(II). As suggested by Sulkowski [3], immobilized Ni(II) requires two exposed histidines for an appreciable retention of a protein, whereas immobilized IDA–Zn(II) or IDA–Co(II) ions seem to recognize such groups if they are in a vicinal position.

Much effort has been devoted to the identification of the nature of the other protein functional groups which may contribute to retention on an IMA column. From the beginning the cysteinyl thiol and tryptophyl groups were considered [1]. Some other groups, such as tyrosyl, carboxylate

---

Correspondence to: Dr. L. Andersson, Biochemical Separation Centre, Biomedical Centre, University of Uppsala, Box 577, S-751 23 Uppsala, Sweden.
　* On leave of absence from the Department of Molecular and Cellular Biology, Roswell Park Cancer Institute, Buffalo, NY 14263, USA.

and α-amino groups, were also proposed. However, none of these has been systematically studied, and the few data now available rather indicate that they are less important. *A priori*, the only group, besides imidazole, on a protein that is likely to be an electron donor for coordination to metals at neutral or near-neutral pH is the α-amino group. Hemdan and Porath [4] and Belew and Porath [5] chromatographed amino acids and short peptides on immobilized IDA–Ni(II) and IDA–Cu(II) ions at or near neutrality and observed the interaction of α-amino groups with these metals. It is reasonable to expect that such an interaction should be pH-dependent because it requires that the amino group occurs in its basic form.

In the present report we have investigated the affinity of the α-amino group for immobilized and chelated Cu(II), Ni(II), Zn(II) and Co(II) ions and its possible role in IMAC. To facilitate the interpretation of data it is necessary to avoid any contribution to binding by an imidazole group. Therefore we chose as models proteins lacking histidine, *i.e.* duck lysozyme, thaumatin and aprotinin. The pH range used was also restricted to ensure that neither lysyl amino groups nor tyrosyl groups coordinated to a metal ion.

EXPERIMENTAL

Chelating Superose was obtained from Pharmacia-LKB (Stockholm, Sweden). The gel was packed in a glass column (21×10 mm I.D.), bed volume 1.65 ml. The capacity for Cu(II) ions was almost 30 μmol/ml.

Barbary duck lysozyme was a gift from Drs. F. Hemman and A. Paraf of the Institut National de la Recherche Agronomique (Nouzilly, France). Its purity was ascertained by sodium dodecyl sulphate (SDS) gel electrophoresis and reversed-phase chromatography and its authenticity was judged from the amino acid analysis. The analysis showed that histidine was not a part of its composition.

Bovine insulin α-chain was prepared by performic acid oxidation and isolated by ion-exchange chromatography on DEAE–Sepharose at pH 9.5. Its purity was checked by amino acid analysis.

The dodecapeptide NH$_2$-Gly-Gly-Gly-Val-Arg-Gly-Pro-Arg-Val-Val-Glu-Lys-COOH was synthesized and purified by Mr. P. Hansen at this institute. Its size was verified by mass spectrometry.

Thaumatin, from *Thaumatococcus danielli* (mol. wt. 21 000), lot No. 108F0299, was from Sigma (St. Louis, MO, USA). Aprotinin (mol.wt. 6500), lot No. 119F8095, was also from Sigma. Those preparations of proteins were found to contain some minor impurities which were readily separated by IMAC. The major components were analysed and found to contain no histidine.

Selective blocking of the α-amino groups of several proteins was achieved by carbamoylation at pH 7.0 with potassium cyanate following the procedure and precautions previously outlined [6]. The extent of carbamoylation as estimated through reaction with trinitrobenzene-sulphonic acid [7] never exceeded 1 mol per mol of protein.

Chromatographic experiments were carried out using a high-performance liquid chromatographic (HPLC) system (LKB) comprising a high-precision pump and a variable-wavelength monitor. Proteins were monitored routinely at 280 nm; dodecapeptide was monitored at 215 nm. Elution profiles were obtained from a Model 2210 recorder. All runs were made at room temperature, 20–22°C.

The column was charged with metal after equilibration with 0.1 *M* sodium acetate (1 *M* sodium chloride), pH 4.0. A 0.70-ml aliquot of 0.050 *M* copper sulphate pentahydrate, nickel nitrate hexahydrate, zinc sulphate heptahydrate or cobalt chloride hexahydrate dissolved in the same buffer was injected followed by washing with 10 ml of the equilibrium buffer. Then the column was re-equilibrated with 15 ml of the starting buffer and the effluent pH-checked. By using this procedure a small portion of the gel remained uncharged with metal and a more stable baseline was obtained.

The buffer systems used were as follows:

(a) pH 4.0–5.5, 0.05 *M* acetic acid–sodium hydroxide (1 *M* sodium chloride).

(b) pH 6.0–6.8, 20 m*M* sodium dihydrogenphosphate–sodium hydroxide (1 *M* sodium chloride).

(c) pH 7.0–8.6, 20 m*M* sodium dihydrogen–phosphate–sodium hydroxide (1 *M* sodium chloride), pH 7.0 and 20 m*M* boric acid–hydrochloric acid (1 *M* sodium chloride), pH 8.6, were mixed in different proportions to give the desired pH.

(d) pH 9.0, 20 m*M* boric acid–sodium hydroxide (1 *M* sodium chloride).

Routinely, the amount of each protein used in a sample was 0.1–0.3 mg dissolved in the equilibrat-

ing buffer or transferred into the buffer by gel filtration on PD-10. The injected volume was 0.20 ml in all runs and the flow-rate was maintained throughout at 1 ml/min.

The chromatographic behaviour of the test substances was expressed as relative retentions $V_r = V_e/V_t$, where V_e and V_t are the elution volumes of the sample in the presence and in the absence of loaded metal, respectively. The recovery of each protein or peptide was estimated assuming that the recovery was 100% in the absence of bound metal.

RESULTS AND DISCUSSION

Chromatography on Cu(II)–IDA–Superose at different pH values

In order to appreciate a contribution of a single α-amino group to the retention on M(II)–IDA columns, some model proteins lacking histidine were selected; a single histidine residue might overwhelm the putative contribution of other groups at neutral pH. Because an influence from cysteine thiol groups cannot be ruled out model proteins should not contain such groups either.

In the first series of experiments aprotinin was chromatographed at many different pH values. Its interaction with the IDA–Cu(II) could be well demonstrated by isocratic elution. As can be seen in Fig. 1, it increased sharply with pH. The same type of
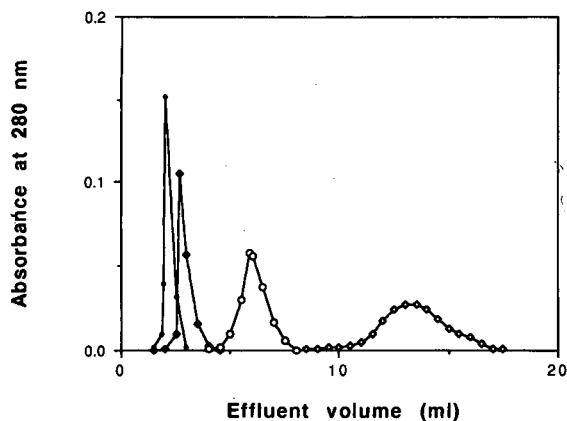
Fig. 2. Effect of pH on the relative retention of peptides and proteins on Cu(II)–IDA–Superose. Samples, 0.10–0.30 mg, were run isocratically at a flow-rate of 1 ml/min. $\square$ = Chicken egg lysozyme; $\lozenge$ = aprotinin; $\blacksquare$ = Barbary duck lysozyme; $\triangle$ = thaumatin; $\blacklozenge$ = cyanate-treated aprotinin; + = bovine insulin α-chain.

behaviour has previously been reported [3] for bovine serum albumin chromatographed isocratically on IDA–Ni(II) in the pH range 6.0–7.0, which was related to the titration of a histidyl group. Fig. 2 describes how the relative retention varies with the pH for native aprotinin and for α-carbamylaprotinin. There is a significant effect of blocking the amino group. These observations are consistent with the notion that the amino group coordinates to immobilized IDA–Cu(II). The pK_a of an α-amino group in a protein may vary, but judging from the pK_a data of peptides one can expect this value to extend down to 7.5 or even lower, especially if there are one or more basic residues nearby. At pH 8, there is a slight retention of the carbamoylated aprotinin which might be caused by unprotonated lysyl amino groups; this effect is presently under study.

The histidine- and thiol-lacking proteins, duck lysozyme and thaumatin, display largely the same behaviour: the relative retention seems to follow the deprotonation of the α-amino group. Blocking the terminal α-amino group in thaumatin clearly impedes the coordination to the metal. Much of the difference between these three proteins might be due to differences in the pK_a value of the terminal amino group. For the sake of comparison one protein which contains a single histidine, chicken egg lyso-

Fig. 1. Composite diagram showing the effect of pH on the retention of aprotinin on a column (21 × 10 mm I.D., 1.65 ml) of Cu(II)–IDA–Superose. Samples were run isocratically at a flow-rate of 1 ml/min. $\bullet$ = pH 6.0; $\blacklozenge$ = pH 6.5; $\bigcirc$ = 7.0; $\lozenge$ = pH 7.5.

zyme, is included in Fig. 2. Clearly, the contribution from the histidine dominates the retention in the pH range 5–7.

Two peptides, oxidized bovine insulin α-chain and a dodecapeptide, were also examined. The retention of the α-chain increased with pH but to a much smaller extent than that of the proteins. In fact, the retention seemed to decrease at pH 8 and above. However, it was found that at this pH the retention was very dependent on the chemical nature of the buffer (not shown). The dodecapeptide displayed grossly a similar behaviour (not shown). These observations may reflect structural changes in the peptides leading to decreased accessibility for coordination or, alternatively, the formation of a high-affinity copper binding site which scavenges Cu^{2+} from IDA and does not contribute much to the retention [8]. The latter phenomenon has been reported for serum albumin [9] and for peptides [5]. The results now described amply illustrate the fact that retention data obtained from experiments with peptides with unblocked α-amino acids and carboxyl terminals cannot be applied to proteins [10].

Chromatography on Ni(II)-, Zn(II)- and Co(II)-chelating Superose

The corresponding chromatographic runs were made using nickel, IDA–Ni(II). The outcome is illustrated in Fig. 3. An obvious observation is that all proteins are much less strongly adsorbed on nickel. Thaumatin, for instance, was in the breakthrough at all pH values up to at least 9. Even chicken egg lysozyme, which has one histidine and one terminal α-amino group, was little retained at alkaline pH. Thus, it seems that the terminal amino group in proteins coordinates weakly or not at all with immobilized nickel ions. In clear contrast to this, both insulin α-chain and the dodecapeptide seem to have amino terminals that interact with the metal. There was no retention of insulin α-chain or any of the proteins on Zn(II)–IDA– or Co(II)–IDA–Superose.
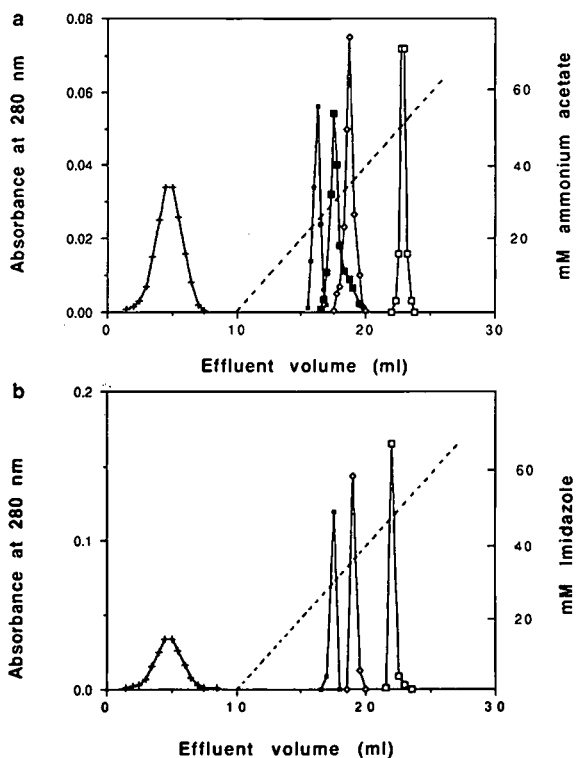
Fig. 4. Composite diagrams showing the elution profiles of some peptides and proteins on a column (21 × 10 mm I.D., 1.65 ml) of Cu(II)–IDA–Superose. Each protein was run separately at a flow-rate of 1 ml/min. Starting buffer was 20 mM boric acid–sodium hydroxide (1 M sodium chloride), pH 8.5. Samples: insulin α-chain, aprotinin and lysozymes. (a) Gradient was formed with 20 mM boric acid–0.10 M ammonia (1 M sodium chloride), pH 8.5. (b) Gradient was formed with 20 mM boric acid–0.10 M imidazole (1 M sodium chloride), pH 8.5. + = Bovine insulin α-chain; ◇ = aprotinin; ■ = Barbary duck lysozyme; □ = chicken egg lysozyme; ■ = cyanate-treated chicken egg lysozyme.

Fig. 3. Effect of pH on the relative retentions of peptides and proteins on Ni(II)–IDA–Superose. Samples, 0.10–0.30 mg, were run isocratically at a flow-rate of 1 ml/min. × = Dodecapeptide; + = bovine insulin α-chain; ◇ = aprotinin; ■ = Barbary duck lysozyme; □ = chicken egg lysozyme; △ = thaumatin.

Comparing the binding of the α-amino group with imidazole group on Cu(II)–IDA–Superose

The following substances were chromatographed one by one on Cu(II)–IDA–Superose in boric acid buffer (1 M sodium chloride), pH 8.5: oxidized bovine insulin α-chain, chicken egg lysozyme, amino-terminal-blocked chicken egg lyzozyme, Barbary duck lysozyme and aprotinin. Shortly after the application the insulin α-chain appeared in the eluate. The other substances were eluted by using an ammonia gradient from 0 to 60 mM, as shown in Fig. 4a. This experiment allows a rough comparison between the binding of an α-amino terminal group and that of histidyl side-chain. A pair of these groups binds much more strongly than any one of them alone. Blocking the amino terminal has a very significant effect in decreasing the interaction. In fact, comparing duck lysozyme, which has one α-amino terminal but no histidine, and carbamoylated chicken egg lysozyme ‚gives the impression that there is no great difference in binding between these two groups.

The outcome of a similar experiment using imidazole instead of ammonia is illustrated in Fig. 4b. Remarkably, imidazole seems to possess little eluting power at pH 8.5. At pH 7, for example, chicken egg lysozyme is readily eluted by 0.01 M imidazole (1 M sodium chloride) (not shown).

CONCLUSION

Taken together, the results of this preliminary study support some important notions. Firstly, our theory that an exposed histidyl group on a protein surface is the primary adsorption site at pH 5–7 is reinforced by the observation that none of the histidine-lacking proteins displays any significant retention. The amino terminal might, in theory at least, become of significance if the group is surrounded by positively charged groups, but this has to be yet experimentally established. Secondly, at a pH above 8, the α-amino terminal has an affinity for immobilized Cu(II) ions that is similar in strength to the affinity of histidine. Therefore, proteins lacking histidine [or with non-interacting histidine(s)] may be chromatographed as a result of the impact of the terminal amino group on binding: they can be separated from proteins with blocked N-terminals. Thirdly, assuming that the peptides in this study are representative of peptides in general, immobilized nickel ions might be useful for fractionation of peptides in slightly alkaline media.

REFERENCES

1 J. Porath, J. Carlsson, I. Olsson and G. Belfrage, *Nature*, 258 (1975) 598.
2 E. S. Hemdan, Y.-J. Zhao, E. Sulkowski and J. Porath, *Proc. Natl. Acad. Sci. U.S.A.*, 86 (1989) 1811.
3 E. Sulkowski, in R. Burgess (Editor), *Protein Purification: Micro to Macro*, Alan R. Liss, New York, 1987, p. 149.
4 E. S. Hemdan and J. Porath, *J. Chromatogr.*, 323 (1985) 255.
5 M. Belew and J. Porath, *J. Chromatogr.*, 516 (1990) 333.
6 G. R. Stark, *Methods Enzymol.*, 25 (1972) 579.
7 A. F. S. A. Habeeb, *Anal. Biochem.*, 14 (1966) 328.
8 E. Sulkowski, *Bioessays*, 10 (1989) 170.
9 L. Andersson, E. Sulkowski and J. Porath, *J. Chromatogr.*, 421 (1987) 141.
10 E. Sulkowski, *Trends Biotechnol.*, 1 (1985) 3.

CHROM. 24 058

Model studies on iron(III) ion affinity chromatography

II.☆ Interaction of immobilized iron(III) ions with phosphorylated amino acids, peptides and proteins

Grażyna Muszyńska☆☆, Grażyna Dobrowolska☆☆, Anders Medin, Pia Ekman and Jerker O. Porath

Biochemical Separation Centre, Uppsala University, Box 577; Department of Biochemistry, Uppsala University, Box 576; and Department of Medical and Physiological Chemistry, Uppsala University, Box 575, S-751 23 Uppsala (Sweden)

ABSTRACT

The chromatographic behaviour of phosphoamino acids, phosphopeptides and phosphoproteins and their non-phosphorylated counterparts was studied on Fe(III)-Chelating Sepharose® and Fe(III)-Chelating Superose®. The phosphorylated compounds, in contrast to their non-phosphorylated or dephosphorylated counterparts, adsorb to immobilized iron(III) ions at pH 5.5 and can be desorbed by an increase in pH. Phosphoamino acids were eluted at pH 6.5–6.7, whereas monophosphopeptides and phosphoprotamine eluted in the pH range 6.9–7.5. Molecules possessing clusters(s) of carboxylic groups are weakly retained (γ-carboxyglutamic acid, Ala-Ser-Glu$_5$) or bound (polyglutamic acid, β-casein) to the immobilized iron(III) ions at pH 5.5. Dephosphorylated β-casein was desorbed at pH 7.0, whereas for elution of native (non-dephosphorylated) β-casein, phosphate buffer of pH 7.7 was required. The homopolymer of polyglutamic acid was desorbed in the pH range 6.0–6.3, whereas copolymers of glutamic acid and tyrosine require pH 7.0–7.3 or even phosphate buffer at pH 7.7 for elution.

INTRODUCTION

Immobilized (chelated) iron(III) ions interact with phosphate groups of phosphoproteins [1,2]. This interaction has been utilized for the separation of phosphopeptides and phosphoproteins [2–5]. Recent studies on the binding of nucleotides to chelated iron(III) ions have established that a free terminal phosphate group is sufficient for the adsorption [6].

It has also been shown that proteins lacking phosphate groups interact with immobilized iron (III) ions [7,8], suggesting an affinity for other acidic groups in a polypeptide chain [9]. In addition, it has been suggested that exposed aromatic side-chains can promote metal complexation [10,11].

This study was undertaken in order to find out which groups on proteins are involved in the interaction with immobilized iron(III) ions.

EXPERIMENTAL

Materials

Amino acids, polymers of amino acids, proteins, 2-(N-morpholino)aminomethanesulphonic acid (MES), tris(hydroxymethyl)aminomethane (Tris) and iron(III) chloride were purchased from Sigma (St. Louis, MO, USA). The basic peptide,

---

Correspondence to: Dr. J. O. Porath, Biochemical Separation Centre, Uppsala University, Box 577, S-751 23 Uppsala, Sweden.
 ☆ For Part I, see ref. 6.
☆☆ Permanent address: Institute of Biochemistry and Biophysics, Polish Academy of Sciences, Rakowiecka 36, 02-532 Warsaw, Poland.

RRKASGP, was purchased from Bachem (Bubendorf, Switzerland) and the acidic peptide, ASEEEEE, prepared as described previously [12], was a kind gift from Professor F. Marchiori of the Centre of Biopolymers (Padua, Italy). [γ^{32}]ATP was purchased from Amersham International (Amersham, UK). Chelating Sepharose® Fast Flow and Chelating Superose® were purchased from Pharmacia LKB Biotechnology (Uppsala, Sweden). All other chemicals were of reagent grade. The protein kinase A (cyclic AMP-dependent protein kinase) and casein kinase IIB from maize seedlings were prepared as described previously [13–15].

Phosphorylation

Protamine (500 μg) and the basic peptide (500 μg) were phosphorylated separately by protein kinase A (18 600 units) using 10^7 cpm of carrier-free [γ^{32}]-ATP (specific radioactivity 3000 Ci/mmol) as the phosphate donor. The incubation, in a total volume of 200 μl, was performed overnight at 30°C in 20 mM MES buffer (pH 6.9) containing 10 mM MgCl$_2$. The acidic peptide (400 μg) was phosphorylated by casein kinase (1000 units) using the same amount of radioactive ATP. The incubation, in a total volume of 200 μl, was performed overnight at 30°C in 10 mM Tris buffer (pH 7.7) containing 10 mM MgCl$_2$. The amount of incorporated phosphate into protamine and the two peptides was detected by determination of the radioactivity by the Cerenkov method.

One phosphorylation unit was defined as the amount of enzyme transferring 1 pmol of phosphate per minute to the protein or peptide acceptor under standard assay conditions.

Protein concentrations

Protein concentrations were monitored by measurements of the absorbance at 280 or 595 nm according to the calorimetric procedure of Bradford [16] using bovine serum albumin as a standard.

Amino acid and peptide concentrations

The concentrations of amino acids and peptides were determined by the ninhydrin reaction at 570 nm [17,18]. The peptides had previously been subjected to alkaline hydrolysis.

Chromatography

The buffers used were as follows: (A) 50 mM MES–1 M NaCl, pH 5.5; (B) 20 mM MES–1 M NaCl, pH 6.5; (C) 100 mM Tris–1 M NaCl, pH 7.5; (D) 20 mM sodiumphosphate–1 M NaCl, pH 7.7; (E) 50 mM Tris–1 M NaCl, pH 7.0. All buffers were degassed and filtered prior to use.

Fe(III)immobilized metal ion affinity chromatography (IMAC) on Chelating Sepharose Fast Flow

The degassed gel was packed in columns (15 mm × 10 mm I.D., $V_t \approx 1$ ml) in distilled water and charged with a few column volumes of 20 mM iron (III) chloride solution. Excess of Fe(III), not bound or loosely bound, was removed from the columns by washing with 10–15 volumes each of water, buffer C and buffer A. Chromatography was conducted at room temperature with a flow-rate of 15 ml/h; 2.0-ml fractions were collected. In each run 0.4–1.0 mg of substance in 0.5–1.0 ml of buffer A was applied to the column. The columns were washed with 10 ml of buffer A, and then eluted in a sequence with 10 ml of buffer B, a continuous pH gradient formed by the gradual mixing of 17 ml of buffer C with 17 ml of buffer B and finally with 20 ml of buffer D. With β-casein and its dephosphorylated form, 2 mg in buffer B were used and chromatography was started from pH 6.5.

After each experiment the chelating gel was regenerated with 100 mM EDTA containing 1 M NaCl and then washed with water. The metal-free columns were stored at room temperature and charged with iron(III) ions immediately before use. Every column was recycled several times.

Fe(III) IMAC on Chelating Superose using the fast protein liquid chromatographic (FPLC) system

Chromatography was performed on a Chelating Superose HR 10/2 prepacked column according to the manufacturer's instructions. Loading and stripping of Fe(III) and the conditions for equilibration were the same as for Chelating Sepharose Fast Flow (see above). The same amount of sample was also applied. Programs for three different procedures were developed on the FPLC system for Fe(III) IMAC. The procedures containing directions for charging with the metal, column prewash, sample application, isocratic elution, gradients in pH and MgCl$_2$, stripping of the metal and regeneration of

the column were included in a single program.

Procedure 1. The conditions were as follows: buffer A, 10 ml; buffer B, 20 ml; a continuous Mg(II) gradient from 0 to 1 M MgCl$_2$ (70 ml), formed by the gradual mixing of buffer B with buffer B containing 1 M MgCl$_2$.

Procedure 2. The conditions were as follows: buffer A, 20 ml; buffer E, 10 ml; a continuous Mg(II) gradient from 0 to 1 M MgCl$_2$ (70 ml), formed by the gradual mixing of buffer E with buffer E containing 1 M MgCl$_2$.

Procedure 3. The conditions were as follows: buffer A, 30 ml; a continuous pH gradient (30 ml), formed by the gradual mixing of buffer A with buffer C; buffer C, 10 ml; a continuous Mg(II) gradient from 0 to 1 M MgCl$_2$ (70 ml), formed by the gradual mixing of buffer C with buffer C containing 1 M MgCl$_2$.

RESULTS

Amino acids

None of the tested nonphosphorylated amino acids was adsorbed on the Fe(II)-Sepharose column at pH 5.5. In contrast, phosphoamino acids were bound to the column and desorption was achieved at pH 6.5. Phosphoserine and phosphotyrosine were eluted at pH 6.5 and phosphothreonine at pH 6.75 (Fig. 1).

Peptides

The basic peptide (RRKASGP) behaved like unmodified amino acids and passed freely through the column. In contrast, the acidic peptide (ASEEEEE) was retarded and emerged as a broad peak in the pH range 5.5–6.2. Both basic and acidic peptides, phosphorylated on the single serine residue, were adsorbed. Their desorption was achieved at pH 7.0 and 7.4, respectively (Fig. 2). The difference in pH required for desorption may be attributed to interactions between iron(III) ions and acidic groups, as indicated by the retardation of the peptide containing a cluster of five glutamic acid residues.

A further increase in the number of COOH groups resulted in a slight strengthening of the binding to the gel, as a homopolymer with an average number of 308 glutamic acid residues was eluted in the pH range 6.0–6.3. Some of the material found in the breakthrough peak probably reflects
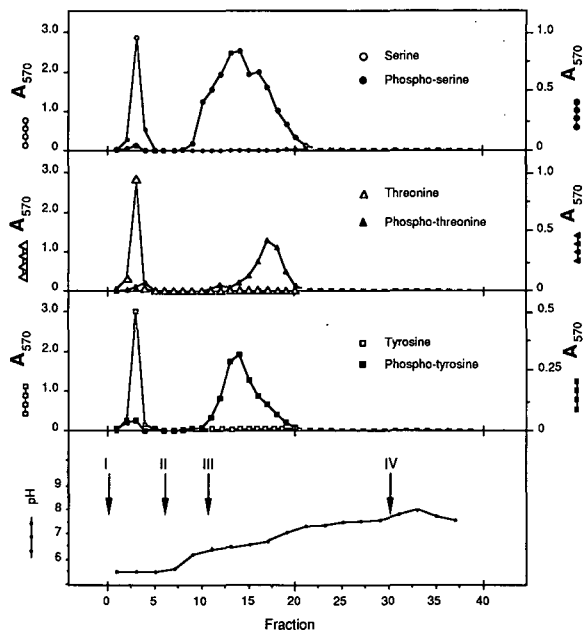
Fig. 1. Elution profiles of phosphoamino acids from Fe(III)-chelated Sepharose. Changes in buffer compositions are marked by arrows: I = buffer A; II = buffer B; III = pH gradient of buffers B and C; IV = buffer D. The internal reference for Tris, which forms coloured complexes with ninhydrin, was always determined along with the amino acid analysis. The absorbance at 570 nm was therefore corrected for the influence of Tris on the absorbance value in the pH gradient.

the presence of impurities of the compound of low or even no degree of polymerization.

The random copolymer of poly(Glu, Tyr), having a ratio of glutamic acid to tyrosine of 4:1, was more strongly bound to the gel than the homopolymer of polyGlu, and was eluted as a broad peak in the pH range 6.75–7.45. Total desorption of the polymer was achieved at pH 7.7 in 20 mM phosphate buffer. Two other peptide copolymers of similar molecular weight, consisting of Glu–Ala–Tyr and Glu–Lys–Tyr in the proportions 6:3:1, were mainly eluted in relatively sharp peaks with the maximum at pH 7.0 (Fig. 3).

The elution conditions for glutamic acid derivatives are presented in Table I. Glutamic acid and its dipeptide were eluted from the column in the breakthrough fraction; γ-carboxyglutamic acid and a heptapeptide containing five glutamic acid residues were slightly retarded on the column.
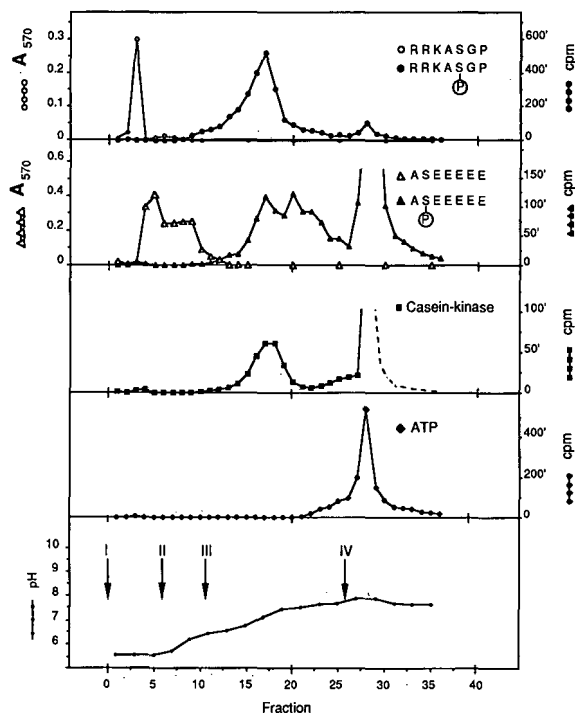
Fig. 2. Elution profiles of phosphopeptides from Fe(III)-chelated Sepharose. Conditions as in Fig. 1. Right-hand scale: primes denote thousands, i.e. 600' is 600 000.
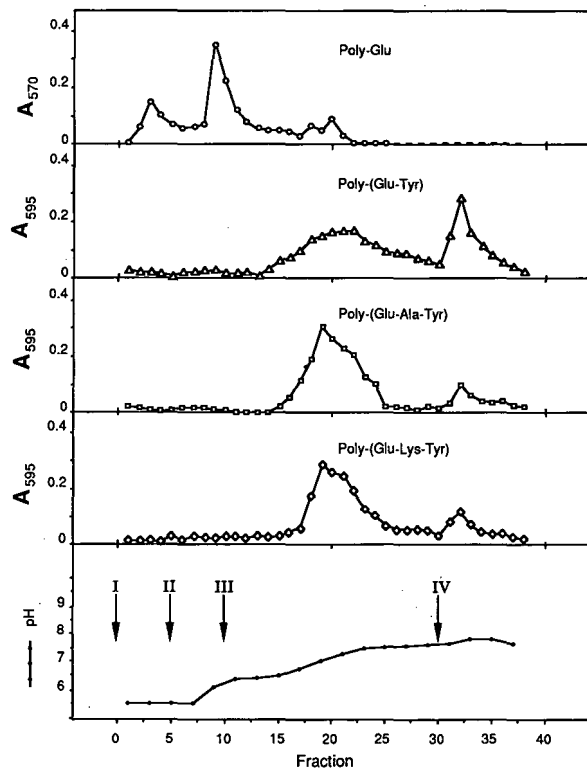
Fig. 3. Elution profiles of polyglutamic acid polymers from Fe(III)-chelated Sepharose. Conditions as in Fig. 1.

Proteins

Owing to the low solubilities of β-casein and its dephosphorylated form at pH 5.5, they were ap-

plied on the column at pH 6.5 (Fig. 4a). Native β-casein, having clusters of glutamic acids and a high degree of serine phosphorylation (see refs. 19

TABLE I

CONDITIONS FOR ELUTION OF GLUTAMIC ACID DERIVATIVES FROM IRON(III)-CHELATED SEPHAROSE

Compound	Number of groups		pH of elution
	Carboxylic	Phenolic	
Glu	2	0	5.5
Glu–Glu	3	0	5.5
Ala–Ser–Glu–Glu–Glu–Glu–Glu	6	0	5.5–6.2 (5.5)[a]
γ-CarboxyGlu	3	0	5.5–5.9 (5.5)[a]
PolyGlu	ca. 308	0	6.0–6.3 (6.0)[a]
Poly(Glu–Tyr)	ca. 210	ca. 52	6.7–7.5 (7.2)[a] 7.7[b]
Poly(Glu–Ala–Tyr)	ca. 110	ca. 18	6.8–7.3 (7.0)[a]
Poly(Glu–Lys–Tyr)	ca. 84	ca. 14	6.8–7.3 (7.0)[a]

[a] The pH of maximum desorption is given in parentheses.
[b] Elution was achieved by a linear pH gradient, followed by 20 mM phosphate buffer.
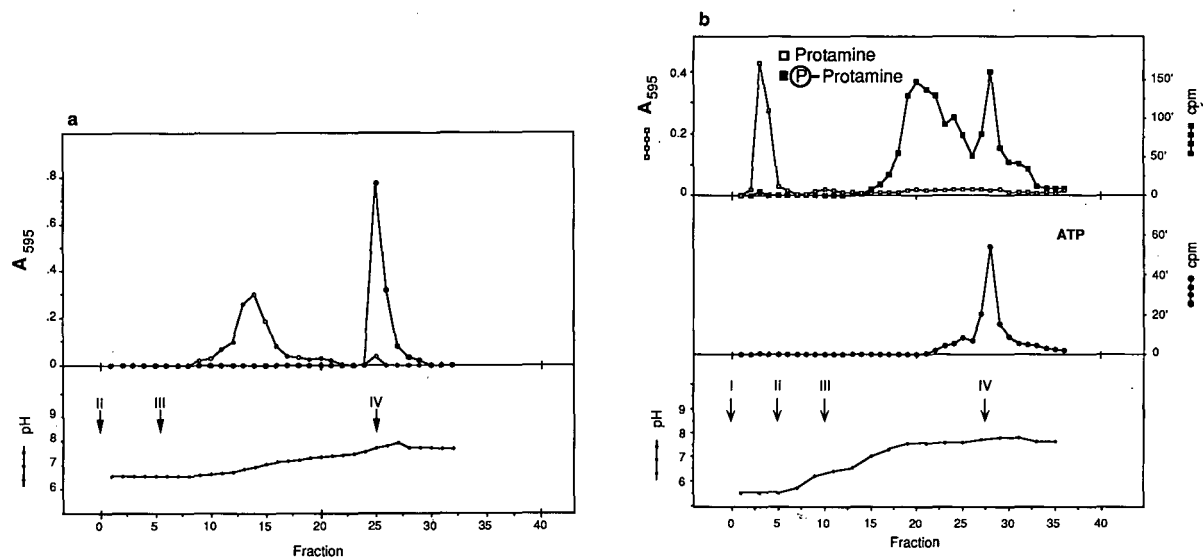
Fig. 4. Elution profiles of phosphoproteins from Fe(III)-chelated Sepharose. (a) ● = β-Casein and ○ = its dephosphorylated form; (b) protamine, phosphorylated and non-phosphorylated. Change of buffers as in Fig. 1.

and 20 and Fig. 5a), was bound very strongly to the immobilized iron(III) ions. For the elution of β-casein, phosphate buffer (pH 7.7) was required. The commercially available, enzymatically dephosphorylated (to about 80%) β-casein did not interact so strongly with the metal. After dephosphorylation the affinity of β-casein for the gel decreased, the major portion of the adsorbed protein was eluted by Tris buffer (pH 7.0) and another minor peak was obtained with phosphate buffer (pH 7.7). As native β-casein required inorganic phosphate to be eluted under these conditions, we conclude that this second peak contains unreacted (native) β-casein (Fig. 4a).

Similarly to other phospho compounds, phosphorylated protamine but not its unmodified form was adsorbed on iron(III)-chelated Sepharose and subsequently eluted at pH 7.5 (Fig. 4b). Three sites on the protamine seem to be available for phosphorylation by protein kinase A (see ref. 21 and Fig. 5b).

Fast protein liquid chromatography (FPLC)

Phosphoprotamine, a basic phosphopeptide and their non-phosphorylated counterparts were chromatographed on iron(III)-chelated Superose columns (prepacked gel bed) with the FPLC system according to procedures 1–3 (see Experimental).

As can be seen in Fig. 6a, in procedure 1, phospho compounds were not eluted at pH 6.5 until the $MgCl_2$ concentration reached 0.4 M. All three elution profiles were broad and were composed of several overlapping peaks.

In procedure 2, where the Mg^{2+} gradient started at pH 7.0, phosphorylated protamine started to appear at pH 6.9; four major peaks were eluted at a constant pH of 7.0 with increasing magnesium concentration, up to 0.3 M. Phosphopeptide was eluted as a single symmetrical peak at pH 6.9 (Fig. 6b).

In a separate experiment, 3 M NaCl instead of the routinely used 1 M NaCl was applied. At this sodium chloride concentration the peptide was desorbed at a pH 0.5 unit lower than when the experiment was performed with 1 M NaCl (data not shown).

In procedure 3, the increase in pH to 7.5 resulted in the elution of three single, relatively symmetrical peaks, at pH 7.1, 7.3 and 7.5 for basic phosphopeptide, phosphoprotamine and ATP, respectively (Fig. 6c).

The elution conditions for phospho compounds from the iron(III)-chelated gels are summarized in Table II. Basic phosphopeptide was eluted at pH 6.9–7.1 from iron(III)-chelated Sepharose and Superose, whereas for the elution of phosphoprotamine from these gels pH values of 7.5 and 7.3 were required, respectively.

a

R-E-L/E-E-L-N-V-P-G-E-I-V-E-S-L-S-S-S-E- (positions 10 ... 20, with encircled P)

-E-S-I-T-R-I-N/K/K-I-E-K-F-Q-S-E-E-Q-Q-Q- (positions 30 ... 40, with encircled P's)

-T-E-D-E-L-Q-D-K-I-H-P-F/A-Q-T-Q-S-L (position 50, with encircled P)

b

Site 1   -R-R-R-R-S-S-S-R-P-I-R-
                          Ⓟ

Site 2   -R-R-A-S-R-P-V-R-
                      Ⓟ

Site 3   -R-R-R-R-S-R-R-A-
                      Ⓟ

Fig. 5. Phosphorylation sites on (a) β-casein and (b) protamine. (a) Serine groups phosphorylated endogenously by the mammary gland casein kinases that could be removed by alkaline phosphatase are designated by an encircled P. According to Traugh and co-workers [19,20]. (b) Sites on protamine available for phosphorylation by protein kinase A are indicated by an encircled P. According to Bramson et al. [21].

DISCUSSION

During the last few years, we have claimed that iron(III) ions, immobilized on chelating gels, display a preferential affinity to phosphate groups in proteins and nucleotides. Our previous results had suggested that an interaction occurs between Fe (III) and the oxygen of the phosphate group [2,6]. The data presented in the first part of this paper have confirmed that suggestion. Unphosphorylated molecules are eluted at a lower pH (pH 5.5) than their corresponding phosphorylated derivatives (Fig. 7).

Although the interactions with immobilized metals have been exploited for phosphopeptide and phosphoprotein separations [2–5], their mechanisms are still not fully clarified.

The present results indicate that the binding of macromolecules to the immobilized iron(III) ions is more complex than assumed earlier [1,2] and is not limited to the iron(III)–phosphate interaction(s). We are now recognizing the role of carboxylic and phenolic groups in the metal ion interaction. Glutamic acid, its derivatives, homo- and heteropolymers (listed in Table I), with different contents of

TABLE II

ELUTION OF PHOSPHOAMINO ACIDS, PHOSPHOPEPTIDES AND PHOSPHOPROTEINS FROM IRON(III)-CHELATED GELS

Compound	Type of chromato-graphy[a]	Elution conditions		Chelating gel
		pH	[MgCl$_2$] (M)	
Phosphoserine	1	6.5	–	Sepharose
Phosphothreonine	1	6.7	–	Sepharose
Phosphotyrosine	1	6.5	–	Sepharose
Ala(Ser P)Glu$_5$	1	7.4	–	Sepharose
Arg$_2$Lys–Ala(Ser P)Gly–Pro	1	7.0	–	Sepharose
	2	6.5	0.56–0.90	Superose
	2	6.9	None	Superose
	2	7.1	None	Superose
Phophoprotamine	1	7.5	–	Sepharose
	2	6.5	0.40–0.58	Superose
	2	7.0	0.08–0.30	Superose
	1	7.3	None	Superose
β-Casein (enzymatically dephosphorylated)	1	7.0	–	Sepharose
β-Casein	3	7.7	–	Sepharose

[a] Type of chromatography: 1, linear pH gradient; 2, stepwise increase in pH followed by a linear MgCl$_2$ gradient (0–1 M); 3, linear pH gradient followed by 20 mM phosphate buffer.

Fig. 6. FPLC separation of phosphopeptide and phosphoprotamine on Fe(III)-chelated Superose. For the three elution conditions, gradient in (a) pH 5.5–6.5, (b) pH 5.5–7.0 and (c) pH 5.5–7.5, procedures I, II and III were used, respectively (for details see Experimental).

glutamic acid and tyrosine residues were chosen for the model studies. Two carboxylic groups in glutamic acid or three in its dipeptide were not sufficient to bind with immobilized iron(III) ions at pH 5.5. However, with three carboxylic groups present very closely assembled, as in γ-carboxyglutamic acid, the elution of the compound from the gel was delayed. A similar chromatographic retardation effect was observed for the acidic heptapeptide consisting of a cluster of five glutamic acid residues.
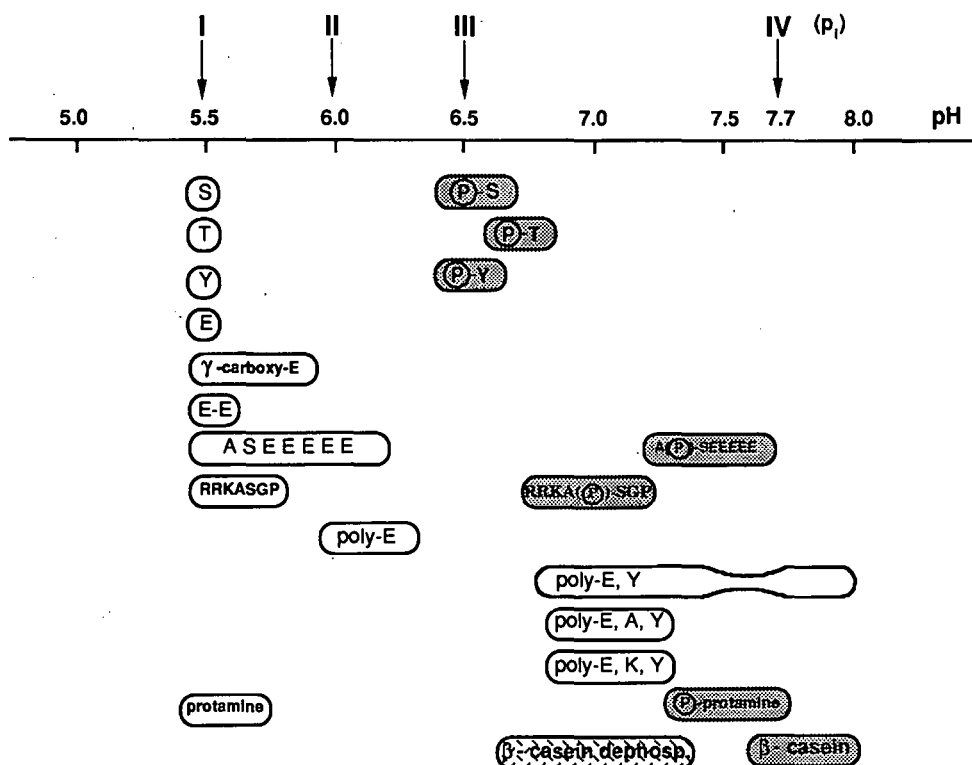
Fig. 7. Comparison of elution, from Fe(III)-chelated Sepharose, of phosphorylated molecules, their non-phosphorylated counterparts and compounds containing different number of carboxylic and phenolic groups. The diagram shows the chromatographic behaviour of amino acids, peptides and proteins. Phosphorylated groups are indicated by an encircled P. Conditions as in Fig. 1; I, II, III, IV = elution buffers A, B, C and D, respectively.

The tremendous increase in carboxylic groups to about 300 on average in the poly-Glu homopolymer results in an increase in the binding strength, but it is still a relatively weak interaction.

It should be pointed out, however, that the copolymers consisting of glutamic acid and tyrosine residues are bound strongly to the iron(III) gels and their desorption requires nearly the same conditions as those for phosphopeptides and phosphoproteins (Fig. 7). The stronger binding of this copolymer than that of the Glu–Ala–Tyr and Glu–Lys–Tyr copolymers may be ascribed to its higher number of phenolic groups (Table I and Fig. 7) and a more direct cooperative effect of adjacent carboxylic and phenolic groups.

The tentative modes of the interaction of phosphate and carboxyl groups with immobilized Fe(III) are presented in Fig. 8. One phosphate

group is sufficient for the binding, whereas the second type of interaction is likely to be promoted by the presence of several carboxyl groups. According to recent suggestions [22], phosphate groups could form a four-membered chelating ring, whereas the carboxylic groups might be involved in the formation of a multi-point attachment, probably a six-membered chelating ring. This could account for the stronger binding of phosphate group to the immobilized iron(III) ions compared with that of the cluster of carboxylic groups. The presence of phenolic rings can enhance the binding of adjacent carboxyl groups, presumably by the involvement of π-electrons of the aromatic ring. The lack of experimental data tends to discourage any further speculation at present.

This work demonstrates again that the adsorption of peptides and proteins to chelated iron(III)
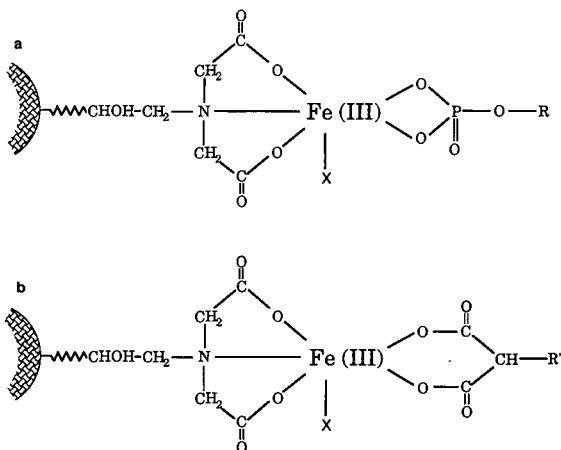
Fig. 8. Postulated mode of interactions of phosphate and carboxyl groups with the immobilized iron(III) ions. (a) Phosphate groups; (b) carboxyl groups. X may be water, hydroxyl, etc., and might also be involved in the binding of macromolecules. R and R' represent the compounds studied.

ions is not based only on a coulombic interaction as the columns were charged in the presence of 1 M sodium chloride, precluding simple ion-exchange chromatography. The strength of binding of phosphorylated basic peptide is slightly decreased in the presence of 3 M sodium chloride. However, it has previously been observed [2] that the elution of phosphorylated histone from iron(III)-chelated gel was not effected by 4 M sodium chloride. The presence of sodium chloride (higher than 1 M) does not greatly affect the binding, possibly because this salt is an intermediate on the Hofmeister scale [23].

Magnesium chloride, on the other hand, has a significant effect on the desorption of phospho compounds and is able to desorb these compounds at a relatively low pH (low pH is insufficient in itself for desorption). At low pH, higher concentrations of Mg^{2+} are required for desorption. At pH < 7.0 $MgCl_2$ elutes phospho compounds in a broad peak, without a distinct maximum. At pH 7.0, a linear increase in $MgCl_2$ concentration causes elution of several peaks containing phospho protamine. This may indicate that the separated peaks are protamine with different degrees of phosphorylation. This supports the previous suggestion [2] that, under certain chromatographic conditions, magnesium ions can be useful for the separation of proteins differing in the number of phosphate groups. The

desorptive action of Mg^{2+} ions can be interpreted as being due to an interaction between the magnesium ions and the phosphate groups. Apart from magnesium, inorganic phosphate was used as a low-molecular-weight affinity eluent for the separation of phospho compounds [1,2].

The elution of the phospho compounds under various conditions is only a part of the total problem. Further studies of the mechanisms of the different binding interactions of iron(III) to proteins are essential to achieve a practical technique for the separation of proteins with respect to their different types of interactions. For affinity eluents directed to other than the iron(III)–phosphate interactions, the approaches based on different types of affinity and/ or various chromatographic conditions must be investigated. The interaction between carboxyl groups and chelated iron(III) ions is very weak compared with the phosphate–iron(III) interactions. However, when there are clusters of both carboxylic and phenolic groups, the chelating effect is increased, becoming comparable to that for phosphate groups. It is possible that by varying the type of salt and its concentration one could enhance the difference in the adsorption strength between phosphoproteins and other proteins. Another approach may involve the inclusion of specific modifiers directed to either phosphate or carboxyl and phenolic groups in order to use them for affinity elution of compounds carrying different numbers of phosphate, carboxyl and phenolic groups. To develop such procedures more information about the way in which specific eluents affect the elution profiles of different compounds is desirable. The possibility of directing the interaction toward a single kind of adsorption on metal-chelated gels provides excellent opportunities for FPLC.

Iron(III)–chelated Superose used together in the FPLC system enables analytical studies on the chromatographic behaviour of different molecules. Moreover, the chromatography on iron(III)-chelated Sepharose, used in regular IMAC, and on iron(III)-chelated Superose was nearly identical, indicating that both systems can be readily compared.

REFERENCES

1 L. Andersson and J. Porath, *Anal.Biochem.*, 154 (1986) 250.
2 G. Muszyńska, L. Andersson and J. Porath, *Biochemistry*, 25 (1986) 6850.
3 H. P. Michel and J. Bennett, *FEBS Lett.*, 212 (1987) 103.
4 G. Muszyńska, in T. W. Hutchens (Editor), *Protein Recognition of Immobilized Ligands*, Alan R. Liss, New York, 1989, p. 279.
5 H. Flotow, P. R. Graves, A. Wang, C. J. Fiol, R. W. Roeske and P. J. Roach, *J. Biol. Chem.*, 265 (1990) 14264.
6 G. Dobrowolska, G. Muszyńska and J. Porath, *J. Chromatogr.*, 541 (1990) 333.
7 E. Sulkowski, *Makromol. Chem., Macromol. Symp.*, 17 (1988) 335.
8 G. Chaga, L. Andersson, B. Ersson and J. Porath, *Biotechnol. Appl. Biochem.*, 11 (1989) 424.
9 N. Ramadan and J. Porath, *J. Chromatogr.*, 321 (1985) 93.
10 J. Porath, *J. Chromatogr.*, 510 (1990) 47.
11 M. Belew and J. Porath, *J. Chromatogr.*, 516 (1990) 333.
12 F. Marchiori, F. Meggio, O. Marin, G. Borin, A. Calderan, P. Ruzza and L. A. Pinna, *Biochim. Biophys. Acta*, 971 (1988) 332.
13 M. J. Zoller, A. R. Kerlavage and S. S. Taylor, *J. Biol. Chem.*, 254 (1979) 2408.
14 G. Dobrowolska, E. Ber and G. Muszyńska, *J. Chromatogr.*, 376 (1986) 421.
15 G. Dobrowolska, F. Meggio and L. A. Pinna, *Biochim. Biophys. Acta*, 931 (1987) 188.
16 M. M. Bradford, *Anal. Biochem.*, 72 (1976) 248.
17 C. H. W. Hirs, S. Moore and W. H. Stein, *J. Biol. Chem.*, 219 (1956) 623.
18 D. H. Spackman, W. H. Stein and S. Moore, *Anal. Chem.*, 30 (1958) 1190.
19 P.T. Tuazon, E. W. Bingham and J. A. Traugh, *Eur. J. Biochem.*, 94 (1979) 497.
20 G. M. Hathaway and J. A. Traugh, in E. Stadtman and B. Horecker (Editors), *Current Topics in Cellular Regulation*, Academic Press, New York, 1982, p. 101.
21 H. N. Bramson, E. T. Kaiser and A. S. Mildvan, *CRC Crit. Rev. Biochem.*, 15 (2) (1984) 93.
22 J. Porath, *J. Mol. Recogn.*, 3 (1990) 123.
23 F. Hofmeister, *Naunyn-Schmiedebergs Arch. Pathol.*, 24 (1888) 247.

Interaction of immunoglobulin G with immobilized histidine: mechanistic and kinetic aspects

A. El-Kak, S. Manjini and M. A. Vijayalakshmi

Laboratoire de Technologie des Séparations, Université de Technologie de Compiègne, B.P. 649, 60206 Compiègne (France)

ABSTRACT

A systematic investigation of coupling methods for and the chemistry and chromatographic parameters of immunoglobulin gamma (IgG) adsorption to histidine- and imidazole-coupled Sepharose gels was undertaken in order to elucidate the interactions involved in the mechanism of recognition between IgG and the immobilized histidine. The effects of pH, salt and temperature effects indicated an ion-pairing mechanism, rather than a mechanism based on the net charge of the protein (IgG), but with some localized complementary charges recognizing the unprotonated imidazole nitrogen. The effects of the addition of ethylene glycol and urea indicated the involvement of hydrogen bonding between the ligand and the protein. The immobilized histidine binds to the Fc fragment of IgG with a fairly low affinity, in a way similar to the N-terminum of protein A binding to the Fc fragment of IgG. The kinetic parameters of the chromatographic system indicated a good capacity but a low adsorption rate constant.

INTRODUCTION

Single amino acids have been reported to be fairly selective and efficient immobilized ligands for the purification of a variety of proteins. Fibronectin and plasminogen were specifically retained on and eluted from Arg- and Lys-immobilized columns, respectively [1,2]. Tryptophan, with its predominant aromatic stacking properties, was shown to adsorb selectively proteins rich in aromatic residues [3]. Histidine has been reported to retain a plethora of biomolecules such as proteins, peptides and bioamines, each selectively under given adsorption conditions, particularly at pH values at or around the isoelectric pH of the molecule [4,5]. Of particular interest are the recent publications of immunoglobulin gamma (IgG) purification using histidine-linked insoluble matrices [6–8]. These investigations showed the possibility of recovering the subclasses IgG$_1$ and IgG$_2$ from serum extracts containing polyclonal antibodies and monoclonal antibodies from cell culture or ascite fluids.

Although the recovery of subclasses of IgG from different sources, by a very mild desorption using 0.2 M NaCl in the adsorption buffer, was demonstrated very clearly, not much is known regarding the mechanism of this selective recognition of IgG subclasses by the polymer-supported histidine ligand. While the ionic properties of both the immobilized ligand and the protein seem to be important in this recognition, the fact that adsorption takes place preferentially at or around the isoelectric pH of the protein is intriguing.

In this work we investigated the possible mechanism(s) of interactions involved in the recognition of IgG by immobilized histidine. Some possibilities of this single amino acid mimicking one of the binding sites of protein A from *Staphylococcus aureus* were evaluated. Moreover, with the aim of eventually scaling up this very simple technique, we studied the kinetic and thermodynamic parameters, such as affinity constants and adsorption rate constants, of this adsorption.

Correspondence to: Dr. M. A. Vijayalakshmi, Laboratoire de Technologie des Séparations, Université de Technologie de Compiègne, B.P. 649, 60206 Compiègne Cedex, France.

EXPERIMENTAL

AH-Sepharose, CH-Sepharose and Sepharose 4B were obtained from Pharmacia (Uppsala, Sweden), carbodiimide, L-histidine and histamine from Sigma (St. Louis, MO, USA), 1,4-butanediol diglycidyl ether from Aldrich (Milwaukee, WI, USA) and epichlorhydrin and sodium tetrahydroborate from Merck (Darmstadt, Germany). The model peptides used were purchased from Bachem (Bubendorf, Switzerland).

Preparation of adsorbents

For the preparation of histidyl-Sepharose (H-Seph) we adopted the experimental protocol described previously [4]. The gel was prepared by introducing reactive oxirane after activation with epichlorhydrin. Then the active oxirane was opened and coupled to the primary amine of the histidine.

For the preparation of histidyl-AH-Sepharose (H-AH-Seph), AH-Sepharose was used as the starting material and histidine was coupled using water-soluble carbodiimide at pH 4.5–6 with lateral stirring for 6 h at room temperature.

All the other gels were prepared either using oxirane intermediates with or without spacer as indicated or using CH-Sepharose as starting material with carbodiimide chemistry.

The different gels are shown schematically in Fig. 1.

Typical chromatography

Purification was performed using a column (6.3 × 1.0 cm I.D.) containing the gels prepared as described above. The bed volume was 5 ml. A linear flow-rate of 45 cm h^{-1} was used throughout. The temperature was kept at 4°C unless specified otherwise. A 184-μl aliquot containing 30 mg of human placental IgG was injected into the column, pre-equilibrated with 25 mM Tris–HCl buffer (pH 7.4). Elution was carried out successively using the same buffer containing 0.2 and 1 M NaCl. The absorbance of the eluate was measured at 280 nm. Fractions of 3 ml were collected. After each use the column was washed with three column volumes of 50 mM NaOH solution followed by washing with water and finally with the equilibrating buffer 25 mM Tris–HCl (pH 7.4).
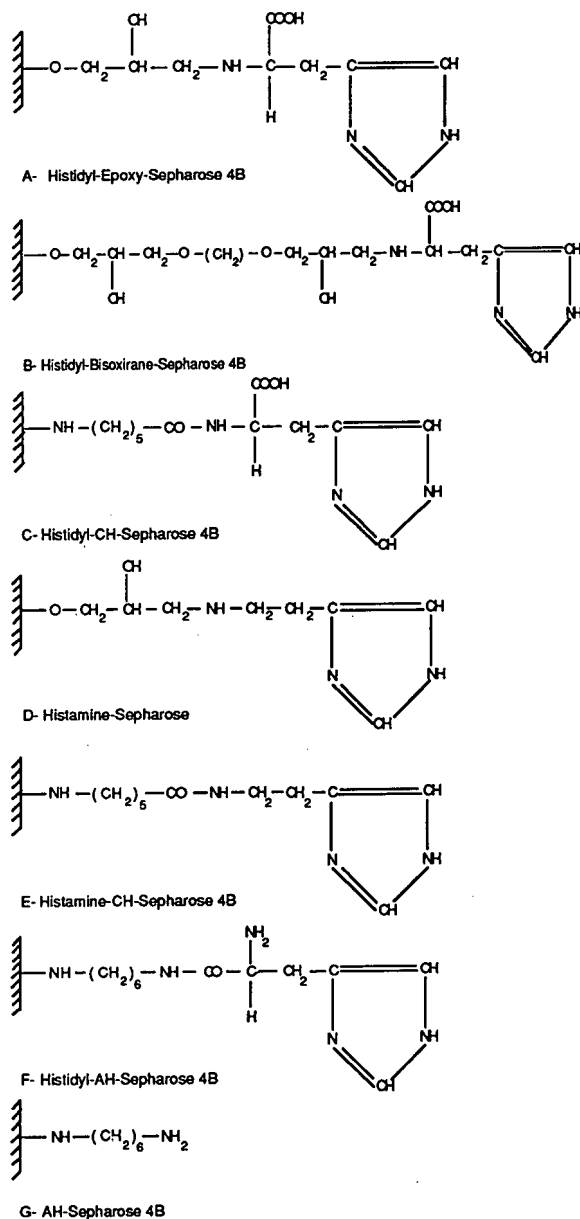
Fig. 1. Schematic structures of the adsorbents.

Study of thermodynamic and kinetic parameters

Determination of dissociation constant, K_D. For this study, a column (1.3 × 1.0 cm I.D.) was filled with H-AH-Seph gel and a preparation of human placental IgG containing 157 mg ml^{-1} of IgG (ca. 95% in IgG) was used.

To the column, equilibrated with 25 mM Tris–HCl (pH 7.4) a protein solution (dissolved in the same buffer) with different concentrations ranging from 0.5 to 25 mg/ml^{-1} of IgG was fed. The absorbance of the effluent at 280 nm was monitored continuously. The injection was continued in a frontal mode until the absorbance of the effluent reached a plateau. The column was then washed with the same buffer until the absorbance of the effluent at 280 nm reached the baseline. The adsorbed IgG was then eluted successively with the same buffer containing 0.2 and 1.0 M NaCl.

For each concentration the capacity of the column was determined as the amount of IgG retained in milligrams per millilitre of the gel. Protein concentrations were determined using a molar absorptivity of 212 000 l mol^{-1} cm^{-1} for IgG. The data obtained were fitted to the Langmuir model as shown below.

$$Q_a = \frac{Q_x K_a [C]}{1 + K_a [C]} \tag{1}$$

where C is the concentration of protein solution (mg ml^{-1} of IgG or M), K_a is the equilibrium association constant (ml mg^{-1} or l mol^{-1}), Q_a is the amount of adsorbed protein (mg IgG ml^{-1} gel) and Q_x is the maximum adsorption capacity of the gel (mg IgG ml^{-1} gel).

The dissociation constant, K_D, which is equal to $1/K_a$, was calculated from the linearized plot of the equation:

$$\frac{[C]}{Q_a} = \frac{[C]}{Q_x} + \frac{1}{Q_x K_a} \tag{2}$$

Determination of adsorption rate constants. This was done by using the split-peak approach as described elsewhere [9]. A solution of IgG (2 mg ml^{-1}) was prepared in 15 ml of equilibrating buffer (Tris–HCl, 25 mM, pH 7.4). Aliquots of 1 ml were injected consecutively into the equilibrated column. Unadsorbed protein was collected as fraction 1 (peak 1) and the adsorbed protein was later recovered as fraction 2 (peak 2). In this manner fifteen fractions representing peak 1 were collected before proceeding with the recovery of the retained protein. In each peak, amounts of protein were determined by multiplying the absorbance at 280 nm by the volume of the fraction collected and dividing by 1.4 (assuming $A_{280\text{ nm}}^{1\%} = 14$ for IgG). From the avail-

able information, the rate constant of adsorption could be calculated from the equation [9]

$$f = \exp\left(-k_a Q_x / \delta\right) \tag{3}$$

where f is the ratio of unretained to injected protein, Q_x is the maximum loading capacity of the column (mol) and δ is the flow-rate (l s^{-1}). Q_x was obtained from the previous experiment (adsorption isotherm) as 10.5 mg.

RESULTS

In a previous paper [7], it was shown that residual charges on immobilized histidine resulting from the coupling chemistry used and the functional group of the histidine implied in the coupling, and also the presence of a spacer arm, play important roles in the efficiency of the IgG purification. Moreover, the selectivity for the IgG$_1$ subclass was unimpaired in all instances whereas the introduction of the spacer, aminohexyl group, allowed the recovery of a second subclass, IgG$_2$ [7].

Fig. 2 shows the elution of IgG from a placental serum extract (containing >95% IgG) at pH 7.4 on the different gels (see Fig. 1). It is clear that the absence of free COOH groups improves the efficiency of IgG adsorption and recovery. This systematic investigation of adsorbents with histidine, with or without a spacer, and histamine instead of histidine has shown that those adsorbents with free COOH groups exhibited lower IgG retention capac-
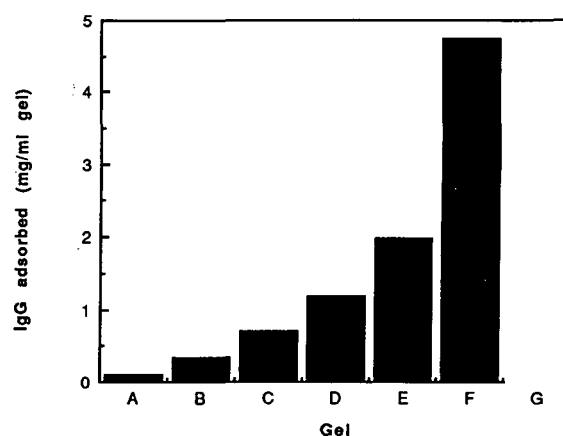
Fig. 2. IgG retention capacity in mg IgG ml^{-1} adsorbent. For A–G, see Fig. 1.

ities when compared with those without the free COOH of the histidine ligand (compare adsorbents A, B and C with D, E and F).

Further investigations reported here were limited to two adsorbents, H-AH-Seph and H-Seph, in order to evaluate the influence of free COOH groups and the presence of a spacer between the matrix and the ligand.

Influence of pH, ionic strength and adsorption temperature on IgG retention

Fig. 3a and b show the efficiency of the purification of IgG subclasses using H-AH-Seph and H-Seph columns, respectively. Although the ionization of the ligand is different in these two adsorbents, the optimum pH of the adsorption was found to be 7.4
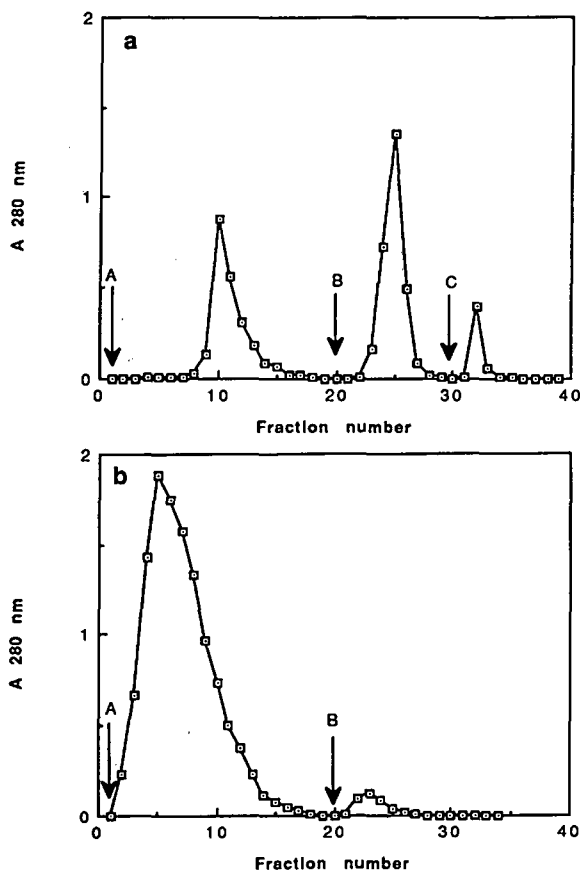
Fig. 3. Typical elution profiles of IgG chromatographed on (a) H-AH-Seph and (b) H-Seph (see text for details). (A) 25 mM Tris–HCl buffer (pH 7.4.); (B) A + 0.2 M NaCl; (C) A + 0.4 M NaCl.
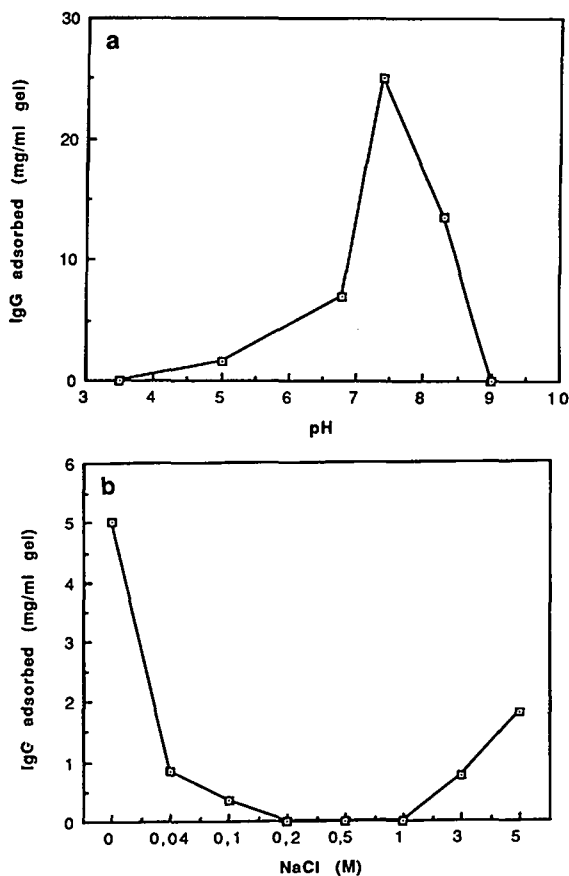
Fig. 4. Influence of adsorption parameters on the retention of IgG on H-AH-Seph: (a) pH; (b) added NaCl concentration.

(Fig. 4a). The difference in their ionization was reflected only in the amount of IgG_1 adsorbed, 5 mg ml^{-1} for H-AH-Seph compared with *ca.* 0.5 mg ml^{-1} for H-Seph. Moreover, both adsorbents retained IgG_1 at low salt concentrations in the adsorption buffer.

This indicates a mechanism of recognition based on ion-pair formation between the ligand and IgG_1. However, secondary interactions such as hydrogen bonding and mild hydrophobicity cannot be excluded. In fact, as shown in Fig. 4b, the efficiency of adsorption is maximum in the absence of any added NaCl in the buffer whereas it passes through a minimum (no adsorption) from 0.2 to 1.0 M added NaCl in the buffer. There was a slight increase in the amount of retained IgG at NaCl concentrations > 3.0 M.
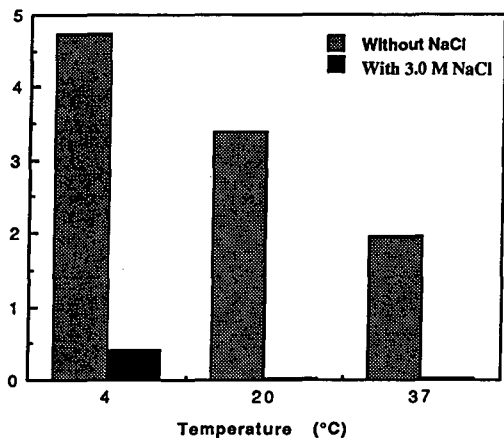
Fig. 5. Effect of temperature and NaCl concentration on IgG adsorption on H-AH-Seph.

The histogram in Fig. 5 shows the influence of temperature and high salt concentration on the adsorption efficiency and selectivity of retention of IgG subclasses on H-AH-Seph. Whereas 4 and 20°C favour the retention of 23.7 and 16.9 mg of IgG_1 and IgG_2, at 37°C no IgG_2 was retained on the column and only 9.8 mg of IgG_1 was retained and eluted when 0.2 M NaCl was added to the buffer. The presence of 3.0 M NaCl in the adsorption buffer showed a moderate retention of IgG at 4°C (2.1 mg ml^{-1}) which is almost ten times lower than that in the absence of NaCl. The retention at 20 and 37°C was almost negligible. This indicates the involvement of electrostatic and hydrogen bond interactions rather than hydrophobic interactions between the protein and the ligand.

Effect of water structure-modifying additives in the adsorption buffer

In order to elucidate better the water structure-mediated interactions, we studied the influence of added urea, ethylene glycol and sorbitol on the retention of IgG. Urea concentrations >3.0 M decreased the IgG retention almost to zero. The graph describing the effect of ethylene glycol was somewhat bell-shaped. The adsorption decreased with increasing concentration of ethylene glycol from 0 to 30%, and then increased with higher concentrations of ethylene glycol from 30 to 50%. Moreover, when the ethylene glycol concentration was increased to 60% the adsorption dropped to the

minimum level (Fig. 6). This can be attributed to the fact that ethylene glycol at concentrations higher than 50% will totally destroy the hydrogen bonds and the structured water molecules, which in turn can result in denaturation of the protein. These effects of the addition of urea or ethylene glycol suggest strongly the involvement of hydrogen bonds in the mechanism of recognition between the IgG and the immobilized histidine. Moreover, when 1.0 M sorbitol was included in the adsorption buffer the IgG retention decreased by up to 60% (data not shown).

Identification of the ligand binding site on IgG

It was important to determine whether IgG was bound to the immobilized histidine at Fc or Fab. We therefore chromatographed separately the Fc and Fab fragments, obtained by papain hydrolysis, under the same conditions as used for IgG retention. It was found that the Fc fragment but not the Fab bound to the adsorbent.

However, we could not probe the specific amino acid residues of Fc implied in this binding mechanism. On the other hand, the data obtained for the adsorption parameters indicated the importance of ion-pairing and hydrogen-bonding mechanisms in IgG binding to the immobilized histidine (Figs. 3–5). In order to pinpoint the specific amino acid residues or peptide sequences involved in this recognition, we used seven synthetic peptides containing N-terminal aspartic acid, based on the fact that the ionic
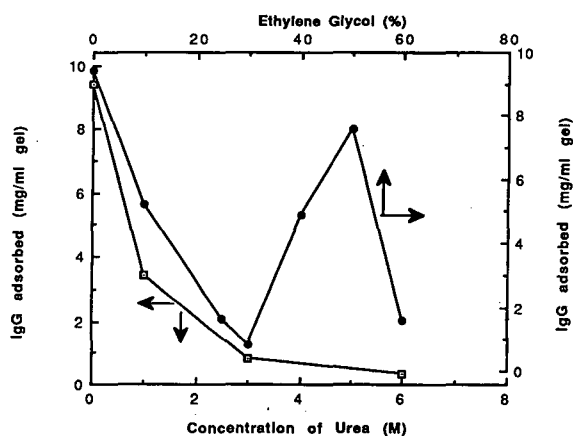
Fig. 6. Influence of water structure-modifying additives on IgG adsorption on H-AH-Seph. □ = Urea; ● = ethylene glycol.

interaction seemed the most predominant. We studied their retention behaviour on both H-Seph and H-AH-Seph at pH 7.4. All the peptides were eluted almost unretarded and without discrimination on the H-Seph column (data not shown). H-AH-Seph showed differences (Fig. 7). In fact, peptide 1 was very strongly retained and eluted from the column only with the addition of 1.0 M NaCl to the adsorption buffer. It was also interesting that peptides 7 and 4, differing only by a sulphate in a tyrosyl residue, showed distinct differences in their retention. Peptide 4 was not adsorbed to the column whereas peptide 7 was totally retained and eluted on addition of 0.2 M NaCl to the adsorption buffer. Another striking feature was that peptide 6 with a C-terminal lysine residue was partially retained and eluted with the addition of 0.2 M NaCl to the initial buffer.

Evaluation of the thermodynamic and kinetic parameters of IgG adsorption to H-AH-Seph

The high efficiency of specifically purifying IgG_1 and IgG_2 from different sources of IgG using H-AH-Seph adsorbent prompted us to study the kinetic aspects of this adsorption for an eventual scale-up of the separation of IgG from either placental serum or plasma.

At the outset it was very important to know the strength of binding and the maximum capacity. It

Fig. 8. Adsorption isotherm of human IgG on H-AH-Seph.

was also important to know the rate of adsorption for automated operation.

Determination of the dissociation constant (K_D). This was done by studying the adsorption isotherm using the frontal elution mode as described under Experimental. The adsorption isotherm, as shown in Fig. 8, follows a Langmuir pattern. From the linearized plot (Fig. 9), K_D was determined as 1.4 · 10^{-6} M and the maximum capacity of the gel was 10.5 mg IgG ml^{-1} gel.

Determination of the adsorption rate constant. This was done by using the split peak method [9] as described under Experimental. The cumulative

Fig. 7. Elution of model peptides on H-AH-Seph with 25 mM Tris–HCl buffer (pH 7.4) at 4°C. ● = DASGE (1); ◆ = DRVYIHPF (2); □ = DYM (3); ◇ = DYMG (4); ■ = DY (5); △ = DAHK (6); ○ = DY(SO₃)MG (7).
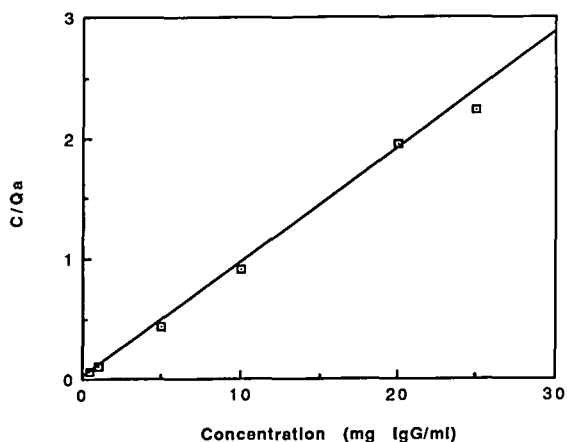
Fig. 9. Linearized plot of Fig. 8 using eqn. 2 (see text for more details). $y = 2.0182 · 10^{-2} + 9.4796 · 10^{-2}x$; $R^2 = 0.981$.
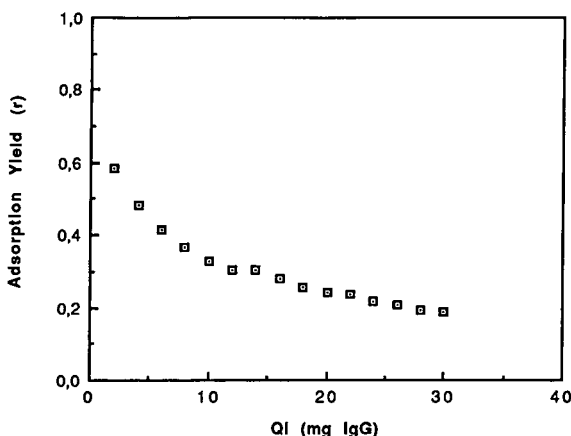
Fig. 10. Effect on adsorption yield of cumulative amounts of IgG injected.

amount of injected protein and the cumulative amount of unadsorbed protein were calculated for fifteen adsorptions. The ratio of the unadsorbed to injected protein was expressed as f, hence $1 - f$ gives the adsorption yield. From Fig. 10 it is clear that the adsorption yield decreases with increasing cumulative amount of injected protein. From eqn. 3, the rate constant was determined to be 56 l mol^{-1} s^{-1} using the values in the linear region of the graph.

DISCUSSION

The adsorption parameters indicated a charge–charge interaction. However, this is not based on the net charge of the protein, but on some localized charges forming ion pairs with the residual charge of the immobilized histidine.

At pH 7.4 IgG has a net positive charge whereas the adsorbent will have a positive charge on the α-NH$_2$ group and the imidazole nitrogen is non-protonated. At lower pH (e.g., pH 5.0) both nitrogens are protonated and IgG also has a net positive charge. Hence there is no retention. Moreover, at pH 6.8, where the imidazole N is non-protonated, the retention was not significant (Fig. 4a), perhaps owing to the lack of perfect charge balancing with a localized protonation in the IgG.

Moreover, the isoelectric point distribution of the total IgG from placenta and that of the retained and non-retained fractions on the histidine adsorbents were determined according Righetti et al. [10]. The

placental IgG had a distribution of pI from 4.36 to 10.11 whereas the fractions (IgG$_1$) retained and consequently eluted with 0.2 M NaCl from H-Seph or H-AH-Seph had pI values from 7.9 to 8.9. Moreover, those eluted with 1.0 M NaCl only from the H-AH-Seph column had pI values only in the range 6.8–7.2. This means that only the isoelectric forms of IgGs within a narrow range of pH were selectively retained on the adsorbents. Moreover, the subsets of IgG were retained more or less strongly on the adsorbent. This again shows the predominance of charge–charge interactions between the localized charges of the protein and the imidazole nitrogen. Nevertheless, the hydrogen-bonding interactions do play a role, as shown by the influence of additives such as urea and ethylene glycol in the elution buffer (Fig. 6).

In order to determine whether the immobilized histidine binds to the Fc or the Fab domain of the IgG, we studied the retention of Fc and Fab fragments, resulting from papain hydrolysis of the IgG as described by Goding [11]. We found that both the H-Seph and H-AH-Seph adsorbents retained only Fc whereas the Fab was unretarded on the columns (data not shown). It is known that protein A from Staphylococcus aureus binds to the Fc region of the IgG [12].

Moreover, the binding of IgG to immobilized histidine seems to be weak. The amino acid residues of protein A binding to Fc of IgG are commonly reported to be FQQNFYLNICK (the B domain) [12]. There are no histidine residues involved here. However, Moks et al. [13] reported the existence of five different domains in protein A binding to Fc region of IgG with differences in their binding strength. In fact the N-terminal sequence, called the E domain, with histidine at position 3 (AQHDEA) has the weakest affinity and binds to immobilized IgG. This weak affinity binding and the presence of histidine, reported as playing an important role, can be compared with the weak affinity of IgG, bound through its Fc region, to the immobilized histidine.

Nevertheless, in another independent investigation, we used some IgG variants differing only in their amino acid sequences at the CDR regions (parts of the Fab domain) for their retention on to the H-AH-Seph column. We found that whereas all six IgG variants studied were retained and eluted with 0.2 M NaCl, the elution volumes were different

for different variants (unpublished data). This indicates that in the whole IgG molecule whereas the primary binding site could be in the Fc region, there could be a minor cooperative effect due to secondary binding sites with long-range forces of interaction with the amino acid residues at the CDR regions.

In an attempt to identify the particular amino acids involved in the ion pairing with the histidine, we studied the retention of a few synthetic model peptides. These data did not show any preferential binding of N-terminal aspartic acid-containing peptides. Peptides with C-terminal E or K showed improved retention, with C-terminal E peptide being strongly retained. This again indicates that the ionic interactions are not the only forces responsible for the selective retention of IgG subclasses on the adsorbent. Further, in a more recent study, we equally successfully eluted the retained IgG_1 by using either E or K at 25 mM concentration, added to the same adsorption buffer, instead of using 0.2 M NaCl as in this study (unpublished data). Moreover, the column was able to distinguish between the sulphated and the non-sulphated Y residue in the peptide sequence. To our knowledge, nothing has been reported about the presence of sulphated tyrosine residues in the IgG.

Hence it is difficult to correlate these observations with the retention of IgG on the histidine-coupled adsorbents.

Kinetic parameters

The capacity of H-AH-Seph was calculated to be 10–12 mg IgG ml^{-1} gel, comparable to that reported for protein A–Sepharose [14] and protein A–Ultrogel [15].

The dissociation constant, K_D, as determined from the adsorption isotherm was 1.4 × 10^{-6} M. This indicates a weak affinity which is consistent with the easy and non-denaturing desorption of the bound IgG. Moreover, in another study in which we compared membrane-based histidine adsorbents with that of protein A coupled to a nylon membrane, we found K_D values in the region of 10^{-5} M [8].

The adsorption rate constant determined by the split peak method [9] gave a value of 56 l mol^{-1} s^{-1}. This indicates slow adsorption kinetics and implies that the flow-rates will influence the IgG adsorption pattern. In fact, a previous study using an ethanol precipitate of human placental serum containing

about 90% IgG did show differences in the retention with varying flow-rate [6]. However, the suitability of this model [9] for the study of the resolution of IgG subclasses using total IgG cannot be clearly demonstrated. Therefore, we are pursuing on the one hand the same study using the prepurified IgG_1 and on the other a different approach based on the variation in flow-rates using both soft (Sepharose) and hard (silica) gels as support matrices to validate these data and the mathematical model. The results will be published elsewhere.

These parameters depend on the porosity and the nature of the supporting polymer matrices. In one of our studies using a low-porosity, small-particle-size support matrix we observed a much higher capacity (unpublished data), indicating diffusion-controlled limitations. Moreover, the systematically observed positive effect of a spacer arm supports this fact.

CONCLUSIONS

This study has shown that a single amino acid residue, histidine, can be very effective in purifying two different subclasses of human IgG from polyclonal sera. The weak affinity interactions are very advantageous for a high recovery of native proteins compared with the protein A-immobilized gels. The high capacity and the reproducibility are favourable features in using this system for scaling-up operations.

REFERENCES

1 M. Vuento and A. Vaheri, *Biochem. J.*, 183 (1979) 331.
2 L. Suamri, F. Spitz and L. Arzadon, *J. Biol. Chem.*, 251 (1976) 3693.
3 M. A. Vijayalakshmi and J. Porath, *J. Chromatogr.*, 177 (1979) 201.
4 S. Kanoun, L. Amourache, S. Krishnan and M. A. Vijayalakshmi, *J. Chromatogr.*, 376 (1986) 259.
5 M. A. Vijayalakshmi, *Ph. D. Thesis*, University of Compiègne, Compiègne, 1980, p. 108.

6 A. Mbida, S. Kanoun and M. A. Vijayalakshmi, in J. F. Stoltz and C. Rivat (Editors), *Biotechnology of Plasma Proteins*, INSERM Publication No. 175, Paris, 1988, p. 237.
7 A. El-Kak and M. A. Vijayalakshmi, *J. Chromatogr.*, 570 (1991) 29.
8 S. Manjini and M. A. Vijayalakshmi, *Biotechnol. Bioeng.*, (1991) in press.
9 H. Place, B. Sebille and C. Vidal-Madjar, *Anal. Chem.*, (1991) in press.
10 P. G. Righetti, E. Gianazza and B. Bjellqvist, *J. Biochem. Biophys. Methods*, 8 (1983) 89.
11 J. W. Goding, *J. Immunol. Methods*, 13 (1976) 215.
12 S. Johnsson and G. Kronvall, *Eur. J. Immunol.*, 4 (1974) 29.
13 T. Moks, L. Abrahmsen, B. Nilsson, U. Hellman, J. Sjöqvist and M. Uhlen, *Eur. J. Biochem.*, 156 (1986) 637.
14 *Pharmacia Handbook of Affinity Chromatography, Principles and Methods*, Pharmacia, Uppsala, 1986, p. 48.
15 *Practical Guide for Use in Affinity Chromatography and Related Techniques*, IBF, Villeneuve la Garenne, 2nd ed., 1983, p. 79.

Purification of complex protein mixtures by ion-exchange displacement chromatography using spacer displacers

Anthony R. Torres

Bio-Fractionations, 1725 S. State Highway 89–91, Logan, UT 84321 (USA)

Elbert A. Peterson

Laboratory of Biochemistry, National Cancer Institute, National Institutes of Health, Bethesda, MD 20205 (USA)

ABSTRACT

The anion-exchange separation of complex protein mixtures by displacement chromatography using spacer displacers driven by high-affinity final displacers is demonstrated. Guinea pig serum was separated on a medium-resolution adsorbent using a single heterogenous mixture of carboxymethyldextran displacers to space the protein components. Mouse liver cytosol was separated on a low-resolution adsorbent using six carboxymethyldextran spacer displacers of increasing column affinity. The demonstration of the purification of alkaline phosphatase from *E. coli* periplasm by displacement chromatography on a high-performance liquid chromatography column is reviewed. The benefits of spacer displacers for separating minor components from complex biological protein mixtures is discussed. A simplified method for preparing carboxymethyldextran displacers is presented.

INTRODUCTION

Although there have been many advances made in the chromatographic separation of proteins, large-scale purification still presents challenges. The purification of a single protein produced by procaryotic or eucaryotic cells is a formidable task because of the complexity of mixtures of proteins produced by organisms. The biotechnology industry has become acutely aware of these problems, as is it estimated that 50–80% of the total production costs of genetically engineered proteins are related to purification [1]. Many purification procedures developed in research laboratories for protein characterization and amino acid sequencing are not suitable for production because of low recoveries from multiple chromatographic and electrophoretic procedures [2]. To reduce the costs of therapeutic pro-

teins, purification methods of high resolution, selectivity, capacity, and recovery must be used [3].

It was recognized over 40 years ago that displacement chromatography offered several advantages for preparative separation. Tiselius and associates published several manuscripts describing the theory of displacement chromatography, using simple mixtures of sugars on charcoal columns as models [4]. Porath and Li [5,6] pioneered the application of displacement chromatography for the separation of polypeptides. They showed that bacitracin and insulin could be highly purified on charcoal columns using various alcohols as carrier displacers. This research showed that very high sample loads of simple mixtures could be separated with high resolution and high recovery [5]. However, it was obvious that the separation of complex mixtures of typical proteins from biological samples was much more difficult. This work was largely abandoned because of the lack of adequate protein adsorbents and carrier displacers. Displacement chromatography for proteins has been revived in recent years, using

---

Correspondence to: Dr. A. R. Torres, Bio-Fractionations, 1725 S. State Highway 89-91, Logan, UT 84321, USA.

modern column technology and synthesized carrier or spacing displacers [3,7–9].

It was shown in the late 1970s that unfractionated preparations of carboxymethyldextran (CM-D) establish multicomponent displacement trains on anion-exchange columns, the affinity of each CM-D molecule being a function of the number of negative charges it can present to the adsorbent. Proteins of human serum were separated within the displacement trains according to their column affinities [10]. These CM-Ds behaved like classic displacers [11] as described by Tiselius [4]. Tailing, noted by Porath with single displacers, was eliminated because of the gradual, progressively increasing affinities of the multiplicity of CM-D species within the displacement train. These displacers have been used to purify proteins from complex biological mixtures, including serum [12] and E. coli periplasm [13]. High recovery, resolution, and capacities have been accomplished on various anion-exchange adsorbents, including high-performance liquid chromatography (HPLC) columns.

Chondroitin sulfate and Nalcolyte 7105 have been used as displacers to separate simple protein mixtures on anion- and cation-exchange columns [14,15]. High-affinity displacers like chondroitin sulfate and Nalcolyte establish displacement trains based upon protein–protein displacement since they have higher affinities than any of the proteins. Subramanian and Cramer [15] have shown that simple mixtures of proteins can be separated by protein–protein displacement when conditions were adjusted to separate crossing isotherms. Although protein–protein displacement can be useful when the target proteins are substantial components of the feed stock, it has not been shown to offer high recovery and high resolution for the separation of a single minor protein component from a complex biological mixture such as serum or a cell culture fluid.

Research in the last 15 years has shown that proteins can be separated by displacement chromatography on many types of protein adsorbents [7,8,10]. However, to be useful in separating therapeutic proteins from complex protein mixtures, effective spacer displacers must generally be used. These displacers must be relatively inexpensive, produced by controlled conditions, cover a wide column affinity range, the nontoxic, and be removeable from the

final product. The CM-D displacers were designed to fulfill these properties.

Our recent work has largely involved simplifying the synthesis and purification of CM-Ds. The present manuscript demonstrates the separating power of displacement chromatography employing carrier or spacer carboxymethyldextrans as displacers in resolving the complex mixtures of proteins present in mouse liver cytosol, guinea pig serum, and alkaline phosphatase from E. coli periplasm on low resolution, medium resolution, and HPLC adsorbents, respectively.

EXPERIMENTAL

Materials

Fractogel DEAE 650S was purchased from Pierce (Rockford, IL, USA). DEAE-cellulose (DE-52) was obtained from Whatman (Hillsboro, OR, USA). The silver staining gel kit, AG1-X8 (OH), and Dowex 50W-X8 (H) were products of Bio-Rad (Richmond, CA, USA). Industrial grade XL dextran of 9000 average molecular weight was a product of Pharmachem (Bethlehem, PA, USA). Chloroacetic acid, lithium hydroxide monohydrate, and sodium borohydride were Fisher Scientific (Pittsburg, PA, USA) products. Phenylmethylsulfonyl fluoride (PMSF), DNase I, RNase A, and molecular weight standards (Dalton Mark VII-L) for gel electrophoresis were obtained from Sigma (St. Louis, MO, USA).

Preparation of spacer carboxymethyldextran

In a 125-ml glass flask, 7.0 g of chloroacetic acid were dissolved in 56 g of water, using a $1\frac{1}{2} \times \frac{5}{16}$ in. magnetic stir bar. Then 47 g of dextran was added in many small portions, reducing the rate of addition as the increasing viscosity slowed dispersion. The resulting solution was cooled to 7°C in a small ice bath; then 6.2 g of LiOH · H$_2$O were added in a trickle to the rapidly stirred solution at a rate adjusted to keep the temperature at 20°C or below as the heat of neutralization was absorbed by the ice bath. When slightly more than half of the LiOH · H$_2$O had been added, a rapid color change to deep yellow indicated that the solution had become strongly alkaline. After this was confirmed with a pH test paper, the ice bath was removed, about 300 mg of sodium borohydride was added, and the re-

maining LiOH · H$_2$O was dropped in. Stirring was continued to complete solution.

The flask was sealed and placed in a weighted screw-cap plastic jar, which was then supported in a 37.5°C water bath for 48 h. The pale yellow product was diluted with partially deaerated deionized water to 450 ml.

CM-D was separated from low-molecular-weight reaction products by passing the diluted reaction mixture at 90 ml/h through a series of three ion-exchange columns; 120 ml of AG1-X8 (OH), 120 ml of Dowex 50W-X8 (H), and 30 ml of AG1-X8 (OH), all 20–50 mesh. In order to provide density stability, the columns were connected to each other in such a way as to produce upward flow through the resin beds. When all the diluted reaction mixture had entered the system, partially deaerated deionized water was pumped after it until all of the purified product had been collected. The CM-D emerged in the free acid form, so collection was begun when the effluent turned a strip of Congo Red paper blue. Soon after this point, the first column was inverted, without disconnecting it from the others, in order to preserve density stability when, much later, the water entered the column. The second and third columns were similarly inverted soon after pumping water into the first column was begun. Collection of the CM-D was ended when the effluent was no longer acid or was very weakly acid to Congo Red paper.

The entire product was adjusted from pH 2.46 to 7.85 with 4.4 ml of 10.0 M NaOH. The final product was 467 ml of 11% CM-D having a reciprocal of pellet volume (RPV) of 7.

Preparation of carboxymethyldextran final displacer

In a 100-ml glass beaker, 8.6 g of chloroacetic acid were dissolved in 17.0 g of water, and 17.0 g of dextran were added in many small portions as in the procedure described above. The resulting solution was cooled in an ice bath to 6°C before starting the addition of 7.6 g of LiOH · H$_2$O. The very high viscosity slowed the addition of the alkali markedly, since mixing and solution were strongly affected. When the mixture became permanently alkaline, the bath was removed, about 110 mg of sodium borohydride was added, and the remaining LiOH · H$_2$O was dropped in. Stirring was continued to complete solution. This mixture was heated at

37.5°C for 48 h in the manner described above for the preparation of low-affinity CM-D. The light yellow product was diluted to 180 ml with partially deaerated deionized water and purified by the ion-exchange procedure described above. The purified acidic fraction was adjusted from pH 2.10 to 7.8 with 5.5 ml of 10.0 M NaOH. The final product was 211 ml of 11% CM-D having an RPV of 26.

Sample preparations

Normal guinea pig serum was dialyzed against 10 mM sodium phosphate, pH 7.0.

Mouse liver cytosol was prepared from livers perfused with 10 ml of phosphate-buffered saline, each. Ten livers were homogenized with a Potter-Elvehjem homogenizer in an equal volume of Littlefield's medium (50 mM Tris · HCl, pH 7.2, 250 mM sucrose, 25 mM potassium chloride and 5 mM magnesium dichloride). The homogenate was filtered through a single layer of silk. The filtrate was centrifuged at 100 000 g for three hours in a Spinco Type 40 rotor. PMSF was added to 0.1 mM, and magnesium acetate was added to 200 mM. DNase I and RNase A were added to 20 μg/ml ad 50 μg/ml, respectively, and the pH adjusted to 7.3 with 0.5 M NaOH. The nucleic acid was digested overnight at room temperature. The protein-rich cytosol was dialyzed against the respective column buffer before use. A Lowry protein determination showed a protein concentration of 13 mg/ml.

Column chromatography

The anion-exchange columns were equilibrated in the appropriate buffers. The flow-rate was 10 ml/h for the serum separation and 5 ml/h for the cytosol chromatography and 2.5-ml fractions were collected in both experiments. The temperature was 5°C.

Gel electrophoresis

The non-denaturing buffering system of Davis [16] was used in a 35-place vertical slab (90 × 244 × 2 mm) of 7.5% acrylamide for evaluation of samples taken directly from the column fractions in the serum and liver cytosol experiments (40 and 70 μl, respectively). The proteins were stained with Coomassie Blue G-250 [17].

Analysis of *E. coli* lysate and purified *E. coli* alkaline phosphatase (see Fig. 3) was performed by so-

dium dodecyl sulfate–polyacrylamide gel electrophoresis (SDS-PAGE) on a 10% acrylamide running gel with a 6% stacking gel [18].

RESULTS AND DISCUSSION

The first two thirds of the chromatographic separation illustrated in Fig. 1 (up to fraction 23) is a displacement of the most lightly bound proteins of the guinea pig serum sample within a frontal analysis of the very heterogeneous low-affinity CM-D

preparation. Application of the final displacer resulted in the emergence in fraction 24 of a brief spike of both CM-D and protein having somewhat higher affinities, with loss of potential resolving power within that range. Adsorption of the very high affinity CM-D used as final displacer resulted in a displacement of counter ion such that the background buffer rose from 10 mM phosphate to 21 mM (not plotted), sufficient to eliminate the affinities of the components of fraction 24. The pH rose only slightly, to 7.27, and therefore did not contrib-
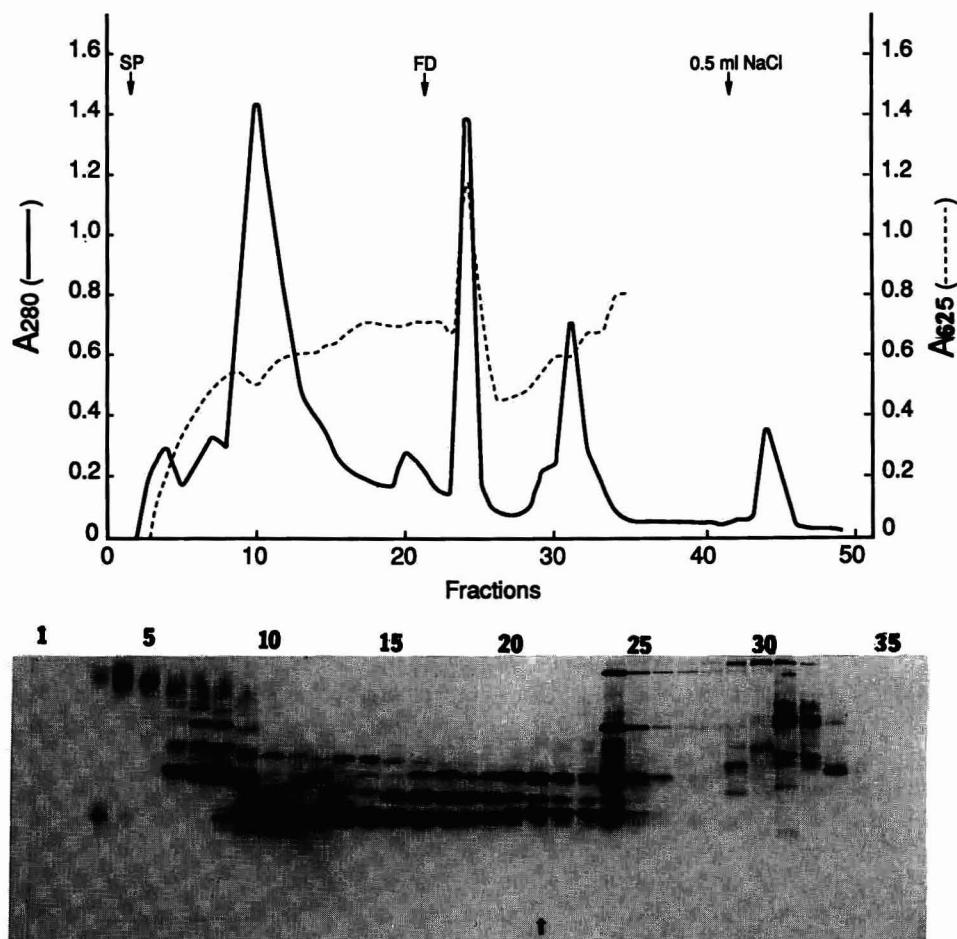
Fig. 1. Displacement chromatography of guinea pig serum on Fractogel DEAE 650S and electrophoretic evaluation of fractions. Sample, 1.1 ml, dialyzed against 10 mM sodium phosphate, pH 7.0, was pumped into the bottom of a 7-ml column equilibrated with the same buffer. Displacers: 51 ml of 0.6% solution of spacer CM-D (RPV = 7) and 50 ml of a 1% solution of the final displacer (FD) (RPV = 26), both in the starting buffer. Heavy line represents absorbance at 280 nm, light line the absorbance at 625 nm after reaction of 10-μl samples with anthrone [23] as a measure of CM-D. For electrophoresis, 40-μl samples were taken directly from the fractions. The point at which FD was applied is marked by the arrow below the electrophoretic pattern of fraction 21.

ute to the desorption of the proteins in fraction 24. Thereafter, the final displacer, much more homogeneous with respect to affinity than the spacer CM-D, drove a classical displacement train comprising the higher affinity components of the serum sample and the spacer CM-D. Finally, the adsorbent was stripped of CM-D by passing 20 ml of 0.5 M NaCl through the column. This CM-D emerged with the salt front in fractions 45 and 46.

Examination of the bands obtained by electrophoresis shows that individual protein species generally emerged in one or two fractions. Some pro-

tein classifications were too heterogeneous to permit such clear resolution: γ-globulins (upper left), in which a progressive increase in electrophoretic mobility revealed their well known extreme heterogeneity; the transferrins (starting in fraction 6), which appear to be more easily separated chromatographically than electrophoretically under these conditions; albumin (starting at fraction 8), which has long been known to be chromatographically heterogeneous in its untreated form because of its ability to bind many low-molecular-weight substances such as fatty acids and other lipids; and albumin
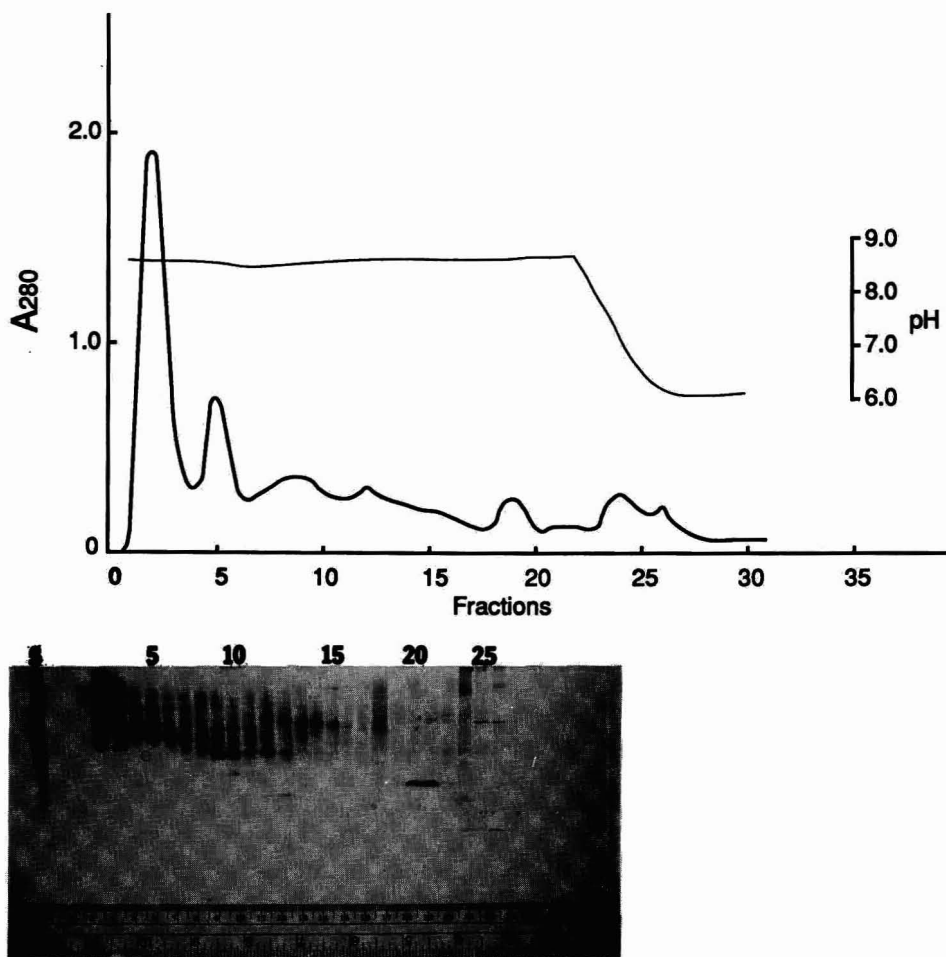
Fig. 2. Displacement chromatography of mouse liver cytosol on DEAE-cellulose and electrophoretic evaluation of fractions. Sample, 2 ml, dialyzed against 40 mM Tris–5 mM phosphate, pH 8.6, was applied to a 3.6-ml column of DE-52 equilibrated with the same buffer. Displacers: six 6-ml portions of 1% solutions of six narrow range CM-Ds [19] increasing progressively in RPV from 5 to 15 and decreasing progressively in pH from 7.5 to 6.5, all containing 5 mM phosphate, were applied successively and followed with 35 ml of an 0.8% solution of CM-D having an RPV of 26 in 5 mM Tris phosphate pH 5.9.

dimer (starting at fraction 15). The extreme heterogeneity of serum protein is evident, and most fractions contain several protein species that have affinities, under these conditions, that are too close for their resolution to be achieved in this system. However, rechromatography of appropriate fractions with the same highly heterogenous displacers at another pH is likely to improve the separation. Group specific globulin, a vitamin D binding protein, for example, was highly purified from human serum by two-step displacement chromatography at pH 7.1 and 8.1 [12].

In work to be published elsewhere, samples of human serum as large as 10 ml (about 600 mg of protein) have been applied to the 7-ml column used here, resulting in the rapid emergence of gamma-globulin, transferrin, and most of the albumin in an unresolved fore peak, leaving proportionately greater amounts of the higher affinity proteins on the column to be separated by displacement within a frontal analysis of a single spacer CM-D solution in a manner analogous to that employed here for the low-affinity serum proteins.

The experiment shown in Fig. 2 provides another example of the resolution by displacement chromatography of a complex natural mixture of proteins, intracellular in this case. Here the small size of the column (3.6 ml) was partly compensated for by the use of six narrow-range CM-Ds [19] applied in succession so as to approximate a partially developed displacement train before they entered the column. This situation is very different from the frontal analysis of heterogeneous CM-D in Fig. 1, where all the constituents of the spacer CM-D entered the column simultaneously until the final displacer was applied. Although dominating heterogeneous classifications such as the γ-globulins, transferrin and albumin of serum are less evident in mouse liver cytosol, the array of proteins presents a formidable problem in resolution. Examination of the gel shows that high- and low-molecular-weight proteins are highly resolved, often in a couple of fractions. In this experiment, a progressive decrease in pH incorporated into the CM-D schedule was buffered by the adsorbent bed (equilibrated at pH 8.6) and did not begin to emerge until fraction 22. Under other conditions of pH and salt a different picture can be expected, and when the objective is the isolation of a single species, poor resolution among
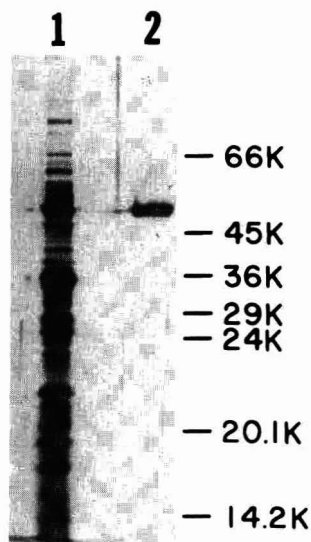
Fig. 3. Silver-stained SDS-PAGE analysis of *E. coli* periplasma sample containing alkaline phosphatase (lane 1) and purified alkaline phosphatase monomer (lane 2). The protein was purified as a dimer of molecular weight 94 000, but examined here in the reduced state. Numbers at the right represent relative positions of molecular weight markers in kilodaltons (K).

other proteins can be ignored.

The analysis of the *E. coli* periplasma sample and purified alkaline phosphatase is shown in lanes 1 and 2, respectively of Fig. 3. This purification of alkaline phosphatase was previously reported by Dunn *et al.* [13] and is not described here except to demonstrate briefly the purification of a single protein from a complex mixture. The resolution of most of the periplasm mixture was ignored in this case in order to achieve the purification of alkaline phosphatase. Only two peaks were displaced from the column: the first containing alkaline phosphatase with two minor components, and the second containing numerous proteins. The minor contaminants were removed by anion-exchange elution chromatography, using a shallow gradient.

The fullest realization of the high capacity inherent in displacement chromatography would be achieved if protein–protein displacement could be made the basis of the separation. However, most of the proteins in biological mixtures are minor constituents surrounded by other minor proteins, and in a displacement train comprised only of proteins, each of these would occupy a volume so small that neighboring and otherwise separable proteins

would be remixed in the column and appear in the effluent with very little separation. Greatly reducing the concentration of the final displacer would reduce the mixing by increasing the volumes of all the bands, but they would remain contiguous. Moreover, one cannot yet assume that all proteins can participate effectively in protein–protein displacement. The model mixtures used for protein–protein displacement studies have been limited to proteins of relatively low molecular weight. From the earliest experiments involving the chromatography of proteins on cellulosic ion-exchangers [20], it has generally been observed that when biological mixtures containing colored adsorbable proteins are applied to adsorbents (e.g. fibrous DEAE-cellulose) that offer more or less uniform access to proteins of essentially all molecular sizes, the adsorbed proteins immediately form a series of colored bands that widen and migrate the accommodate the increasing widths of the bands behind them as additional sample enters the column. However, an attempt to drive such a train of human serum proteins through a column by applying a high-affinity displacer without spacers resulted in very poor resolution [10], in part because the fractions collected were too large to preserve whatever separation survived remixing in the column.

The application of suitable intermediate-affinity displacers subsequent to the application of the sample does not reduce the amount of sample that can be applied to the column, but it does greatly improve the spacing of the numerous minor species. Also, the passage of low concentrations of such displacers through the developing train on their way to appropriate positions ahead can be expected to increase the rate at which the higher-affinity proteins attain their appropriate positions in the later portions of the train. When the adsorbent employed does not provide uniform access for all the proteins to potential adsorption sites (i.e., some degree of molecular sieving occurs), the presence of displacing molecules of intermediate affinity and relatively low molecular weight prevents the retention of low-molecular-weight proteins within the inner recesses of the adsorbent, away from competition with higher-affinity proteins of higher molecular weight.

The use of displacers having intermediate affinities for spacing does, of course, increase the volume of the effluent. However, much more can be achieved in a single pass, and when only one protein species is being isolated, the added spacer can be limited to the region of the train containing that protein, with reliance on protein–protein displacement in the rest of the train and even sharp elution with salt after the desired protein has been collected. Generally, displacement chromatography would be the first chromatographic step in the isolation of the product, so subsequent fractionation to attain final purity provides opportunity for the removal of spacing displacers, whether by ion exchange [12], hydrophobic interaction [22], molecular sieving, affinity chromatography or electrophoresis.

The very fine, uniform beads and compact packing of HPLC columns are very helpful in small-scale displacement separations for maintaining the sharp boundaries that are developed in the trains [21]. For example, E. coli alkaline phosphatase was purified on an HPLC DEAE-5PW column with excellent results. However, the self sharpening effect of a displacement train allows high resolution on a relatively low-resolution adsorbents. Molecular forms of ovalbumin which differ by 0.1 pH units in their isoelectric points have been separated on DE-52 [19]. In this manuscript we have demonstrated the separation of guinea pig serum on a medium-resolution beaded adsorbent (DEAE-Fractogel), and the separation of mouse liver cytosol on a low-resolution microgranular cellulose (DE-52). All three of these separations showed high resolution as demonstrated by the electrophoretic evaluation of fractions. It has been our experience that once the chromatographic conditions are established, the columns are interchangeable. For example, the β-lactoglobulins A and B were separated by the same spacer displacer on low-pressure anion-exchange columns [19] and HPLC anion-exchangers [21]. General conditions for preparative columns can thus be worked out rapidly on HPLC columns. In large-scale separations relatively inexpensive beaded adsorbents such as those now available for chromatography at moderate pressure should be very effective because the much larger volumes of the developed protein bands will make any effects of the increase in the size of the beads less significant. The close packing that is possible with beaded adsorbents remains important in large-scale work since it minimizes the interstitial volume, thus reducing

mixing at the boundaries. On the other hand, separation problems vary so widely in the challenges they impose that it is likely that in some cases non-beaded adsorbents will be effectively employed and in others the full power of HPLC will be required.

ACKNOWLEDGEMENTS

REFERENCES

1 N. E. Pfund, *Genet. Eng. News*, 8 (1988) 30.
2 J. Bonnerjea, S. Oh, M. Hoare and P. Dunnill, *Biotechnology*, 4 (1986) 954.
3 A. R. Torres and E. A. Peterson, in M. S. Verrall and M. J. Hudson (Editors), *Biotechnology*, Ellis Horwood, Chichester, 1987, Ch. 11, pp. 176–184.
4 A. Tiselius, *Ark. Kemi Mineral Geol.*, 16A V.18 (1943).
5 J. Porath, *Acta Chem. Scand.*, 6 (1952) 1237.
6 J. Porath and C. H. Li, *Biochim. Biophys. Acta*, 13 (1954) 268.
7 E. A. Peterson and A. R. Torres, *Methods Enzymol.*, 104 (1984) 113.
8 J. Frenz and Cs. Horváth, in Cs. Horváth (Editor), *High-Performance Liquid Chromatography —Advances and Perspectives*, Vol. 5, Academic Press, Orlando, FL, 1988, p. 211.
9 S. M. Cramer and G. Subramanian, Sep. Purif. Methods, 19 (1990) 31.
10 E. A. Peterson, *Anal. Biochem.*, 90 (1978) 767.
11 A. R. Torres and E. A. Peterson, *J. Biochem. Biophys. Methods*, 1 (1979) 349.
12 A. R. Torres, G. G. Krueger and E. A. Peterson, *Anal. Biochem.*, 144 (1985) 469.
13 B. E. Dunn, S. C. Edberg and A. R. Torres, *Anal. Biochem.*, 168 (1988) 25.
14 A. W. Liao, Z. El Rassi, D. M. LeMaster and Cs. Horváth, *Chromatographia*, 24 (1987) 881.
15 G. Subramanian and S. M. Cramer, *Biotechnol. Prog.*, 5 (1989) 92.
16 B. J. Davis, *Ann. N.Y. Acad. Sci.*, 121 (1964) 404.
17 A. H. Reisner, P. Nemes and C. Bucholtz, *Anal. Biochem.*, 64 (1975) 509.
18 V. K. Laemmli and M. Favre, *J. Mol. Biol.*, 80 (1973) 575.
19 E. A. Peterson and A. R. Torres, *Anal. Biochem.*, 130 (1983) 271.
20 H. A. Sober, F. J. Gutter, M. M. Wyckoff and E. A. Peterson, *J. Am. Chem. Soc.*, 78 (1956) 756.
21 A. R. Torres, B. E. Dunn, S. C. Edberg and E. A. Peterson, *J. Chromatogr.*, 316 (1984) 125.
22 A. R. Torres, S. C. Edberg and E. A. Peterson, *J. Chromatogr.*, 389 (1987) 177.
23 T. A. Scott, Jr. and E. H. Melvin, *Anal. Chem.*, 25 (1953) 1656.

Rapid displacement chromatography of melittin on micropellicular octadecyl-silica

Krishna Kalghatgi, Irén Fellegvári and Csaba Horváth

Department of Chemical Engineering, Yale University, New Haven, CT 06520 (USA)

ABSTRACT

Rapid high-performance liquid chromatographic analysis and displacement purification of melittin and its variants were carried out by reversed-phase chromatography. High speed of separation was achieved by the use of columns packed with a micropellicular stationary phase consisting of a thin C_{18} hydrocarbonaceous layer on the surface of 2-μm fluid-impervious silica microspheres at elevated temperature. In the case of melittin from bee venom or its synthetic variants the plots of the logarithmic retention factor against acetonitrile concentration in the eluent were straight lines whereas the van 't Hoff plots in the temperature range from 20 to 80°C were non-linear. Purification of melittins by displacement was carried out with benzyldimethylhexadecyl ammonium chloride as the displacer. In a 20-min displacement run at 40°C about 5 mg of highly pure melittin were isolated from 10 mg of synthetic mixture by using a 105 × 4.6 mm column. The results demonstrate that columns packed with micropellicular sorbents not only facilitate rapid high-performance liquid chromatographic analysis but are also suitable for fast peptide purification with high recovery.

INTRODUCTION

Melittin, a polypeptide consisting of 26 amino acids is the main component of honey bee venom. It binds strongly to natural and synthetic phospholipid bilayers and has served as a model peptide in numerous biochemical and pharmacological studies [1–4]. Its physico-chemical properties are well established. The amino acid sequence of melittin is as follows

NH$_2$– G–I–G–A–V–L–K–V–L–T–T–G–L–
  1   12
P–A–L–I–S–W–I–K–R–K–R–Q–Q–COOH
14   26

In a separate study, two structural variants of melittin have been synthesized to investigate their structure and interaction with biological membranes in comparison to those of melittin proper [5]. These two peptides are G12A and P14A melittins in which alanine is substituted for glycine in the 12th

position and for proline in the 14th position, respectively.

The need for highly pure melittin and its variants prompted us to investigate the potential of reversed-phase chromatography in the displacement mode for their purification. Whereas reversed-phase chromatography in the elution mode has widely been used for analysis and purification of peptides by high-performance liquid chromatography (HPLC) [6,7], the merits of displacement for preparative-scale purification have only recently been recognized [8–14]. Introduction of micropellicular sorbents that offer higher separation speed and product recovery than conventional porous stationary phases has further advanced the chromatography of biopolymers [15–18]. Therefore, columns packed with micropellicular stationary phases were employed for both the rapid HPLC analysis and displacement purification of melittins. In order to facilitate the analysis of fractions obtained in preparative chromatography, a rapid HPLC method was developed for the rapid assay of melittin by appropriate modifications of the instrument as described below in the Experimental section.

Correspondence to: Professor Csaba Horváth, Department of Chemical Engineering, Yale University, 9 Hillhouse Avenue, New Haven, CT 06520, USA.

EXPERIMENTAL

Materials

Reagent-grade trifluoroacetic acid (TFA), formic acid (88%) and HPLC-grade acetonitrile (ACN) were obtained from Baker (Phillipsburgh, NJ, USA). Benzyldimethylhexadecyl ammonium chloride was from Fluka (Rokonkoma, NY, USA). Bee venom, melittin, apamin, and phospholipase A_2 were purchased from Sigma (St. Louis, MO, USA). The two melittin variants P14A and G12A were gifts from Dr. C. Dempsy. Hy-Tach columns (30 × 4.6 and 105 × 4.6 mm), packed with silica-based C_{18} micropellicular sorbents of 2-μm particle diameter were from Glycotech (Hamden, CT, USA). Eluents were prepared with deionized water from NanoPure unit (Barnstead, Boston, MA, USA), filtered through 0.45-μm membranes and degassed by sparging with helium.

Instruments

The liquid chromatograph consisted of a Series 4 pump, Model LC-85B variable-wavelength detector, Model LCl-100 printer plotter and Model 7500 laboratory computer (Perkin-Elmer, Norwalk, CT, USA). Before entering the column the eluent passed through a 500 × 0.25 mm heat exchanger coil and a Model 7125 sample injector (Rheodyne, Cotati, CA, USA) that were placed in a Model DL-8 constant-temperature bath (Haake-Buchler, Saddlebrook, NJ, USA). A 3.0-ml sample loop was used in displacement experiments. Some of the analytical separations were obtained with Model 1090 liquid chromatograph equipped with column compartment, diode array detector and Model 79994A analytical work station (Hewlett-Packard, Avondale, PA, USA).

Methods

Analytical separations. HPLC analysis of bee venom and synthetic melittins was carried out with short columns (30 × 4.6 mm) packed with micropellicular octadecyl silica. Elevated temperature and relatively high flow-rates were employed for the analysis by gradient elution with increasing ACN concentration in aqueous TFA as described previously for other peptide mixtures [15–17]. The actual gradient profiles were determined by tracer technique as described earlier [16].

Displacement chromatography. Instrumentation and methodology for displacement chromatography were similar to those described elsewhere [8,11,13]. The column (105 × 4.6 mm) was first equilibrated with a solution of 0.1% (v/v) TFA in water that served as a carrier. Thereafter, a solution of the sample mixture (feed) in the carrier was introduced into the column, and the separation was carried out with the displacer; 25 mM benzyldimethylhexadecyl ammonium chloride in 10% (v/v) aqueous ACN containing 0.1% (v/v) TFA. The "light" and "heavy" impurities shown on displacement chromatograms refer to those components of the sample that are retained less or more than the key product, *i.e.*, melittin or its analogue, respectively, as shown by the analytical separation of individual samples (Fig. 1). Fractions of the column effluent were collected at 30- and 15-s intervals for displacement experiments carried out at 23 and 40°C, respectively. A 5-μl aliquot from each fraction was mixed with 95 μl of 0.1% TFA in water and 20 μl from the diluted sample were analyzed by rapid HPLC. Quantitative measurements were made by the peak area and a calibration curve was prepared using melittin from bee venom as the reference. This preparation (Sigma Lot No. 116F-4011) was 73% (w/w) pure, according to the supplier and this value was used for the calibration curve. In the case of impurities present in the crude samples, it was assumed that these compounds have the same extinction coefficient as melittin.

Column regeneration. After emergence of the displacer front, the column was washed first with 3 ml of 50% (v/v) formic acid in 2-propanol then with 3 ml of 95% (v/v) aqueous ACN containing 0.1% (v/v) TFA. Subsequently, the column was reequilibrated with 6 ml of the carrier. Regeneration of the column was carried out at 80°C and at a flow-rate of 3 ml/min. In most cases the entire process was completed in less than 5 min.

RESULTS AND DISCUSSION

Analysis of bee venom and synthetic melittins

Bee venom is a complex biological material and contains besides melittin, which comprises nearly 50% of the total dry weight, proteins such as phospholipase A_2, hyaluronidase as well as other peptides such as apamin, minimine and mast cell de-
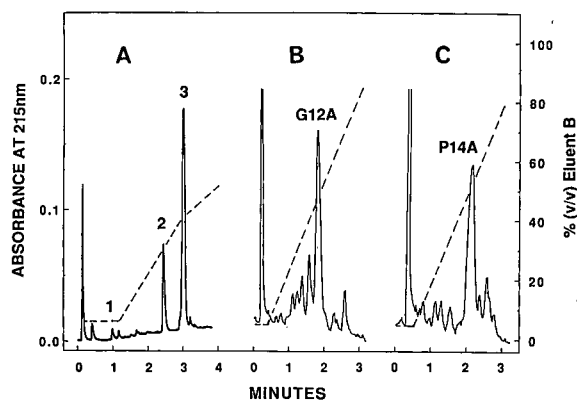
Fig. 1. Analytical chromatograms of samples containing (A) bee venom, (B) G12A melittin and (C) P14A melittin from synthetic mixtures. Column, Hy-Tach micropellicular C_{18} silica, 30 × 4.6 mm; eluent A, 0.1% (v/v) TFA in water; eluent B, 0.1% (v/v) TFA and 95% (v/v) ACN in water; flow-rate, 1 ml/min; temperature, 23°C. Elution: (A) linear increase of eluent B from 10 to 60% in 3 min and from 60 to 80% in 2 min; (B and C) linear gradient of eluent B from 5 to 80% in 3 min. Bee venom components identified were apamin (1), phospholipase A_2 (2) and melittin (3). Dotted lines represent the actual gradient profile of eluent B during the separation.

granulating (MCD) peptide. Fig. 1A shows an analytical chromatogram of bee venom obtained by rapid HPLC with a short column containing C_{18} micropellicular stationary phase. As seen the separation of bee venom constituents is brought about in 3 min. Similarly, samples of synthetic G12A and P14A melittins were also analyzed rapidly using the same column but different gradient as illustrated by the chromatograms in Fig. 1B and C. The relative hydrophobicity increased in the order, melittin < G12A < P14A. The weight percentage of melittin in bee venom and those of G12A and P14A melittins in the synthetic mixtures were found to be 54, 28 and 30%, respectively, as measured by the peak area in the analytical chromatograms.

Effect of mobile phase composition and temperature on the retention behavior of melittins

Crystallographic studied [1] suggest that the melittin molecule contains two α-helices comprising the amino acid residues 1–10 and 13–26, which are
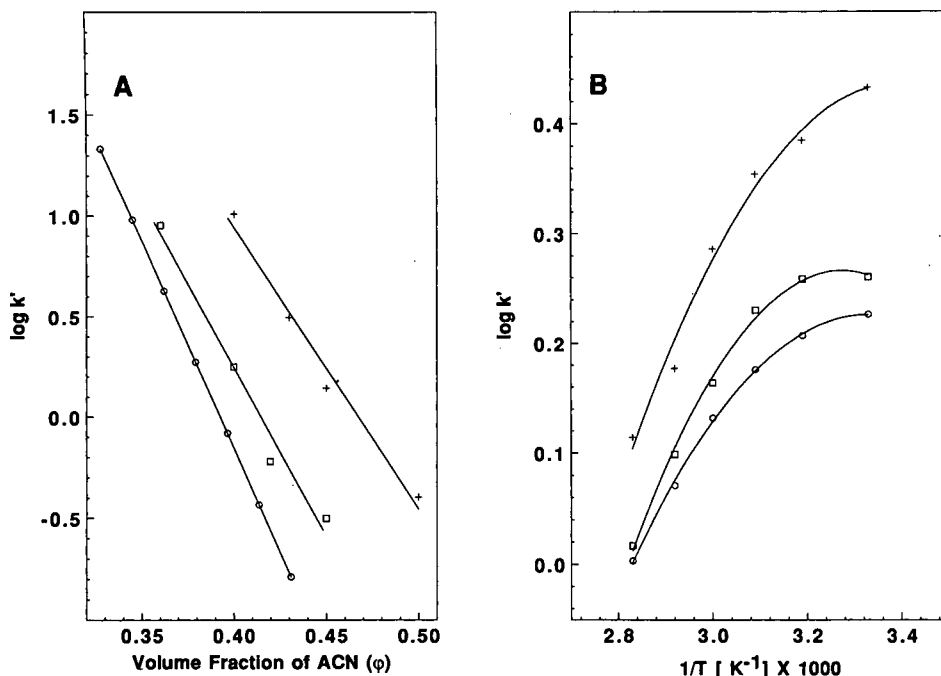
Fig. 2. (A). Effect of ACN concentration on the retention of melittins. Hy-Tach micropellicular C_{18} silica column, 105 × 4.6 mm; isocratic elution with aqueous eluents containing 0.1% (v/v) TFA and various concentrations of ACN; flow-rate 0.2 ml/min; temperature, 23°C. Samples were 2 μg each of melittin (○), G12A (□) and P14A (+) melittins. (B). Van 't Hoff plots for the retention of melittins. Hy-Tach micropellicular C_{18} silica column, 105 × 4.6 mm, isocratic elution with aqueous eluent containing 0.1% (v/v) TFA with 36% (v/v) ACN for both melittin (○) and G12A melittin (□) and with 38% (v/v) ACN for P14A melittin (+). k' = Retention factor; T = temperature.

linked together by residues 11 and 12, to give the molecular shape of a bent rod. One side of each helix contains 10 hydrophobic residues and a group of 6 polar amino acids is clustered at the opposite end. High-resolution NMR studies [2] have shown that at acidic pH and low ionic strength, melittin exists predominantly as an extended monomer and the residues 5–9 and 14–19 in the helices are maintained in highly structured order. This conformer is in equilibrium with a low abundant form of melittin due to cis–trans isomerism of the L-13–P-14 peptide bond.

Plots of logarithmic retention factor for melittin and its two synthetic analogues against ACN concentration in the eluent are depicted in Fig. 2A. Melittin elutes at about 40% of eluent B (organic modifier) and the substitution of Ala by Gly or Pro at positions 12 and 14, respectively, results in increasingly stronger binding of the peptide to the hydrophobic chromatographic surface. The latter peptides eluted nearly at 43% and 50% of eluent B, respectively. The data suggest that melittin proper and P14A melittin have the smallest and the largest hydrophobic contact area upon binding to the stationary phase, respectively. It is noted that the plots of $\log k'$ versus φ are non-parallel straight lines suggesting reversal of selectivity for the three peptides in a range of organic concentration lower than that shown for the data in Fig. 2A.

The retention behavior of melittin and the two synthetic analogues was further investigated by measuring the effect of temperature and the resulting van 't Hoff plots are shown in Fig. 2B. The composition of the eluent used to measure the retention of melittin and G12A melittin was 36% (v/v) aqueous ACN containing 0.1% TFA. As P14A melittin was found to be the most hydrophobic among the three melittin variants and it was eluted with 38% (v/v) aqueous ACN containing 0.1% TFA. In the absence of conformational changes of the eluite or structural changes in the stationary phase, the van 't Hoff plots are usually straight lines in reversed-phase chromatography [19]. As seen in Fig. 2B, the van 't Hoff plots for melittin and the two synthetic variants are curved suggesting changes in eluite conformation and concomitantly in the binding mechanism upon varying the temperature. Further investigations are needed to elucidate physico-chemical aspects of changing temperature on

the chromatographic retention behavior of such relatively complex molecules as melittins.

Displacement chromatography of melittins

So far, displacement chromatography in the laboratory has been carried out exclusively by HPLC columns packed with conventional porous sorbents that have relatively large accessible surface area required in the chromatography of small molecules. Recent studies with micropellicular sorbents from this and other laboratories have revealed that with stationary phase particles which consist of fluid-impervious microspherical support coated with a thin retentive layer, analytical speed and column efficiency can be enhanced, particularly for separation of large molecules. Although the chromatographic surface area in columns packed with micropellicular stationary phases is relatively low, the enhanced efficiency, column stability and increased sample recovery makes them useful also for micropreparative isolation of proteinaceous compounds [15–18, 20–22]. The analysis of fractions collected during the displacement experiment was carried out with micropellicular C_{18} columns (30 × 4.6 mm) operated at 80°C. Under these conditions melittin containing samples were analyzed in less than a minute and a typical chromatogram is shown in Fig. 3.

Displacement chromatography on 105 × 4.6 mm columns yielded several milligrams of pure melittin from bee venom or melittin variants from synthetic mixtures. The feed was dissolved in 0.1% (v/v)
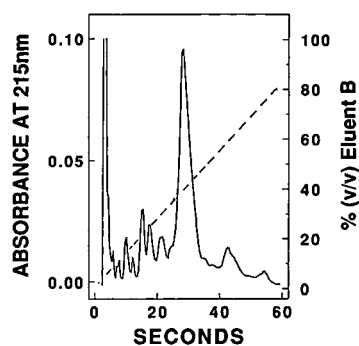
Fig. 3. Rapid HPLC analysis of melittin. Hy-Tach micropellicular C_{18} silica column, 30 × 4.6 mm; eluents as in Fig. 1; linear gradient from 0 to 80% B in 1.0 min, flow-rate, 3.0 ml/min, temperature 80°C. Sample: 5 μg melittin from Sigma. Dotted lines represent the actual gradient profile of eluent B.
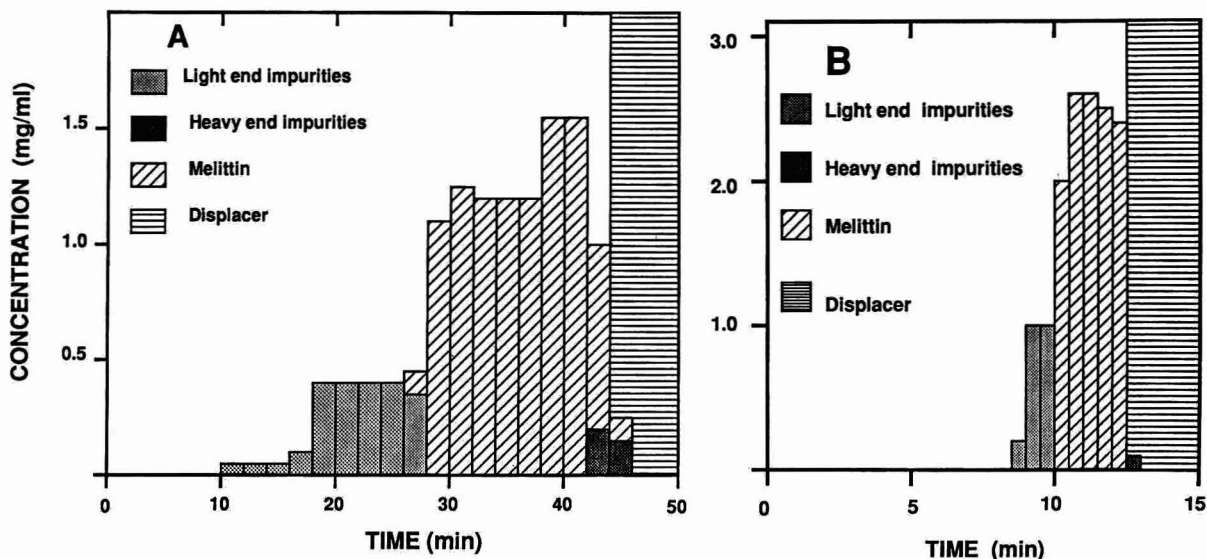
Fig. 4. Displacement chromatogram of crude synthetic P14A melittin at 23°C (A) and 40°C (B). Column, Hy-Tach micropellicular C_{18} silica, 105 × 4.6 mm, carrier, 0.1% (v/v) TFA in water; displacer, 25 mM benzyldimethylhexadecyl ammonium chloride in 10% (v/v) aqueous ACN containing 0.1% TFA; flow-rate, 0.2 ml/min (A) and 0.6 ml/min (B); feed: 10 mg of P14A melittin in 1.5 ml. Fractions were collected at 30 and 15 s at 23°C and 40°C, respectively. Aliquots of 5 μl of each fraction were mixed with 95 μl of 0.1% TFA and 20-μl aliquots of the diluted samples were analyzed by the procedure described in Fig. 3. The concentration of melittin was calculated on the basis of peak area and from the calibration curve (not shown) obtained at 215 nm using Sigma melittin as the reference.

aqueous TFA which was used also as the carrier to facilitate strong binding of the sample components to the chromatographic surface during loading on the the the column. The displacer was 25 mM benzyldimethylhexadecyl ammonium chloride in aqueous solution containing 10% (v/v) ACN and 0.1% (v/v) TFA. This compound has been used successfully as the displacer for the separation of various peptides in our laboratory [10]. A displacement chromatogram of 10 mg of synthetic P14A melittin obtained at 23°C and at a flow-rate of 0.2 ml/min is shown in Fig. 4A. Under these conditions the breakthrough of the displacer front occurred in 45 min and the bands of product and the impurities show some overlap.

In order to speed up the separation the column temperature was increased to 40°C so that the viscosity of the mobile phase was reduced and the favorable effect of elevated temperature on both the diffusivity and sorption kinetics could be exploited for anhancement of separation efficiency. The displacement of the crude P14A melittin at 40°C and at flow-rate of 0.6 ml/min is illustrated by the chromatogram in Fig. 4B. Comparison of chromato-

grams obtained at 23°C (Fig. 4A) and 40°C (Fig 4B) shows that the efficiency of separation improved considerably and the time of separation decreased significantly with respect to the results obtained at 23°C and at 0.2 ml/min. The complete cycle including separation by displacement chromatography and column regeneration was completed in about
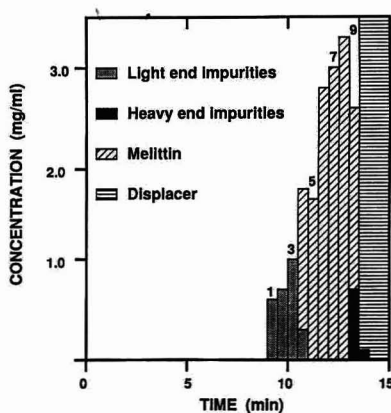
Fig. 5. Displacement chromatogram of bee venom. Conditions as in Fig. 4B except the feed was 10 mg of bee venom.
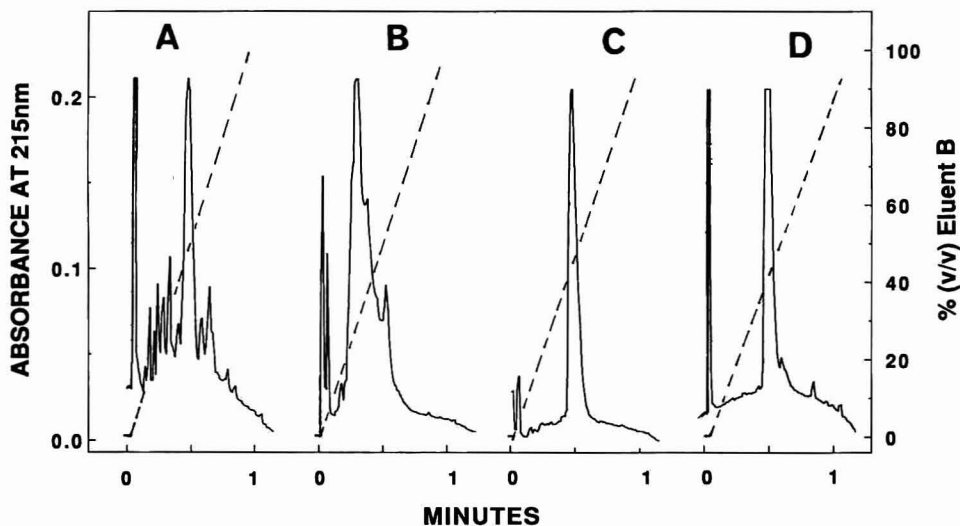
Fig. 6. Monitoring of the column effluent during displacement chromatography of bee venom. Chromatograms are shown for the analysis of fractions corresponding to (A) the feed, (B) impurities (fraction 3), (C) melittin (fraction 7) and (D) heavy-end impurities (fraction 9) as shown by the displacement diagram in Fig. 5. Dottes lines represent the actual gradient profile of eluent B.

20 min. Similar results were obtained for isolation of melittin from bee venom as shown in Fig. 5. The versatility of the rapid HPLC method is illustrated by good-resolution and high-speed analysis of the column effluent during the displacement chromatography of bee venom. The results of analysis of the feed and fractions containing the light-end impurities, melittin and heavy-end impurities are depicted in Fig. 6. The fractions of melittin collected between 11.5 and 13 min and free from other peptide components as determined by rapid HPLC were pooled. Total yield of purified melittin was 5.23 mg and the purity of the pooled sample was 99.1% as determined from the area under the peak by reversed-phase chromatography and from a calibration curve prepared from Sigma melittin as reference. It is noted that the elution pattern of the primary component in the displacement chromatogram varied resulting in steps in the bar diagram as depicted in Figs. 4 and 5. This could be due to incomplete development of the displacement train that can be improved by using longer columns. Under these conditions the bar heights are expected in to increase in sample concentration.

CONCLUSIONS

Displacement chromatography with micropellic-

ular sorbents offers significant advantages for rapid purification of proteins and peptides on a micro-preparative scale. The advantages of this approach are particularly pronounced when the column is operated at elevated temperature and at relatively high flow-rates as illustrated by the purification of melittin and its variants in less tan 15 min. Regeneration of the column, a generally time consuming step with traditional porous packings, required less than 5 min. Columns packed with micropellicular stationary phases are eminently suitable also for rapid analysis of fractions of the column effluent in preparative chromatography and offer the potential for process monitoring by HPLC.

REFERENCES

1 T. C. Terwilliger and D. Eisenberg, J. Biol. Chem., 257 (1982) 6016.
2 J. Lauterwein, L. R. Brown and K. Wütrich, Biochim. Biophys. Acta, 622 (1980) 219.

3 A. W. Bernheimer and B. Rudy, *Biochim. Biophys. Acta*, 864 (1986) 123.

4 W. F. DeGrado, F. J. Kézdi and E. T. Keiser, *J. Am. Chem. Soc.*, 103 (1981) 679.

5 C. Dempsy and D. Engelman, Department of Molecular Biology and Biophysics, Yale University, New Haven, CT, personal communication.

6 W. R. Melander and Cs. Horváth, in Cs. Horváth (Editor), *High-Performance Liquid Chromatography —Advances and Perspectives*, Vol. 2, Academic Press, New York, 1980, pp. 114–319.

7 J. Frenz, W. S. Hancock, W. J. Henzel and Cs. Horváth, in K. M. Gooding and F. E. Regnier (Editors), *HPLC of Biological Macromolecules —Methods and Applications*, Marcel Dekker, New York, 1990, pp. 145–177.

8 J. Frenz and Cs. Horváth, in Cs. Horváth (Editor), *High-Performance Liquid Chromatography —Advances and Perspectives*, Vol. 5, Academic Press, New York, pp. 211–314.

9 H. Kalász and Cs. Horváth, *J. Chromatogr.*, 215 (1981) 295.

10 G. Viscomi, S. Lande and Cs. Horváth, *J. Chromatogr.*, 440 (1988) 157.

11 S. Cramer and Cs. Horváth, *Prep. Chromatogr.*, 1 (1988) 29.

12 Gy. Vigh, Z. Varga-Purchony, G. Szepesi and M. Gazdag, *J. Chromatogr.*, 386 (1987) 353.

13 A. Liao, Z. El Rassi, D. M. LeMaster and Cs. Horváth, *Chromatographia*, 24 (1987) 881.

14 A. Liao and Cs. Horváth, *Ann. N.Y. Acad. Sci.*, 589 (1990) 182.

15 K. Kalghatgi and Cs. Horváth, *J. Chromatogr.*, 398 (1987) 335.

16 K. Kalghatgi and Cs. Horváth, *J. Chromatogr.*, 443 (1988) 343.

17 Y. F. Maa and Cs. Horváth, *J. Chromatogr.*, 445 (1988) 71.

18 Y. F. Maa, S-C. Lin, Cs. Horváth, U-C. Yang and D. M. Crothers, *J. Chromatogr.*, 508 (1990) 61.

19 W. Melander, D. E. Campbell and Cs. Horváth, *J. Chromatogr.*, 158 (1978) 215.

20 K. Kalghatgi, *J. Chromatogr.*, 499 (1990) 267.

21 A. L. Lee, A. W. Liao and Cs. Horváth, *J. Chromatogr.*, 443 (1988) 31.

22 K. Kalghatgi and Cs. Horváth, in Cs. Horváth and J.G. Nickely (Editors), *Analytical Biotechnology —Capillary Electrophoresis and Chromatogrpahy (ACS Symposium Series, No. 434)*, American Chemical Society, Washington, DC, 1990, pp. 162–180.

CHROM. 24 094

Adsorption chromatography on cellulose

VII. Chiral separations on cellulose with aqueous solvents

M. Lederer

Institut de Chimie Minérale et Analytique, Université de Lausanne, Boîte Postale 115, Centre Universitaire, CH-1015 Lausanne 15 (Switzerland)

ABSTRACT

The chiral properties of different celluloses were examined in adsorption chromatography from aqeous solvents. Much better separations were obtained on microcrystalline cellulose than on "native" cellulose for D- and L-tryptophan and D- and L-methyltryptophan. The separation of D- and L-5-fluorotryptophan was achieved using long (40 cm) thin layers of microcrystalline cellulose.

INTRODUCTION

In Part VI [1], some variables of the separation of D- and L-5-methyltryptophan on cellulose with aqueous solvents were described. It was observed that the usually good separation obtained on Merck DC Plastikfolien (Art. 5577) could not be obtained on MN Polygram CEL 300 layers.

Wollenweber [2] subsequently confirmed these observations, commenting that the Merck layers contain microcrystalline cellulose (Avicel) whereas the MN Polygram CEL 300 layers are made from native cellulose. If the MN Polygram CEL 400 layers of microcrystalline celulose had been used, a separation equal to that on the Merck layers would have been obtained. We could confirm this as shown in Fig. 1. No explanation can be offered for this difference in behaviour [2].

From the vast literature on partition chromatography on cellulose we had the general impression that different kinds of cellulose behave essentially alike. They could differ in ion-exchange capacity and in the amounts of amorphous regions in the crystalline structure, but were still essentially the same anhydroglucose units joined together in the 1–4 configuration in chains of about 3000 units.

Since we started to investigate this problem, we have found two other examples of large differences in chromatographic behaviour between various celluloses.

Müller [3] separated mixed chloro- and bromoosmiates(IV) and mixed chloro- and bromorhenates (IV) on MN Polygram CEL 300-50 layers 40 cm long with 30% aqueous sulphuric acid. Although the R_F differences between members of the series are only 0.02–0.03, "baseline" separations were obtained (and could be repeated by us). On microcrystalline MN Polygram CEL 400 layers, however, no separation took place. It was also found that not all lots of the CEL 300-50 layers gave good separations [4]. here is another interesting aspect to these separations. It is generally assumed that in thin-layer chromatography (TLC) a maximum plate number is achieved with 10–12 cm development (and thus most ready-made layers are sold in dimensions based on this). However, Müller [3] obtained his separations with 40 cm development (or more). This is consistent with our inability to obtain good

---

Correspondence to: Professor M. Lederer, Institut de Chimie Minérale et Analytique, Université de Lausanne, Boîte Postale 115, Centre Universitaire, CH-1015 Lausanne 15, Switzerland.
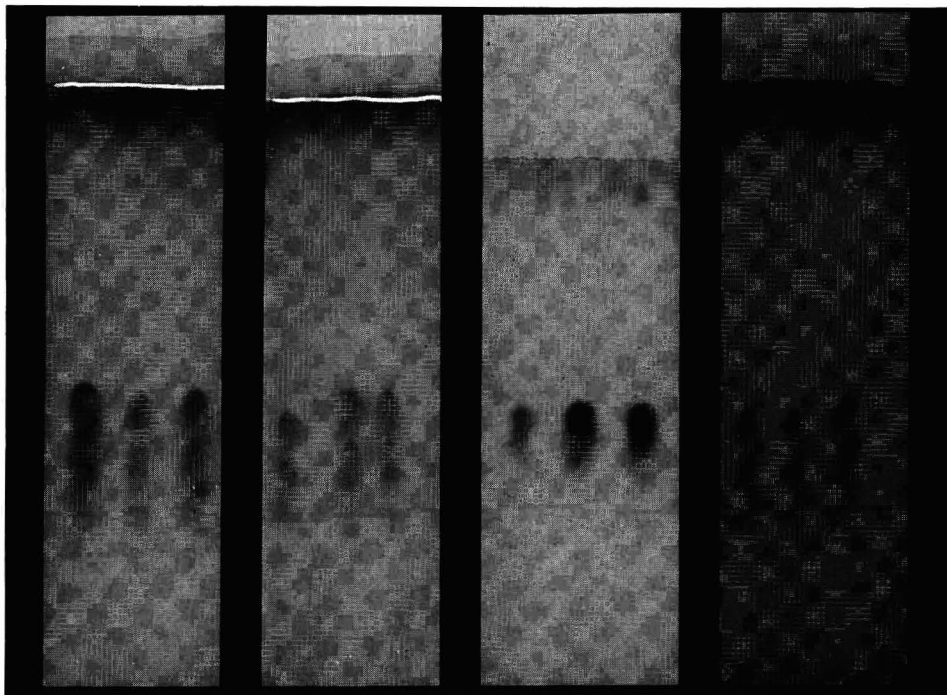
Fig. 1. Chromatograms of DL-5-methyltryptophan developed with 1 M NaCl on (from left to right) Merck Art. 5577 Plastikfolien, the same, MN CEL 300 and MN CEL 400 cellulose thin layers.

separations on shorter layers (20 × 20 cm). A re-examination of these generally accepted principles might therefore be justified.

Another example is shown in Fig. 2. In Fig. 2a the chromatograms of some ball-point pen inks are compared for Whatman No. 3MM (i.e., native cellulose), CEL 300 and CEL 400 thin layers. Whatman 3MM and CEL 400 (i.e., microcrystalline cellulose) are similar, whereas CEL 300 ("native" cellulose) shows much stronger adsorption. In Fig. 2b another set of ball-point pen inks (chosen at random) are compared for CEL 300, CEL 400 and Merck 5577 thin layers. Again, CEL 300 shows much stronger adsorption. Ion exchange should play only a minor role in these systems as a high salt concentration was used throughout [5].

In this paper some results from a comparison of thin layers of native cellulose, microcrystalline cellulose and cellulose papers in the separation of optical isomers are presented.

EXPERIMENTAL

All chromatograms were obtained by ascending development in glass containers with a tightly closed glass lid. For Whatman 3MM papers and for the 40-cm thin layers this usually took 7–8 h. The chromatograms were then dried in an oven at 70–80°C. Colour with ninhydrin developed very slowly on the thin layers. The following media were used: Whatman No. 3MM papers extra thick for chromatography; Merck Art. 5577 DC Plastikfolien Cellulose, layer thickness 0.1 mm, 20 cm × 20 cm; Merck Art. 5787 HPTLC-Fertigplatten Cellulose, 10 cm × 10 cm; Macherey–Nagel MN-Polygram CEL 300 precoated plastic sheets for TLC, 40 cm × 80 cm; Macherey–Nagel MN Polygram CEL 300-50 layers, 0.5 mm Cellulose MN 300 on glass, 40 cm × 20 cm; and Macherey–Nagel MN Polygram CEL 400 for TLC, Art. 801114, 0.1 mm microcrystalline cellulose precoated plastic sheets, 40 cm × 20 cm.
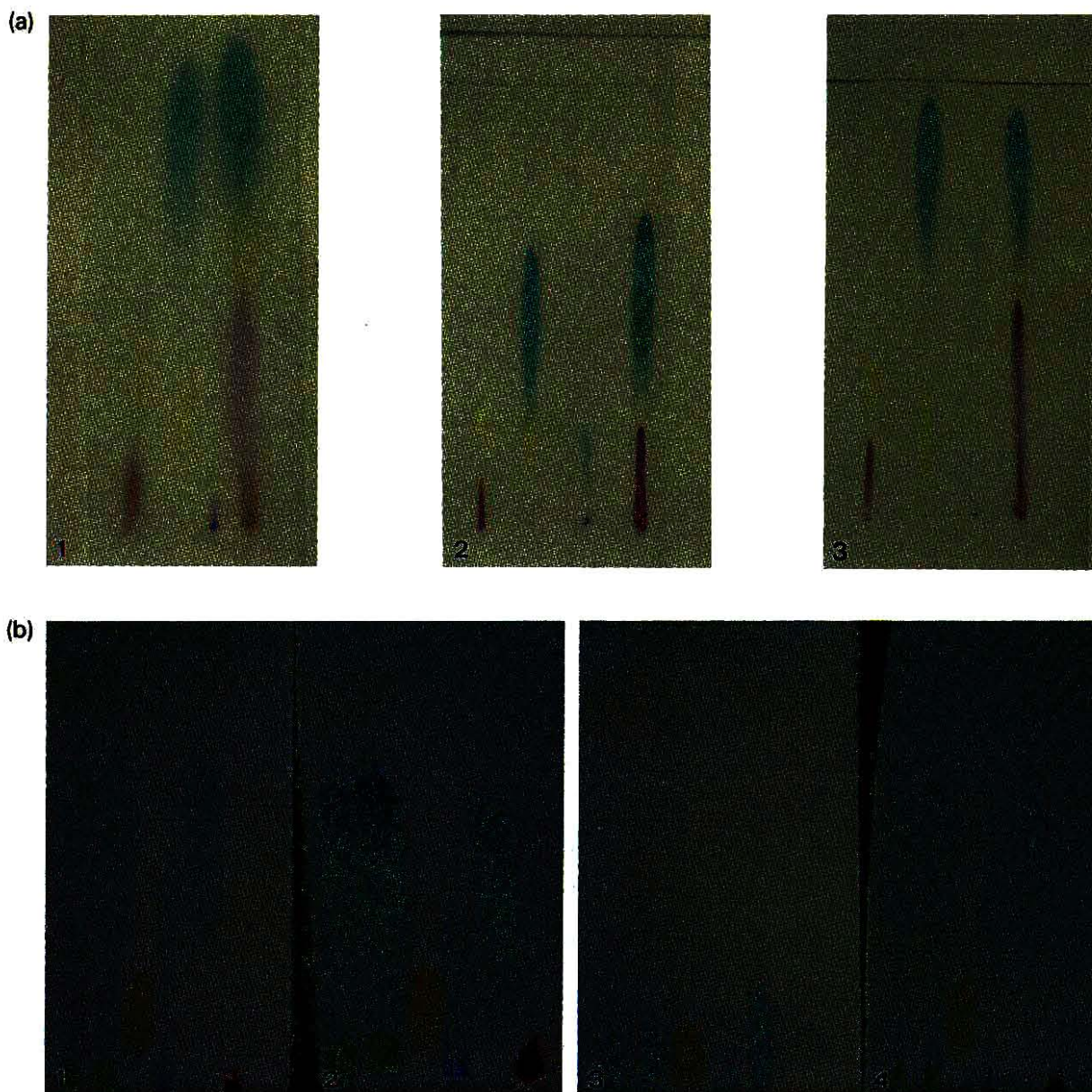
Fig. 2. Chromatograms of ball-point pen inks developed with (a) (1) Whatman 3MM paper, (2) MN CEL 300 cellulose thin layer and (3) MN CEL 400 cellulose thin layer, all developed with 1 *M* NaCl; (b) (1) MN CEL 400 thin layer cellulose, (2) Merck Art. 5577 thin layer cellulose, (3) MN CEL 300 thin layer and (4) MN CEL 400 thin layer cellulose.

RESULTS

Separations of the antipodes of 5-methyltryptophan

Figs. 3 and 4 show the chromatograms obtained on short and long thin layers and on Whatman 3MM paper.

The chromatogram on the long CEL 300 layer shows that there is a separation that cannot be discerned on the short layers. The R_F values on all three media were calculated and the results are given in Table I. Thus, on the CEL layer, made of "native" cellulose, there is merely a smaller separa-
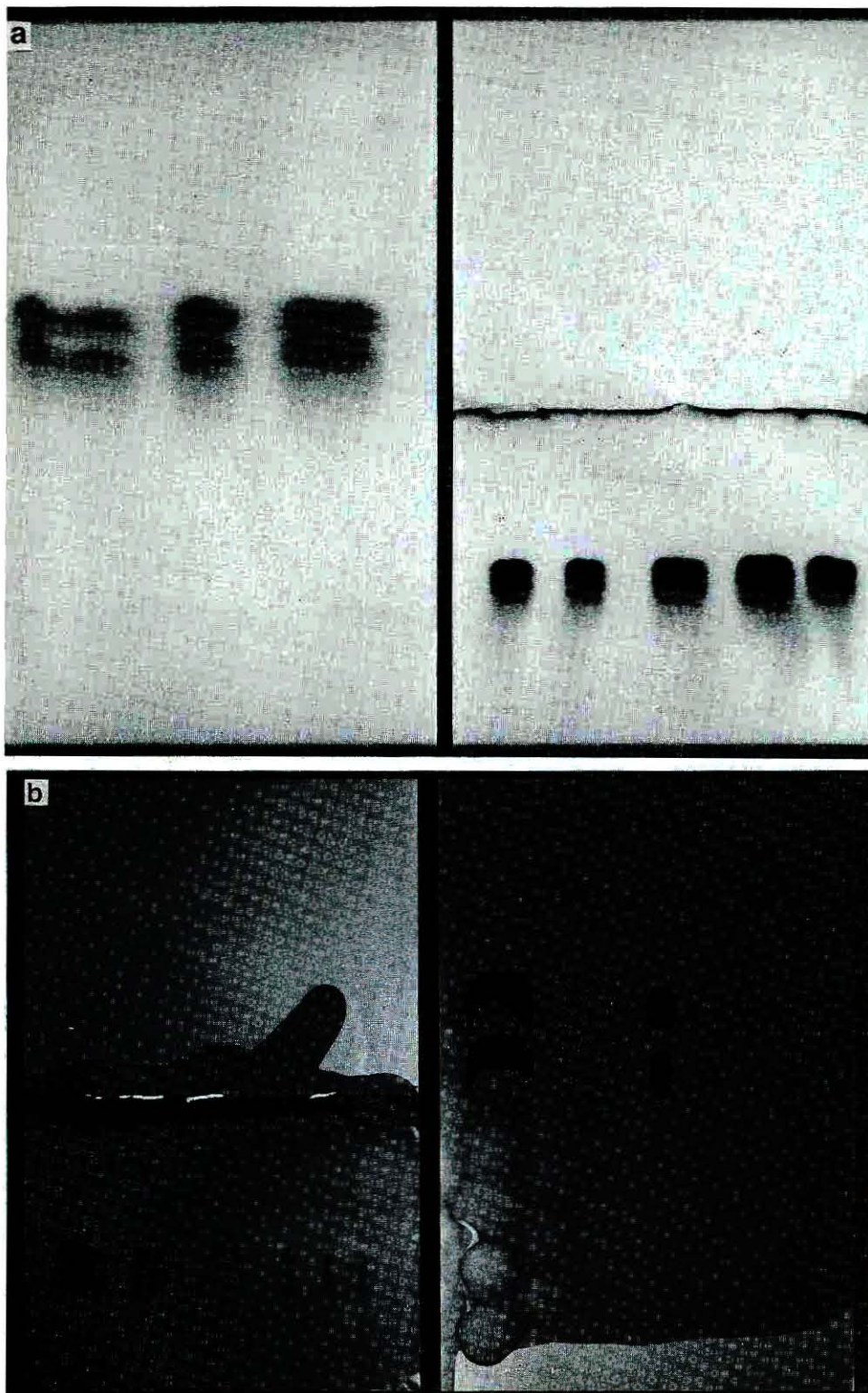
Fig. 3. Chromatogram of 5-methyltryptophan developed with 1 M NaCl on (a) 40-cm long MN Polygram CEL 300-50 layer, (left) long development and (right) short development; (b) 40-cm MN Polygram CEL 400 sheets, (left) short development and (right) long development. This chromatogram later developed a spotted background owing to the oven shelf on which it was dried. The actual spots were emphasized with ink.

tion factor, which means that visual detection of the two adjacent zones is difficult on short layers. On the chromatogram in Fig. 4 D- and L-tryptophan are also shown. As was previously recorded by Weichert [6], there is an R_F difference of about 0.03, which, however, is insufficient for a complete separation. It is also interesting that the plate numbers for the three media are not radically different when the same length of development is compared.

Separations of other methyltryptophans

In a previous paper [5], good separations of 1-, 5-, 6- and 7-methyltryptophan on short (20 cm × 20 cm) Merck cellulose layers were reported. We therefore wanted to examine how these would behave on long layers. Fig. 5a is a drawing of a chromatogram obtained on CEL 400 showing baseline separation of all the four methyltryptophans; D- and L-phenylalanine move too fast in this system and do not separate (Fig. 5b). On CEL 300 layers (Fig. 6) only adjacent zones are obtained with long development. On Whatman No. 3MM paper 1-methyltryptophan produces a single spot, whereas the 6- and 7-methyltryptophan each produce two discernible adjacent spots (Fig. 7). α-Methyltryptophan is not separated even with long development or on short Merck plates [7].

Kynurenine

Kynurenine has previously been separated into its antipodes by Dalgleish [8] and Weichert [6] by paper chromatography. The antipodes separated well on all the thin layers used (see Figs. 5 and 6) except for the Whatman 3MM paper. We used this separation to calculate some plate numbers (Table II).
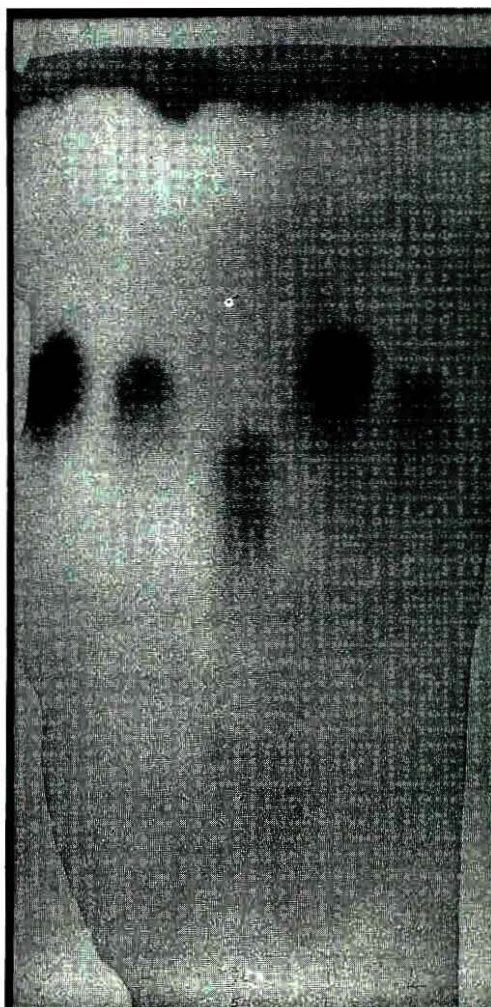
Fig. 4. Chromatogram of (from left to right) D-tryptophan, L-tryptophan, DL-5-methyltryptophan, D-tryptophan and L-tryptophan on Whatman 3MM paper, 40-cm long, with 1 M NaCl.

TABLE I

DATA FOR THE SEPARATION OF D- AND L-5-METHYLTRYPTOPHAN

Medium	R_F		Separation factor, α	Plate number of the faster spot, n
	D-	L-		
MN CEL 300-50 (40 cm long)	0.50	0.45	1.22	2000
Whatman 3MM paper	0.54	0.47	1.32	1600
CEL 400 (40 cm long)	0.48	0.385	1.46	1800
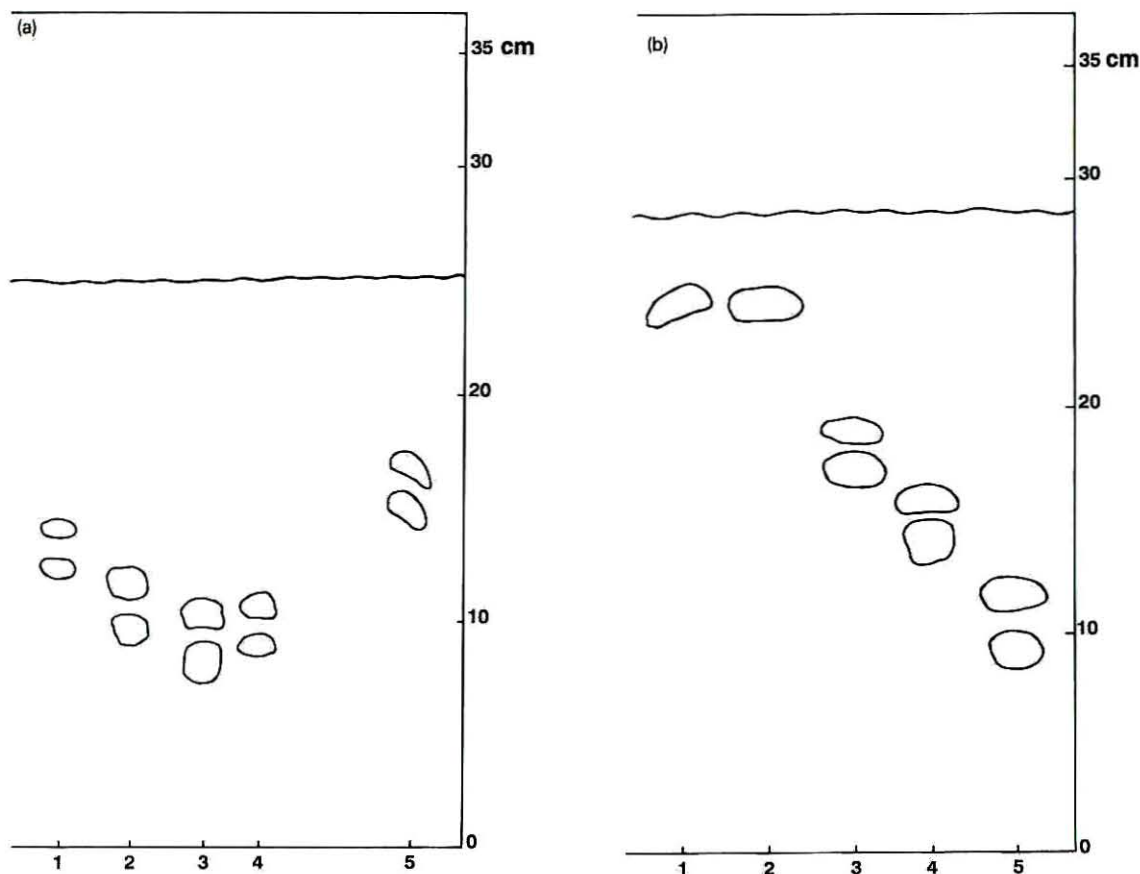
Fig. 5. Chromatograms on 40-cm long MN CEL 400 developed with 1 *M* NaCl: (a) 1 = 1-methyltryptophan; 2 = 5-methyltryptophan; 3 = 6-methyltryptophan; 4 = 7-methyltryptophan; 5 = kynurenine; (b) 1 = D-phenylalanine; 2 = L-phenylalanine; 3 = kynurenine; 4 = 1-methyltryptophan; 5 = 6-methyltryptophan.

5-Fluorotryptophan

To our knowledge, this compound has not been examined before on cellulose. As shown in Table III, it yields well separated spots of the antipodes only on the long CEL 400 layers and on Merck HPTLC cellulose layers with R_F differences of 0.06 and 0.04, respectively.

DISCUSSION

The results presented here indicate that the highest chiral discrimination for all the compounds is obtained on microcrystalline cellulose, followed by Whatman No. 3MM paper, and least on "native" cellulose layers. What is the cause of the different behaviours of the various celluloses? We have

shown that the differences are only a matter of degree.

From our results the reasons for the differences are not clear; however, if we assume that microcrystalline cellulose has a greater surface area than "native" cellulose, this could account for some of the results, but not all (*e.g.*, the results of Müller [3]). Obviously, however, there is a close resemblance with the observations made from experiments with cellulose triacetate, in which case the ordered structure, associated with microcrystalline regions of the sorbent, has been found to play a major role in the chiral discrimination process [9].

Against the general opinion in TLC we obtained a better result with long development although the plate numbers calculated by the usual procedure
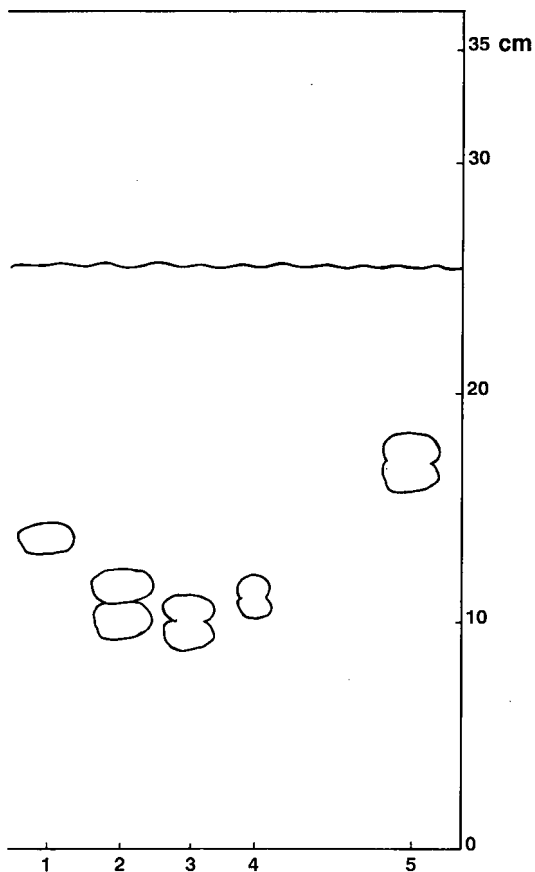
Fig. 6. Chromatogram on 40-cm long MN CEL 300 developed with 1 M NaCl. 1 = 1-methyltryptophan; 2 = 5-methyltryptophan; 3 = 6-methyltryptophan; 4 = 7-methyltryptophan; 5 = kynurenine.
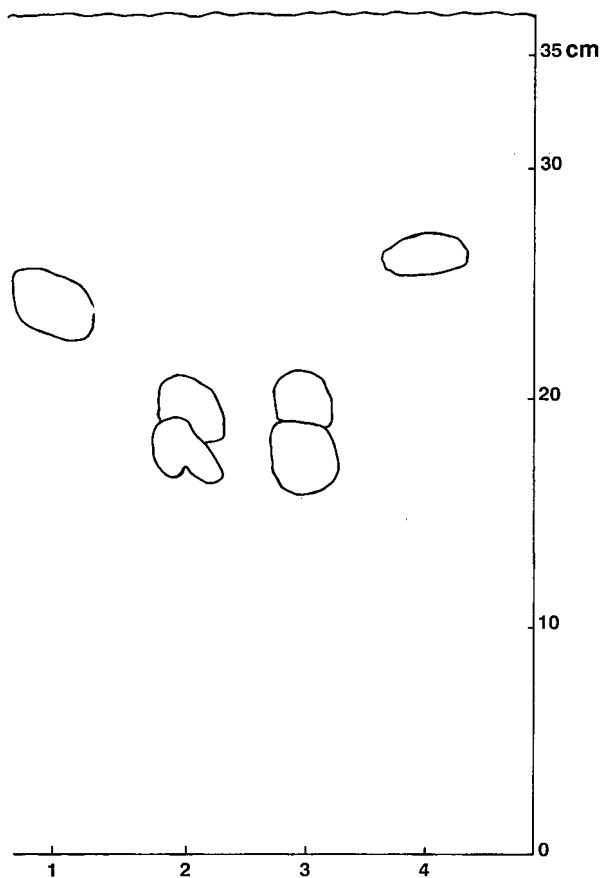
Fig. 7. Chromatogram on 40-cm long Whatman No. 3MM paper developed with 1 M NaCl. 1 = 1-Methyltryptophan; 2 = 6-methyltryptophan; 3 = 7-methyltryptophan; 4 = α-methyltryptophan.

TABLE II

DATA FOR THE SEPARATION OF D- AND L-KYNURENINE

Medium	Isomer	Spot front (mm)	Spot rear (mm)	Liquid front (mm)	n
Merck Art. 5577 DC	L-	64	61	103	7000
Plastikfolien Cellulose	D-	58.5	53	103	1600
Merck Art. 5787	L-	60	57	86	6100
HPTLC-Fertigplatten Cellulose	D-	55	51	86	2610
MN CEL 400	L-	263	247	373	4000
(40 cm long)	D-	243	225	373	2700
MN CEL 300-50 plates	L-	181	169	254	4050
(40 cm long)	D-	169	157	254	2550

TABLE III

DATA FOR THE SEPARATION OF D- AND L-FLUORO-TRYPTOPHAN

Medium	R_F	
	D	L
MN CEL 400 (40 cm long)	0.57	0.51
Merck Art. 5787 HPTLC-Fertigplatten Cellulose	0.51	0.47
Merck Art. 5577 DC Plastikfolien Cellulose	0.54 (single spot)	
MN CEL 300 (40 cm long)	0.54 (single spot)	
Whatman 3MM paper	0.56 (single spot)	

were then lower than with short development.

In all the chromatograms the slower spot is longer and hence has a lower plate number. This could be explained by the Dalgleish "three-point" model: When three interactions are really involved, the ad-sorption process kinetics are slower than when mainly "two points" are involved.

We calculated the ΔR_M values for the usual functional groups on cellulose [10]. The maximum ΔR_M between two optical isomers observed here was 0.165 (for 5-methyltryptophan on MN CEL 400 layers), which is less than the ΔR_M of the usual functional groups (about half of the ΔR_M of the NH_2 group).

REFERENCES

1 M. Lederer, *J. Chromatogr.*, 510 (1990) 367.
2 P. Wollenweber, Macherey–Nagel, personal communication.
3 H. Müller, *Fresenius' Z. Anal. Chem.*, 247 (1969) 145.
4 H. Müller, personal communication.
5 M. Lederer and M. Schudel, *J. Chromatogr.*, 475 (1989) 451.
6 R. Weichert, *Acta. Chem. Scand.*, 8 (1954) 1542.
7 A. O. Kuhn, M. Lederer and M. Sinibaldi, *J. Chromatogr.*, 469 (1989) 253.
8 C. E. Dalgleish, *Biochem J.*, 64 (1956) 483.
9 T. Shibata, I. Okamotor and K. Ishii, *J. Liq. Chromatogr.*, 9 (1986) 313.
10 A. O. Kuhn and M. Lederer, in T. W. Hutchens (Editor), *Protein Recognition of Immobilized Ligands*, Alan R. Liss, New York, 1988 pp. 179–192.

Adsorption behavior of milk proteins on polystyrene latex

A study based on sedimentation field-flow fractionation and dynamic light scattering

Karin D. Caldwell, Jianmin Li and Jenq-Thun Li

Center for Biopolymers at Interfaces, University of Utah, Salt Lake City, UT 84112 (USA)

Douglas G. Dalgleish

Department of Food Science, University of Guelph, Guelph, Ontario N1G 2W1 (Canada)

ABSTRACT

Sedimentation field-flow fractionation (SdFFF) has been used to characterize the adsorption of the proteins β-casein (BCN) or β-lactoglobulin (BLG) on colloidal polystyrene latices; this system was used to model hydrophobic interactions between the proteins and the surfaces of fat droplets in protein-stabilized emulsions. It was found that the SdFFF technique could determine directly the surface concentrations of BCN and BLG irreversibly adsorbed to the latex surface, provided care was taken to maintain the ionic strength of the carrier at a level which suppressed particle–wall repulsion in the separation channel. The measured surface concentrations were similar for the two proteins (about 1 mg/m^2), and this was verified by quantitative amino acid analysis. These concentrations were smaller than those found in depletion studies (3 and 4 mg/m^2 respectively for BCN and BLG), in which loosely associated protein may have been included in the determinations. The thickness of the adsorbed layers was determined *in situ* by dynamic light scattering and was found to differ significantly for the two proteins (up to 15 nm for BCN *vs.* 2–3 nm for BLG). The implication of these findings in terms of different surface arrangements of the two proteins is discussed.

INTRODUCTION

Since the pioneering work of Kautzmann [1] it has been well known that proteins are marginally stable structures the conformation of which to a more or less pronounced degree is due to hydrophobic interaction between non-polar residues in their peptide chains. On the thermodynamic balance sheet, the folding of the peptide chain into a compact structure is a costly process in terms of entropy. Any opportunity for the molecule to interact with a hydrophobic surface is therefore likely to re-

sult in some relaxation of its folded structure, with a gain in entropy, as it exchanges intramolecular hydrophobic interactions for similar bonds with the surface. During this process, accomodation of the protein to the surface may lead to the exposure of previously buried hydrophobic residues which themselves can serve as adsorption sites for subsequent layers of protein molecules. Processes as different as emulsification, colloid stabilization and surface fouling may be affected by this type of protein adsorption, and the subject has therefore been given much attention [2].

If the hydrophobic groups are dispersed on an otherwise hydrophilic surface, such as a support used for hydrophobic interaction chromatography (HIC), the driving force behind the adsorption of

Correspondence to: Dr. K. D. Caldwell, Center for Biopolymers at Interfaces, University of Utah, Salt Lake City, UT 84112, USA.

proteins is ideally the weak interaction between matrix-bound non-polar ligands and hydrophobic patches on the protein surface which, for steric reasons, have failed to become buried in the interior of the molecule. With an appropriate spacing between ligands the adsorption process is reversible, and the protein structure remains essentially intact and biologically active during its contact with the matrix.

In the early 1970s Jerker Porath and coworkers [3–5] devoted much attention to the development of stationary phases for HIC. By increasing the degree of substitution of primarily agarose matrices from a level suitable for chromatography it was found that proteins could be irreversibly adsorbed with significant levels of retained activity, and could remain active for periods of months even under continuous percolation with the mobile phase [6–8]. Batch experiments showed the adsorption of several enzymes to be virtually instantaneous. After transfer of the adsorption complex into a minicolumn, a slow partial desorption was initially accomplished by the continuous introduction of protein-free buffer. Within hours, however, the desorption rate became negligible, and the remaining protein load was for all practical purposes immobilized. Although these and similar observations in chromatographic systems may give qualitative information regarding the behavior of proteins in contact with non-polar surfaces, the lack of a well defined surface area of the stationary phase precludes exact determinations of such parameters as the surface concentration and spatial extension of the adsorbed protein.

Processes underlying the formation and stability of protein-based emulsions are in part dependent on the conformational behavior of the proteins as they adsorb at the oil–water interface. Among the proteins which have been studied from this perspective are the different caseins and β-lactoglobulin from bovine milk [9,10]. Because of the difficulty in characterizing the adsorbed layer of protein in emulsions, which are composed of polydisperse mixtures of oil droplets, it has been assumed that the behavior of the oil droplet can be simulated by the behavior of similarly hydrophobic polystyrene (PS) latex particles [11] suspended in a comparable protein solution. Such latex particles are available in a variety of discrete and uniform sizes. The high level of cross-linking produced during the polymerization process causes these particles to behave as

solid spheres with well defined surface areas. This makes them particularly useful as substrates in adsorption experiments intending to shed light on the surface concentration of the adsorbed component and the thickness of the adsorbed layer.

Several studies have followed the build-up of adsorbed layers of protein on such hydrophobic colloids by means of photon correlation spectroscopy (PCS) [12,13]. These have shown that it is possible to make *in situ* measurements of increases in particle hydrodynamic radius resulting from increased concentrations of protein in the suspension medium. If the thicknesses of the adsorbed layers are in excess of 2–3 nm, and the core particles are less than about 300 nm in diameter (so that uncertainties because of experimental error can be avoided), PCS will reproducibly define the increase in particle size. However, this increase can result either from irreversible adsorption or from a loose association of protein with the particle, or both, and PCS alone cannot define which of the two occurs. The surface concentration of adsorbed material can in principle be calculated from the layer thickness, but this requires making certain assumptions about the protein arrangement on the surface, which in view of the different measured thicknesses of adsorbed layers of different proteins [12,13] are not likely to be valid.

Recently, we have demonstrated that sedimentation field-flow fractionation (SdFFF) can be used to determine directly the surface concentration of materials adsorbed to colloidal particles [14,15]. The substrates in these studies were monodisperse PS latex spheres, and the adsorbed layer was a synthetic block co-polymer with known colloid stabilizing properties. If the adsorbed layer represents at least 15% of the mass of the core particles, and if the core particles can be well retained by the system, which for substrates such as PS the density of which is so close to that of the aqueous suspension medium (1.053 vs. 0.997 g/ml) implies particles larger than about 125 nm, the SdFFF retention is a direct measure of the mass adsorbed to each particle. In general, the process involves a separation of the adsorption complex from its supernatant using a mobile phase which is free from the adsorbing substance. As a result, the determined surface concentration of this substance is that which represents an irreversibly adsorbed layer.

In this study, we will examine the interaction between PS latex particles and the two milk proteins β-casein (BCN) and β-lactoglobulin (BLG) using both the PCS and the SdFFF technique. Although the proteins are of similar molecular weight (23 000 vs. 18 000 dalton), their structures are very different. BCN is believed to possess very little structural order [16], and is known to be highly surface active in spread films [17] and emulsions [18], while BLG with its tightly folded β-barrel core [19] is less surface active, but once adsorbed gives a much stronger interfacial layer [20]. As expected, the two experimental techniques discussed here give complementary information on the surface arrangement of these proteins.

EXPERIMENTAL

Sizing methods

SdFFF. At the end of the protein adsorption process, 5-μl samples of the 1% (w/v) suspended particles were injected directly into the thin separation chamber the highly polished Hastelloy walls of which were clamped together around a Mylar spacer which defined the geometry of the separation channel. The 94 $\times$ 2 $\times$ 0.0254 cm channel was curved to fit inside a rotor basket, allowing it to spin at some preset centrifugal acceleration G, which can be considered constant across the thin channel. The system was configured to allow the flow of mobile phase through the channel while it was spinning. Samples were injected with a syringe directly into the stationary channel under a slow flow of mobile phase (0.2 ml/min). After 30 s the flow was turned off and the rotor was accelerated to the selected spin rate.

Under the influence of the field, the injected components migrate to one of the channel walls and concentrate into exponentially distributed particle clouds the average thickness of which (l) depends on the interplay between the field-induced force on the particles and the sample's diffusivity [21]. This concentration distribution $c(x)$ in the direction of the field varies with distance x from the accumulation wall in the following manner

$$c(x) = c(0) \exp(-x/l) = c(0) \exp(-x/\lambda w) \qquad (1)$$

where $c(0)$ is the concentration at the wall, and λ is

the dimensionless layer thickness, defined as the ratio of l and the channel thickness w.

Parameter λ can be given a general definition, valid for all types of field-flow fractionation

$$\lambda = kT/Fw \qquad (2)$$

where F is the force acting on a particle in the field, and k and T have the usual meaning of Boltzmann constant and temperature. In the case of a sedimentation field of acceleration G, the reduced layer thickness is described by

$$\lambda = kT/m'Gw = kT/m(\Delta\rho/\rho_s)Gw = 6kT/d^3\Delta\rho\pi Gw \qquad (3)$$

The leftmost of these three expressions casts λ as a function of the buoyant mass m' of the sample particle, while in the middle m' is replaced by the product of the actual mass m and the bouyancy factor, consisting of the density difference $\Delta\rho$ between the particle (density ρ_s) and the mobile phase. The right hand expression, obtained by replacing m with the product of volume and density, is particularly useful for the sizing of spherical particles, as λ is seen to depend inversely on particle diameter d raised to the third power.

After a "relaxation time" of 20 min, during which the sample equilibrates under the influence of the field, the mobile phase flow is initiated at a rate of 2.6 ml/min while the system remains spinning. The thin channel ensures laminar flow of liquid, which implies that the various particle clouds are transported downstream at rates governed by their level of compression near the wall. The more compact its distribution, the slower will a zone move through the channel and the larger will be its retention volume V_r. For the "infinite parallel plate" type channels used here [21], the retention ratio R bears the following relationship to λ:

$$R = V_0/V_r = 6\lambda[\coth(1/2\lambda) - 2\lambda] \approx 6\lambda \qquad (4)$$

Here, the approximate relationship between R and λ is accurate to within 5% for R values less than 0.1. Experimentally R, the ratio between the channel void volume V_0 and the observed retention volume, can be directly converted into a value for parameter λ which, in turn, gives information on particle mass or size through use of eqn. 3.

While the basic sample characteristic given by this approach is the buoyant mass m', this quantity is frequently less useful than the size d or actual mass m which are obtainable only for particles of known density. If the density is unknown, as is the case for colloidal substrates with coatings or adsorbed layers of unknown thickness, the retained particle fraction can readily be sized by independent techniques, e.g. electron microscopy or PCS. Although these techniques are applicable to direct sizing of the sample without prior fractionation [22], the introduction of the separation step ensures removal both of loosely associated protein and of the particle aggregates which may have formed during the adsorption process and which would disturb the sizing. In a recent study [15] we have demonstrated that the mass m_2 of material adsorbed to a colloidal particle is amenable to determination from SdFFF retention data, provided the densities of the (unsolvated) coating (ρ_2) and the moile phase (ρ_3) are both known

$$m_2 = [kT/Gw(1 - \rho_3/\rho_2)](1/\lambda_2 - 1/\lambda_1) \qquad (5)$$

Here, λ_1 and λ_2 are the retention parameters recorded at a fixed field strength G for the bare and coated particles, respectively. If the field strength is chosen so that both particle types are retained more than 10 column volumes, an approximate value for m_2 is given by a combination of eqns. 4 and 5.

$$m_2 \approx [6kT/V_0Gw(1 - \rho_3/\rho_2)]\Delta V_r \qquad (6)$$

where ΔV_r is the difference in retention volume between coated and bare particles. Since the retention volume for the bare particles gives their size d, provided their density is known, one can easily evaluate the surface area A per particle

$$A = \pi d^2 \approx \pi(6kT/\lambda_1\pi\Delta\rho Gw)^{2/3} \qquad (7)$$

Therefore, the SdFFF observations lead directly to determinations of the surface concentration Γ ($= m_2/A$) of adsorbed material. In the limit of well retained zones for which the approximate form of eqn. 4 applies, the value for Γ can be simply expressed in terms of ΔV_r

$$m_2/A = \Gamma \approx$$
$$0.55(kT/\pi V_0Gw)^{1/3}(\Delta\rho/V_1)^{2/3} (1 - \rho_3/\rho_2)^{-1} \Delta V_r \quad (8)$$

In the above approximate expression, $\Delta\rho$ symbolizes the density difference between bare particles and mobile phase, and V_1 is the retention volume of the bare particles.

Photon correlation spectroscopy. PCS measurements were made at a scattering angle of 90° on a spectrometer attached to a 7032 Multi-8 autocorrelation system (Malvern Instruments). Diffusion coefficients were calculated from the correlation functions using the method of cumulants [23], and apparent diameters of the particles were calculated from the diffusion coefficients using the Stokes equation. All measurements were made at a temperature of 25°C.

For the depletion experiments, a sample of latex (20 μl of a 10% suspension of diameter 190 nm) was suspended in 10 ml of buffer (20 mM imidazole, pH 7.0), and 20 μl of of a 10 mg/ml solution of BCN were added. The diameter of the latex was measured before and after addition of the protein. The mixture was then centrifuged using an Eppendorf 5414 centrifuge, operating at 16 000 g, and the supernatant liquid was removed. The latex was then resuspended in buffer containing no protein. This washing procedure was repeated six times, and the diameter of the residual latex–protein complex was measured and compared with the original values.

Quantification of colloid surface area

The freshly acquired suspension of PS latex particles had a manufacturer-assigned solids content of 100 mg/ml. From this stock a series of samples was prepared the concentrations of which were based on the assigned value for the stock, and the optical densities of which were determined at a wavelength of 232 nm, using a Perkin-Elmer Model Lambda 6/PECSS spectrophotometer. From these measurements a calibration curve was established which allowed the determination of particle concentration, and thus surface area, in a sample of unknown particle concentration.

Quantification of adsorbed protein

Two techniques were employed to quantify the amount of protein adsorbed to a given amount of particles. The first method, which assessed the total amount of protein taken up by the particles, was based on a depletion study. Here, the concentration of a given protein solution was determined by ami-

no acid analysis (AAA). To 1-ml samples of each of these two solutions, containing around 1.6 mg/ml protein, were added 100-μl portions of a 10% (w/v) suspension of latex spheres. The samples were gently mixed for 10 min on a rotating shaker, and at the end of this incubation period the particles, with their protein load, were pelletted by spinning at 16 000 g in the Eppendorf centrifuge. The protein content in the supernatant was again determined by AAA, and the amount adsorbed calculated from the difference in concentration before and after exposure to the particles.

The second method involved determination of the amount of protein that was irreversibly bound to the particles. Here, the coated particles were carefully washed, either by multiple suspension/centrifugation steps in which the supernatant was removed between spins and replaced by fresh buffer, or by the fractionation process through which the 5 μl injected sample was carried downstream by the mobile phase to elute at a retention volume of around 40 ml. In either case, the turbidity of the washed suspension was determined spectrophotometrically as described above, whereupon the sample was freeze-dried and submitted to amino acid analysis. The AAA procedure has been described elsewhere [24,25], and is based on a 20-h hydrolysis of the freeze-dried sample in 6 M HCl at 105°C, followed by derivatization with phenyl isothiocyanate and reversed phase liquid chromatography using a Hewlett-Packard Model HP 1050 liquid chromatograph. The total protein content was determined as the total area under peaks corresponding to the standard amino acids (*i.e.* all common amino acids with the exception of Trp).

Microcalorimetry

The thermal stability of the two proteins, in solution and in their adsorption complexes with PS latex particles, was determined using a differential scanning microcalorimeter (Model 4207) from Hart Scientific. The protein was dissolved in a 20 mM imidazole buffer of pH 7.0, and portions (final concentrations 12 mg/ml) were filled into the three measuring cells (volumes 1.0 ml each) prior to ramping up the temperature by 1°C/min. The calorimetric enthalpy, ΔH_{cal}, was found by integration of the heat capacity curve after baseline identification and correction for the change in heat capacity ΔC_p be-

tween the fully native and fully denatured forms of the protein [26].

Materials

PS latex samples were obtained from Duke Scientific and from Seradyn; they were used without further preparation. BLG was obtained from Sigma, while BCN was prepared by isolating the whole casein fraction from skimmed bovine milk by acid precipitation, followed by chromatography on a column of S Sepharose-FF (Pharmacia LKB Biotechnology) in a buffer containing 20 mM acetate and 6 M urea at pH 5.0 [27]. This separated the four different caseins. The BCN fraction was collected and dialyzed exhaustively against four changes of distilled water, and was lyophilized. Analysis of the protein using fast protein liquid chromatography [28] did not show any other protein components to be present. The densities of both proteins were taken as 1.365 g/cm^3, while densities for the latex and buffer were 1.053 g/cm^3 and 0.997 g/cm^3, respectively.

RESULTS AND DISCUSSION

The two whey proteins BCN and BLG were adsorbed onto PS latex particles with a nominal diam-
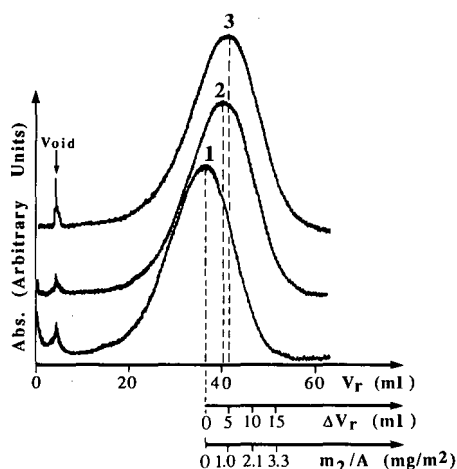
Fig. 1. Fractograms of PS bare and protein-coated PS particles with nominal diameter of 272 nm. Traces 1–3 represent bare, BCN-coated and BLG-coated particles, respectively. SdFFF parameters used were: field strength, 173 g; flow-rate, 2.9 ml/min. The ΔV_r expresses the excess retention volume caused by the uptake of protein, which in turn proportional to the mass (m_2) adsorbed per unit area.

TABLE I

ADSORPTION OF MILK PROTEINS

Surface concentrations Γ of the two proteins on PS latex are determined by four methods: Γ_{FFF} by FFF, via eqns. 5 and 7; $\Gamma_{FFF/AAA}$ by AAA on coated particles after fractionation; $\Gamma_{AAA}(W)$ by AAA on particles extensively washed after adsorption; $\Gamma_{AAA}(T)$ by AAA of the supernatant, before and after protein adsorption to the latex. Coating thickness δ (PCS, nm) is determined from the size difference between bare and coated particles.

Proteins	Mol.wt. (dalton)	Γ_{FFF} (mg/m^2)	$\Gamma_{FFF/AAA}$ (mg/m^2)	$\Gamma_{AAA}(W)$ (mg/m^2)	$\Gamma_{AAA}(T)$ (mg/m^2)	δ (PCS, nm)
BCN	23 000	1.00	1.28	1.26	2.99	10
BLG	18 000	0.88	1.06	1.00	4.12	3

eter of 272 nm from solutions containing 8 mg/ml of protein and 1% (w/v) (surface area 0.21 m^2/ml) of the latex. The adsorption was rapid for both proteins, and no difference was seen in the fractionation behavior whether sampling was done after 5 min or several hours after mixing. Fig. 1 illustrates the typical fractionation patterns gathered for the bare PS latex particles, as well as for the particles coated with BCN and BLG, respectively. The approximate relationship (eqn. 6) between adsorbed mass, on the one hand, and the difference in retention volume between bare and coated particles on the other, serves as a qualitative indication of the similarities in amounts adsorbed encountered for the two proteins. A more exact assessment of the particle uptake of each protein is obtained via eqn. 5, in conjunction with the retention volumes measured for the bare particles and for each of the protein–particle complexes, respectively. The surface concentrations for the two proteins, obtained from eqns. 5 and 7, are listed in Table I. These concentrations are seen to be very similar. The similarity is particularly striking if they are expressed as area per molecule. However, the values of around 1 mg/m^2 are significantly lower than the concentrations (around 3 mg/m^2) reported by others performing adsorption of these milk proteins on PS substrates [29,30]. The explanation to this discrepancy may be that these other studies were based on the depletion of protein from a solution exposed to a known amount of particles, and therefore include both irreversibly and loosely bound protein, although the binding isotherms do not show biphasic adsorption.

There are, however, some potential sources of error that can affect the SdFFF measurement, and

which therefore must be examined. First, it is known that mobile phases of low ionic strength can give rise to significant Coulombic repulsions between sample particles and the channel wall [31,32]. Such repulsions add a term to the flux equation which forms the basis for establishing the concentration distribution given by eqn. 1; if present, they lead to premature elution of a sample the size or mass of which therefore appears smaller than its actual value. By systematically varying the ionic strength (I) of the carrier and recording the effect of I on retention, one can easily detect whether such unwanted effects are present. This process is illustrated in Fig. 2 for the adsorption complex between BCN and the 272-nm PS latex; a similar curve was recorded for BLG. Although premature elution is clearly observed in mobile phases of low ionic strength, the gradual increase in I leads to a plateau value for the retention indicative of a complete suppression of any Coulombic interaction with the
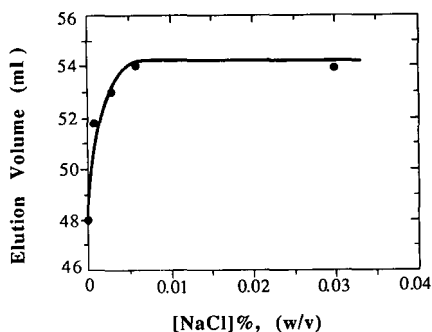
Fig. 2. Effect of carrier ionic strength on the elution volume of casein-coated PPS particles. The plateau is reached for salt concentrations above 0.015% (w/v).
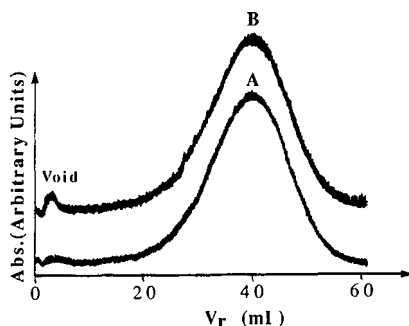
Fig. 3. Fractograms of BCN-cated PS particles in carriers of different compositions. Traces: A = 20 mM imidazole + 0.015% NaCl; B = as A, buth with the addition of 2 mg/ml BCN. SdFFF conditions were: field strength, 173 g; flow-rate, 2.9 ml/min.

channel wall. It is this plateau retention which is used to compute the surface concentrations given in Table I.

A second source of error in these measurements would be encountered if the adsorbed protein were to repartition from the particle surface to the channel wall during the fractionation. In order to ensure that this did not occur, fractograms were collected for the PS–BCN complex using mobile phases consisting of imidazole buffer alone or with the addition of 2 mg/ml of soluble BCN. The slight difference in retention, and therefore in adsorbed mass, which is seen in Fig. 3 may account for some loosely associated protein withstanding the shear of the carrier and thus co-migrating with the particles in the BCN-containing buffer. However, the difference in too small to in any way indicate that a significant loss of protein occurs from the particles during the SdFFF procedure in protein-free buffers.

To further scrutinize the validity of the FFF derived surface concentrations of BCN and BLG, PS latex samples of known concentration were incubated with solutions of each of the two proteins (8.03 and 7.79 mg/ml, respectively), as described in the Experimental section. The protein solutions were sampled before and after exposure to the particles, and these samples were subjected to amino acid analysis for quantification of the protein loss due to adsorption. In addition, the coated particles were removed from the supernatant by centrifugation and washed thoroughly with pure imidazole buffer to remove any loosely adsorbed protein. Giv-

en portions of coated particles, quantified by their turbidity, were also submitted to amino acid analysis. Similarly, samples which had been subjected to the SdFFF procedure were collected at the peak elution positions in the fractograms. From the turbidities of these fractions, the amounts of particles were determined prior to amino acid analysis of their protein loads. Thus it was found that the depletion experiments do indeed indicate higher surface concentrations of both proteins (2.94 ± 0.03 mg/m^2 for BCN and 4.12 ± 0.05 mg/m^2 for BLG) than that found after extensive wash (1.26 mg/m^2 for BCN vs. 0.96 mg/m^2 for BLG). The latter pair of data is very similar to that found for the fractions from SdFFF, either by AAA or from the level of retention (See Table I). The slight discrepancy between the retention-based values and those based on a turbidity-related surface area, may well be due to an error in the assumed particle concentration for the latex sample, as it is of the same sign and similar magnitude for both proteins.

Errors in substrate concentration, and therefore in surface area available for adsorption, are easy to make with samples the limited availability of which make dry weight determinations and subsequent concentration assignments impractical. In relying on SdFFF retention to determine surface concentration of adsorbed materials this source of error is eliminated, since the difference in elution volume between bare and coated particles is a measure of the amount of protein adsorbed per particle, i.e. per a well defined surface area.

In addition to determinations of protein surface concentration, the two latex–protein adsorption complexes were examined by PCS to determine the thickness of the adsorbed protein layer on the 272-nm latex particles. Here, the previously noted differences between the two proteins [33] were confirmed, as seen in Table I. Thus, while the surface concentrations of BCN and BLG were very similar, the spatial extension of these molecules from the PS surface was quite different. Indeed, the BLG layer was within the measurement error of PCS, and can therefore not exceed 2–3 nm in thickness, whereas the BCN layer appeared to be around 15 nm thick. The latter value agrees with previous PCS measurements reported on by one of us [12]. Experiments where the latex–protein complexes were exhaustively washed gave a layer thickness of 13.5 nm before
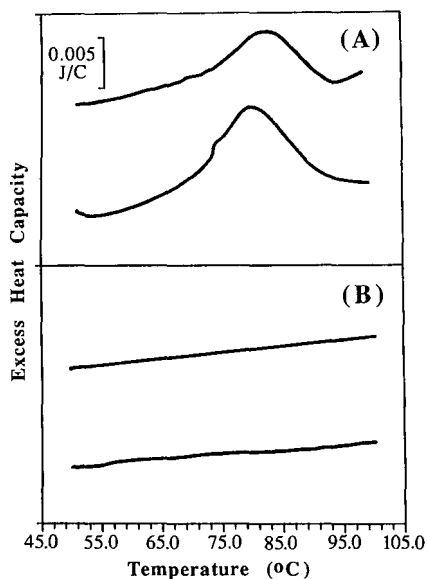
Fig. 4. Thermograms of proteins in free and adsorbed forms: (A) the lower trace represents free BLG in 20 m*M* imidazole buffer and the upper trace shows the protein adsorbed to PS latex with diameter of 90 nm. The unfolding enthalpies were 3.5 J/g and 1.8 J/g for the free and adsorbed forms, respectively; (B) as (A) but for BCN. The unfolding enthalpies are zero for both forms of the protein. The scan rate of the instrument is 1°C/min. The excess heat capacity (J/C) is in Joules per centigrade.

PS + BLG   PS + BCN

Fig. 5. Proposed surface arrangements for BCN and BLG on the PS latex particles. The BLG is heavily structured and compact even in the adsorbed state, while the BCN, a good surfactant protein, remains flexible and structureless on the particle surface.

washing and 9.5 nm afterwards. While this confirmed that there was a change in the surface as a result of washing, it was clear that the thickness of the layer was not diminished proportionately to the amount of protein which was lost, according to the surface coverage figures quoted above.

Although of comparable molecular weight, the two proteins of interest here are structurally very different. BCN appears to be a flexible molecule, with a highly hydrophobic "tail", which may be the site of adsorption to fat droplets and similarly nonpolar surfaces, while the remaining hydrophilic portion of the molecule reaches out into an aqueous environment in which the fat is solubilized [34]. In contrast, the BLG molecule is known from X-ray crystallography [19] to be folded into a stable β-barrel. It is thought that after adsorption on to a hydrophobic surface, the BLG undergoes a slow structural rearrangement [35]. However, calorimetric examination of BLG adsorbed to the 90-nm PS latex shows that a significant amount of structure

remains in the molecule even after adsorption. In fact, the melting temperature for the protein in its adsorbed state was found to be somewhat higher (by 2.6°C) than for the protein in solution, as seen in Fig. 4. This observation supports the notion of a molecule which remains relatively compact even when it is adsorbed on a solid substrate. This notion is illustrated by the cartoon in Fig. 5.

In these experiments we have considered the adsorption of two proteins of similar chain length. Both adsorb with about the same surface density, but one retains a significant amount of structure, although in the adsorbed state it may be forced to flatten out somewhat for better contact with the surface. The other, in turn, is virtually structureless, allowing its long and highly hydrophilic tails to penetrate deeply into the aqueous solvent which surrounds the complex.

CONCLUSIONS

The ability to accurately assess the surface concentration and layer thickness of adsorbed macromolecules is crucial for the understanding of their function in the adsorbed state. This is particularly true for molecules of surfactant character, the ability of which to create a stable emulsion is directly linked to their ability to interact both with the oil and the water phase. Here, the milk surfactant protein β-casein is compared in its adsorption behavior to the structurally more rigid β-lactoglobulin. With the help of SdFFF we have been able to quantify the surface concentration of irreversibly adsorbed protein of both types and found it to differ significantly from adsorption data gathered earlier from depletion experiments. The SdFFF data are verified by the significantly more labor intensive amino acid

analysis procedure. It is noted that in determining surface concentrations by means of SdFFF one needs no prior knowledge of the exact amount of colloidal surface area exposed to protein. Rather, the measurement indicates mass increase per particle, where the surface area is easily determined from observations on the bare particles. The size increase associated with the uptake of protein can not be determined by SdFFF, since the composite density of the adsorption complex is unknown. Instead, the use of PCS has made it possible to demonstrate that the thickness of the β-casein adsorbed layer is at least five times that of the more structured companion protein.

ACKNOWLEDGEMENTS

REFERENCES

1 W. Kautzmann, *Adv. Prot. Chem.*, 14 (1959) 1–63.
2 E. Dickinson, *Food Hydrocolloids*, 1 (1986) 3–23.
3 J. Porath, T. Låås and J. C. Janson, *J. Chromatogr.*, 103 (1975) 49–62.
4 J. Porath, J. C. Janson and T. Låås, *J. Chromatogr.*, 60 (1971) 167–177.
5 J. Porath, L. Sundberg, N. Fornstedt and I. Olsson, *Nature (London)*, 245 (1973) 465–466.
6 K. D. Caldwell, R. Axén and J. Porath, *Biotech. Bioeng.*, 18 (1976) 1573–1588.
7 K. D. Caldwell, R. Axén and J. Porath, *Biotech. Bioeng.*, 18 (1976) 1605–1614.
8 J. Porath and K. D. Caldwell, in Z. Bohak and N. Sharon (Editors), *Biotechnological Applications of Proteins and Enzymes*, Academic Press, New York, 1977, Ch. 6, pp. 83–102.
9 D. E. Graham and M. C. Phillips, *J. Colloid Interf. Sci.*, 70 (1979) 415–426.
10 E. Dickinson, S. E. Rolfe and D. G. Dalgleish, *Food Hydrocolloids*, 3 (1989) 193–203.
11 E. Dickinson, R. H. Whyman and D. G. Dalgleish, in E. Dickinson (Editor), *Food Emulsions and Foams*, (*RSC Special Publication*, No. 58), Royal Society of Chemistry, London, 1987, pp. 40–51.
12 D. G. Dalgleish, *Colloids Surf.*, 46 (1990) 141–155.
13 E. E. Uzgiris and H.P.M. Fromageot, *Biopolymers*, 15 (1976) 257–263.
14 J. T. Li, K. D. Caldwell and J. S. Tan, in T. Provder (Editor), *Particle Size Distribution II* (*ACS Symposium Series*, No. 472), American Chemical Society, Washington, DC, 1991, Ch. 16, pp. 247–262.
15 J. T. Li and K. D. Caldwell, *Langmuir*, 7 (1991) 2034–2039.
16 E. R. B. Graham, N. M. Malcolm and H. A. McKenzie, *Int. J. Biol. Macromol.*, 6 (1984) 155–161.
17 D. E. Graham and M. C. Phillips, *J. Colloid Interf. Sci.*, 70 (1979) 427–439.
18 E. Dickinson, S. E. Rolfe and D. G. Dalgleish, *Food Hydrocolloids*, 2 (1988) 397–405.
19 M. Z. Papiz, L. Sawyer, E. E. Eliopoulos, A. C. T. North, J. B. C. Finlay, R. Silvaprasadarao, T. A. Jones, M. E. Newcomer and P. J. Kraulis, *Nature (London)*, 324 (1986) 383–385.
20 E. Dickinson, S. E. Rolfe and D. G. Dalgleish, *Int. J. Biol. Macromol.*, 12 (1990) 189–194.
21 J. C. Giddings, and K. D. Caldwell, in B. W. Rossiter and J. F. Hamilton (Editors), *Physical Methods of Chemistry*, Vol. 3B, Wiley, New York, 1989, pp. 867–938.
22 B. B. Weiner, in H. G. Barth (Editor), *Modern Methods of Particle Analysis*, Wiley-Interscience, New York, 1984, pp. 93–116.
23 D. E. Koppel, *J. Chem. Phys.*, 57 (1972) 4814–4820.
24 R. L. Heinrikson and S. C. Meredith, *Anal. Biochem.*, 136 (1984) 65–74.
25 G. Yan, G. Nyquist, K. D. Caldwell, R. Payor and E. C. McCraw, *Inv. Ophthalm. Vis. Sci.*, submitted for publication.
26 P. L. Privalov and N. N. Khechinashvili, *J. Mol. Biol.*, 86 (1974) 665–684.
27 C. M. Hollar, A. J. R. Law, D. G. Dalgleish and R. J. Brown, *J. Dairy Sci.*, 74 (1991) 2403–2409.
28 D. T. Davies and A. J. R. Law, *J. Dairy Res.*, 54 (1987) 369–376.
29 E. Dickinson, E. W. Robson and G. Stainsby, *J. Chem. Soc. Farad. Trans. 1*, 79 (1983) 2937–2952.
30 D. G. Dalgleish, E. Dickinson and R. H. Whyman, *J. Colloid Interf. Sci.*, 108 (1985) 174–179.
31 M. E. Hansen, and J. C. Giddings, *Anal. Chem.*, 61 (1989) 811–819.
32 Y. Mori, K. Kimura and M. Tanigaki, *Anal. Chem.*, 62 (1990) 2668–2672.
33 D. G. Dalgleish and J. Leaver, *J. Colloid Interf. Sci.*, 141 (1991) 288–294.
34 J. Leaver and D. G. Dalgleish, *Biochim. Biophys. Acta*, 1041 (1990) 217–222.
35 E. Dickinson and Y. Matsumura, *Int. J. Biol. Macromol.*, 13 (1991) 26–30.

CHROM. 24 060

Recycling isoelectric focusing: use of simple buffers*

Milan Bier and Terry Long**

Center for Separation Science, University of Arizona, Tucson, AZ 85721 (USA)

ABSTRACT

Using the recycling free-flow focusing (RF3) apparatus, we have demonstrated that single ampholytes can be utilized to establish very stable pH regions, separating all proteins into three groups: a sharply resolved zone of proteins isoelectric at the prevailing pH, this "pH window" being bracketed by zones of more acidic and/or basic proteins. The ampholytes used are either amino acids or their dipeptides and other derivatives. Where necessary, because of lack of an ampholyte with the required pH, a binary mixture of ampholytes can be utilized. The closer their isoelectric points (pI), the narrower will be the pH window, *i.e.*, the sharper the resolution of the bracketed proteins. This method overcomes the necessity of using ill-defined comnmercial carrier ampholytes, such as Ampholine, for preparative isoelectric focusing. It is recommended that the ampholytes be utilized at relatively high concentration, 100 mM or higher, this contributing to pH stability and minimizing protein precipitation.

INTRODUCTION

Borrowing from the vocabulary of another "high-tech" discipline, scaling up of electrophoresis for the processing of relatively large quantities of proteins presents both hardware and software problems. Our prior work on the hardware problems resulted in the design of several instruments embodying novel concepts for regulation of fluid flow. While for scale-up of liquid chromatography enlarging column diameters is a feasible option, enlarging gel-based analytical electrophoretic instruments is rather unproductive. Gels and other solid support matrices complicate dissipation of Joule heat as well as product recovery. Thus, it was found necessary to devise new types of instruments, operating in free solution without gels or other supports. This requires control of fluid flow and avoidance of unwanted convection. In our hands, three strategies for convection control were found to be particularly effective for the scaling of isoelectric focusing: (i) stabilization of fluid flow by means of screen elements, in the RIEF [1] apparatus; (ii) stabilization by screen elements and rotation in the Rotofor [2] apparatus (available from Bio-Rad Labs., Richmond, CA, USA); and (iii) stabilization by means of rapid flow through narrow gaps, in the recycling free-flow focusing (RF3) instrument [3] (available from Rainin Instrument Co., Woburn, MA, USA).

Software problems are concerned with the selection of buffers and other operational parameters for optimal resolution. In the past, we have addressed this problem through computer modeling [4]. In the present paper we wish to address the problem inherent in the use of commercial carrier ampholytes (CAs) for the establishment of pH gradients. These CAs are chemically ill-defined, which makes it difficult to document their complete removal, where necessary. In analytical work, pH gradients are indispensable, but in preparative applications, the isolation of a single protein is usually sufficient.

Thus, we are in the process of developing a novel strategy for preparative isoelectric focusing based on the concept of "pH windows" rather than pH gradients.

A single simple ampholyte, such as an amino acid or a dipeptide, suffices to cut a broad spectrum of proteins, isolating a narrow zone of proteins within the prevailing pH. Used at rather high concentration, the ampholyte produces an exceptionally stable pH profile, separating the proteins into three fractions: those with isoelectric points (pI) more basic than the ampholyte, those with pI values more acidic, and those with the same pI as the ampholyte. It is this third fraction which has the narrowest pI distribution of proteins and exhibits highest resolution. If a suitable single ampholyte with the required pI is not available, a mixture of two ampholytes bracketing the desired pH value can be substituted. It is an extension of the concept of the use of amino acids as discrete spacers in isotachophoresis, introduced a number of years ago [5]. Such ampholytes are chemically well defined and biologically acceptable. Equally important, because of the high concentration, they minimize the isoelectric precipitation often encountered otherwise. Many are also lower in cost than commercial CAs. Thus, their use opens the possibility of cost effective high resolution large scale focusing.

THE CONCEPT AND USE OF pH WINDOWS

In isoelectric focusing (IEF) the essential pH gradient is usually generated naturally, through the migration of buffer components to their isoelectric points, the proteins migrating within this gradient to their own steady state distribution. Realizing the need for a large number of ionizable species, Vesterberg [6] synthesized a random mixture of polyamino–polycarboxylic acids, commercialized under the tradename of Ampholine. Ampholine and other similar CA mixtures have found widespread acceptance for analytical focusing, even if chemically ill-defined.

In a seminal paper, Svensson (now Rilbe) [7] examined the possible use of amino acids and other simple ampholytes for establishment of a pH gradient. He has given formulas for calculation of degree of ionization, conductivity and buffering of individual compounds. Svensson also established the

now classical distinction between good and poor ampholytes. The pI of a simple ampholyte is given by the algebraic mean of its two dissociation constants, pI = (pK_1 + pK_2)/2. For an ampholyte with more than two ionizable groups, only the dissociation constants proximal to its pI are of consequence. Due to the logarithmic definition of pH, buffering decreases by a factor of 10 for every pH unit away from the pK. Thus, the degree of ionization of the ampholyte and its buffering at or near its pI will depend of the quantity pI−pK_1. Svensson rejected as unsuitable all ampholytes where (pI−pK_1) > 2.5, defining them as poor ampholytes, *i.e.* exhibiting too low conductivity to act as good carriers of the electrical current. Table I reproduces Svensson's [7] listing of acceptable ampholytes. Albert and Serjeant [8] have given a concise review of the methods for the determination of ionization constants and list additional data.

The Svensson calculations of the ionization, conductance and buffering were cumbersome and are greatly simplified by our computer program [4]. In previous work [4,9] we have published computer predictions of pH gradients resulting from focusing of various binary and ternary mixtures of amino acids. For instance, the ternary mixture of an acidic, a neutral and a basic amino acid (glutamic acid, cycloserine, and lysine) [9] creates two broad pH windows, between the acidic and neutral, and neutral and basic amino acids, respectively. These windows capture proteins isoelectric at those pH values. We have often used such systems to demonstrate the performance of our instruments for the admittedly easy separation of hemoglobin and bromophenol blue stained albumin, taken as models because of their color.

We now wish to present results obtained with single ampholytes, used in high concentration. These suffice to establish very stable pH zones isolating proteins isoelectric at the prevailing pH from those more acidic or more basic. In practice, we have found that good ampholytes, such as histidine or cycloserine, give good results at 100 mM concentration, but that even poor ampholytes can be used, provided the concentration is increased. Thus, we have used glycine at 1.5 M concentration and ε-aminocaproic acid (EACA) or glycyl-glycine at 0.5 M concentration. The upper concentration is mainly limited by the solubility of the compound. A rea-

TABLE I

LISTING OF CARRIER AMPHOLYTES ACCORDING TO SVENSSON [7]

Ampholyte	pI	pI − pK_1
Aspartic acid	2.77	0.89
Glutathione	2.82	0.70
Aspartyl-tyrosine	2.85	0.72
o-Aminophenylarsonic acid	3.00 (?)	0.77 (?)
Aspartyl-aspartic acid	3.04	0.34
p-Aminophenylarsonic acid	3.15 (?)	0.92 (?)
Picolinic acid	3.16	2.15
L-Glutamic acid	3.22	1.03
β-Hydroxyglutamic acid	3.29	0.96
Aspartyl-glycine	3.31	1.21
Isonicotinic acid	3.35	1.51
Nicotinic acid	3.44	1.37
Anthranilic acid	3.51	1.47
p-Aminobenzoic acid	3.62	1.30
Glycyl-aspartic acid	3.63	0.82
m-Aminobenzoic acid	3.93	0.81
Diiodotyrosine	4.29	2.17
Cystinyl-diglycine	4.74	1.62
α-Hydroxyasparagine	4.74	2.43
α-Aspartyl-histidine	4.92	1.90
β-Aspartyl-histidine	4.94	2.00
Cysteinyl-cysteine	4.96	2.31
Pentaglycine	5.32	2.27
Tetraglycine	5.40	2.35
Triglycine	5.59	2.33
Tyrosyl-tyrosine	5.60	2.08
Isoglutamine	5.85	2.04
Lysyl-glutamic acid	6.10	1.65
Histidyl-glycine	6.81	1.00
Histidyl-histidine	7.30	0.50
Histidine	7.47	1.50
L-Methylhistidine	7.67	1.19
Carnosine	8.17	1.34
α, β-Diaminopropionic acid	8.20	1.40
Anserine	8.27	1.23
Tyrosyl-arginine	8.38 (?)	1.00 (?)
	8.68 (?)	1.13 (?)
L-Ornithine	9.70	1.05
Lysine	9.74	0.79
Lysyl-lysine	10.04	0.59
Arginine	10.76	1.72

sonable estimate of the conductivity and the pI can be obtained by direct measurement on solutions of the pure ampholytes in distilled water, at the desired concentration.

As most ampholytes have very low concentrations of anionic or cationic species at their pI, they migrate only imperceptibly toward cathode or anode, and remain distributed throughout the system. This was confirmed experimentally as well as by the use of our computer program, recently utilized to model the performance of single ampholytes, and of binary mixtures of ampholytes, with closely similar electrokinetic properties [10]. At this point, it will suffice to give some general conclusions applicable to all simple ampholytes at their isoelectric state.

(1) Near neutrality, the conductivity of the solution is a linear function of concentration. Below pH 5 and above pH 9, the conductivity increases somewhat less than proportionally to concentration because of the contribution of hydrogen and hydroxyl ions.

(2) Near neutrality, the conductivity of the solution is a linar function of the electrophoretic ion mobility, this linearity decreasing at low or high pH. Ion mobility is roughly an inverse function of ion molecular weight.

(3) At same ionic mobility and close to neutrality, the conductivity of the solution decreases by roughly a factor of 9, when the value (pI − pK_1) increases from 1 to 2. This factor decreases to about 6 at pH 4.

(4) At same ion mobility, conductivity is nearly the same between pH 5 and 9, increasing at more extreme pH values.

(5) If the desired pH window cannot be established using a single ampholyte, binary mixtures of compounds with very close pI values seem to be equivalent. The resulting pH is intermediary to their individual pI values. Thus, such close binary mixtures permit the establishment of any desired pH window. As the ionization at the intermediate pH is still very low, there is little migration of the component ampholytes and the pH remains stable. A good approximation of the conductivity is given by the algebraic mean of component conductivities.

Above guidelines may suffice to lead the experimenter in the selection of appropriate ampholytes for the desired pH window. Detailed computer modeling data will be published separately.

EXPERIMENTAL

RF3 Apparatus (RF3)

Fig. 1 shows a schematic presentation of the recycling free flow focusing (RF3) apparatus. The work was carried out in a commercial RF3 apparatus
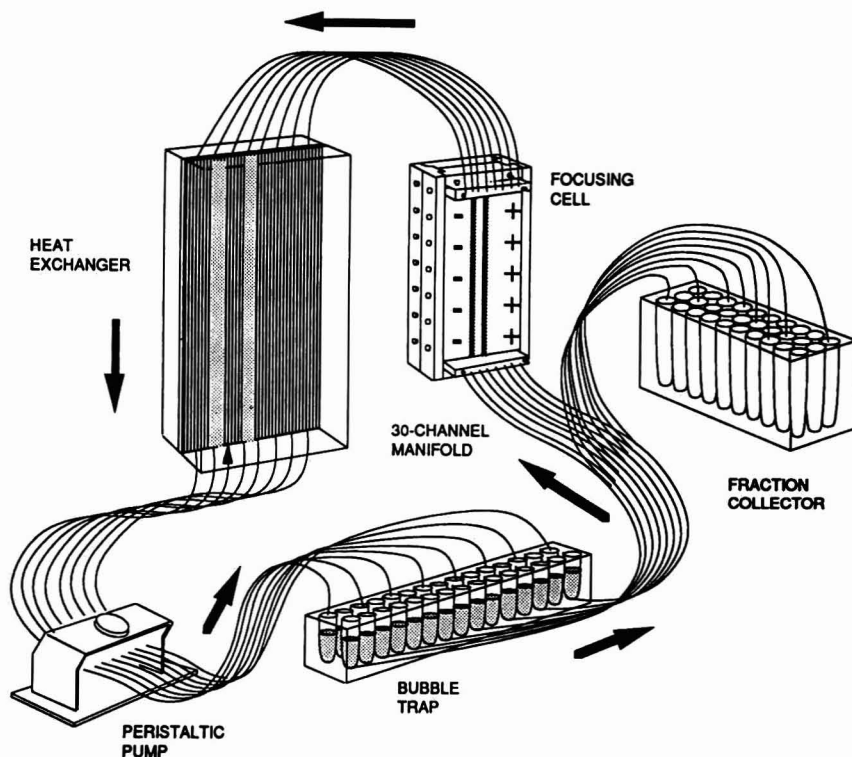
Fig. 1. A schematic presentation of the fluid flow pattern in the recycling free-flow focusing (RF3) apparatus. The main components are the focusing cell, the heat exchanger, a multichannel peristaltic pump and a bubble trap. See text for explanation.

(Protein Technologies, Tucson, AZ, USA) as well as in a home-made prototype. No difference in performance was noticed, though the commercial apparatus is simpler in usage.

The process fluid, containing the CAs and proteins to be fractionated, is continuously recycled through the focusing cell and a heat exchanger by means of a 30-channel peristaltic pump. The array of bubble traps inserted into the recycling loops are sealed by silicone septa, permitting addition of protein or withdrawal of small sample volumes during the focusing process. The key component of the apparatus is the focusing cell, illustrated schematically in Fig. 2. The cell is constituted by two parallel plexiglass plates defining a focusing cavity, 20 × 4 cm in size. Key to the stability of laminar flow through the cavity is its shallow depth, 0.75 mm, combined with the rapid flow of process fluid and the appropriately machined fluid inlet and outlet manifolds. Quick-connectors simplify the attachment of the 30 PTFE

tubing loops to the focusing chamber. A multichannel peristaltic pump directs the flow of the focusing process fluid upward through the cell with a residence time of about 2–4 s. Thus, in each pass through the cell, only incremental migration of components toward their isoelectric points is achieved. Rapid flow is essential to avoid electrohydrodynamic distortion [3].

An external power supply can impose a d.c. voltage of up to 1500 V, 400 mA. The electrodes are lateral, separated from the focusing cavity by ion-permselective membranes. These can be utilized in two modes. In the electrodialysis mode, the cation-selective membrane will face the cathodic compartment, the anion-selective membrane facing the anodic compartment. This will result in transport of low-molecular-weight ions from the processing to the electrode compartments. Using commercial CAs, such an arrangement may cause loss of some buffering components. Thus, in focusing, we often
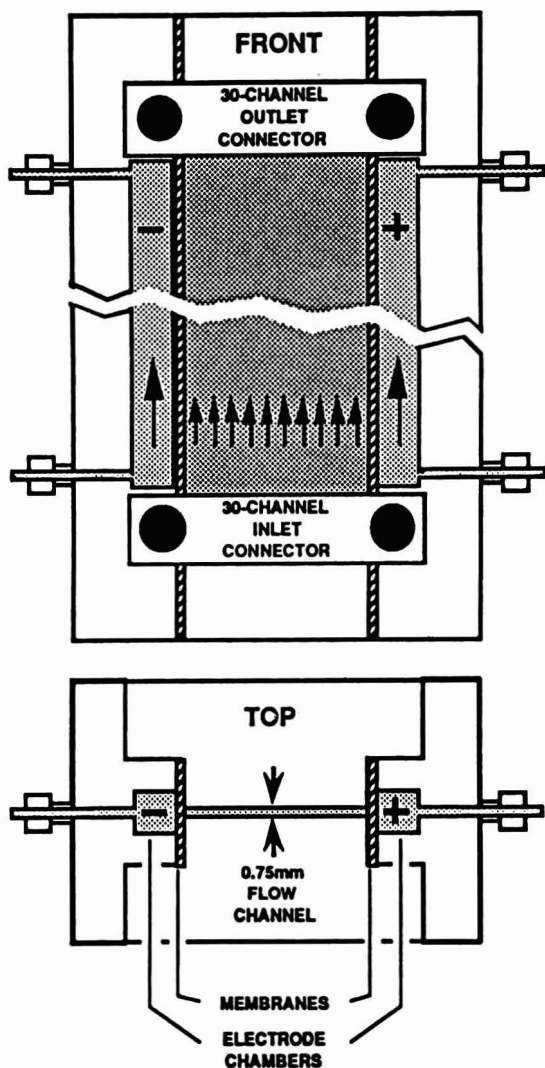
Fig. 2. A schematic presentation of the focusing cell of the RF3 apparatus. Of critical importance is the flow channel depth, indicated in the bottom panel.

use the reverse arrangement, cationic membrane facing the anode and vice versa. In such arrangement, no ions can escape from the processing compartment and are, instead, polarized proximally to the membranes. 0.1 M NaOH and phosphoric acid solutions are used typically as catholyte and anolyte, respectively.

Operating procedure

The cell volume is only about 6 ml, while total priming volume of the cell, the loops and the bubble trap is about 100 ml but can be increased up to 500 ml. The apparatus was primed with amino acid solutions of concentrations specified further on. Once recycling was started and current applied, the model protein solution to be fractionated was slowly injected into a central recycling loop by means of a Harvard apparatus syringe pump. The injection was carried out over a 30-min period, so as not to cause an excessive local protein concentration, which may alter to local pH value.

The focusing was carried out for 2 h at constant voltage of 1000V, the current varying as specified in figure legends. In some experiments, the field was decreased to 500 V during the last 30 min of focusing. With commercial CAs, current decreases significantly due to focusing of CA components. This is not the case in the present method, as the ampholyte is already loaded very close to or at its isoelectric pH. Thus, there is only a minor decrease of current density. At the end of the focusing, recycling and electrical power are stopped. The focusing chamber contents (6 ml) remix and are collected separately. The bulk of the fluid (94 ml) remains contained in the fluid loops and is collected simultaneously by shifting the bottom quick-connector from the cell to a test-tube array. Each of the 30 fractions contains approximately 3 ml of the fractionated fluid.

Amino acids

The EACA, histidyl-β-alanine, and lysyl-glutamine were obtained as gift from Vega Biotechnology (Tucson, AZ, USA). The other compounds were purchased from Sigma (St. Louis, MO, USA). No tests were made to ascertain the purity of the compounds.

Serum proteins

For most separations, a 10-ml aliquot (approx. 500 mg protein) of a frozen specimen of bovine serum was used as the model protein. In one experiment, a commercial sample of bovine immunoglobulin G (Sigma) was used. Both models were chosen as they represent rather broad distribution of proteins. To avoid overloading of the system with serum electrolytes, the serum was first equilibrated against 5 mM Tris buffer, pH 9.

TABLE II

PROPERTIES OF THE AMPHOLYTES USED

Ampholyte	pI	pK_a [a]	pK_b [a]	$\mu \cdot 10^4$ [b]	Exp. pI [c]
ε-Aminocaproic acid	7.6	4.4	10.8	?	N.A.
Cycloserine	5.9	4.4	7.4	3.42	5.9
Glycyl-glycine	5.7	3.15	8.25	3.08	5.9
Histidine	7.65	6	9.3	3.17	7.9
Histidyl-β-alanine	6.8	?	?	2.3	6.73
Lysyl-glutamic acid	6.1	4.47	8.45	1.96	6.15

[a] For histidine and other polyprotic ampholytes, only the two dissociation constants proximal to the pI are given.

[b] Electrophoretic mobility (cm^2/V s).

[c] Experimental pI, as obtained in the reported fractionations.

Analysis

The pH, ultraviolet adsorption and conductivity of all fractions were recorded. In addition, every second fraction was analyzed by conventional isoelectric focusing in polyacrylamide gels (PAG), using pH 3–10 Ampholine, the protein patterns being stained by Commassie Blue.

RESULTS

Of the many experiments carried out, we will report only a few illustrative examples. Serum proteins were used as a model, because of their polydispersity. In Table II are listed the pI, dissociation constants and electrophoretic mobility of the am-
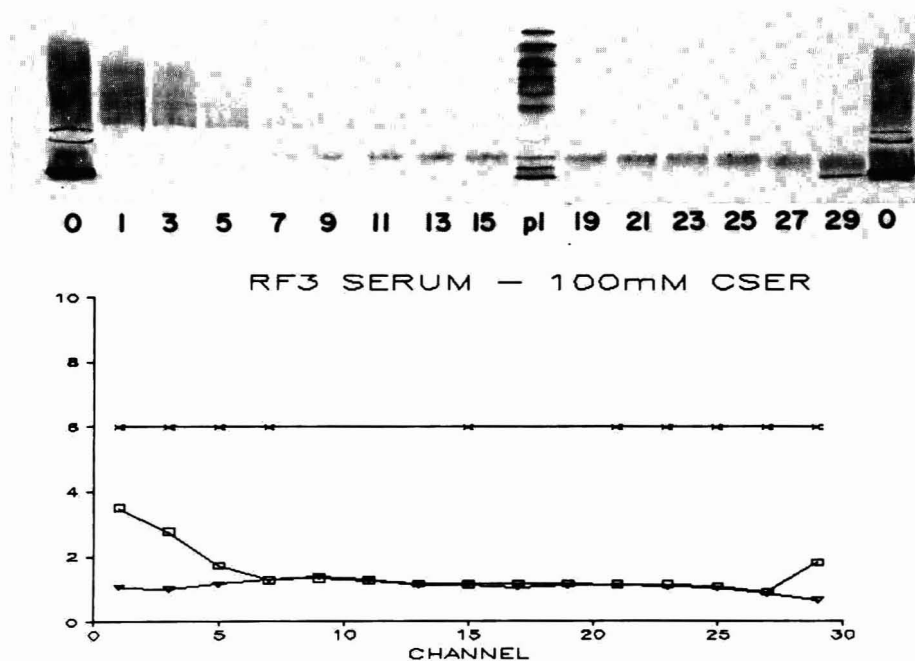
Fig. 3. RF3 separation of 10 ml of dialyzed serum using 90 ml of 100 mM cycloserine (CSER) as the sole buffering agent. Every second fraction was analyzed by focusing in PAG, 3–10 Ampholine (0 = original serum, pI = pH standard). Bottom plots present profiles of pH (x), absorbance at 280 nm (□) and conductivity in mS · 10 (▽). Initial conditions: 1000 V, 69 mA; final, after 2 h focusing: 1000 V, 42 mA. Throughout all the fractions, pH 5.9 was measured.

pholytes used. The last column in the table lists the pH of the plateaus seen in the reported experiments. There is in general a good agreement between the literature pI and the measured pH. Unfortunately, reliable literature data are not available for many potential ampholytes.

Fig. 3 illustrates the separation of the bovine serum proteins, using as the buffering agent a 100 mM solution of cycloserine, a "good" ampholyte. The upper part of the figure shows the IEF pattern of the separated fractions: basic proteins were found in the first 5 fractions, acidic in the last two. The original serum patterns are marked as 0. The bulk of the fractions, 11 to 27, contain essentially a single proteins, isoelectric at or near pH 6, coinciding with the band of the carbonic anhydrase, contained in the pI standard (marked pI). We have made no effort to identify this serum protein.

The bottom part of the figure shows the remarkable constancy of the pH across all the fractions. The pH 5.9 measured across all channels corresponds to

the literature one, given in Table II. There was no polarization of low-molecular-weight ions in the terminal fractions, as the electrodialysis mode of perm-selective membrane arrangement was utilized. Absorbance readings at 280 nm, document the accumulation of proteins close to the two electrodes.

Fig. 4 shows quite similar results obtained using as the sole buffer a 500 mM solution of glycyl-glycine. This dipeptide is a rather "poor" ampholyte, therefore the current density was much lower, yet the resolution was comparable to that obtained with cycloserine. As the focusing mode of membrane arrangement was utilized, there was significant ion polarization, causing sharp increases of conductivity in the terminal fractions. These ions may have been contributed by the protein sample as well as by the buffering glycyl-glycine, used at high concentration.

Fig. 5 reproduces comparable data obtained with 100 mM lysyl-glutamic acid dipeptide. The polarization effect, noticed above for glycyl-glycine, is
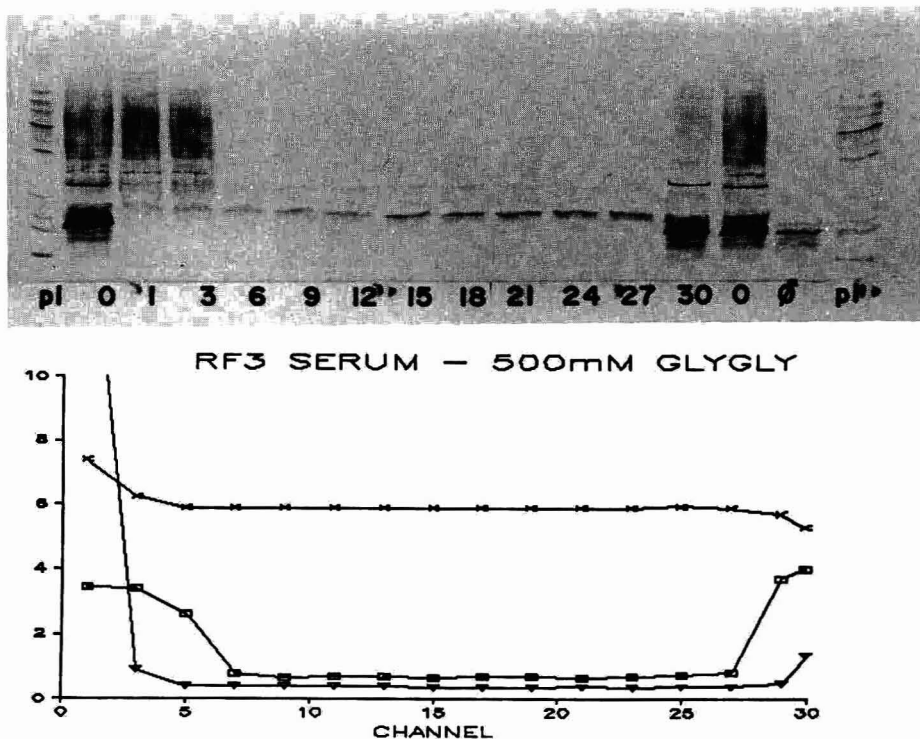
Fig. 4. RF3 separation in 500 mM glycyl-glycine (GLYGLY) buffer, a "poor" ampholyte. Initial: 1000 V, 19 mA; after 120 min: 1000 V, 16.4 mA; final 30 min: 500 V, 7.5 mA. Poor ampholytes result in lower current densities. A stable pH of 5.9 was measured between fractions 5 and 27. Symbols as in Fig. 3. $\varnothing$ = Sample irrelevant for example shown.
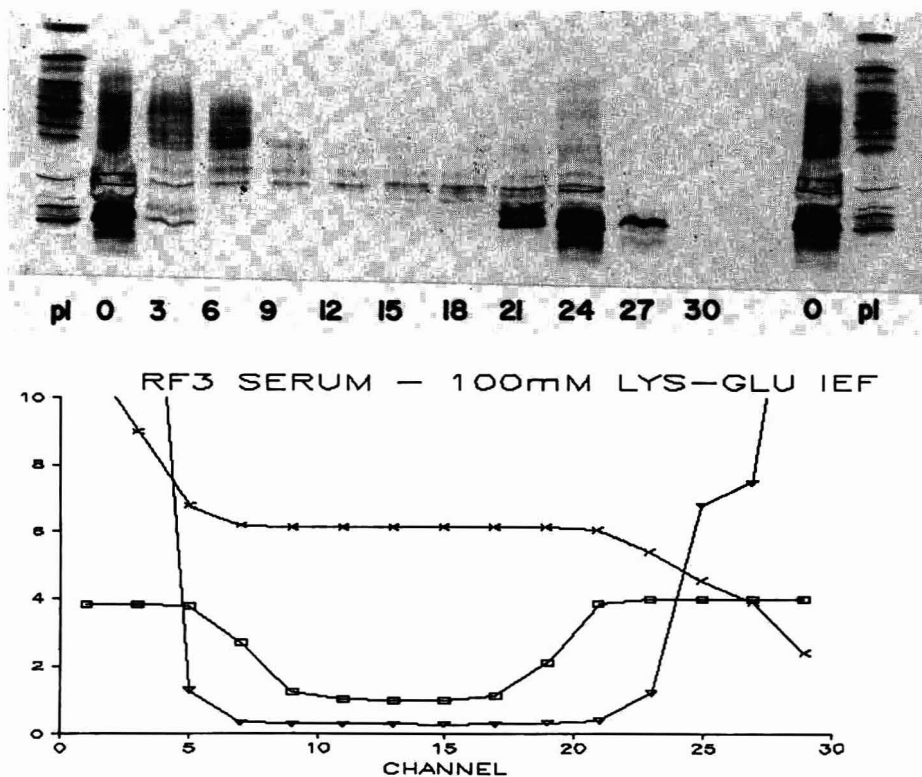
Fig. 5. Fractionation of 10 ml of serum in 100 mM lysyl-glutamic acid (LYS-GLU) dipeptide. Initial: 450 V, 200 mA; final: 500 V, 8.7 mA. The drastic decrease in current was due to the contamination of the lysine-glutamic acid by free glutamic acid, which focused at the anode, displacing all proteins. Nevertheless, a constant pH of 6.15 was measured in fractions 8 to 20. Symbols as in Fig. 3.

greatly accentuated, particularly in the acid region (fractions 25–30), where even the serum proteins were excluded. This effect was probably due to the presence of unreacted glutamic acid in the dipeptide used, which focused at the anode. This impurity notwithstanding, reasonable separation was obtained.

A separation of serum proteins within the histidyl-β-alanine pH window is presented in Fig. 6. The peptide concentration was lower, only 50 mM, and probably insufficient to properly buffer the apparatus contents during protein injection. Thus, fraction 30, which should comprise only acidic proteins, is heavily contaminated by basic proteins as well. Once proteins become trapped in regions close to the electrodes, they are slow to focus. The prevailing high conductivity results in a low local electric field and slow migration.

The results of separation using a binary mixture

of two quite "poor" ampholytes is presented in Fig. 7. The combination of 500 mM each of EACA (pI 7.6) and glycyl-glycine (pI 5.7) resulted in an extended pH zone of pH 6.4–6.5, *i.e.*, close to the mean value. Being poor ampholytes, their ionization at this pH is still minimal, insufficient to bring about separation of the two amino acids even at the prolonged focusing time of 3 h. Thus, the mixture resulted in a very stable pH profile.

Finally, Fig. 8 shows the separation of 500 mg of bovine γ-globulin, using 100 mM histidine, a typical "good" ampholyte. The analysis of the fractions was carried out in a narrow range gel, pH 5–8 Ampholine. The data show that the spectrum of gamma globulins was resolved with high resolution.

DISCUSSION

Svensson [7] was the first to examine the use of
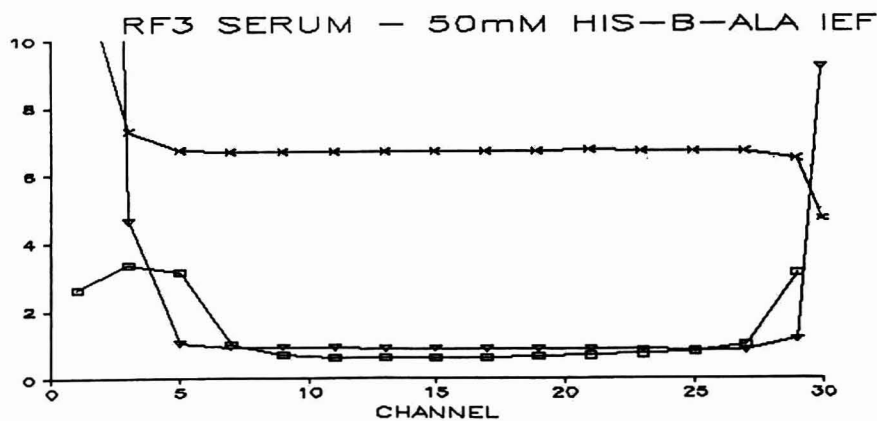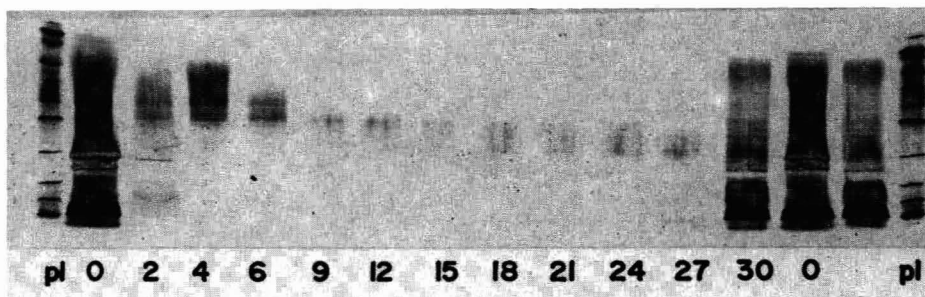
Fig. 6. Serum fractionation using 50 mM histydyl-β-analine (HIS-B-ALA) as the pH knife. Some basic protiens were trapped in the anodic compartment 30, possibly because of too low ampholyte concentration. Starting at 950 V, 110 mA, final 500 V, 24 mA. Channels 6 to 27 exhibited a constant pH of 6.73. Symbols as in Fig. 3.

amino acids and other simple ampholytes as current carrying buffers for isoelectric focusing. Nguyen and Chrambach [11] and others followed suit, while we have analyzed this possiblity by computer simulation [4,9]. The results, as a whole, were disappointing, because of the lack of sufficient ampholytes. More important, the gradients formed presented too many conductivity gaps, acting as protein traps.

We now propose a novel usage of amino acids and other similar simple ampholytes. Rather than trying to form pH gradients, we use individual amino acids to establish very stable regions of constant pH, into which the proteins to be separated are slowly injected. Due to the absence of any significant pH gradient, proteins do not focus in the conventional sense, but migrate by zone electrophoresis toward one or the other electrode. A third, intermediate zone is formed by the proteins isoelectric at the prevailing pH window imposed by the amino

acid. These are sharply resolved from the more acidic or more basic ones. Where a single ampholyte of desired pI is not available, binary mixtures can be used. The closer their pI values, the sharper the resolution.

The proposed method is a software analogue to the hardware one developed by Righetti et al. [12]. Using the principle of recycling focusing [1], Righetti et al. recycle the protein to be purified though a compartment bounded on both sides by polyacrylamide gels, rendered isoelectric at the desired pH by incorporation of copolymerized buffering components (known as Immobiline). The advantage of our method is the avoidance of the need for controlled gel synthesis.

In is projected that for optimal use of our method, it would be advantageous to have available ampholytes covering the pH scale at 0.1 pH intervals. Table I lists the ampholytes proposed already by Svensson [7]. We are presently engaged in preparing
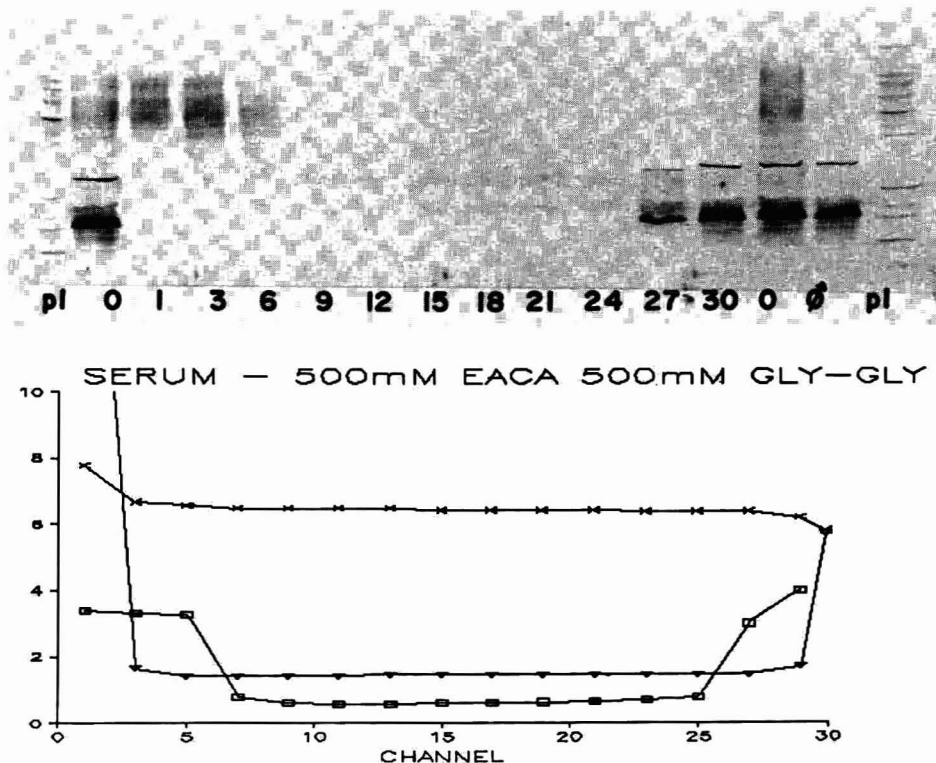
Fig. 7. Serum fractionation in a binary mixture of 500 mM ε-aminocaproic acid (EACA) and 500 mM of glycyl-glycine (GLY-GLY), two "poor" ampholytes. A shallow pH gradient, pH 6.5 in channel 6 decreasing to pH 6.4 in channel 27, was obtained. Few proteins were focused in this range. 1000 V were applied throughout the 3 h run, the current decreasing from 91 to 61 mA. Obviously, the two amino acids were poorly resolved, their ionization at this average pH value being minimal, but excellent resolution was obtained. Symbols as in Fig. 3.

an extended list of compounds, rendered possible through advances in amino acid chemistry and peptide synthesis. Moreover, we have demonstrated that intermediate pH regions can be established using binary mixtures of ampholytes. The closer their pI values, the narrower will be the pH window and the sharper the resolution. In addition, we are engaged in extensive computer modeling of such systems, to be published separately.

We feel that this method has overcome the main shortcoming of conventional preparative focusing by avoiding use of the chemically ill-defined commercial CAs. The amino acids are easily analyzed and, if necessary, easily removed by dialysis or gel sieving. In addition, protein precipitation is avoided or greatly decreased. Because of the low cost of many amino acids and other ampholytes, it opens the possibility of large scale focusing for production of therapeutic proteins. In work not yet reported [10], we were able to scale focusing to a rate of 500 ml/h, using a RIEF apparatus [1] with an effective cross-area of 100 cm^2.
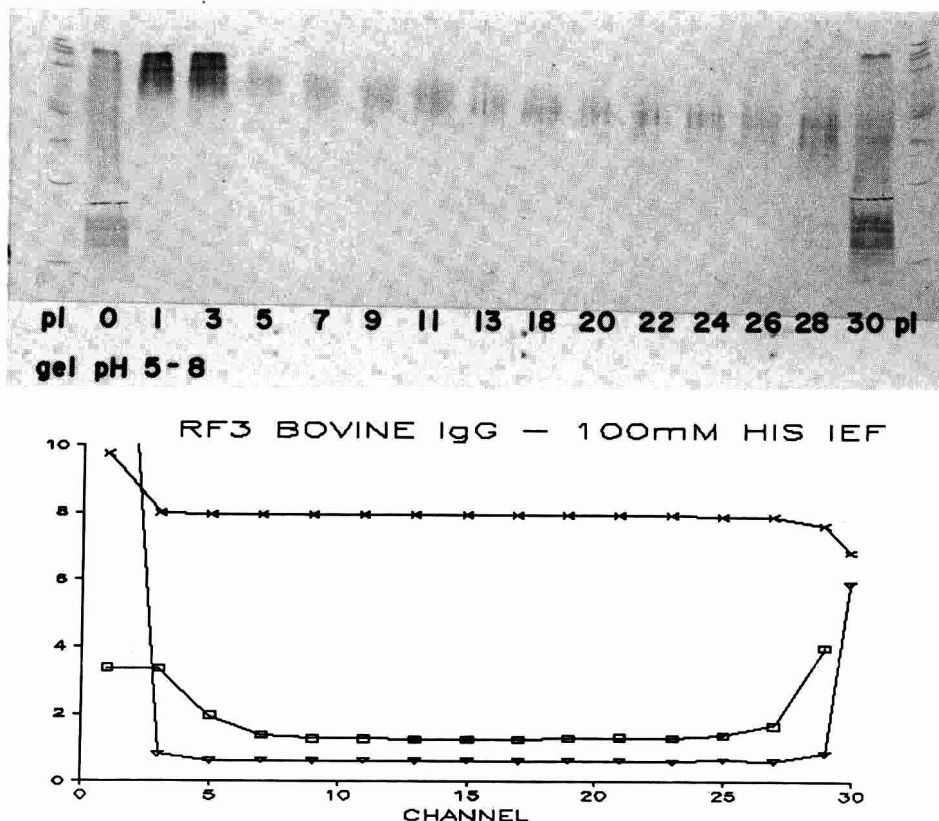
Fig. 8. Fractionation of 500 mg of bovine immunoglobulin G in 100 mM histidine (HIS) buffer. Clear subfractionation was obtained. Initial condition: 1000 V, 55 mA, final conditions: 500 V, 16.5 mA, pH 7.90 between channels 5 and 27. Symbols as in Fig. 3.

REFERENCES

1 M. Bier, N. B. Egen, T. T. Allgyer, G. E. Twitty and R. A. Mosher, in E. Gross and J. Meienhofer (Editors), *Peptides: Structure and Biological Function*, Pierce, Rockford, IL, 1979, pp. 35–48.

2 N. B. Egen, W. Thormann, G. E. Twitty and M. Bier, in H. Hirai (Editor), *Electrophoresis 83*, Walter de Gruyter, Berlin, 1984, pp. 547–550.

3 M. Bier, G. E. Twitty and J. E. Sloan, *J. Chromatogr.*, 470 (1989) 369.

4 M. Bier, O. A. Palusinski, R. A. Mosher and D. A. Saville, *Science (Washington, D.C.)*, 219 (1983) 1281.

5 M. Bier, R. M. Cuddeback and A. Kopwillem, *J. Chromatogr.*, 132 (1977) 437.

6 O. Vesterberg, *Acta Chem. Scand.*, 23 (1969) 2653.

7 H. Svensson, *Acta Chem. Scand.*, 16 (1962) 456.

8 A. Albert and E. P. Serjeant: *The Determination of Ionization Constants*, Chapman & Hall, London, New York, 1984.

9 M. Bier, R. A. Mosher and O. A. Palusinski, *J. Chromatogr.*, 211 (1981) 313.

10 M. Bier, unpublished results.

11 N. Y. Nguyen and A. Chrambach, *Anal. Biochem.*, 74 (1976) 145; 79 (1977) 462.

12 P. G. Righetti, B. Barzaghi and M. Faupel, *J. Biochem. Biophys. Methods*, 15 (1987) 163.

Simple multi-point detection method for high-performance capillary electrophoresis

Tasanee Srichaiyo and Stellan Hjertén

Department of Biochemistry, University of Uppsala, Biomedical Centre, Box 576, S-751 23 Uppsala (Sweden)

ABSTRACT

A simple device for multi-point detection was designed to record the course of an analysis by high-performance capillary electrophoresis (HPCE). Determinations of mobilities and relative peak areas can be performed with an accuracy higher than that obtained with conventional HPCE equipment. Two principles were utilized (in both instances the polyimide coating is removed at the detection points desired). In one approach, the fused-silica tubing, following a first recording, is moved "backwards" to a new position for a second recording, and so on. The other approach utilizes a piece of tubing which, after a straight stretch, is curved into loops; the first monitoring takes place as the solutes leave the straight stretch, the second when they leave the first loop, the third when they leave the second loop, and so on (the straight stretch can, of course, be replaced with a loop). The technique is illustrated with an electrophoretic analysis in free solution of DNA and peptides. Interestingly, λ DNA is separated into several extremely narrow zones. By using multi-point detection it could be demonstrated that the appearance of the DNA pattern changed in an unexpected, discontinuous way during a run.

INTRODUCTION

Free zone electrophoresis in capillaries with diameters around 1 mm requires rotation of the capillary around its long axis in order to minimize zone distortions caused by convection [1]. The capillaries, which are made of quartz, are ground and polished on both the inside and the outside to make them straighter and to ensure very small variations in the inner diameter and the wall thickness along the length of the capillary. Owing to this high optical quality, the capillaries permit scanning with UV radiation for the detection of the solute zones without giving disturbing fluctuations of the baseline on the recorder chart (when the ratio of the absorption at two wavelengths is recorded, one of them not being absorbed by the solutes, the fluctuations are even smaller). The advantages of scanning these high-quality quartz capillaries are that an

electrophoresis experiment can be followed from the start to its termination and that mobilities and peak areas can be determined with high accuracy because the diameter of the capillary varies very little throughout its length and also because several measuring points are obtained.

Fused-silica tubing is not of the same high quality as the above quartz capillaries and therefore does not give a satisfactory baseline on scanning. Further, silica tubing cannot be used with UV scanning, as it is delivered with a non-UV transparent polyimide coating (without the coating it is extremely brittle). In addition, the variations in the diameter of the tubing along its length are too large to permit accurate mobility determinations. Accordingly, in practice it is not straightforward to design a simple scanning device with satisfactory performance. We present here another very simple approach which overcomes partially the problems discussed above: the scanning is replaced with detection at two or more selected migration distances. Only slight modifications of existing monitors for high-performance capillary electrophoresis are required. Multiple

Correspondence to: Professor S. Hjertén, Department of Biochemistry, University of Uppsala, Biomedical Centre. Box 576, S-751 23 Uppsala, Sweden.

monitoring has been reported previously, but the equipment was designed such that each detection point required its own detector [2–5]. Our version requires only one detector.

EXPERIMENTAL

Apparatus

The detector was an LKB/Pharmacia (Uppsala, Sweden) HPLC 2141 variable-wavelength monitor, modified for on-tube detection of the solutes. In one version of the equipment the fused-silica tubing was mounted in a V-groove for a fixed position relative to the UV beam, but could still be moved longitudinally in the groove for detection at different points on the tubing (Fig. 1a). The height of the opening in the V-groove was approximately equal to the outer diameter of the tubing and the width was 0.15 mm. In another version, the tubing was bent into loops for detection of the solutes as they entered and left a loop (Fig. 1b). The segments of the tubing that correspond to the beginning and the end of a loop were placed on top of each other in a slit. The height of the slit was slightly larger than the sum of the

outer diameters of all the segments. The silica tubing was cooled by means of a fan and the V-groove by flowing water.

For determination of migration times and peak areas we used a Spectra-Physics SP 4270 inegrator. The DNA experiment was monitored with the aid of a recorder (Servograph REC 61) from Radiometer (Copenhagen, Denmark).

Treatment of the fused-silica tubing

By means of an electrically heated tungsten wire [6] the polyimide coating of the tubing was burnt off from places where detection was desired. The non-coated sections must be relatively narrow, otherwise the tubing will break when bent into a loop. The inside of the silica tubing was coated with a monolayer of linear polyacrylamide to eliminate adsorption and electroendosmosis [7]. This coating is stable also at high pH: no changes in migration velocities or the appearance of the electropherograms were observed during a test period of 4 weeks with a coated capillary stored at pH 11.

RESULTS AND DISCUSSION

Four consecutive detections of λ DNA by displacement of the fused-silica tubing (method I, see Fig. 1a)

The electropherograms in Fig. 2a, b, c and d show the patterns obtained when the migration distances were 12, 17, 27 and 37 cm, respectively. The fourth, third and second electropherograms are not simply monotonic extrapolations of the third, second and first electropherograms, respectively. In fact, one reason why we were interested in multiple-point detection was that we wanted to follow the separation of λ DNA, as we had earlier found that λ DNA can be resolved electropheretically into many extremely narrow zones, but not reproducibly [8]. In a forthcoming paper we shall discuss the separation mechanism and the unexpected alterations in the electropherograms. The separations may be dependent on the diameter of the electrophoresis capillary, as the lengths of the λ DNA molecules approach the diameter of the caillary.

In several experiments the unexpected differences between the appearances of consecutive electropherograms were even more pronounced than those in Fig. 2.
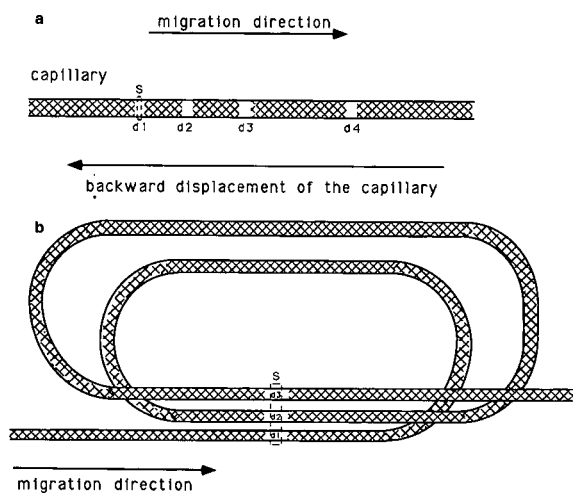
Fig. 1. The principle of multi-point detection in high-performance capillary electrophoresis. S = slit. (a) Method I: following a first detection at d1 the tubing is moved "backwards" for a second recording at d2, and so on. (b) Method II: the tubing is stationary. The first electropherogram is obtained when the solutes pass d1, the second when passing d2, and so on.
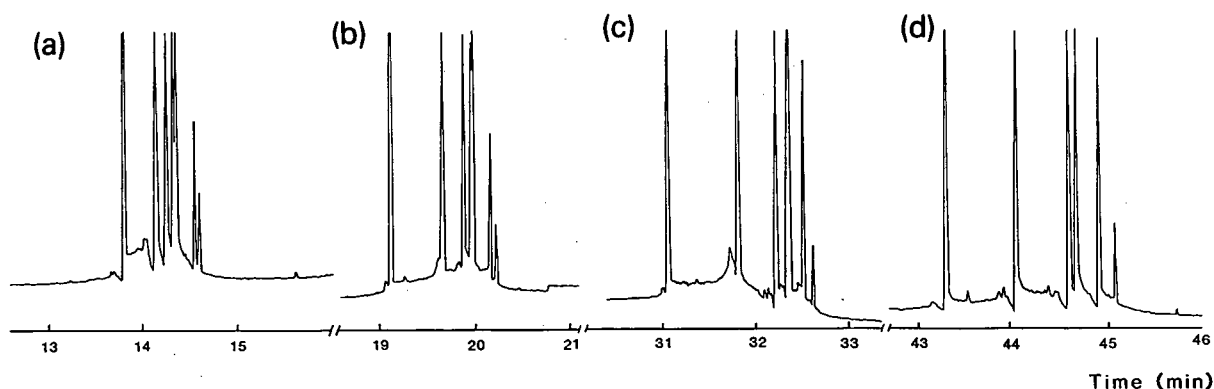
Fig. 2. Electropherograms of λ DNA obtained from four consecutive detections by displacement of the fused-silica tubing (see Fig. 1a). λ DNA was applied electrophoretically at 2000 V for 30 s and analysed at the same voltage in TBE buffer (0.09 M Tris–0.09 M boric acid–0.002 M EDTA) (pH 8.2). When the first detection (a) (migration distance 12 cm) was completed, the fused-silica tubing was drawn backwards to a new position for a second recording (b) (migration distance 17 cm). In (c) and (d) the migration distances were 27 and 37 cm, respectively. Capillary: 540 mm × 0.075 mm I.D. Detection wavelength: 260 nm.

Three consecutive detections of peptides by monitoring the solutes at different points in the stationary fused-silica tubing (method II, see Fig. 1b)

The model peptides were from Bio-Rad Labs. (Richmond, CA, USA). It is striking how an increase in the migration distance increases the resolution (Fig. 3). In contrast to the electropherograms in Fig. 2, those in Fig. 3 exhibit no anomalies.

Determination of relative peak areas and absolute mobilities.

The electropherograms in Fig. 3 show that four, six and all nine peptides were baseline resolved when the migration distances were 4.0, 14.0 and 44.0 cm, respectively. Accurate determinations of peak areas and mobilities could therefore only be obtained for the four peptides bradykinin, luteinizing hormone-
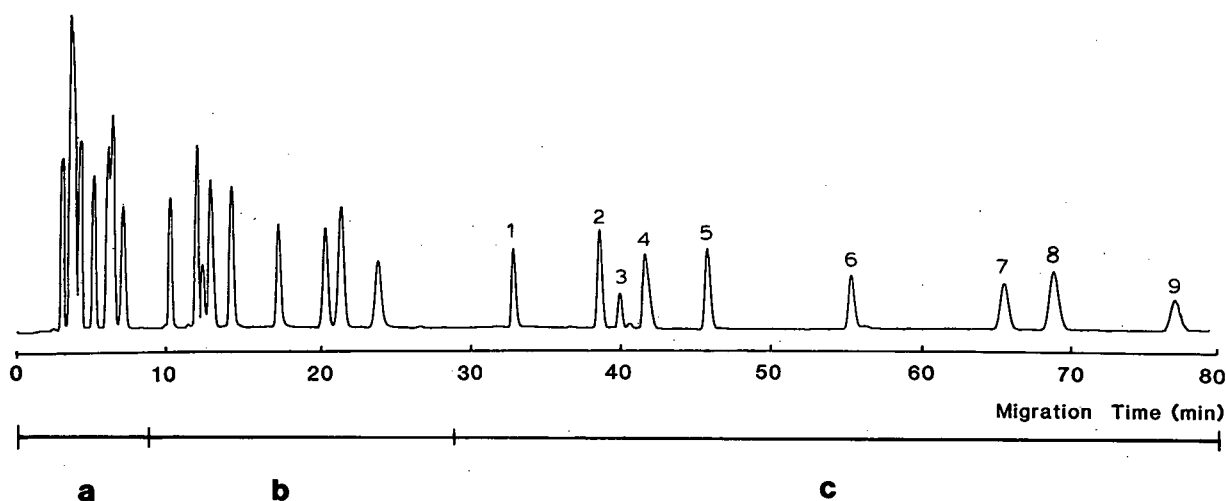
Fig. 3. Electropherograms obtained from three consecutive detections by monitoring the solutes (standard peptides) at different points in the stationary fused-silica tubing (see Fig. 1b). The sample was applied electrophoretically at 8000 V for 10 s. Buffer: 0.1 M sodium phosphate (pH 2.5). Running voltage: 8000 V. Dimensions of the capillary: 580 mm × 0.05 mm I.D. Detection wavelength: 200 nm.

TABLE I

DETERMINATION OF RELATIVE PEAK AREAS

Recording	. Bradykinin	Luteinizing hormone-releasing hormone	[2–5]Leucine enkephalin	Oxytocin
1st	1.00	1.30	0.91	0.90
2nd	1.00	1.28	0.94	0.91
3rd	1.00	1.33	0.94	0.90

releasing hormone, [2–5]leucine enkephalin and oxytocin (peaks 1, 5, 6 and 9, respectively).

As the light intensity varies over the cross-section of the detecting UV beam and also because the diameters of the capillary are not exactly equal at the different detection points, the area of any particular peak is not the same in the consecutive electropherograms (see Fig. 3). However, this disadvantage should be eliminated if the absolute values of the peak areas are converted into relative units by dividing the areas of all peaks in an electropherogram by that of one of the peaks (*e.g.*, the first). This is confirmed in Table I.

In Fig. 4 the migration distance is plotted against migration time for the four peptides listed in Table I. The points lie surprisingly well on a straight line, indicating that the multi-point detection technique described here gives reliable mobility values (u), provided that the field strength can be determined accurately [$u = v/F$, where v is the migration velocity (cm s^{-1}) (the slope of a line in Fig. 4)].
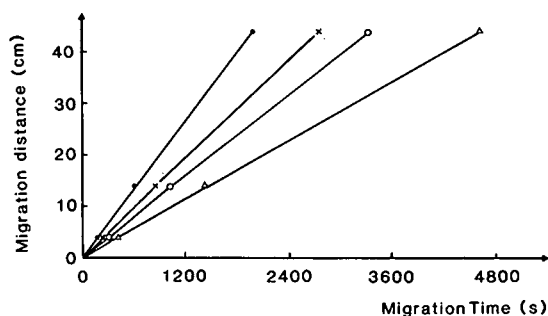
Fig. 4. Plot of migration distance against migration time. The plot refers to peaks 1 (bradykinin), 5 (luteinizing hormone-releasing hormone), 6 ([2–5]leucine enkephalin) and 9 (oxytocin) in Fig. 3. All points fall on straight lines, which indicates good accuracy in the determination of mobilities with the multi-point detection method presented.

Using a field strength obtained by dividing the voltage applied by the length of the capillary, the mobility values for bradykinin, luteinizing hormone-releasing hormone, [2–5]leucine enkephalin and oxytocin were calculated to be $1.61 \cdot 10^{-4}$, $1.17 \cdot 10^{-4}$, $0.96 \cdot 10^{-4}$ and $0.69 \cdot 10^{-4}$ cm^2 s^{-1} V^{-1}, respectively.

As the field strength in an electrophoresis tube is determined primarily by the current in the tube and not by the voltage between the electrodes, it is theoretically safer to use the equation $F = I/q\kappa$, where I is the current (A), q the cross-sectional area (cm^2) and κ the electrical conductivity (Ω^{-1} cm^{-1}) [9]. It is important that the average cross-sectional area is determined accurately, *e.g.*, by weighing the tubing empty and filled with a heavy liquid of known density.

Sensitivity

A small change in the position relative to the capillary and the photodiode of a light beam with a height as small as that of the inner diameter of the capillary may give rise to a relatively large alteration in sensitivity (deflction of the recorder pen) and in the level of the baseline, as the reflection losses (according to Fresnel's equation) and the light path through the capillary vary with the angle of incidence and also because the photodiode has a different response in different parts of the photosensitive surface. This displacement of the light beam, which can be caused by alterations in the temperature of the detection system, is less pronounced if the light beam is higher than the diameter of the capillary as in Fig. 1. This approach to bathing the capillary in light has been used previously with success [1]. One can therefore expect the detection methods described here to give a relatively small change in the position of the baseline and in

sensitivity if the temperature of the detection system changes during a run. This may explain why the drift in the baseline is extremely small in the electropherogram shown in Fig. 3, despite the long analysis time (80 min).

The slit height is considerably larger in the multipoint detection method II than in method I (see Fig. 1). Accordingly, even when a solute zone absorbs almost all of the light entering the zone, the total light striking the photodiode in method II will be reduced only by about $(1/n) \cdot 100\%$, where n is the number of detection points (most of the light will pass outside the zone). The sensitivity of the multipoint detection method II is, from this point of view, relatively low. However, as a photodiode has more favourable characteristics at high light flux and functions better, the fluctuations in the baseline, including the drift, are smaller in method II than in method I. If one amplifies the photocurrent in method II until the disturbances in the baseline become the same as in method I, one obtains a peak height (for a given solute concentration) which may approach that obtained in method I. Accordingly, the difference in sensitivity between the two methods need not be large. A similar detection technique was utilized in the design of the detector in the first capillary electrophoresis apparatus and worked satisfactorily [1]: the height of the slit was not sufficiently small to restrict the light beam to the centre of the capillary, but was larger than the outside diameter to minimize the variations in the baseline.

Method II works satisfactorily also when the capillaries are placed side-by-side instead of on top of each other as in Fig. 1b.

In any plot of absorption against solute concentration, the curve obtained may deviate considerably from a straight line when the absorption is not zero at infinite concentration, as in the experiments shown in Figs. 2 and 3, where part of the light beam passed outside the solute zone. This case is treated in detail in ref. 1 (pp. 182–190). When a linear relationship is required over a large absorption (concentration) range, only the central part of the tubing should be illuminated. In such experiments, Method II must be used in the version with the capillaries placed side-by-side.

An electrophoresis tube bent into loops gives greater zone broadening than does a straight tube of the same length, as molecules migrating at the outside of the loop lag behind those migrating at the inside. Neglecting the influence of diffusion, it is easy to show that the attendant zone broadening $\Delta X = n2\pi\phi$, where n is the number of loops and ϕ is the inner diameter of the tubing. Method I should, accordingly, be chosen when optimum resolution is required, which was verified experimentally by running DNA fragments in a gel-filled straight tube and in a gel-filled coiled tube (the runs are not shown here). The inner diameter was 0.2 mm. The gel (polyacrylamide) was cast in the coiled tubing. The same result was obtained when the straight gel-filled tube was bent into a loop. By giving the tubing such a shape (e.g., a figure-of-eight or a serpentine path) that the "inner lane" turns into an "outer lane", the zone broadening can be decreased. Another alternative is to cut the end of the tubing where the sample is applied at such an angle that the length of the "inner lane" becomes equal to the "outer lane" at the detection point (suggested by Professor Paul Roos of this Department).

ACKNOWLEDGEMENTS

REFERENCES

1 S. Hjertén, Chromatogr. Rev., 9 (1967) 122–219.
2 B. J. Wanders and F. M. Everaerts, presented at the 3rd International Symposium on High Performance Capillary Electrophoresis, San Diego, CA, February 3–6, 1991, Abstract LW-1.
3 J. L. Beckers, T. P. E. M. Verheggen and F. M. Everaerts, J. Chromatogr., 452 (1988) 591–600.
4 S. Terabe and O. Shibata, presented at the 3rd International Symposium on High Performance Capillary Electrophoresis, San Diego, CA, February 3–6, 1991, Abstract LW-3.
5 S. Terabe and T. Isemura, J. High Resolut. Chromatogr., 14 (1991) 52–55.
6 J. A. Lux, U. Häusig and G. Schomberg, J. High Resolut. Chromatogr., 13 (1990) 373–374.
7 S. Hjertén, J. Chromatogr., 347 (1985) 191–198.
8 S. Hjertén, T. Srichaiyo and K. Elenbring, paper presented at the 3rd International Symposium on High Performance Capillary Electrophoresis, San Diego, CA, February 3–6, 1991, Abstract LM-5.
9 S. Hjertén, Electrophoresis, 11 (1990) 665–690.

Short Communication

Lectin affinity electrophoresis of α-fetoprotein

Increased specificity and sensitivity as a marker of hepatocellular carcinoma

Hidematsu Hirai

Tumour Laboratory, Kokubunji, Tokyo (Japan)

Kazuhisa Taketa

Department of Public Health, Okayama University Medical School, Okayama (Japan)

ABSTRACT

α-Fetoprotein (AFP) is widely used as a marker of hepatocellular carcinoma (HCC) for assisting diagnosis and also for screening purposes, even though its sensitivity has been decreased slightly as a result of the earlier detection of HCC by ultrasonography. Using lectin-dependent fractionation of AFP, the diagnostic sensitivity as well as the specificity of AFP can be increased compared with measurement of total AFP. Furthermore, lectin-reactive forms of AFP, AFP-L3 and AFP-P4, have been shown to serve as preclinical markers of HCC. Accordingly, AFP is still the most reliable marker of HCC in screening and monitoring high-risk patients.

INTRODUCTION

Since the implementation of radioimmunoassay of α-fetoprotein (AFP), which was developed by Ruoslahti and Seppälä [1] and Nishi and Hirai [2] nearly twenty years ago, AFP has played an important role in screening for and diagnosing hepatocellular carcinoma (HCC) and other AFP-producing tumours. As a result of applying several types of imaging to screening high-risk patients with chronic hepatitis and liver cirrhosis, the AFP-positive rate of

HCC has decreased significantly, *e.g.* for a cut-off level of 200 ng/ml the positive rate has decreased from 75 to 30–43% during this period (Table I). It is also evident that there is a wide overlap between the serum AFP level in benign and malignant liver diseases. In fact, the number of patients with chronic hepatitis and liver cirrhosis who have slightly increased serum levels of AFP, ranging from 11 to 200 ng/ml, is always higher than the number of patients with HCC. These patients obviously need further evaluation, preferably by analysing the elevated serum AFP, before considering invasive examinations such as angiography or biopsy of suspected hepatic lesions.

Correspondence to: Professor H. Hirai, Tumour Laboratory, Higashitokuna 1-15-3, Kokubunji, Tokyo, Japan.

TABLE I

SENSITIVITIES AND SPECIFICITIES OF AFP FOR DIFFERENT RANGES OF SERUM AFP LEVELS

CH = Chronic hepatitis; LC = liver cirrhosis; HCC = hepatocellular carcinoma. Numbers of patients are given. Values in parentheses are percentages.

Calendar year and disease	Serum AFP level (A) (ng/ml)		
	$A \leqslant 10$	$10 < A \leqslant 200$	$A > 200$
1971–1975			
CH	31 (44.3)	35 (50.0)	4 (5.7)
LC	23 (37.1)	38 (61.3)	1 (1.6)
HCC	2 (10.0)	3 (15.0)	15 (75.0)
April 1983–July 1985			
CH	71 (71.7)	20 (20.2)	8 (8.1)
LC	49 (43.0)	53 (46.5)	12 (10.5)
HCC	8 (19.0)	10 (23.8)	24 (57.1)
Aug. 1985–March 1987			
CH	106 (80.3)	24 (18.2)	2 (1.5)
LC	123 (64.0)	65 (33.9)	4 (2.1)
HCC	33 (34.4)	34 (35.4)	29 (30.2)
April 1987–March 1989			
CH	173 (72.4)	65 (27.2)	1 (0.4)
LC	147 (52.7)	131 (47.0)	1 (0.3)
HCC	10 (10.5)	44 (46.3)	41 (43.2)

A recently developed technique, affinity electrophoretic separation of AFP, appears to serve this purpose. Bręborowicz et al. [3] and Miyazaki et al. [4] have reported increased proportions of lentil lectin (LCA)-reactive AFP in patients with HCC and yolk sac tumours. They detected separated AFP components by crossed immunoelectrophoresis and protein staining. However, this system is not sensitive enough to be applied to low serum levels of AFP as described above. We have developed a highly sensitive method of antibody-affinity blotting for the detection of separated AFP bands [5,6]. Clinical evaluation of this method coupled with affinity electrophoresis of AFP is reported in this article.

Antibody-affinity blotting

This method is a blotting technique using nitrocellulose membranes which are precoated with purified horse antibodies to human AFP, followed by enzymatic amplification of transferred AFP with rabbit antibodies to human AFP and goat anti-rabbit

IgG(H + L)-horseradish peroxidase conjugate (Bio-Rad Labs., Richmond, CA, USA). By this method, AFP bands of only a few per cent of applied AFP (4 μl of 200 ng/ml) can be quantitatively detected. The sensitivity of the detection system can be increased to 4 μl of 50 ng/ml by employing Vectastain ABC kit (Vector Labs., Burlingame, CA, USA) [7].

In this study, erythroagglutinating phytohaemagglutinin (E-PHA) was used in addition to LCA-A as affinity media by including these lectins in agarose gels at a concentration of 0.2 mg/ml for LCA-A and 0.5 mg/ml for E-PHA. Separated AFP bands were identified by the system of nomenclature proposed by Taketa and Hirai [6]. The major AFP bands are numbered consecutively from the anode so that the most anodal band is band 1, and the band numbers are suffixed by the capitalized initial letters of the lectins used: for example, AFP-L1, -L2 and -L3 for LCA-A and AFP-P1, -P2, -P3, -P4 and -P5 for E-PHA. Those bands may be readily identified, as shown in Fig. 1.

Altered lectin-reactive patterns of AFP in malignancies

Representative patterns of AFP bands separated by LCA-A and E-PHA affinity electrophoresis of sera from patients with benign and malignant diseases associated with AFP production are shown in Fig. 1. The proportion of AFP-L3 increases in HCC, while AFP-L2 increases in yolk sac tumours. Broad unresolved bands of AFP-L2 and AFP-L3 are frequently seen in gastric carcinomas. With E-PHA,
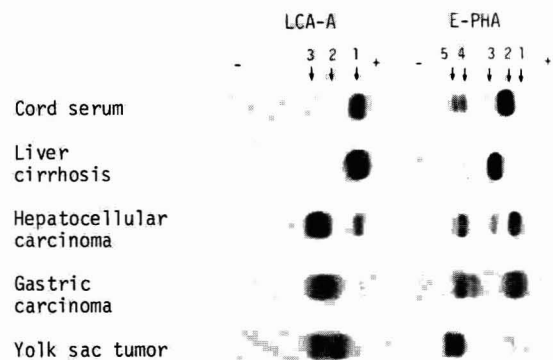
Fig. 1. Representative patterns of AFP bands separated by lectin affinity electrophoresis.

AFP separates into five bands, although only three bands are seen in cord serum AFP, namely AFP-P2 as a major band and AFP-P4 and AFP-P5 as minor ones. The proportions of AFP-P4 and AFP-P5 in liver cirrhosis are much less than those in cord serum, while the proportion of AFP-P4 is increased in HCC and that of AFP-P5 is increased in gastric carcinomas. In yolk sac tumours, AFP-P4 and AFP-P5 are major components. AFP-P3 is frequently present in patients with chronic hepatitis and liver cirrhosis with or without HCC. AFP-P1 is seen in most patients with extrahepatic tumours.

Accordingly, the AFP band pattern of HCC is characterized by increased proportions of AFP-L3 and AFP-P4. The degree of the increase varies from one case to another, reaching a value of over 90% for AFP-L3 and a value as high as 50% for AFP-P4. AFP-L3 and AFP-P4 increase independently, resulting in an increased sensitivity when these two markers are used in combination.

Clinical significance as early diagnostic markers

In an attempt to discriminate chronic hepatitic and cirrhotic patients without HCC from those with HCC, cut-off levels of AFP-L3 and AFP-P4 were determined using the values in those chronic liver disease patients who had no signs of HCC for at least one year after analysis of AFP-L3 and AFP-P4. Since the fractionation of AFP with lectin was carried out to increase the sensitivity of AFP as a diagnostic marker, not a screening marker, cut-off levels were set at the means plus three standard deviations of the values obtained for the benign liver diseases. From the cumulative frequency distribution of the values for a group of patients with chronic hepatitis and liver cirrhosis, the specificities for AFP-L3 and AFP-P4 may be calculated to be 99.9% for both. The actual cut-off levels and sensitivities of LCA-A- and E-PHA-dependent AFP bands are given in Table II.

Among the single bands of AFP used as markers of HCC of varying stages with serum AFP levels above 200 ng/ml, AFP-P4 has the highest sensitivity, 88%, followed by AFP-L3 with a sensitivity of 78% and AFP-P5 with a sensitivity of 57%. The addition of AFP-P4 and AFP-P5 gives a sensitivity of 91%, which is higher than either alone. Combined evaluation of AFP-L3 and AFP-P4, taking the result positive when either alone or both exceed the respective cut-off levels, gives the highest sensitivity of 97% at nearly the same specificity of 99.7%. Incidentally, the importance of AFP-C1, AFP-L2 and AFP-P5 as markers of gastrointestinal tumours and yolk sac tumours is also clearly shown in Table II.

In patients in whom serum AFP levels are below 200 ng/ml, a slightly reduced sensitivity of 68% is reported for AFP-L3 and 63% for AFP-P4, and 88% for AFP-L3 and/or AFP-P4 with a serum AFP level as low as 16 ng/ml [7]. When these results are taken together with the positive rate of total serum AFP level of HCC for the latest two-year period using a cut-off level of 10 ng/ml, the positive rate of AFP in HCC is calculated to be $46.3 \times 0.88 + 43.2 = 83.9\%$. This indicates that the overall positive rate of AFP assay, including AFP-L3 and AFP-P4, in the latest two years is greater than the initial positive rate of total serum AFP level alone in 1971–1975 shortly after the development of radioimmunoassay of AFP. Thus, AFP is still the most sensitive and specific marker of HCC notwithstanding the current prevalence of diagnostic imaging directed to HCC.

In our studies monitoring the variation in AFP-L3 and AFP-P4 content during the follow-up of

TABLE II

PERCENTAGE SENSITIVITIES OF AFP BANDS AT A SPECIFICITY OF 99.9%

CLD = Chronic liver disease (chronic hepatitis plus liver cirrhosis); GIT = gastrointestinal tumours; YST = yolk sac tumour. Numbers of cases studied were 43 for CLD, 58 for HCC, 21 for GIT and 7 for YST. Modified from ref. 7.

AFP band	Cut-off levels for CLD	HCC	GIT	YST
C1	9	34	95	100
L2	0	3	57[a]	100
L3	15	78	71[a]	71
L2 + L3 (or L2-3)	15	78	90	100
P1	1	22	57	86
P3	11	5	38	57
P4	12	88	90	86
P5	6	57	86	100
P4 + P5 (or P4-5)	16	91	100	100

[a] L3-2 is included when present.

TABLE III

TEMPORAL RELATIONSHIP BETWEEN ALTERED LECTIN REACTIVITY OF AFP AND DETECTION OF HCC BY IMAGING

HCC = Definite diagnosis of HCC; HCC(?) = HCC suspected; HCC(−) = HCC not demonstrated. Modified from ref. 8.

Date		AFP (g/l) (<20)	Scintigraphy	Ultrasonic examination	CT	Angiography	Lectin-reactive pattern of AFP
1981	Sept. 28	33.9					
	Oct. 7						LC
	Oct. 21		LC				
	Dec. 8						
1983	Jan. 19			LC			
	Jan. 24		LC				
	Aug. 31	47.5			HCC(?)		
	Oct. 18	40.4		HCC(?)			
1984	March 13						LC
	May 25	45.0					HCC
	Oct. 12	29.1		HCC(?)			
1985	Feb. 1	34.2		LC			
	March 19				HCC		
	March 27			HCC			
	July 11	41.4		HCC		HCC	
	Sept. 11				HCC		
1986	Feb. 14	747				HCC	
	March 29					HCC	
	Aug. 7	53, 100		HCC		HCC	
	Aug. 12			+			

patients with AFP-positive liver cirrhosis, as early as 10 months before localization of HCC, AFP-L3 and AFP-P4 were shown to become positive (Table III). The altered lectin-reactive pattern of AFP also precedes by 1 year the rise in total AFP level. In studies on another group of 35 cirrhotic patients we have demonstrated that AFP-L3 and AFP-P4 became positive at almost the same time in eight patients, AFP-L3 became positive first in three patients, and AFP-P4 became positive first in six patients 1–25 months before detection of HCC by diagnostic imaging [9]. The results suggest that the AFP-L3 and AFP-P4 serve as preclinical markers of HCC. Whether the altered lectin-reactive patterns of AFP represent the presence of HCC cells or of merely a preneoplastic state of hepatocytes remains to be solved in future studies.

REFERENCES

1 E. Ruoslahti and M. Seppälä, *Int. J. Cancer*, 8 (1971) 374–383.
2 S. Nishi and H. Hirai, *Gann Monogr. Cancer Res.*, 14 (1973) 79–81.
3 J. Bręborowicz, A. Mackiewicz and D. Bręborowicz, *Scand. J. Immunol.*, 14 (1981) 15–20.
4 J. Miyazaki, Y. Endo and T. Oda, *Acta Hepatol. Jpn.*, 22 (1981) 1559–1568.
5 K. Taketa, E. Ichikawa, H. Taga and H. Hirai, *Electrophoresis*, 6 (1985) 492–497.
6 K. Taketa and H. Hirai, *Electrophoresis*, 10 (1989) 502–567.
7 K. Taketa, C. Sekiya, M. Namiki, K. Akamatsu, Y. Ohta, Y. Endo and K. Kosaka, *Gastroenterology*, 99 (1990) 508–518.
8 H. Taga, H. Hirai, H. Ishizuka and W. Kaneda, *Tumor Biol.*, 9 (1988) 110–115.
9 Y. Endo, H. Taga and H. Hirai, *Physico-Chem. Biol.*, 34 (1990) 250.

High-performance hydroxyapatite chromatography of integral membrane proteins and water-soluble proteins in complex with sodium dodecyl sulphate

Per Lundahl

Department of Biochemistry, Biomedical Centre, Uppsala University, Box 576, S-751 23 Uppsala (Sweden)

Yasushi Watanabe and Toshio Takagi

Institute for Protein Research, Osaka University, 3-2 Yamadaoka, Suita, Osaka 565 (Japan)

ABSTRACT

Integral membrane proteins from human erythrocytes were fractionated in the presence of sodium dodecyl sulphate (SDS) on four types of high-performance hydroxyapatite columns. A column of 2-μm sintered hydroxyapatite beads from Asahi Optical (Tokyo, Japan) gave the best resolution. With this column, glycophorin was eluted early in a gradient of increasing sodium phosphate buffer concentration, the glucose transporter was eluted later in two zones, one of which contained this protein alone, and the anion transporter was eluted last. Water-soluble proteins applied in complex with SDS also separated reasonably well upon elution. The water-soluble proteins and the membrane proteins were all eluted mainly in the order of increasing polypeptide length, but with considerable individual variation. SDS–polypeptide complexes are probably adsorbed onto hydroxyapatite by the interaction of positively charged amino acid side groups with phosphate ions (at P-sites) and of negatively charged amino acid side groups and polypeptide-bound dodecyl sulphate anions with calcium ions (at C-sites). As a rule, the number of charged side groups and dodecyl sulphate anions, and thus the number of binding sites, increases with the polypeptide chain length, which explains the general order of release of the polypeptides.

INTRODUCTION

Hydroxyapatite chromatography of water-soluble proteins in the presence of sodium dodecyl sulphate (SDS) was introduced by Moss and Rosenblum in 1972 [1]. Later applications failed to contribute any persuasively efficient example of such separations and often suffered from unsatisfactory reproducibility. Sintered hydroxyapatite and other new preparations afford improved reproducibility between runs and between different batches of hydroxyapatite. A significant reduction in the run time was achieved upon development of the high-performance liquid chromatography (HPLC) type hydroxyapatite packing materials that are now commercially available from several sources. Recently, Horigome *et al.* [2] efficiently fractionated rat erythrocyte membrane proteins solubilized in SDS on HPLC columns of ceramic (sintered) or coral-shaped hydroxyapatite and could resolve several components. They identified one transmembrane protein, the anion transporter. This might be the first successful application of this technique for separation of membrane proteins in the presence of SDS.

It seemed important to examine the performance of the HPLC-type hydroxyapatite chromatography in the presence of SDS for integral (intrinsic) membrane proteins only, the major ones in erythrocytes being the anion transporter, the glucose transporter

Correspondence to: Dr. P. Lundahl, Department of Biochemistry, Biomedical Centre, Uppsala University, Box 576, S-751 23 Uppsala, Sweden.

and glycophorin, rather than a more complicated mixture containing also several other proteins. Mascher and co-workers [3,4] have previously fractionated integral membrane proteins from human erythrocytes by molecular sieve chromatography on Superose 6 in the presence of SDS after thorough removal of cytosolic proteins, cytoskeletal proteins and other peripheral membrane proteins. We have now fractionated such integral membrane proteins by HPLC on sintered and coral-shaped hydroxyapatite in the presence of SDS. Several water-soluble globular proteins were also complexed with SDS and the behaviour of the corresponding SDS-polypeptide complexes was investigated to ascertain whether there was something special about the behaviour of intrinsic membrane proteins.

Horigome et al. [2] found a positive correlation between the retention time of SDS complexes of 24 water-soluble proteins and the logarithm of their molecular weight upon phosphate buffer gradient elution from hydroxyapatite. The proteins were not specified. The authors discuss this in terms of the binding of SDS to water-soluble proteins in proportion to the polypeptide length and imply that SDS-polypeptide complexes bind to hydroxyapatite mainly as a result of the negative charge derived from the dodecyl sulphate (DS) anions in the complexes. This is probably correct, and the purpose of our present work was to verify or disprove that polypeptides are released from hydroxyapatite in the presence of SDS essentially in the order of increasing polypeptide chain length, for membrane proteins as well as for water-soluble proteins, as the phosphate buffer concentration is increased. However, we want to emphasize that charged amino acid side groups can contribute to the binding and cause individual variations in the elution of polypeptides of similar lengths. A tentative model is thus presented for the equilibrium state of binding of SDS-polypeptide complexes to hydroxyapatite: we propose that positively charged amino acid side groups interact with the "phosphate sites" (P-sites) of the hydroxyapatite, whereas negatively charged side groups and dodecyl sulphate anions interact with the "calcium sites" (C-sites) [5–8].

The structure of free SDS–polypeptide complexes may be described by the "necklace model" [9–11] or by the "protein-decorated micelle modell" [12], but the complexes probably rearrange upon binding. As

discussed below, it is important that SDS is released upon binding of the complexes to hydroxyapatite, as shown by Watanabe et al. [13].

EXPERIMENTAL

Materials

SDS (AnalaR No. 10807) was obtained from BDH Chemicals (Poole, UK). Low-molecular-weight calibration proteins for electrophoresis were purchased from Pharmacia-LKB Biotechnology (Uppsala, Sweden). Carbonic anhydrase (C-7500), cytochrome c (C-7752) and chicken egg ovalbumin (A-7641) were bought from Sigma (St. Louis, MO, USA). β-Lactoglobulin was obtained from Miles (UK) and β-galactosidase was a gift from Daiichi Chemicals (Tokyo, Japan). Rabbit IgG was prepared and purified on DEAE–cellulose by T. Takagi. Bovine serum albumin (No. 002, "reagent grade") was bought from Chiba Chikusan Kogyo (Chiba, Japan). Chemicals were of reagent grade and high-quality deionized water was used. All solutions were filtered through 0.3-μm filters (PHWP 04700, Nihon Millipore Kogyo, Yonezawa, Japan).

Four hydroxyapatite columns were used: (a) Tonen Taps-020810, 2-μm beads (Toa Nenryo Kogyo K. K., Tokyo, Japan); (b) PENTAX SH-0710F, 2-μm beads (Asahi Optical); (c) A-7610, 3-μm beads, with guard column C-3201 (Koken, Tokyo, Japan) and (d) TSKgel HA-1000, 5-μm beads, with TSK guard HA-1000 column (Tosoh, Tokyo, Japan). Columns a and b were used without guard columns. The dimensions of columns a, b and d were 100 mm × 7.5 mm I.D., and those of column c were 100 mm × 7.6 mm I.D.

The chromatographic equipment consisted of an ERC-3510 degasser from Erma Optical Work (Kawaguchi, Japan), a CCPM HPLC pump with a controller for gradient programming and an injector, a CM-8000 conductometer, a UV-8 Model II spectrophotometer set at 280 nm and a TSK two-channel recorder, all from Tosoh.

Sample preparation

(1) Integral membrane proteins together with membrane lipids from human erythrocytes (i.e. membranes stripped of peripheral proteins and free from water-soluble proteins) were prepared and finally adjusted to 10 mg of protein per ml of 50 mM

Tris–HCl (pH 6.7 at 25°C), frozen in liquid nitrogen and stored at −70°C as described previously [4]. A 2.5-ml aliquot of the preparation was mixed with 1 M sodium phosphate buffer (pH 6.56), 350 mM SDS and other components to a final composition of 2 mg of protein per ml, 10 mM Tris–HCl, 10 mM sodium phosphate buffer (final pH 6.8), 0.5 mM dithioerythritol (DTE), 100 mM SDS and 2 mM sodium azide. The solution was stirred for 5 min at 25°C and centrifuged at 160 000 g for 40 min at 25°C. A very small pellet was formed. The supernatant was collected, frozen immediately in 350-μl aliquots and kept at −70°C.

(2) Low-molecular-weight calibration proteins for electrophoresis (60–130 μg of each of bovine milk α-lactalbumin, soybean trypsin inhibitor, bovine erythrocyte carbonic anhydrase, egg white ovalbumin, bovine serum albumin and rabbit muscle phosphorylase b) were mixed with 1.2 ml of solution S (10 mM sodium phosphate buffer, pH 6.8, 0.1 mM calcium chloride, 100 mM SDS and 3 mM sodium azide. DTE (3.0 mg) was added to give a final concentration of 16 mM. The solution was heated to 80°C over 2 min, kept at that temperature for 6 min and then cooled to 25°C and centrifuged at that temperature at 100 000 g for 30 min. No pellet was seen. The solution was divided into aliquots, frozen immediately and kept at −70°C.

(3) Horse heart cytochrome c (1.4 mg), β-lactoglobulin (1.5 mg), bovine erythrocyte carbonic anhydrase (1.5 mg), rabbit IgG (2.4 mg) and β-galactosidase (1.4 mg) were mixed and dissolved in 5 ml of solution S. DTE (16.3 mg) was added and the solution was treated as described in (2) above except that it was filtered through a 0.22-μm filter (type SLGV025LS, Nihon Millipore Kogyo, Yonezawa, Japan) before freezing.

(4) Cytochrome c (1.1 mg), β-lactoglobulin (0.8 mg), carbonic anhydrase (0.7 mg), ovalbumin (0.7 mg), rabbit IgG (1.1 mg), bovine serum albumin (0.6 mg) and β-galactosidase (0.7 mg) were dissolved separately, each in 2 ml of solution S. DTE (6 mg) was added to each sample. The samples were treated as in (3) above.

Hydroxyapatite chromatography

Before each experiment the column was equilibrated with at least 120 ml of solution A 10 mM sodium phosphate buffer (10 mM phosphorus), pH 6.82, 0.1 mM calcium chloride, 3.5 mM (0.1%) SDS and 3 mM sodium azide] at 0.8 ml/min, except for the PENTAX column (see below). The ionic strength of this solution is 27 mM and the corresponding critical micelle concentration (CMC) of SDS is about 3.1 mM according to Fig. 7-2 in ref. 14. During this equilibration the column became saturated with SDS [13] and the conductivity of the eluted buffer stabilized at 2.10 ± 0.02 mS/cm. The end solution, solution B, was 585 mM sodium phosphate buffer (585 mM phosphorus), pH 6.56, 5 μM calcium chloride, 3.5 mM SDS and 3.5 mM sodium azide. This solution was stable at and above 25°C; at lower temperatures SDS precipitated. The experiments were performed at 25–27°C. Solutions A and B were both prepared from stock solutions of (a) 1.00 M sodium phosphate buffer containing 6 mM sodium azide, pH 6.51 at 25°C, (b) 10 mM calcium chloride and (c) 350 mM SDS containing 6 mM sodium azide. The given final pH values were those obtained after dilution of the stock buffer; no adjustment was done. The SDS solutions were stored in glass bottles as plastic bottles containing SDS solutions can release components which become adsorbed to hydroxyapatite.

After column equilibration, 250 μl of protein sample were applied at a flow-rate of 0.8 ml/min. At 5 min after the start of sample application the percentage of solution B was linearly increased to 50% (298 mM phosphate buffer) over 1 min and was then increased linearly to 100% (585 mM phosphate buffer) over another 38 min (slope 9.4 mM/ml). The elution with solution B was continued until the UV absorption became constant. The flow-rate was 0.8 ml/min throughout the elution. With the PENTAX column, which tolerated high pressure, re-equilibration was performed at 1.5–1.8 ml/min, but the flow-rate was lowered to 0.8 ml/min about 30 min before each run, since lowering the flow-rate resulted in the elution of a broad zone of slightly increased conductivity.

Electrophoresis

SDS polyacrylamide gel electrophoresis (PAGE) was done essentially as described by Laemmli [15] with a 70-mm-long and 0.5-mm-thick separation gel of 12.2% acrylamide and 0.34% N,N' methylenebisacrylamide. The stacking gel contained 4.4% acrylamide and 0.12% of the cross-linker. A 30-μl sample was mixed with 10 μl of

water containing 40% (v/v) glycerol and 8% (w/v) SDS and with 2 μl of water containing 0.6 μg of bromophenol blue. A 10-μl volume of the mixture was applied in 4-mm-wide wells. The gels were stained with the silver-staining kit 2D-Silver Stain II DAIICHI (Daiichi Pure Chemicals).

RESULTS

Integral erythrocyte membrane proteins

Fig. 1 shows the elution patterns obtained for the SDS complexes of the human erythrocyte integral (intrinsic) membrane proteins using the four HPLC-type hydroxyapatite columns. As is clear from the comparison, the PENTAX column gave the best overall resolution (Fig. 1B). Electrophoret-

ic analysis of fractions from this column, as illustrated in Fig. 2, showed good separation between the major proteins glycophorin (Figs. 1B and 2, fraction a), the glucose transporter (broad zones [3,4], in fractions d and e) and the anion transporter (fractions f–h). However, only the peak corresponding to fraction e in Fig. 1B contained a single essentially pure component, namely the glucose transporter. For details, see the legend to Fig. 2. With the other three columns the elution profiles were compressed (Fig. 1A, C and D) and the resolution was lower.

Nine runs were made on the PENTAX column with essentially the same result (Fig. 1B) in the last eight. Four to six runs were made on the other columns, also with consistent results.
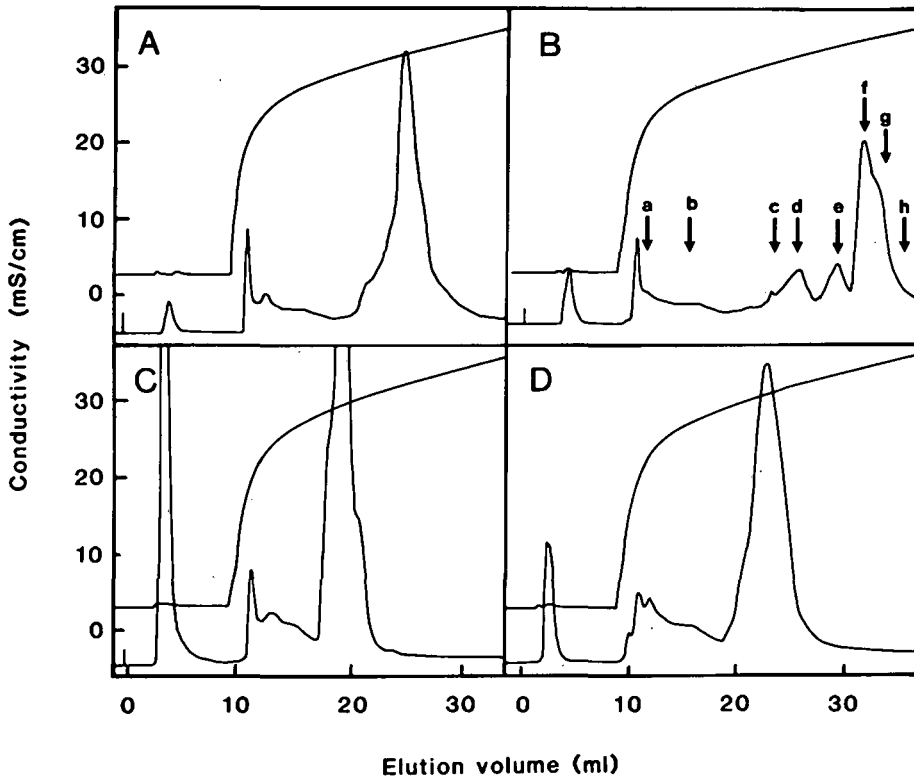
Fig. 1. Elution patterns (absorbance at 280 nm) obtained for solubilized human erythrocyte integral (intrinsic) membrane proteins (see Experimental) in complex with SDS using the HPLC-type hydroxyapatite columns: (A) Tonen Taps-020810, (B) PENTAX SH-0710F, (C) A-7610 and (D) TSKgel HA-1000. Protein amount: 0.5 mg. The SDS–polypeptide complexes were eluted with a gradient in phosphate buffer concentration, as described in the Experimental section. Flow-rate: 0.8 ml/min. The height of the panels corresponds to an absorbance of 0.12. The arrows indicate fractions analysed by electrophoresis (see Fig. 2). A conductivity of 10, 20 and 30 mS/cm at 25°C corresponds to a phosphate concentration of 85, 205 and 370 mM, respectively, in the eluent.
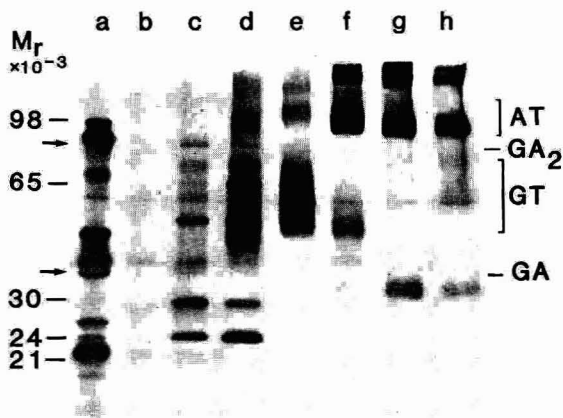
Fig. 2. Electrophoretic analysis of fractions a–h in the chromatogram in Fig. 1B. (a) Glycophorin A monomers and dimers (arrows, denotations GA and GA$_2$, respectively) and other components; (b) mainly lipids, appearing as a clear zone near the front in the original gel; (c) unidentified protein zones; (d) broad zones probably corresponding to the glucose transporter monomer and dimer, and sharper zones corresponding to other components similarly as in (c); (e) pure glucose transporter monomer, dimer and trimer; and (f–h) mainly the anion transporter and different proportions of unidentified slowly migrating components. The broad zones in (d) have migrated slightly faster than the corresponding zones in (e), possibly because of differences in the glucose transporter oligosaccharide.

Electrophoretic analyses (not illustrated) confirmed that the order of elution of the components was the same with all four columns, although the resolution differed. No attempt was made to optimize the resolution by changing the chromatographic conditions.

Water-soluble proteins

Only the PENTAX column was used for water-soluble proteins. The resolution of low-molecular-weight electrophoresis calibration proteins was reasonably good, as illustrated in Fig. 3A (fourth run with these proteins). The resolution was slightly better in three earlier runs, possibly because of a small batch-to-batch change in the composition of starting buffer before the fourth run. α-Lactalbumin (j), carbonic anhydrase (k), ovalbumin (l) and phosphorylase b (m) were identified by electrophoresis. The mixture of proteins that was prepared as described in the Experimental section (Sample preparation 3) was resolved as shown in Fig. 3B. Electrophoresis revealed the order of elution: cyto-

chrome c (n), H-chain of IgG (o), carbonic anhydrase (k) and β-galactosidase (p). To confirm the identification of the zones, several of the water-soluble proteins were converted to SDS protein complexes as described in the Experimental section (Sample preparation 4) and were run separately. The results were as expected (not illustrated).

Elution order

The buffer concentrations corresponding to the positions of the SDS-polypeptide peaks in the chromatograms were plotted against the relative molecular weights (M_r) of the polypeptides. This was done for several water-soluble proteins and for two integral membrane proteins, the glucose transporter (polypeptide M_r 54 117) [16] and the anion transporter (polypeptide M_r 101 791) [17] (Fig. 4). Glycophorin is small (131 amino acid residues, M_r about 31 000, including oligosaccharides) [18] and was eluted early (see Figs. 1B and 2). This is not shown in Fig. 4 as the elution of glycophorin preceded the main gradient elution with the slope 9.4 mM/ml.

Glycophorin contains only one transmembrane α-helix, which is perhaps inserted into a single SDS micelle, and the extracellular part of the polypeptide is long and heavily glycosylated. This explains the special behaviour of glycophorin. The diagram in Fig. 4 shows that the longer polypeptides were in general eluted at higher buffer concentration than the shorter ones. For proteins with similar polypeptide lengths the elution positions varied considerably. The two large, major integral membrane proteins, the glucose and anion transporters, which are thought to contain twelve and fourteen hydrophobic transmembrane α-helices, respectively [16,17], were eluted at about the same positions as water-soluble proteins of similar polypeptide chain lengths.

DISCUSSION

The performances of the four hydroxyapatite columns that we have studied differed considerably under the single set of chromatographic conditions used. Changes in the conditions can perhaps improve the result for each individual column. All of them gave reproducible elution profiles and the same order of elution of integral (intrinsic) erythro-
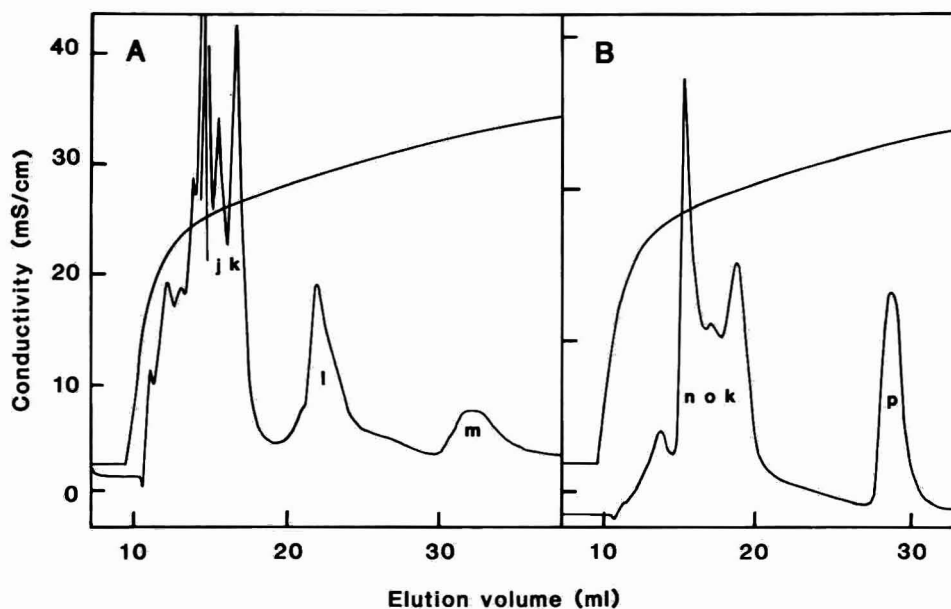
Fig. 3. Elution patterns (absorbance at 280 nm) of water-soluble proteins on the PENTAX column. Mixtures of proteins were prepared as described in the Experimental section (A, *Sample preparation* 1, B, *Sample preparation* 2) and the order of elution was identified by electrophoresis (not shown). (A) Low-molecular-weight electrophoresis calibration proteins: j = α-lactalbumin; k = carbonic anhydrase; l = ovalbumin; and m = phosphorylase *b*. (B) Protein mixture: n = Cytochrome *c*; o = H-chain of IgG; k = carbonic anhydrase; and p = β-galactosidase. Protein amount: 13–27 μg of each protein in (A) and about 70 μg of each protein (polypeptide) in (B). Flow-rate: 0.8 ml/min. The height of (A) corresponds to an absorbance of 0.03 and that of (B) to 0.13. A conductivity of 40 mS/cm at 25°C corresponds to a phosphate concentration of approximately 540 mM in the eluent.
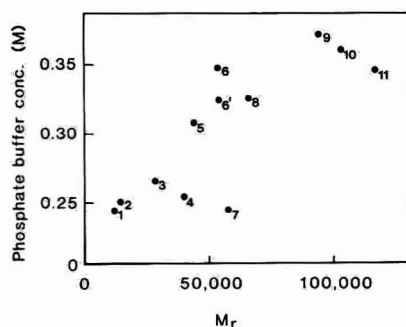
Fig. 4. SDS–polypeptide complexes eluted from the ceramic PENTAX hydroxyapatite column. The phosphate buffer concentration corresponding to each polypeptide peak was estimated from the recorded conductivity and a calibration curve and was plotted against the polypeptide relative molecular weight (M_r). This was done for nine water-soluble proteins and for two integral membrane proteins from human erythrocytes, the glucose transporter and the anion transporter. Data are from experiments illustrated in Figs. 1–3 and an experiment with β-lactoglobulin (not illustrated). The proteins were: 1 = cytochrome *c*; 2 = α-lactalbumin; 3 = carbonic anhydrase; 4 = β-lactoglobulin; 5 = ovalbumin; 6 = the glucose transporter (e in Figs. 1B and 2); 6′ = the glucose transporter (d in Figs. 1B and 2); 7 = H-chain of IgG; 8 = bovine serum albumin; 9 = phosphorylase b, 10 = the anion transporter (f in Figs. 1B and 2); and 11 = β-galactosidase.

cyte membrane proteins, but the resolution differed. The PENTAX column SH-0710F showed the best separation of the membrane proteins, as illustrated in Fig. 1, and allowed a high flow-rate. However, even with this excellent column only one fraction contained a pure protein, the glucose transporter. This transporter also appeared in another fraction. The reason for this dual elution is not known, but the tendency of integral membrane proteins to form dimers and to appear in both monomeric and dimeric forms in the presence of SDS (as in the presence of non-ionic detergents) may be of importance. Monomers may be released earlier than dimers, and dimers may dissociate upon electrophoresis. Most fractions contained several components, and the result of hydroxyapatite chromatography of membrane proteins in the presence of SDS therefore usually has to be analysed by electrophoresis.

The chromatographic experiments presented here were all done with 3.5 mM SDS in the eluent, which is above the CMC of SDS even at the low ionic strength (27 mM) of the starting buffer, as men-

tioned above. As is well known, the CMC for ionic detergents decreases with increasing ionic strength. Later experiments on the PENTAX column showed that the resolution of the intrinsic membrane proteins decreased, whereas the resolution of water-soluble proteins increased, when the SDS concentration was increased to 35 mM (1%). We do not know why this was so. The SDS/protein binding ratio for a membrane protein, at an equilibrium concentration of free SDS near the CMC, can be similar to that for water-soluble proteins [19]. Nevertheless, differences in the SDS/protein binding ratios and in the homogenity of binding may occur upon adsorption to hydroxyapatite and may depend on the SDS concentration. However, although the glucose transporter and the anion transporter contain several hydrophobic α-helices which may bind especially large amounts of dodecyl sulphate, they did not bind exceptionally strongly to hydroxyapatite in the presence of SDS in the present experiments. The contribution of dodecyl sulphate to the adsorption of the complex to hydroxyapatite is thus probably similar for integral membrane proteins and water-soluble proteins at a concentration of free SDS near the CMC, although the distribution of hydrophobic amino acid side groups along the polypeptide chains differs.

The structure of SDS–protein complexes has recently been studied by small-angle neutron scattering in Brookhaven [10,11] and in Grenoble [12]. The recent result of Guo et al. [11] indicated, for example, that eight SDS micelles of an average aggregation number of 43 were associated with the bovine serum albumin (BSA) polypeptide (M_r 66 267) [20] in the presence of 1.5 g of SDS per g of BSA at an ionic strength of 0.2 M. The structure of the complex was described as being of the "necklace" type. The normal binding level of 1.5 g of SDS per g of BSA ($344 = 8 \times 43$ SDS molecules per BSA molecule) at the CMC of SDS is consistent with the data of Guo et al. [11]. However, a certain concentration of free SDS is required for equilibrium to prevail. This was not explicitly taken into account in the paper of Guo et al. [11]. The results of Ibel et al. [12] indicated that three SDS micelles of about 42, 101 and 73 SDS molecules (from the polypeptide N-terminus to the C-terminus) are part of the SDS complex with a water-soluble enzyme of M_r 49 484, i.e. smaller than BSA, near the saturation level and at

an ionic strength of 0.1 M. The structural model is denoted "the protein-decorated micelle model". The number of SDS molecules in these three micelles, 216, corresponds to 1.26 g of SDS per g of the enzyme. The limit of error in the SDS aggregation numbers observed by Ibel et al. [12] is about $\pm$ 5%, and it cannot be excluded that an additional small SDS micelle has escaped detection. The discrepancy between the reported numbers of SDS micelles in the complexes [11,12] is thus reasonably small when the differences in polypeptide lengths and experimental conditions are taken into consideration.

For the binding of SDS–polypeptide complexes to hydroxyapatite it is probably important to realize that ionic amino acid side chains can participate in the equilibrium state of binding of the polypeptides to the hydroxyapatite. As recently shown by Watanabe et al. [13] the binding process is accompanied by release of a substantial amount of SDS from the hydroxyapatite or the SDS–polypeptide complex, probably from both. Release of an amount of SDS corresponding to about 80% of the SDS initially bound to the polypeptide was observed. It is likely that the SDS–polypeptide complex changes its structure upon binding to hydroxyapatite and that the binding involves ionic bonds between negatively and positively charged amino acid side groups and the C-sites and P-sites of the hydroxyapatite, respectively. This will lead to different binding strengths depending on the number of charges and the distribution of charges along the polypeptide chain, in agreement with the spread of the elution positions for polypeptides of similar sizes in earlier chromatographic experiments [2] and in our present experiments. It will also lead to the strongest binding of a polypeptide to hydroxyapatite near its isoelectric point (pI), where the net charge is low but where the number of charged amino acid side groups usually has a maximum. This is consistent with the results illustrated in Fig. 6, left panel, in ref. 2. However, as a rule, at a given pH value and for polypeptides of similar pI values the overall number of charged groups and therefore of potential binding sites increases with the length of the polypeptide. The number of polypeptide-bound dodecyl sulphate anions increases with the polypeptide length in free complexes and probably also in the hydroxyapatite-adsorbed state. These two circumstances explain the results summarized in our
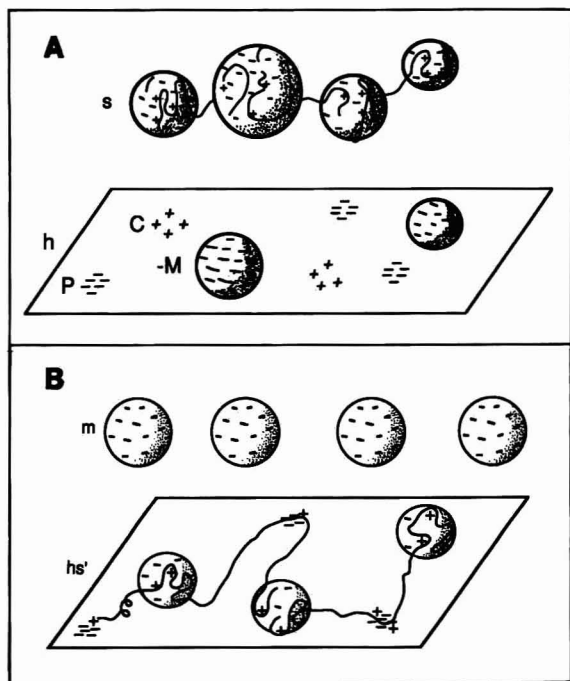
Fig. 5. Schematic illustration of the binding of an SDS–polypeptide complex to hydroxyapatite. (A) An SDS–protein complex (s) depicted according to the "protein-decorated micelle model" [12] approaches a hydroxyapatite surface (h) with P- and C-sites [6] where SDS micelles (M) are bound. (B) Hypothetical model of an equilibrium state with bound polypeptide (hs'). Part of the SDS has been released (micelles m) [13] and charges on the rearranged polypeptide bind electrostatically to P- and C-sites, whereas residual dodecyl sulphate anions interact electrostatically with the C-sites and by hydrophobic interaction and possibly also by hydrogen bonding [21] with the polypeptide.

Fig. 4 and the results illustrated in Fig. 6, middle panel, of ref. 2.

Taking the above into consideration, and using the "protein-decorated micelle structure" [12] for SDS–protein complexes as a starting point, since this is the most detailed model yet available, we envisage that the binding of an SDS–polypeptide complex to hydroxyapatite, schematically and hypothetically, is as illustrated in Fig. 5.

Molecular sieve chromatography separates SDS–protein complexes mainly according to size and shape, as exemplified in ref. 3, and hydroxyapatite chromatography is probably based on polypeptide chain length and the number of charged amino acid side groups, as discussed above. These two methods, in combination, can therefore be expected to give good results in many cases, and require little time with the modern HPLC materials.

REFERENCES

1 B. Moss and E. N. Rosenblum, *J. Biol. Chem.*, 247 (1972) 5194.
2 T. Horigome, T. Hiranuma and H. Sugano, *Eur. J. Biochem.*, 186 (1989) 63.
3 E. Mascher and P. Lundahl, *Biochim. Biophys. Acta*, 856 (1986) 505.
4 P. Lundahl, E. Greijer, S. Cardell, E. Mascher and L. Andersson, *Biochim. Biophys. Acta*, 855 (1986) 345.
5 G. Bernardi, *Methods Enzymol.*, 27 (1973) 471.
6 T. Kawasaki, S. Takahashi and K. Ikeda, *Eur. J. Biochem.*, 152 (1985) 361.
7 S. Shimabayashi, H. Tanaka and M. Nakagaki, *Chem. Pharm. Bull.*, 35 (1987) 3539.
8 H. Tanaka, K. Miyajima, M. Nakagaki and S. Shimabayashi, *Chem. Pharm. Bull.*, 37 (1989) 2897.
9 K. Shirahama, K. Tsujii and T. Takagi, *J. Biochem. (Tokyo)*, 75 (1974) 309.
10 S. H. Chen and J. Teixeira, *Phys. Rev. Lett.*, 57 (1986) 2583.
11 X. H. Guo, N. M. Zhao, S. H. Chen and J. Teixeira, *Biopolymers*, 29 (1990) 335.
12 K. Ibel, R. P. May, K. Kirschner, H. Szadkowski, E. Mascher and P. Lundahl, *Eur. J. Biochem.*, 190 (1990) 311.
13 Y. Watanabe, T. Okuno, K. Ishigaki and T. Takagi, *Anal. Biochem.*, (1992) in press.
14 C. Tanford, *The Hydrophobic Effect: Formation of Micelles and Biological Membranes*, Wiley, New York, 2nd ed., 1980.
15 U. K. Laemmli, *Nature*, 227 (1970) 680.
16 M. Mueckler, C. Caruso, S. A. Baldwin, M. Panico, I. Blench, H. R. Morris, W. J. Allard, G. E. Lienhard and H. F. Lodish, *Science*, 229 (1985) 941.
17 S. E. Lux, K. M. John, R. R. Kopito and H. F. Lodish, *Proc. Natl. Acad. Sci. U.S.A.*, 86 (1989) 9089.
18 M. Tomita and V. T. Marchesi, *Proc. Natl. Acad. Sci.*, U.S.A., 72 (1975) 2964.
19 M. Wallstén and P. Lundahl, *J. Chromatogr.*, 512 (1990) 3.
20 R. G. Reed, F. W. Putnam and T. Peeters, Jr., *Biochem. J.*, 191 (1980) 867.
21 P. Lundahl, E. Greijer, M. Sandberg, S. Cardell and K.-O. Eriksson, *Biochim. Biophys. Acta*, 873 (1986) 20.

Short Communication

Thiophilic interaction chromatography of sweet potato β-amylase

Laura Franco-Fraguas and Francisco Batista-Viera

Cátedra de Bioquímica, Facultad de Química, Gral. Flores 2124, Casilla de Correos 1157, Montevideo (Uruguay)

ABSTRACT

The affinity of sweet potato β-amylase toward two kinds of thiophilic adsorbents [the so-called thiophilic or T-gel and 3-(2-pyridylsul-phido)-2-hydroxypropylagarose or PyS-gel] was demonstrated. Enzyme adsorption on both gels was promoted by antichaotropic salts. Lower salt requirements and higher protein recoveries were observed for the PyS gel, even though its ligand concentration was half that of T-gel. For the former gel, the effectiveness series for sulphates was $Na_2SO_4 > (NH_4)_2SO_4 > K_2SO_4 > MgSO_4$. Based on the thiophilic character exhibited by the pure sweet potato β-amylase and the reversibility of the salt effects, a new method for its purification from crude extracts was developed.

INTRODUCTION

Sweet potato β-amylase (EC. 3.2.1.2) is a gluca-nomaltohydrolase, practical interest in which centres on its capacity to produce maltose syrups acting on liquefied starch from several sources, especially if it is combined with the use of pullulanase (debranching enzyme). The interest in this enzyme also resides in its application in continuous processes in immobilized form and the study of its mechanisms of action. For such purposes highly purified preparations are needed. There are many reports on purification procedures for sweet potato β-amylase, based on crystallization or acetone precipitation of the enzyme [1–3], affinity chromatography [4], glycogen precipitation [5,6], thymol–amylose complexation [7], ion exchange on DEAE-Sephadex A-50

[8,9] and hydrophobic interaction chromatography [10].

Porath *et al.* [11] introduced the use of a new class of group-specific adsorbents for protein chromatography, consisting of T-gel, with the general structure $M–OCH_2SO_2CH_2CH_2SCH_2CH_2OH$, and 2-thiopyridineagarose gel (PyS-gel) [12], with the structure $M–OCH_2CH(OH)CH_2SPy$, where M = matrix and Py = pyridyl. So far, their main applications have been in the purification of immunoglobulins from serum [11–13] and of monoclonal antibodies [14].

As demonstrated by Hutchens and Porath [15], the affinity of the T-gel is not restricted to immunoglobulins because, depending on the experimental conditions, other proteins also show thiophilic character. In this work, we found that pure sweet potato β-amylase also exhibits thiophilic behaviour and the quantitative effects of antichaotropic salts on its adsorption were evaluated. Based on these studies, a new procedure for its fast and efficient

Correspondence to: Dr. F. Batista-Viera, Cátedra de Bioquímica, Facultad de Química, Gral. Flores 2124, Casilla de Correos 1157, Montevideo, Uruguay.

purification of the enzyme from unpigmented extracts by thiophilic interaction chromatography was developed.

EXPERIMENTAL

Materials

Sepharose 6B and DEAE-Sephadex A-50 were kindly provided by Pharmacia (Uppsala, Sweden). β-Mercaptoethanol, 2-mercaptopyridine and divinyl sulphone were purchased from Sigma (St. Louis, MO, USA). Soluble starch and 3,5-dinitrosalicylic acid were obtained from Carlo Erba (Milan, Italy). All other chemicals were of analytical-reagent grade.

Pure sweet potato β-amylase was obtained by hydrophobic interaction chromatography [10]. Its purity was tested by polyacrylamide gel electrophoresis.

Determination of enzyme activity and protein

Enzyme activity was assayed by the 3,5-dinitrosalicylic acid method [16] using 0.05 M sodium acetate (pH 4.8). Protein was determined spectrophotometrically at 280 nm, using an extinction coefficient ($E^{1\%}$, 280 nm) for β-amylase of 17.1 [17]; for the unpigmented extract the protein concentration was taken from the absorbance at 280 nm.

Enzyme unit, specific activity and enrichment ratio

One unit (U) of β-amylase activity is defined as the amount of enzyme that catalyses the production of 1 mg of maltose in 3 min at pH 4.8 under the assay conditions. The specific activity was defined as the number of enzyme units per milligram of protein. The enrichment ratio was expressed as the ratio of the specific activity after a given step and the initial step.

Synthesis of the thiophilic gels

T-gel was synthesized according to Porath et al. [11]. Essentially, 40 g of suction-dried Sepharose 6B were suspended in 40 ml of 0.5 M sodium carbonate solution (pH 11) and 2 ml of divinyl sulphone were added. The suspension was incubated with shaking for 18 h at room temperature and then thoroughly washed. The suction-dried activated gel was suspended in 40 ml of 0.1 M sodium hydrogencarbonate solution (pH 8.5) containing 2 ml of β-mercaptoethanol. The gel suspension was gently stirred for 20 h at room temperature and then thoroughly washed until free of β-mercaptoethanol. The ligand concentration was calculated to be 1312 μmol of ligand per gram of dried gel from sulphur elemental analysis of the gel before and after coupling with β-mercaptoethanol. PyS-gel was synthesized according to Porath and Oscarsson [12]. The ligand concentration calculated from sulphur and nitrogen elemental analysis was 657 μmol per gram of dried product.

Salt effects on the thiophilic adsorption of β-amylase

Aliquots of 0.5 g of suction-dried gels were incubated batchwise with gently mixing for 1 h at room temperature with 3.0 ml of sample (0.5 mg ml^{-1}) in the adsorption buffer i.e., 0.1 M phosphate (pH 7.4) containing 0.5 M salts. Elution of the adsorbed protein was performed by salt deletion and quantified only in cases when more than 50% adsorption was obtained. The same procedure was followed to determine the optimum concentrations of ammonium sulphate and sodium sulphate to reach 90% enzyme adsorption on both gels.

Preparation of sweet potato unpigmented extract

A 200-g amount of peeled and sliced sweet potato (Ipomea batata) was blended in a Waring blender with 200 ml of water and then centrifuged for 30 min at 3000 g at 4°C. The supernatant was collected and diluted twofold with 0.1 M phosphate (pH 6.0)–0.6 M sodium sulphate. Pigments were removed by ion exchange on DEAE-Sephadex A-50 batchwise. Before application to PyS-gel, the pH was raised to 7.4.

Purification of β-amylase by thiophilic interaction chromatography

A 45-ml volume of an unpigmented extract was applied to a column of PyS-gel [6.0 ml of packed gel equilibrated in 0.1 M phosphate (pH 7.4)–0.3 M sodium sulphate]. The flow-rate was 25-ml h^{-1} and 5.0-ml fractions were collected. Desorption was performed by sodium sulphate deletion and with 30% ethylene glycol.

Disc polyacrylamide gel electrophoresis

This was carried out according to Orstein and Davis [18]. Protein staining was performed with 1%

amido black solution in 7% acetic acid. For enzyme activity detection, gels run in parallel with stained gels were sliced into 3-mm pieces and incubated with 1 ml of activity buffer for 2 h. The enzyme activity was determined in the supernatants as described above.

RESULTS AND DISCUSSION

When pure β-amylase was applied to PyS-gel or T-gel in 0.1 M sodium phosphate (pH 7.4), only 10% of the protein applied was adsorbed. A possible way to promote protein adsorption on thiophilic gels was described by Porath et al. [11] for immunoglobulins using water-structuring salts. We investigated the effects of different sulphates at 0.5 M concentration on the enzyme adsorption on both gels (Table I).

These antichaotropic salts promoted adsorption on both gels to different extents; in both instances sodium sulphate was the most efficient. However, a difference in recovery of adsorbed protein by deletion of the salt was observed, viz., 65% from T-gel and 90% from PyS-gel.

The percentage adsorption of β-amylase on both gels was quantified as a function of the final concentration of sodium sulphate in the range 0–0.5 M (Fig. 1). To reach 90% adsorption of the pure enzyme, the T-gel required 0.5 M and the PyS-gel 0.3 M sodium sulphate. The same experiments were performed with ammonium sulphate owing to its versatility and wide use in protein fractionation (Fig. 2). Higher ammonium sulphate concentrations were required to reach similar protein adsorption levels on both gels.

Fig. 1. Effect of sodium sulphate on the thiophilic adsorption of β-amylase on (□) PyS-gel and (▲) T-gel.

The lower salt requirements of Pys-gel justified its selection for β-amylase purification. The reversibility of the binding allowed quantitative desorption and made possible the application of this procedure to the purification of the enzyme starting with unpigmented extracts of sweet potatoes (Fig. 3).

Most of the other proteins present in the extract passed through the column, showing a lack of thiophilicity under the chromatographic conditions. The enzyme activity can be eluted as a sharp peak by deleting salt from the sample buffer, allowing its quantitative recovery in a very concentrated form. Other thiophilic proteins adsorbed on the gel were eluted under stronger conditions (30% ethylene glycol). The one-step purification procedure by thiophilic interaction chromatography for sweet potato β-amylase was highly reproducible and allowed an enrichment ratio of 29 to be obtained with a yield of 56.3% (Table II). The observed variations of these values in three independent experiments were ca. 10%.

TABLE I

SALT EFFECTS ON THE THIOPHILIC ADSORPTION OF β-AMYLASE

Salt	T-gel		PyS-gel	
	Protein bound (%)	Recovery (%)	Protein bound (%)	Recovery (%)
$(NH_4)_2SO_4$	25	—	57	78
$MgSO_4$	36	—	21	—
K_2SO_4	21	—	54	58
Na_2SO_4	89	65	94	90
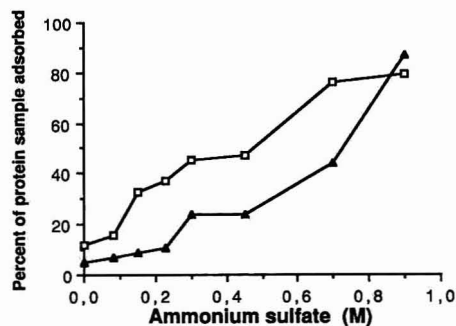
Fig. 2. Effect of ammonium sulphate on the thiophilic adsorption of β-amylase on (□) PyS-gel and (▲) T-gel.
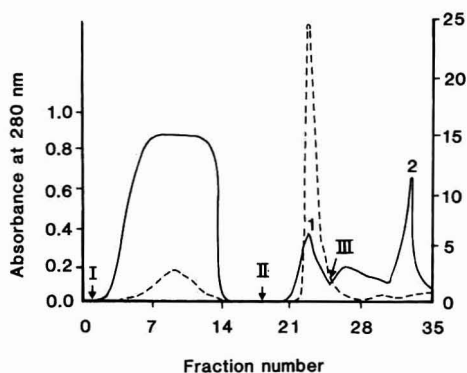
Fig. 3. Purification of β-amylase by thiophilic interaction chromatography on PyS-gel. I = sample application; II = desorption by sodium sulphate deletion; III = desorption with 30% ethylene glycol. Solid line, protein; dashed line, activity.

Electrophoretic analysis (Fig. 4) demonstrated the presence of only one band which was coincident with enzyme activity.

In conclusion, the thiophilic character of sweet potato β-amylase has been demonstrated. Enzyme adsorption on both types of gels was promoted by antichaotropic salts. As reported for immunoglobulins [13], sodium sulphate was the most effective of the four sulphates studied; ammonium, potassium and magnesium sulphates were much less effective in promoting adsorption of the enzyme on both thiophilic gels. Lower salt requirements (e.g., 0.3 M sodium sulphate) and higher protein recoveries (e.g., 90% of adsorbed enzyme) were observed for the PyS-gel, thus justifying its choice for the purification of the enzyme from crude extracts. In spite of the fact that the ligand content of PyS-gel was only half that of the T-gel, better binding properties
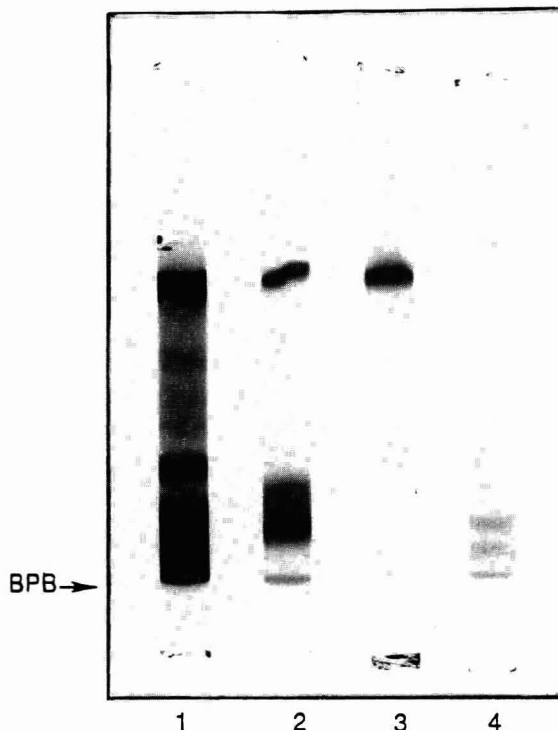
Fig. 4. Polyacrylamide gel electrophoresis (7.5% acrylamide, pH 8.3) at various stages in the purification of β-amylase: crude extract (lane 1), unpigmented extract to be applied to the column (lane 2), peaks 1 and 2 from Fig. 3 (lanes 3 and 4, respectively). BPB = bromophenol blue tracking dye.

toward β-amylase were exhibited by the former adsorbent. The high capacity and the possibility of reusing the same bed several times after regeneration make thiophilic interaction chromatography an extremely useful technique for enzyme purification.

TABLE II

SUMMARY OF β-AMYLASE PURIFICATION PROCEDURE

Fraction	Volume (ml)	Total activity (U)	Total protein (mg)	Specific activity (U mg^{-1})	Recovery (%)	Enrichment ratio
Unpigmented extract	45	222	51	4.3	100	–
Active peak	5	125	1	125	56.3	29

REFERENCES

1 A. K. Balls, M. K. Walden and R. R. Thompson, *J. Biol. Chem.*, 173 (1948) 9.
2 S. Englard and T. P. Singer, *J. Biol. Chem.* 187 (1950) 213.
3 S. Nakayama and S. Amagase, *J. Biochem.*, 54 (1963) 375.
4 S. K. Dube and P. Nordin, *Arch. Biochem. Biophys.*, 94 (1961) 121.
5 C. T. Greenwood, A. W. MacGregor and E. A. Milne *Carbohydr. Res.*, 1 (1965) 350.
6 D. French and M. Abdullah, *Cereal Chem.*, 43 (1966) 555.
7 M. V. Hedge, F. Roy and P. N. Joshi, *Prep. Biochem.*, 9 (1979) 71.
8 J. J. Marshal and W. J. Whelan, *Anal. Biochem.*, 52 (1973) 642.
9 F. Roy and M. V. Hedge, *Indian J. Biochem. Biophys.*, 17 (1980) 2.
10 T. Díaz, L. Franco-Fraguas, B. Luna, B. Brena and F. Batista-Viera, *J. High Resolut. Chromatogr.*, 12 (1989) 570.
11 J. Porath, F. Maisano and M. Belew, *FEBS Lett.*, 185 (1985) 306.
12 J. Porath and S. Oscarsson, *Makromol. Chem. Macromol. Symp.*, 17 (1988) 359.
13 T. W. Hutchens and J. Porath, *Anal. Biochem.*, 159 (1986) 217.
14 M. Belew, N. Juntti, A. Larsson and J. Porath, *J. Immunol. Methods*, 102 (1987) 173.
15 T. W. Hutchens and J. Porath, *Biochemistry*, 26 (1987) 7199.
16 P. Bernfeld, *Methods Enzymol.*, 1 (1955) 149.
17 K. Uehara, T. Mizoguchi and S. Mannen, *J. Biochem.*, 68 (1970) 359.
18 L. Orstein and B. J. Davis, *Ann. N. Y. Acad. Sci.*, 121 (1964) 321.

Selective adsorption of immunoglobulins and glucosylated proteins on phenylboronate–agarose

Beatriz M. Brena⋆ and Francisco Batista-Viera⋆

Biochemical Separation Centre, Uppsala University, Uppsala Biomedical Centre, Box 577, S-751 23, Uppsala (Sweden)

Lars Rydén

Department of Biochemistry, Uppsala University, Uppsala Biomedical Centre, Box 576, S-751 23, Uppsala (Sweden)

Jerker Porath

Biochemical Separation Centre, Uppsala University, Uppsala Biomedical Centre, Box 577, S-751 23, Uppsala (Sweden)

ABSTRACT

Aminophenylboronate-substituted agarose in 20 mM N-2-hydroxyethylpiperazine-N'-2-ethanesulphonic acid, pH 8.5, selectively adsorbs immunoglobulins and complement factors C3 and C4 from human serum. The selectivity of binding is strongly influenced by the presence of magnesium chloride in the sample buffer. Adsorbed immunoglobulins are quantitatively eluted by sorbitol, but only partially by ethylene glycol or methylcellosolve. Aniline–agarose of a similar degree of substitution shows only weak adsorption of serum proteins under similar experimental conditions, thus indicating the important contribution of the boronate moiety to this interaction. Immunoglobulin adsorption seems not to be due to the *cis*-diol complexation used extensively for the chromatographic determination of non-enzymatically glucosylated proteins. Hydrophobic and π–π interactions with the aromatic structure of the ligand seem also to contribute to protein binding. The behaviour of aminophenylboronate-liganded agarose is, in some respects, rather similar to that of the so-called "thiophilic adsorbents".

INTRODUCTION

Boronate is known to reversibly esterify certain carbohydrates containing 1,2-*cis*-diol structures, and this is also the case with organic boronic acids [1,2]. Aminophenylboronic acid coupled to agarose (PBA) is therefore a potential adsorbent for carbohydrate-containing proteins. It has been used successfully for monitoring diabetes [3,4] since glucosylated haemoglobin and glycosylated albumin and other serum proteins are markers of blood glucose control [5]. The non-enzymatically glucosylated proteins interact via the exposed glucose groups.

However, non-glucose-containing glycoproteins and other proteins may also interact with the aromatic boronate ligand. The present investigation was undertaken to find out whether other serum proteins might be adsorbed and, if so, to reveal the nature of the interaction.

The following reaction schemes summarize the steps employed for the synthesis of aminophenylboronate–agarose:

(1) Activation of the agarose matrix.

$$\text{M-OH} + \text{ClCH}_2\text{-CH-CH}_2 \longrightarrow \text{M-O-CH}_2\text{-CH-CH}_2 \qquad (1)$$
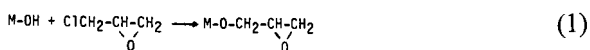
(2) Coupling of *m*-aminophenylboronic acid.

Correspondence to: Dr. B. M. Brena, Facultad de Química, Gral. Flores 2124, Casilla de Correo 1157, Montevideo, Urugay.
⋆ Permanent address: Facultad de Química, Gral. Flores 2124, Casilla de Correo 1157, Montevideo, Uruguay.

$$\text{M-O-CH}_2\text{-CH-CH}_2 + \underset{\underset{H_2N}{\overset{|}{\bigcirc}}}{\overset{OH}{\underset{|}{\bigcirc}}}\text{-B-OH} \longrightarrow \text{M-O-CH}_2\text{-CH-CH}_2\text{-NH}\underset{OH}{\overset{OH}{\underset{|}{\bigcirc}}}\text{-B-OH} \qquad (2)$$
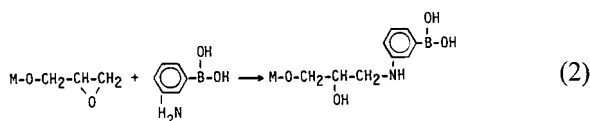
MATERIALS AND METHODS

Materials

Agarose (Ultrogel A-6) was purchased from LKB (Bromma, Sweden); m-aminophenylboronic acid hemisulphate, aniline, sodium borohydride and epichlorohydrin were obtained from Fluka (Buchs, Switzerland) and Glico Gel B was from Pierce (Rockford, IL, USA). N-2-Hydroxyethyl-piperazine-N′-2-ethanesulphonic acid (HEPES) and nicotinamide adenine dinucleotide (NAD$^+$) were products from Sigma (St. Louis, MO, USA). Human serum albumin (HSA) was kindly supplied by Kabi Vitrum (Stockholm, Sweden). Human total serum was obtained from the University Hospital in Uppsala (Sweden). Antisera against human serum proteins were kindly supplied by Professor C.-B. Laurell (Malmö Hospital, Malmö, Sweden). All other chemicals used were of reagent or analytical grade.

Analytical procedures

The distribution of proteins in column effluents was determined spectrophotometrically at 280 nm. Electrophoretic analysis was done on 1% agarose gels at pH 8.6. Serum proteins were immunologically identified by the conventional Ouchterlony immunodiffusion techniques using monospecific antibodies [6].

Glucosylation of human serum albumin

The glucosylation procedure was carried out essentially as described by Mereish et al. [7] by incubating for 15 days at 37°C solutions of albumin (47.5 mg/ml) in 0.01 M sodium phosphate, pH 7.4, containing 0.1 M D-glucose. Glucosylated albumin was monitored at 279 nm assuming an absorbance of 0.531 for a 1 mg/ml solution.

Synthesis of phenylboronate agarose

Activation. Agarose was activated essentially as described by Porath and Fornstedt [8]. A 100-g aliquot of Ultrogel A-6, filter dried and washed with water, was suspended in 64 ml of 2.5 M sodium hydroxide containing 100 mg of sodium borohydride. Epichlorohydrin (8 ml) was added and the mixture was shaken at room temperature for a total time of 18 h. The gel was then washed with water until neutral and immediately used for coupling.

Coupling. The activated gel was incubated for 48 h at room temperature with 6 g of m-aminophenylboronic acid hemisulphate dissolved in 200 ml of 1 M sodium carbonate, pH 10. The gel was then washed consecutively with 0.1 M sodium hydrogencarbonate, pH 8.5, water, 95% ethanol, water, 10% (v/v) acetic acid and finally water.

Deactivation. To hydrolyse residual epichlorohydrin-activated groups the gel suspension was incubated in a boiling water bath for 30 min. The excess liquid was filtered off and the moist gel was stored in 0.05 M sodium acetate, pH 5.0, at 4°C until use.

Synthesis of aniline–agarose

The activation of agarose was carried out as described above. A 60-g aliquot of filter-dried epoxiactivated agarose was suspended in 120 ml of 0.2 M sodium carbonate buffer, pH 9.5, and 10 ml of freshly distilled aniline were added dropwise with gentle shaking. Incubation was performed for 16 h at room temperatrue. The gel was then thoroughly washed as indicated above.

Ligand content

The total ligand contents of the phenylboronate and aniline gels were determined by micro-Kjeldahl nitrogen analysis.

Determination of binding capacities towards carbohydrates

Low-molecular-weight cis-diols: NAD. The capacity was determined essentially as reported by Maestas et al. [9]. Packed gel beds were fed with 0.1 mM NAD$^+$ in 0.05 M HEPES, pH 8.5–0.1 M magnesium chloride until saturation (a Uvicord unit equipped with a 254-nm UV detector and a strip chart recorder were used). After exhaustive washing with HEPES buffer, bound NAD$^+$ was eluted with 0.2 M borate buffer, pH 10.2, and the absorbance at 260 nm was measured. A molar extinction coefficient of $1.78 \cdot 10^4$ was used to calculate the amount of bound NAD$^+$ per ml of packed gel.

High-molecular-weight cis-diols: glucoproteins. The capacities were determined by saturating the

gel beds with glucosylated human serum albumin in 0.25 *M* ammonium acetate, pH 8.5. After washing with several column volumes of acetate buffer, the albumin was eluted with 0.2 *M* sorbitol in the same buffer and quantified spectrophotometrically.

Chromatography of serum proteins

Phenylboronate–agarose. Human serum was diluted ten-fold with the following application buffers: (a) 0.02 *M* HEPES, pH 8.5 (standard conditions); (b) 0.02 *M* HEPES, pH 8.5, containing 0.01–0.16 *M* magnesium chloride; (c) 0.02 *M* HEPES, pH 7.2; and (d) 0.25 *M* ammonium acetate, pH 8.5. The serum samples were applied at a flow-rate of 16 ml/h into 3 ml gel beds (1.0 × 4.0 cm) at room temperature (22°C). After sample application the column was washed with several volumes of application buffer. Elution was effected with 0.2 *M* sorbitol in 0.25 *M* ammonium acetate buffer, pH 8.5, unless otherwise specified. Before re-use the columns were washed with 6 *M* urea.

Aniline–agarose. Serum samples diluted in 0.02 *M* HEPES, pH 8.5, with or without 0.04 *M* magnesium chloride, were applied under the above-mentioned conditions. After washing the gel beds with several volumes of application buffer, elution was effected with 30% ethyleneglycol and finally with 6 *M* urea.

RESULTS

Characterization of synthesized phenylboronate–agarose

The adsorbent was obtained as a brownish gel that was stable for at least several months. The av-

erage ligand densities for several preparations of phenylboronate– and aniline–agarose gels, as estimated by nitrogen analysis, were 43 μmol and 37 μmol per ml of packed gel bed, respectively (Table I).

The binding capacity of phenylboronate–agarose for a low-molecular-weight *cis*-diol as determined by saturating the adsorbent with NAD$^+$ was 5.0 ± 0.2 μmol per ml of packed gel.

For comparison, a commercially available phenylboronate–agarose (Glico Gel B, containing 17 μmol of ligand per ml of packed gel, according to the manufacturer) was analysed (Table I). As expected from the lower degree of substitution, the adsorption capactity was only 40% of ours, *i.e.* 2.2 μmol/ml.

Less than 4% of human serum albumin was adsorbed in 0.25 *M* ammonium acetate, pH 8.5. However, after extensive *in vitro* non-enzymatic glucosylation, the albumin became quantitatively adsorbed under the same conditions. It was eluted with near 100% recovery by 0.2 *M* sorbitol. The adsorption capacity for this glucosylated protein was 46 mg (0.7 μmol) per ml of packed gel, which on a molar basis correponds to 1–2% utilization of the ligands (Table I) assuming single-point adsorption.

The adsorbent can be stored for at least 3 months at 4°C without significant decrease in adsorption capacity. Gel beds can be used repeatedly after washing with 6 *M* urea.

Aniline–agarose does not bind NAD$^+$ or glucosylated HSA under the above conditions, proving that the boronate moiety is essential for these interactions.

TABLE I

GEL-BINDING CAPACITIES FOR LOW- AND HIGH-MOLECULAR-WEIGHT *cis*-DIOLS

See Materials and methods section for details. Values reported (±S.D.) are the average of five determinations.

Gel derivative	Ligand content (μmol/ml)	Binding capacity for	
		NAD (μmol/ml)	Glycosylated HSA (mg/ml)
Phenylboronate agarose (this study)	43	5.01 ± 0.2	46.0 ± 2.3
Glico Gel B	17	2.2 ± 0.1	35.5 ± 1.8
Aniline–agarose	37	Negligible	Negligible

TABLE II

CHROMATOGRAPHY OF SERUM PROTEINS ON PHENYLBORONATE–AGAROSE: INFLUENCE OF BUFFERS

A 30-ml aliquot of diluted serum sample (corresponding to 3 ml of serum or approximately 200 mg of protein) was chromatographed on 1×4 cm gel beds in the indicated buffers. In the case of 0.02 M HEPES, pH 7.2, 150 ml of diluted serum sample were applied (overloading conditions). Desorption was achieved by including 0.2 M sorbitol in 0.25 M ammonium acetate buffer, pH 8.5. Protein was estimated by 280 nm absorption and in some runs identified by electrophoresis and immunodiffusion (Figs. 1 and 2). About 19% of the applied protein was adsorbed

Adsorption conditions		Desorbed by sorbitol elution	
Buffer	Magnesium chloride (M)	Percentage of total protein	Proteins identified
0.05 M HEPES, pH 8.5	0.00	14.5	IgG, IgA, C3, C4
0.02 M HEPES, pH 8.5	0.01	16.5	IgG, IgA, C3, C4, small amounts α_2-macroglobulin, HSA, transferrin, haptoglobin
0.02 M HEPES, pH 8.5	0.04	14.7	
0.02 M HEPES, pH 8.5	0.16	9.6	
0.02 M HEPES, pH 7.2	0.00	Overloading conditions	IgG, IgA, C3, C4, small amounts α_2-macroglobulin, transferrin, haptoglobin
0.25 M ammonium acetate pH 8.5	0.00	10.4	

Chromatography of human serum proteins

In 0.02 M HEPES buffer, pH 8.5 (standard conditions), essentially only immunoglobulins and the complement factors C3 and C4 were adsorbed (Table II). HEPES has been reported to enhance *cis*-

diol interactions and was therefore chosen as the adsorption buffer [4,10]. Sorbitol elution in this buffer did not give sharp peaks. Excellent elution profiles were obtained with sorbitol included in 0.25 M ammonium acetate, pH 8.5. Sorbitol was necessary for the desorption. An additional 1–2% of the protein was recovered upon a final washing of the column with 6 M urea. About 95% of serum proteins were accounted for.

Influence of pH, magnesium chloride and decreased polarity on protein adsorption

The use of a lower pH, pH 7.2, only marginally affected the chromatographic performance (Table
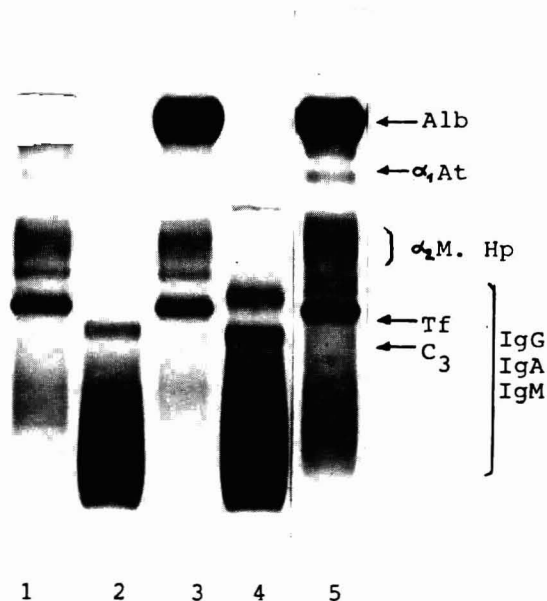
Fig. 1. Electrophoretic analysis of human serum proteins chromatographed on phenylboronate–agarose. Effect of pH of the application buffer. In each run the proteins that passed unretarded through the column are shown on the left and those eluted by 0.2 M sorbitol in 0.25 M ammonium acetate, pH 8.5, are shown on the right. Lanes: 1 and 2 = 0.02 M HEPES, pH 8.5 (overloading conditions); 3 and 4 = 0.02 M HEPES, pH 7.2 (overloading conditions); 5 = serum reference. Alb = Albumin; α_1At = α_1-antitrypsin; α_2M = α_2-macroglobulin; Hp = haptoglobulin; Tf = transferrin; C_3 = complement factor 3; Ig = immunoglobulin.
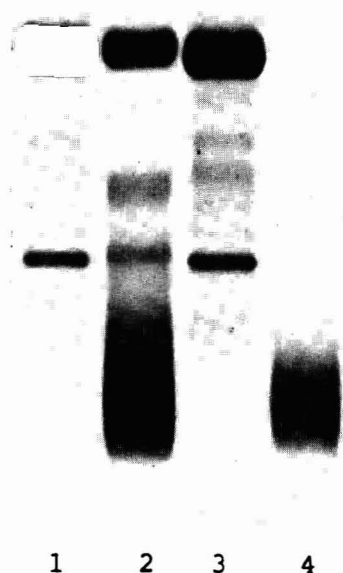
1   2   3   4

Fig. 2. Electrophoretic analysis of human serum proteins chromatographed on phenylboronate–agarose. Effect of including magnesium chloride in the application buffer. In each run, the proteins that passed unretarded through the column are shown on the left and those eluted by 0.2 M sorbitol in 0.25 M ammonium acetate, pH 8.5, are shown on the right. Lanes: 1 and 2 = 0.02 M HEPES, pH 8.5, containing 0.02 M magnesium chloride; 3 and 4 = 0.02 M HEPES, pH 8.5.

1   2   3   4   5   6   7   8   9

Fig. 3. Electrophoretic analysis of human serum proteins chromatographed on phenylboronate–agarose. Effect of deleting magnesium chloride on the desorption of adsorbed proteins. The proteins were applied in 0.02 M HEPES, pH 8.5, containing varying concentrations of magnesium chloride and eluted first by passing HEPES buffer without magnesium chloride and finally by 0.2 M sorbitol in 0.25 M ammonium acetate, pH 8.5. In each run the proteins that passed unretarded are shown on the left, those eluted by buffer lacking magnesium chloride in the middle and those eluted by sorbitol on the right. In each of the three experiments, the initial magnesium chloride concentrations were as follows: lanes: 1–3 = 0.16 M; 4–6 = 0.04 M; 7–9 = 0.01 M.

II and Fig. 1), but a few more proteins were adsorbed at the lower pH.

The presence of magnesium chloride in the application buffer increased the adsorption capacity and decreased the selectivity. Additional proteins became adsorbed, namely serum albumin, α_2-macroglobulin, transferrin and haptoglobin (Fig. 2). Most of these proteins were eluted simply by deleting magnesium chloride (Fig. 3).

TABLE III

EFFECTS OF LOW-POLARITY AGENTS ON ELUTION OF ADSORBED SERUM PROTEINS (IMMUNOGLOBULINS) FROM PHENYLBORONATE–AGAROSE

A 10-ml aliquot of 10-fold diluted human serum, corresponding to a total of 70 mg of protein and about 10–15 mg of immunoglobulin, was applied on the column (1 × 4 cm) in 0.02 M HEPES buffer, pH 8.5. The column was eluted as indicated in the two experiments. Protein was estimated by 280 nm absorption. About 19% of applied protein was adsorbed

Experiment	Elution conditions	Applied protein eluted (%)
(1) First eluent	40% Ethyleneglycol	8.4 (broad peak)
Second eluent	0.2 M Sorbitol in 0.25 M ammonium acetate, pH 8.5	8.6 (total 17.0)
(2) First eluent	30% Methylcellosolve	7.3 (broad peak)
Second eluent	40% Ethyleneglycol	1.7 (broad peak)
Third eluent	0.2 M Sorbitol in 0.25 M ammonium acetate, pH 8.5	7.9 (total 16.9)

The possible influence of hydrophobic effects on the binding of serum proteins to phenylboronate ligand was investigated under conditions that favour *cis*-diol interactions (0.02 *M* HEPES, pH 8.5) and ethyleneglycol and 2-methoxyethanol (methylcellosolve) were tested for their ability to elute hydrophobically bound proteins (immunoglobulins) (Table III). Relatively high concentrations of these agents (30–40, v/v) were required for elution; broad and extended peaks were obtained, and only 50% of the adsorbed protein was recovered. Aniline–agarose with a similar degree of substitution only adsorbed 4–6% of applied serum proteins under the same experimental conditions. This compares with the approximately 19% of protein adsorbed in standard conditions on the PBA. The adsorbed proteins were eluted by 30% ethyleneglycol and 6 *M* urea.

DISCUSSION

Immobilized aminophenylboronate ligand readily forms complexes under mild conditions with molecules containing two vicinal hydroxyl groups in the *cis* configuration. 1,2-*cis*-Diol compounds, such as sorbitol, act as displacers [11]. The adsorbent described herein behaves accordingly, as demonstrated by its ability to bind NAD$^+$ and *in vitro* glucosylated HSA.

Immunoglobulins and complement factors C3 and C4 are adsorbed selectively from human serum upon chromatography under conditions that favor *cis*-diol interactions (20 m*M* HEPES buffer, pH 8.5). Unexpectedly, however, protein binding also occurs at pH 7.2, at which pH the boronate–carbohydrate interaction is supposed to be negligible [9,12].

This observation and the fact that many serum glycoproteins, *e.g.* ceruloplasmin and transferrin, were not adsorbed while immunoglobulins in which the carbohydrate moieties is not readily available stayed on the column indicate that *cis*-diol binding to carbohydrate is of little importance here. Since glucose-containing albumin binds, we conclude that the carbohydrates in the oligosaccharide side chains in the glycoproteins which lack glucose do not interact significantly with the boronate moiety.

It is clear (Table II) that under standard conditions the proteins which are absorbed by the bor-
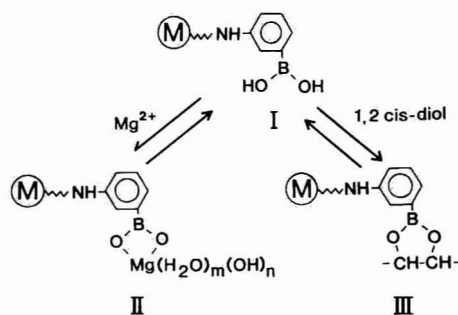
Fig. 4. Postulated interconvertible structures of ligand involved in various adsorption phenomena observed on aminophenylboronate–agarose gel.

onate gel generally are the same as those which are absorbed by thiophilic adsorbents with the uncharged ligands 2-hydroxy-ethylsulphonyl [13] and 2-pyridine-sulphido groups [14], but there are differences. α_2-Macroglobulin has a lower affinity for the boronate gel than for the thiophilics. In any case, ionic interactions may not necessarily be involved. This assumption is supported by the fact that only a smaller part of the protein adsorption at pH 8.5 is lost by adding 0.25 *M* ammonium acetate. This concentration is high enough to efficiently suppress ionic interactions.

We observed that the adsorption capacity of aniline–agarose was very low. The boronate substitution makes the ligand more hydrophilic but, paradoxically, the adsorption, which appears to be related to hydrophobicity, increases.

Let us discuss the protein–aminophenylboronate adsorption in terms of equilibrium conditions between the three forms, I, II and III, in Fig. 4. Adsorption may be essentially due to form I, and the contribution of form II may be negligible. This could explain why sorbitol is also a more efficient elution agent with respect to the hydrophobic/thiophilic part of the adsorption. Sorbitol reacts with the ligand to give III.

Upon addition of magnesium chloride to 0.02 *M* HEPES buffer the adsorption increases to a maximum (Table II). Mg^{2+} at high concentrations lowers the adsorption capacity and selectivity at the same time, as evidenced by the increasing amount of serum albumin in the desorbed fraction (Fig. 3). Magnesium chloride is a chaotropic salt and the effect at high concentration is therefore expected.

However, there must be another explanation for the behaviour of the magnesium-loaded adsorbent (form II, Fig. 4). In the range 0.01–0.16 M the effects of chaotropic magnesium chloride and the antichaotropic magnesium sulphate were similar (results not shown), suggesting that it is not the anion but the metal ion that is important for adsorption. Mg^{2+} and the boronate group may form an ion pair. Magnesium chloride has been reported to increase the stability of the phenyl–boronate–carbohydrate (nucleotide) interaction [15] and is currently used in standard buffers for carbohydrate–boronate chromatography. Proteins show some kind of rather non-specific affinity for magnesium. Carboxylic oxygen may enter into the coordination sphere of the immobilized magnesium. Magnesium is also likely to cause a redistribution of the π electron cloud over the ligand, thus possibly affecting π–π complexation. An alternative, perhaps more likely, explanation is that Mg^{2+} interacts with the proteins, diminishing ionic repulsion between protein carboxylates and the boronate ligand.

The complexity of the overall adsorption is further revealed by the experiments referred to in Table III. Hydrophobic and hydrophilic interaction may explain the effect of ethylene glycol and methylcellosolve on the desorption. The incomplete and slow desorption by these solvents points to additional operational factor(s). The efficient elution of the proteins by sorbitol clearly shows that boronate–protein interaction is involved. In conclusion, we suggest that the behaviour observed is the combined effect of several kinds of interactions: boronate interactions, hydrophobic and π–π interactions and possibly hydrogen bonding. All of these interactions are abolished when sorbitol is included in the medium. A weak ionic interaction may play a role at low ionic strength.

REFERENCES

1 Ch. A. Zittle, *Adv. Enzymol. Relat. Areas Mol. Biol.*, 12 (1951) 495.
2 J. P. Lorand and J. O. Edwards, *J. Org. Chem.*, 24 (1959) 769.
3 B. J. Gould and P. M. Hall, *Clin. Chim. Acta*, 163 (1987) 225.
4 F. A. Middle, A. Bannister, A. J. Bellingham and P. D. G. Dean, *Biochem. J.*, 209 (1983) 771.
5 S. F. Kemp, R. H. Creech, and T. R. Horn, *J. Pediatr.*, 105 (1984) 394.
6 A. Milford-Ward, in R. A. Thompson (Editor), *Techniques in Clinical Immunology*, Blackwell, Oxford, 1981, p. 1.
7 K. A. Mereish, H. Rosemberg and J. Cobby, *J. Pharm. Sci.*, 71 (1982) 235.
8 J. Porath and N. Fornstedt, *J. Chromatogr.*, 51 (1970) 479.
9 R. Maestas, J. Prieto, G. Kuehn and J. Hageman, *J. Chromatogr.*, 189 (1980) 225.
10 P. D. G. Dean, F. A. Middle, C. Lonstaff, A. Bannister, J. J. Dembinski, in I. M. Chaiken, M. Wilcheck and I. Parikh (Editors), *Affinity Chromatography and Biological Recognition*, Academic Press, New York, 1983, p. 433.
11 S. Hjertén and J. P. Li, *J. Chromatogr.*, 500 (1990) 543.
12 A. M. Yurkevich, I. I. Kolodkina, E. A. Ivanova and E. I. Pichuzkina, *Carbohydr. Res.*, 43 (1975) 215.
13 J. Porath, F. Maisano and M. Belew, *FEBS Lett.*, 185 (1985) 306.
14 J. Porath and S. Oscarsson, *Macromol. Chem., Macromol. Symp.*, 17 (1988) 359.
15 V. Boutoris, I. J. Galpin and P. D. G. Dean, *J. Chromatogr.*, 210 (1981) 267.

Immobilized hemoglobin in the purification of hemoglobin-based oxygen carriers

Emilia Chiancone

CNR Center of Molecular Biology, Department of Biochemical Sciences, University "La Sapienza", 00185 Rome (Italy)

Clara Fronticelli

Department of Biological Chemistry, Medical School, University of Maryland, Baltimore, MD 21201 (USA)

Maurizio Gattoni

CNR Center of Molecular Biology, Department of Biochemical Sciences, University "La Sapienza", 00185 Rome (Italy)

Barbara K. Urbaitis

Department of Medicine (Nephrology Division), Medical School, University of Maryland, Baltimore, MD 21201 (USA)

Enrico Bucci

Department of Biological Chemistry, Medical School, University of Maryland, Baltimore, MD 21201 (USA)

ABSTRACT

Chemically modified hemoglobins can be used as oxygen carriers in cell-free fluids provided that they have a low oxygen affinity and are stable towards dissociation into subunits. The latter species are undesirable because they are filtered rapidly through the kidneys, have renal toxicity and are characterized by a high oxygen affinity. A most important step in the preparation of hemoglobin-based oxygen carriers is therefore their purification from any dissociable material. Hemoglobin immobilized as $\alpha\beta$ dimers on Sepharose lends itself naturally to this purpose as it is able to interact in a specific and reversible way with soluble $\alpha\beta$ dimers. Hemoglobin affinity columns are very effective in the purification of cross-linked and pseudo-cross-linked human and bovine hemoglobin. The applicability of the technique is enhanced by the ease with which $\alpha\beta$ dimers from different species cross-interact to yield hybrid $\alpha_2\beta_2$ tetramers. It is shown that hemoglobin affinity columns may provide analytical information on the cross-linking reaction itself.

INTRODUCTION

In the search for alternatives to blood for transfusion or perfusion purposes, the use of cell-free hemoglobin as an oxygen carrier has been proposed

by several laboratories [1]. The hemoglobin molecule has to be modified chemically to stabilize the tetrameric state and hence impede the rapid renal clearance of the dissociated $\alpha\beta$ dimers. Further, the oxygen affinity of the molecule has to be rendered similar to that of whole blood as the physiological modulators such as 2,3-diphosphoglycerate are no longer segregated in the red cells.

Among the most promising modifications of hu-

man hemoglobin studied to date are those in which an intramolecular cross-link has been introduced between the βEF5 lysines [2] or between the αG6 lysines [3] or, alternatively, a pseudo-cross-link between the βEF5 lysines [4]. Such modifications endow human hemoglobin with the proper stability and oxygen affinity. Bovine hemoglobin has also been modified in similar ways [5,6]. Interest in this readily available protein is growing as it can be employed when the use of human hemoglobin may be unnecessary and too costly (*e.g.*, for organ perfusion and organ storage). Moreover, the stroma-free bovine hemoglobin has unusual oxygen-binding properties; owing to its marked sensitivity to chloride ions, at physiological concentrations of chloride its oxygen affinity is lower than that of human blood [7].

Irrespective of the source of protein, a most important step in the preparation of hemoglobins to be used as oxygen carriers is represented by the purification of the cross-linked material from all dissociable forms of hemoglobin which are undesirable owing to their high oxygen affinity and very short intravascular retention time and renal toxicity. On a laboratory scale, purification is achieved by ion-exchange chromatography [5]. On an industrial level advantage is taken of the higher thermal stability of the cross-linked material [8].

We propose the use of subunit-affinity columns of immobilized hemoglobin to purify hemoglobin-based oxygen carriers. Human hemoglobin is known to be immobilized on cyanogen bromide (CNBr)-activated Sepharose as $\alpha\beta$ dimers which maintain the capacity to interact in a highly specific and reversible way with soluble $\alpha\beta$ dimers under conditions where the latter are in association–dissociation equilibrium with the $\alpha_2\beta_2$ tetramers [9,10]. The experiments presented here demonstrate that immobilized $\alpha\beta$ dimers extract very effectively any dissociable hemoglobin from preparations of cross-linked or pseudo-cross-linked protein. The versatility of the approach is enhanced by the cross-interaction between dimers from hemoglobins of different species which leads to the formation of hybrid $\alpha_2\beta_2$ tetramers.

EXPERIMENTAL

Hemoglobin

Human hemoglobin (HbA) was prepared from expired blood obtained from the Blood Bank of the University Hospital in Baltimore following a published procedure [4]. Bovine hemoglobin (HbBv) was prepared from bovine blood using the standard procedure of Fronticelli *et al.* [5].

HbA and HbBv were pseudo-cross-linked between the βEF5 lysines by reaction with mono-(3,5-dibromosalicyl)fumarate (FMDA) as described in refs. 4 and 6, respectively. The pseudo-cross-linked hemoglobins, HbA–FMDA and HbBv–FMDA, are predominantly non-dissociable tetramers stabilized by electrostatic and hydrophobic interactions.

HbA covalently cross-linked between the two αG6 lysyl residues with a fumaryl residue (α–αXL HbA) [3] was a gift from the Department of Defense (LAIR, San Francisco, CA, USA). Following the chemical modification, the cross-linked material was purified by heating for 10 h at 60°C in the presence of reducing agents such as sulfites and dithionite. This treatment sterilizes the preparation and precipitates the residual less stable non-cross-linked material; α–αXL HbA is a tetramer which does not dissociate into dimers [3]. Typically the preparations have concentrations of 13 g/dl and contain 10–13% of iron(III) hemoglobin.

HbBv was cross-linked covalently with a fumaryl residue (β–βXL HbBv) by treatment of either the oxygenated or the deoxygenated derivative with bis (3,5-dibromosalicyl) fumarate as described in refs. 11 and 5, respectively. Reaction of the oxygenated protein leads to cross-linking between the two βEF5 lysyl side-chains, whereas reaction of the deoxygenated protein modifies both the α- and the β-subunits [5]. Unless stated otherwise, the protein cross-linked in the oxygenated state was purified by high-performance liquid chromatography on a Toyopearl 650M DEAE anion-exchange resin (Toso-Haas) using a gradient formed by 0.015 *M* Tris buffer (pH 8.0) and 0.015 *M* Tris buffer (pH 7.7) in 0.2 *M* sodium acetate; the main fraction was collected and concentrated by forced filtration. In contrast, the protein cross-linked in the deoxygenated state was not purified and thus contained both non-reacted and over-reacted protein, namely protein reacted at sites other than βEF5 and/or αG6. In all

instances, purified preparations of β–βXL HbBv are stable tetrameric hemoglobins.

Coupling procedure

Covalent coupling of hemoglobin was performed on Sepharose 4B activated by the CNBr method or on commercial CNBr-activated Sepharose 4B (from Pharmacia, Uppsala, Sweden). The concentration of immobilized protein was determined by means of spectrophotometric measurements on a Cary 14 spectrophotometer using a 2-mm cell; the effect of turbidity was minimized by the use of protein-free gel in the reference beam as described [10].

Determination of associating capacity of immobilized hemoglobin

The capacity of the various preparations of immobilized hemoglobin to interact with the soluble protein was assessed with a chromatographic column containing 5–6 ml of immobilized protein, thermostated at 8–10°C and eluted at a constant flow rate of 10–12 ml/h. The absorbance of the effluent was monitored at 541 nm with a Gilford apparatus equipped with flow-through cells. The experiments were of two kinds. For a semi-quantitative indication of the associating capacity, a small volume (1 ml) of protein solution in associating buffer [0.1 M phosphate buffer (pH 7.0)] was percolated through the column equilibrated with the same buffer. For a quantitative measure of the associating capacity the column was saturated, i.e., sufficient protein solution was applied until a steady state was reached and the absorbance of the effluent was the same as that of the inflowing solution. In either type of experiment, interaction of the soluble protein with the immobilized protein results in an increase of the elution volume with respect to a non-interacting protein, i.e., with respect to the void volume of the column, V_0 [12,13]. The column was freed from the retained protein with dissociating buffer, 1.98 M NaCl–0.01 M phosphate (pH 6.7) [9,10].

Gel electrophoresis

The fractions eluted from the hemoglobin affinity column were analyzed by polyacrylamide gel electrophoresis (PAGE) performed with the buffer system of Laemmli [14] at pH 8.6 in the presence of 0.1% sodium dodecyl sulfate (SDS); the stacking

and running gels were 5 and 15% in acrylamide, respectively.

Intravascular retention time in the rat

The protocol described by Urbaitis et al. [15] was used. The rats received a bolus injection of 20 mg per 100 g body weight. Timed blood and urine samples were collected and analyzed for their hemoglobin content. Semi-logarithmic plots of hemoglobin concentration vs. time allowed the half-time of intravascular retention to be calculated. The urine samples were used to determine the fraction of hemoglobin eliminated through the kidneys.

RESULTS AND DISCUSSION

Effect of coupling conditions on the associating capacity of immobilized hemoglobin and formation of hybrid tetramers

Previous experiments on human hemoglobin immobilized on CNBr-activated Sepharose 4B have shown that the capacity of immobilized αβ dimers to interact specifically with $\alpha_1\beta_1$ dimers in solution is influenced markedly by the coupling conditions [9,10]. Hence the associating capacity of the hemoglobin subunit affinity columns, expressed as milligrams of hemoglobin retained per milligram of immobilized protein, was assessed for bovine and human hemoglobin coupled to CNBr-activated Sepharose under the conditions detailed in Table I. In line with observations by Rossi Fanelli et al. [10], the highest capacity is displayed by the protein immobilized in the presence of ethanolamine, which facilitated single-point attachment of the protein to the matrix, thus leaving the subunit interfaces unaltered.

Thereafter the capacity of immobilized HbA and HbBv to cross-interact with soluble hemoglobin from the other species was determined. The results, included in Table I, show that immobilized hemoglobin interacts essentially with the same strength with either hemoglobin in solution. This finding reflects the ease with which hybrid tetramers are formed owing to the similarity of the relevant αβ interfaces in the two proteins [9,10].

Purification of cross-linked hemoglobin from the non-cross-linked protein

After the characterization of their associating ca-

TABLE I

EFFECT OF COUPLING CONDITIONS ON THE ASSOCIATING CAPACITY OF IMMOBILIZED HEMOGLOBIN DIMERS

In all experiments, 1 ml of solution was applied.

Sample No.	Hb immobilized	Coupling conditions[a]	Hb per ml Sepharose (mg)		Hb applied		Hb retained per 100 mg Hb immobilized (mg)
			Added	Immobilized	Type	Concentration (mg/ml)	
1	HbBv	1	6.3	5.2	HbBv	10	8.3
2	HbA	1	6.0	6.0	HbA	9.2	7.8
					HbBv	18	8.1
3	HbA	2	4.6	3.7	HbA	9.7	8.6
					HbA	2.4	7.5
					HbBv	10.3	7.3
4	HbA	3	8.1	6.8	HbA	10.5	15.0
				6.5[b]	HbA	12.7	11.0
5	HbA	3	17.5	11.1	HbA	15.5	17.0

[a] Coupling conditions 1: commercial CNBr-activated Sepharose 4B, coupling carried out under standard Pharmacia conditions, namely 0.1 M NaHCO$_3$ (pH 8)–0.5 M NaCl for 2 h at room temperature, deactivation with 1 M ethanolamine. Coupling conditions 2: commercial CNBr-activated Sepharose 4B, coupling in 0.1 M phosphate buffer (pH 7.8) for 18 h in the cold. Coupling conditions 3: Sepharose 4B activated with 600 mg of CNBr per 12 ml of resin, coupling in 0.1 M NaHCO$_3$ (pH 8) containing 0.012 M ethanolamine for 1 h at room temperature, deactivation with 1 M ethanolamine.
[b] Experiment performed after keeping the immobilized hemoglobin for 4 months in the cold in the presence of sodium azide.

pacity, the different preparations of immobilized hemoglobin were employed to separate cross-linked from non-cross-linked hemoglobin. Only the latter protein is expected to interact with the hemoglobin affinity column as the cross-linked proteins, namely α–αXL HbA and β–βXL HbBv, which are stable tetramers, do not undergo reversible association–dissociation reactions into subunits and therefore elute in the void volume, V_0.

The use of immobilized HbA is depicted in Fig. 1. In all experiments 1 ml of soluble hemoglobin was applied to the column. First the capacity for soluble HbA was calculated to be 4.2 mg (panel A). In the control experiment depicted in panel B, in which the amount of hemoglobin percolated was less than the column capacity (1.4 mg), all the protein was retained on the affinity column and eluted only after application of dissociating buffer. Thereafter α–αXL HbA purified by heat treatment at 60°C was applied to the column (panel C); most of the protein eluted in the void volume, but 5.4% was retained, indicating that this amount of dissociable hemoglobin had been left in solution after heat treatment. HbBv cross-linked in the oxygenated state (β–βXL HbBv) displayed a similar behaviour in that part of

the protein was retained on the affinity column. On the other hand, β–βXL HbBv purified by ion-exchange chromatography contained no dissociable material, demonstrating the effectiveness of this purification procedure (panel D). Panel C also shows that on SDS-PAGE [14] the mobility of the retained protein corresponds to that of hemoglobin chains (lane c); thus, as expected, exclusively dissociable $\alpha\beta$ dimers interact with the hemoglobin affinity column.

For large-scale purifications the column capacity, of course, has to be fully exploited in saturation experiments. Two major factors determine the extent to which a given subunit affinity column can be loaded under a set of experimental conditions, namely the amount of matrix-bound polymer formed per milligram of immobilized protein and the elution volume difference between the interacting protein and any other non-interacting protein present in solution. Both properties depend on the solution concentration of the interacting protein, but act against each other: when the concentration of soluble interacting protein is low, the difference in elution volume between the interacting protein and any other protein in solution is large; however,
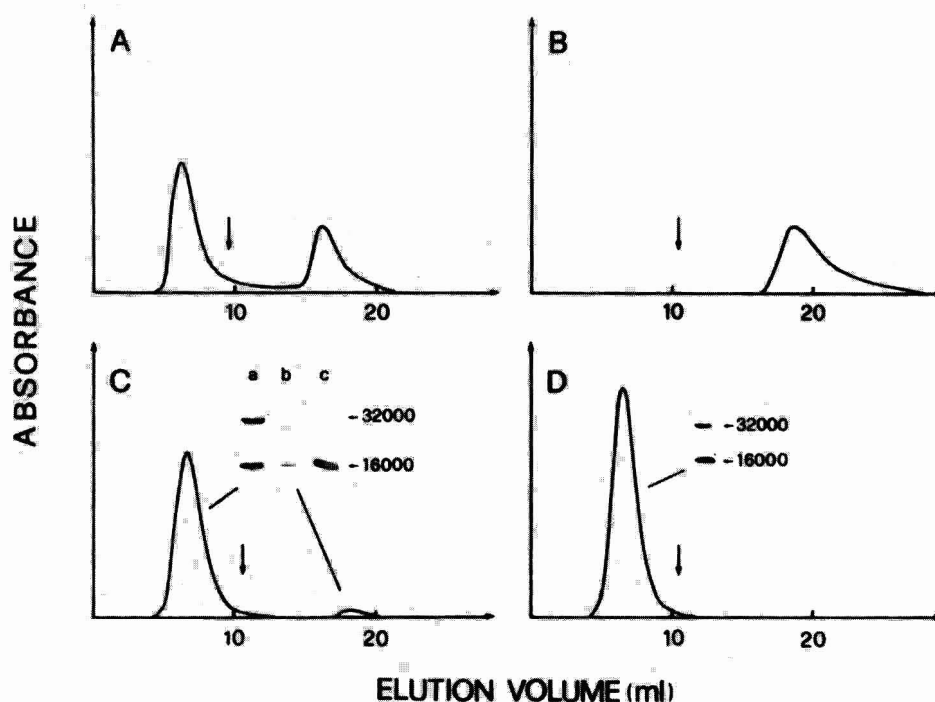
Fig. 1. Elution profiles of native and cross-linked hemoglobin solutions from a column containing Sepharose-bound HbA. The column (6 ml) was thermostated at 8°C and equilibrated with associating buffer, 0.1 M phosphate buffer (pH 7.0); 1-ml pulses of the various hemoglobin solutions in the same buffer were applied. Arrows indicate the application of dissociating buffer, 0.01 M phosphate buffer–1.98 M NaCl (pH 6.7). A = HbA at 12.7 mg/ml; B = HbA at 1.4 mg/ml; C = α–αXL HbA at 5.2 mg/ml; D = β–βXL HbBv, cross-linked in the oxygenated state and purified by ion-exchange chromatography, at 10.3 mg/ml. The inset of panel C shows the SDS-PAGE patterns of the fractions indicated on the elution profile (a and b) and of HbA (c). Lane a = α–αXL dimers and β-chain monomers; lanes b and c = α- and β-chain monomers. The inset of panel D shows the SDS-PAGE pattern of the indicated fraction containing β–βXL dimers and α-chain monomers.

the amount of protein retained is low owing to a mass action effect [10,12,13]. Hence, unless the cross-linking procedure is standardized to yield similar concentrations of dissociable protein in the mixture, it is best to check every preparation of cross-linked hemoglobin on a small scale before performing a large-scale purification.

A column saturation experiment involving immobilized HbA to purify HbBv cross-linked in the deoxygenated state is given in Fig. 2. This specific example also illustrates that hemoglobin affinity columns may yield information on the cross-linking reaction itself. The occurrence of modifications at sites other than lysines αG6 and βEF5 was indicated by SDS-PAGE experiments which showed a substantial amount of tetramers, corresponding to overreacted hemoglobin, in addition to the expect-

ed dimeric and monomeric species (compare with panels and C and D in Fig. 1). The component retained on the column, analysed by SDS-PAGE, contained not only monomeric species derived from unmodified, dissociable $\alpha\beta$ dimers, but also dimeric species deriving from undissociable $\alpha_1\beta_1$ dimers. Such dimers, which are absent in the purified cross-linked material [5], are still able to interact with the immobilized protein.

Purification of pseudo-cross-linked hemoglobin

HbA–FMDA and HbBv–FMDA are stabilized tetramers at neutral and slightly acidic pH values on the basis of sedimentation velocity experiments [4,6]. Consistent with this observation, a major fraction disappears from plasma in the rat at significantly slower rates (half-time $\approx$ 190 min) than na-
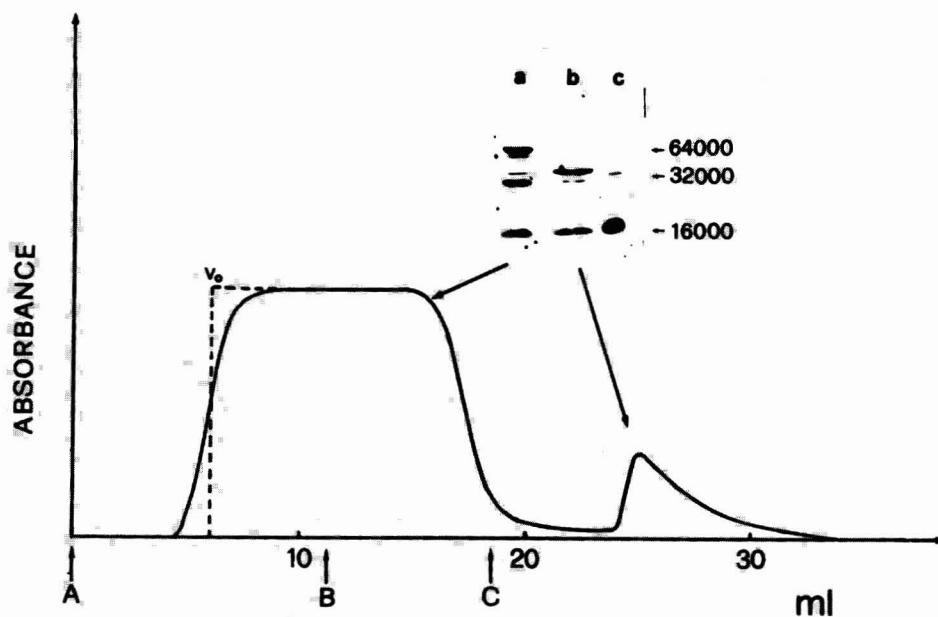
Fig. 2. Purification of dissociable hemoglobin from HbBv cross-linked in the deoxygenated state by means of immobilized HbA. Experimental conditions as in Fig. 1. Arrows indicate application of (A) cross-linked bovine hemoglobin at 5 mg/ml, (B) associating buffer and (C) dissociating buffer. The inset shows the SDS-PAGE pattern of the starting solution (lane a, any fraction in the plateau region), of the retained protein (lane b) and of HbA (c). The high-molecular-mass bands correspond to cross-linked tetramers and dimers in lane a and to $\alpha_1\beta_1$XL dimers in lane b; the 16 000 M_r band corresponds in all three lanes to α- and β-chains.

tive HbA and HbBv (half-time 40 min). However, a fraction is excreted very quickly (half-time $\approx$ 20 min); its relative amount, although erratic, is always higher in HbBv–FMDA [6].
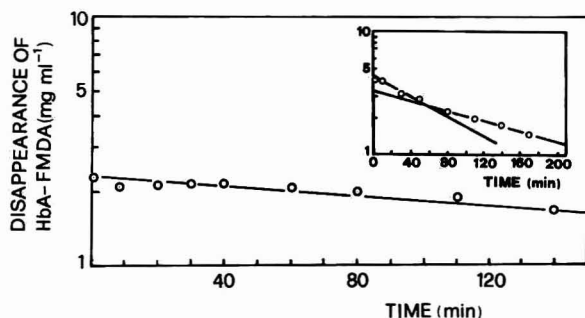
Fig. 3. Time course of disappearance from plasma of purified pseudo-cross-linked HbA–FMDA in the rat. The inset shows the biphasic curve obtained from the same material before purification on the hemoglobin affinity column. In the inset the fast component has a half-time of retention of 20 min and the slow component the same half-time as the purified material, 190 ± 10 min. The experimental protocol is described under Experimental.

In order to check whether the minor component filtered quickly by the kidney corresponds to dissociable hemoglobin, HbBv–FMDA was applied to a column of immobilized HbA in a pulse experiment. Surprisingly, most of the material (about 75%) behaved as dissociated hemoglobin and was retained on the column. In order to verify the possible existence of a slow dissociation equilibrium in the small fraction containing tetrameric protein which eluted in the void volume, this component was applied again to the hemoglobin affinity column on the following day. No protein was retained, pointing to the absence of a slow equilibrium.

A similar behaviour was observed with HbA–FMDA. In this instance the stability towards dissociation of the HbA–FMDA tetramer purified by means of the hemoglobin affinity column was checked *in vivo* by measuring the intravascular retention in the rat. The slope of the intravascular retention, shown in Fig. 3, was monophasic with a half-time (190 ± 10 min) similar to that measured for intramolecularly cross-linked hemoglobins [5].

This finding indicates that the purified species is stable also *in vivo*. There is, however, an inconsistency between the experiments *in vivo*, where the major fraction is retained by the kidney as a non-dissociable tetramer, and *in vitro*, where the major fraction interacts with the affinity column as a dissociable tetramer. Any explanation will reflect the difficulty of comparing biological and biochemical data. It is possible that the capillaries in the kidney favour or are neutral with regard to tetramer formation, whereas the column favours the dissociation of pseudo-cross-linked species. More probably the reason lies in the presence of isomeric species that are not resolved by the standard purification of the pseudo-cross-linked material and are recognized differently by the glomeruli in the kidney and by the immobilized hemoglobin in the column.

CONCLUSIONS

The experiments presented here demonstrate that hemoglobin affinity columns can be used effectively to purify modified hemoglobins to be used as oxygen carriers. The versatility of the technique is enhanced by the cross-interaction between dimers from different hemoglobin species, which reflects the ready formation of hybrid hemoglobin tetramers in solution; hence, for example, a column of bovine hemoglobin can be used to purify the human protein.

In addition, hemoglobin affinity columns may provide analytical information. They can be used to establish whether other purification techniques are effective in removing all the non-cross-linked material. More importantly, they can furnish information on the modification reaction itself, as exemplified by the case of bovine hemoglobin cross-linked in the deoxygenated state in which formation of intradimer cross-links in $\alpha_1\beta_1$ dimers was demonstrated for the first time.

REFERENCES

1 A. G. Greenburg, in T. M. Chang and R. P. Geyer (Editors), *Blood Substitutes*, Marcel Dekker, New York, 1989, p. 71.
2 J. A. Walder, R. Y. Walder and A. Arnone, *J. Mol. Biol.*, 141 (1980) 195.
3 R. Chatterjee, E. V. Welty, R. Y. Walder, S. L. Prvitt, P. H. Rogers, A. Arnone and J. A. Walder, *J. Biol. Chem.*, 261 (1986) 9929.
4 E. Bucci, A. Razynska, B. Urbaitis and C. Fronticelli, *J. Biol. Chem.*, 264 (1989) 6191.
5 C. Fronticelli, T. Sato, C. Orth and E. Bucci, *Biochim. Biophys. Acta*, 874 (1986) 76.
6 C. Fronticelli, E. Bucci, A. Razynska, J. Sznajder, B. Urbaitis and Z. Gryczynsky, *Eur. J. Biochem.*, 193 (1990) 331.
7 C. Fronticelli, E. Bucci and A. Razynka, *J. Mol. Biol.*, 202 (1988) 343.
8 T. N. Estep, M. K. Bechtel. T. J. Miller, A. Bagdasarian, in T. M. Chang and R. P. Geyer (Editors), *Blood Substitutes*, Marcel Dekker, New York, 1989, p. 129.
9 E. Antonini, M. R. Rossi Fanelli and E. Chiancone, in H. Sund and G. Blauer (Editors), *Protein–Ligand Interactions*, Walter de Gruter, Berlin, 1975, p. 45.
10 M. R. Rossi Fanelli, G. Amiconi and E. Antonini, *Eur. J. Biochem.*, 92 (1978) 253.
11 C. Fronticelli, E. Bucci, N. Higgins, M. Sassaroli and J. Kowaleczyk, in R. B. Bolin, R. P. Gever and G. J. Nemo (Editors), *Advances in Blood Substitutes Research*, Alan Liss, New York, 1983, p. 51.
12 E. Chiancone and M. Gattoni, *Methods Enzymol.*, 135 (1987) 484.
13 E. Chiancone and M. Gattoni, *J. Mol. Recognition*, 3 (1990) 142.
14 U. K. Laemmli, *Nature (London)*, 227 (1970) 680.
15 K. B. Urbaitis, A. Razynska, Q. Corteza, C. Fronticelli and E. Bucci, *J. Lab. Clin. Med.*, 117 (1991) 115.

Synthetic metal-binding protein surface domains for metal ion-dependent interaction chromatography

I. Analysis of bound metal ions by matrix-assisted UV laser desorption time-of-flight mass spectrometry

T. William Hutchens

US Department of Agriculture/Agricultural Research Service, Children's Nutrition Research Center, Department of Pediatrics, Baylor College of Medicine and Texas Children's Hospital, Houston, TX 77030 (USA)

Randall W. Nelson

Vestec Corporation, 9299 Kirby Drive, Houston, TX 77054 (USA)

Chee Ming Li and Tai-Tung Yip

US Department of Agriculture/Agricultural Research Service, Children's Nutrition Research Center, Department of Pediatrics, Baylor College of Medicine and Texas Children's Hospital, Houston, TX 77030 (USA)

ABSTRACT

To extend the analytical capabilities of immobilized metal ion affinity chromatography (IMAC) for evaluation of biologically relevant peptide–metal ion interactions, we have prepared synthetic peptides representing metal-binding protein surface domains from the human plasma metal transport protein known as histidine-rich glycoprotein (HRG). Three synthetic peptides, representing multiples of a 5-residue repeat sequence (Gly–His–His–Pro–His) from within the histidine- and proline-rich region of the C-terminal domain were prepared. Prior to immobilization, the synthetic peptides were evaluated for identity and sample homogeneity by matrix-assisted UV laser desorption time-of-flight mass spectrometry (LDTOF-MS), a method developed recently for the mass determination of high-molecular-mass biopolymers. 2,5-Dihydroxybenzoic acid was evaluated as a matrix to facilitate the laser desorption and ionization of intact peptides and was found to be ideally suited for determinations of mass within the low-mass region of interest (641.7 to 1772.8 dalton). We observed minimal chemical noise from photochemically generated peptide-matrix adduct signals, clustering, and multiply-charged peptide species. Peptides with bound sodium and potassium ions were observed; however, these signal intensities were reduced by immersion of the sample probe tip in water. Mixtures of the three different synthetic peptides were also evaluated by LDTOF-MS after their elution through a special immobilized peptide-metal ion column designed to investigate metal ion transfer. We found LDTOF-MS to be a useful new method to verify the presence of peptide-bound metal ions. Thus, LDTOF-MS is ideally suited for the rapid (3–5 min), sensitive (< 1 pmol), accurate ($\pm 0.05\%$), and relatively high resolution ($m/\Delta m = 300$–500, full width at half maximum, where m = mass) evaluation of synthetic peptides. Further, LDTOF-MS was found to be an important tool for the characterization of peptide mixtures and peptide–metal ion interactions.

Correspondence to: Dr. T. William Hutchens, Department of Pediatrics (CNRC), Baylor College of Medicine, 1100 Bates, Houston, TX 77030, USA.

INTRODUCTION

We have investigated the preparation of synthetic peptides for the purpose of building bioactive model surfaces which may mimic naturally occurring metal-binding domains identified on the surface of known metal transport proteins. Histidine-rich glycoprotein (HRG) is a 75 000-dalton Zn(II)- and Cu(II)-binding plasma protein with unique arrangements of repeating His (11–13 mol%) and Pro (14–16 mol%) residues in the C-terminal region [1–7]. A 5-residue primary sequence of GHHPH is found in tandem repeats of up to 25 residues [6]. We have synthesized HRG peptides of the type (GHHPH)$_n$G, where n = 1–3, to investigate the affinity of this protein surface metal-binding domain for free metal ions and to evaluate metal ion-dependent macromolecular recognition of the native peptide.

Matrix-assisted UV laser desorption time-of-flight mass spectrometry (LDTOF-MS) has been introduced recently [8–13] as a means for the mass determination of high-molecular-mass biomolecules. One purpose of this communication is to discuss LDTOF-MS as a routine method for monitoring the accuracy and completeness of automated peptide synthesizers. More importantly, we have found LDTOF-MS to be a new method to evaluate directly the interaction of transition metal ions with synthetic peptides representing metal-binding protein surface domains (see also refs. 14–17 and Note added in proof).

EXPERIMENTAL

Synthesis of HRG metal-binding peptides (GHHPH tandem repeats)

The 6-residue HRG peptide (GHHPH)$_1$G (1-mer), the 11-residue HRG peptide (GHHPH)$_2$G (2-mer), and the 16-residue HRG peptide (GHHPH)$_3$G (3-mer) were synthesized on an Applied Biosystems Model 430A automated peptide synthesizer using 9-fluorenylmethyloxycarbonyl (Fmoc)–N-methylpyrrolidone (NMP) chemistry (FastMoc, Applied Biosystems). C-Terminal residues were attached onto p-hydroxymethylphenoxymethyl (HMP) resin using standard dicyclohexylcarbodiimide (DCC) procedures. The remaining active hydroxyl groups on the resin were capped with benzoic anhydride before initiation of peptide synthesis. Coupling of amino acid derivatives to the C-terminal residue was achieved stepwise by removal of the N-terminus Fmoc group (with piperidine) followed by coupling of the next amino acid using 2-(1H-benzotriazol-1-yl)-1,1,3,3-tetramethyluronium hexafluorophosphate (HBTU) as the coupling reagent. Upon completion, the N-terminus Fmoc protecting group was removed with piperidine. Deprotection of side chain residues and decoupling from resin was achieved by incubation for 1–2 h at room temperature in 95% trifluoroacetic acid. Peptide purity was verified by reversed-phase high-performance liquid chromatography on a Waters RCM Delta-Pak C_{18} Prep Pak cartridge (100 mm × 25 mm I.D.; 15-μm particle size; 30-nm pore size). Peptide amino acid sequences were verified by Edman (see ref. 18) degradation with an Applied Biosystems Model 473A automated peptide sequence analyzer. The calculated mass of each synthetic peptide was verified by UV LDTOF-MS [14,17] and by electrospray ionization mass spectrometry [17]. The calculated mass values were based upon IUPAC average atomic masses for C (12.011), N (14.007), O (15.999), H (1.008), S (32.060) and P (30.974).

Preparation of synthetic peptides for LDTOF-MS

Synthetic peptides were deblocked and cleaved from the resin and either lyophylized directly or purified by reversed-phase high-perforance liquid chromatography. Saturated solutions of 2,5-dihydroxybenzoic acid (M_r = 154.12) were prepared fresh for each experiment in Milli-Q water. Typically, 1–2 μl of a 1–100 nmol/ml peptide solution (in water, buffer or 70% acetonitrile in water was mixed with 1–2 μl of 2,5-dihydroxybenzoic acid; 2 μl of this mixture were applied to the 2-mm diameter stainless-steel probe tip and air-dried at room temperature (25°C). Where indicated, the dried peptide-matrix deposit on the probe tip was washed in Milli-Q water (25°C) and redried. The probe was then inserted through a vacuum lock into the mass spectrometer. Vacuum pump down time averaged 2–4 min.

UV laser desorption time-of-flight mass spectrometry

MS was performed on a Vestec Model 2000 laser

TABLE I

VERIFICATION OF AMINO ACID SEQUENCE AND MASS FOR SYNTHETIC HRG PEPTIDES

Code	Peptide sequence	Molecular mass (M_r)	$[M + H]^+$	
			Calculated	Observed
1-mer	GHHPHG	640.7	641.7	641.6
2-mer	GHHPHGHHPHG	1206.3	1207.3	1207.5
3-mer	GHHPHGHHPHGHHPHG	1771.8	1772.8	1772.5

desorption linear time-of-flight mass spectrometer. Frequency-tripled output from a Q-switched neodymium–yttrium aluminum garnet (Nd-YAG) pulsed laser (355 nm, 5 ns pulse, Lumonics HY400) or a pulsed nitrogen laser (337 nm, 3 ns pulse, Laser Science) was focused (12-in. focal length) through a fused-silica window to irradiate a spot (ca. 150 μm × 300 μm) of the insertion probe tip on which the matrix/analyte solution had been dried. A variable attenuator was used to maintain the laser power density at the optimal threshold for desorption/ionization of the analyte species (ca. 1–2 · 10⁶ W/cm). Ions desorbed by pulsed laser irradiation were accelerated to 30 keV and allowed to drift along a 2-m flight path (maintained at 30 μPa) to a 20-stage focused mesh electron multiplier. A Lecroy model TR8828D transient recorder (5-ns time resolution) and LeCroy 6010 MAGIC controller were used with software permitting real-time signal averaging of multiple laser shots (all spectra presented are the signal average of 100 laser shots). Data were transferred from the MAGIC controller to a Compaq 386/33 personal computer. The resulting mass spectrum, calculation of peak centroids, and data reduction were performed using PC-based software (Lab-Calc, Vestec).

RESULTS AND DISCUSSION

The accurate mass determination of synthetic peptides has been recognized as a valuable tool in preparation of high-quality peptides [19,20]. It has been reported [21] that as many as 50% of the synthetic peptide preparations characterized by MS at protein chemistry core laboratories contained peptides with incorrect masses; others were not homogeneous. For analytical (i.e., quantitative) affinity chromatography, the accuracy with which synthetic

ligands are prepared is essential to avoid ambiguities in data reduction and interpretation.

The amino acid sequence of each of the three synthetic peptides was verified by sequential Edman degradation. Each of the synthetic peptides was also evaluated by LDTOF-MS. We found excellent agreement between the calculated and observed mass values; there was no evidence of incomplete or intermediate products resulting from peptide synthesis. These results are summarized in Table I. Representative mass spectra around the parent molecular ions are shown for the case of the synthetic HRG peptide (GHHPH)₂G.

Fig. 1. shows the LDTOF mass spectrum obtained for the synthetic HRG peptide (GHHPH)₂G (2-mer). In this case, the peptide sample [prepared in 40% acetonitrile–0.1% trifluoroacetic acid (TFA)] was mixed with an equal volume of 2,5-dihydroxybenzoic acid matrix, applied to the probe tip, and allowed to air-dry at room temperature. Analysis by LDTOF-MS revealed an M_r of 1207.5 for the protonated molecule $[M + H]^+$. The smaller peak observed at an M_r of 1229.1 (Fig. 1) represents the mass of the sodium adduct $[M + Na]^+$. The relative quantities of free peptide and the peptide-sodium adduct were found to vary with the solvent concentration of sodium ions. This is an important consideration for the routine evaluation of peptides after affinity chromatography in high salt buffers and, therefore, was investigated further.

The full effects of added buffer salts on the LDTOF mass spectrum obtained for the synthetic HRG peptide (GHHPH)₂G (2-mer) is illustrated in Fig. 2. The peptide sample was prepared in a commonly used buffer (20 mM sodium phosphate, 0.5 M NaCl, pH 7.0), applied to the probe tip with 2,5-dihydroxybenzoic acid (in water) as the matrix, allowed to air-dry, and analyzed by LDTOF-MS.
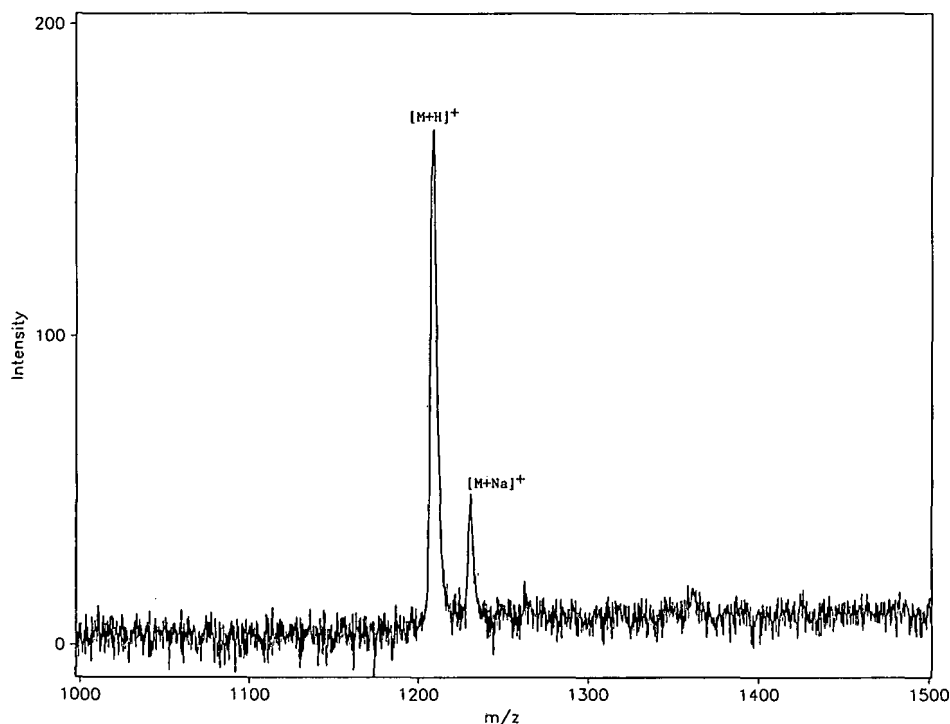
Fig. 1. LDTOF mass spectrum obtained for the synthetic HRG peptide (GHHPH)$_2$G with 2,5-dihydroxybenzoic acid as the matrix. The peptide sample (in acetonitrile–TFA) was applied to the probe tip, air-dried, washed gently with Milli-Q water and analyzed.

The protonated molecule (M_r 1207.5) observed originally (Fig. 1) was absent. Instead, two peaks were observed. The first peak represents the peptide with one sodium adduct (M_r 1229.1). The second peak represents the peptide with two sodium adducts (M_r 1251.7). This particular example represents one of the more extreme cases we have observed. The effects of buffer salts on the mass of the synthetic HRG peptide (i.e., the presence of sodium and potassium adducts), however, could be reduced or eliminated. When the dried peptide sample on the probe tip was washed with Milli-Q water (by immersion of the inverted probe tip into a reservoir), subsequent analysis by LDTOF-MS revealed the protonated molecule and one additional peak, $[M + K]^+$ (Fig. 3). A summary of molecular ions observed for the synthetic 2-mer peptide is presented in Table II.

We have also explored the use of LDTOF-MS for the direct evaluation of transition metal ion interactions with known metal-binding peptides and even with mixtures of these peptides. The results shown in Fig. 4 reveal the LDTOF mass spectrum observed for a mixture of all three synthetic HRG peptides (1-mer, 2-mer and 3-mer) after receiving Cu(II) ions by metal ion transfer from a stationary phase of immobilized metal ions (see Table III). In this example, the mixture of three HRG peptides had been passed through a column of the immobilized HRG peptide (GHHPH)$_2$G loaded with Cu(II) ions. The immobilized HRG peptide had been coupled at a low ligand density (3 μmol metal ion bound/ml gel) to a commercial preparation of activated agarose (Affi-10, Bio-Rad). The eluted HRG peptide (GHHPH)$_1$G (1-mer) was observed as a protonated molecule free of bound metal ions (peak labeled 1.0; M_r 641.6), with one bound Cu(II) ion (peak labeled 1.1; M_r 703.0), and with two bound Cu(II) ions (peak labeled 1.2; M_r 764.5). The middle set of peaks revealed the mass of the (GHHPH)$_2$G peptide free of bound metal ions (peak labeled 2.0; M_r 1207.7), with one bound Cu(II) ion (peak labeled 2.1; M_r 1269.9), with two bound Cu(II) ions (peak labeled 2.2; M_r 1332.1),
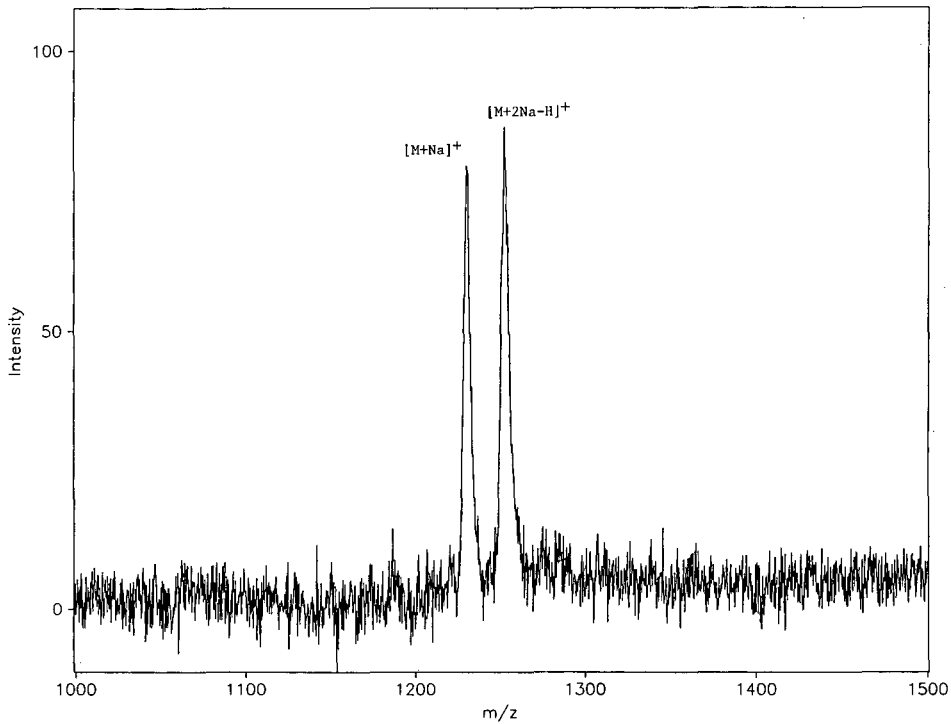
Fig. 2. Effects of buffer salts on the LDTOF mass spectrum obtained for the synthetic HRG peptide (GHHPH)$_2$G. The peptide sample was applied to the probe tip with 2,5-dihydroxybenzoic acid as the matrix, allowed to air-dry and analyzed.
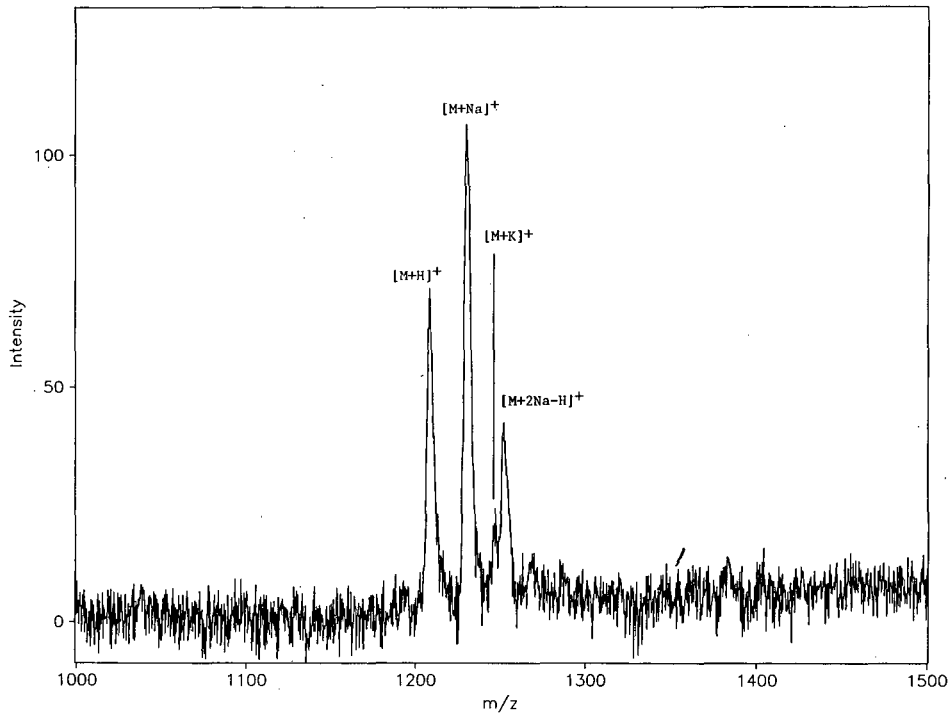
Fig. 3. Removing the effects of buffer salts on the mass of the synthetic HRG peptide (GHHPH)$_2$G. The peptide sample was applied to the probe tip with 2,5-dihydroxybenzoic acid as the matrix, allowed to air-dry, washed briefly with Milli-Q water and analyzed by LDTOF-MS.

TABLE II

MOLECULAR ION MASS ASSIGNMENTS FOR PEAKS OBSERVED IN FIGS. 1–3

Synthetic HRG peptide: GHHPHGHHPHG (2-mer).

Molecular ion	M_r	
	Calculated	Observed
$[M+H]^+$	1207.3	1207.5
$[M+Na]^+$	1229.3	1229.1
$[M+K]^+$	1245.3	1246.1
$[M+2Na-H]^+$	1250.3	1251.7

with three bound Cu(II) ions (peak labeled 2.3; M_r 1394.3), and some with four bound Cu(II) ions (peak labeled 2.4; M_r 1456.8). The last group of peaks on the right represents the mass of the (GHHPH)$_3$G (3-mer) peptide free of any bound metal ions (peak labeled 3.0; M_r 1772.5), with one

bound Cu(II) ion (peak labeled 3.1; M_r 1835.0), with two bound Cu(II) ion (peak labeled 3.2; M_r 1897.3), with three bound Cu(II) ions (peak labeled 3.3; M_r 1959.5), and with four bound Cu(II) ions (peak labeled 3.4; M_r 2022.4). The small peaks marked by an asterisk indicate the presence of an additional sodium adduct. The incremental differences of approximately 62.5 dalton (as opposed to the 63.5 dalton difference expected) observed for the molecular ions with multiple bound Cu(II) ions suggests that, in all cases, the addition of each metal ion results in the displacement of one proton; this effect is under further investigation (see Note added in proof). The near baseline resolution of these peaks within a narrow mass range, and the apparent absence of multiply-charged molecular ions, illustrates the analytical potential of LDTOF-MS.

These results suggest that LDTOF-MS, aside from being a rapid and efficient method for the routine verification of peptide mass, may be an effective tool to investigate directly the interaction of peptides with various metal ions. On the basis of our

TABLE III

MOLECULAR ION MASS ASSIGNMENTS FOR PEAKS OBSERVED IN FIG. 4

The small intermediate peaks in Fig. 4 marked with an asterisk (e.g., between peaks 1.0 and 1.1 and between peaks 2.0 and 2.1) represent a sodium adduct, for example $[M+Na]^+$.

Peak No.	Molecular ion[a]	Calculated[b]	Observed	Difference in mass
1-mer (GHHPH)$_1$G				
1.0	$[M+H]^+$	641.7	641.6	0
1.1	$[M+Cu]^+$	704.2	703.0	61.4
1.2	$[M+2Cu]^+$	766.7	764.5	61.5
2-mer (GHHPH)$_2$G				
2.0	$[M+H]^+$	1207.3	1207.7	0
2.1	$[M+Cu]^+$	1269.8	1269.9	62.2
2.2	$[M+2Cu]^+$	1332.3	1332.1	62.2
2.3	$[M+3Cu]^+$	1393.8	1394.3	62.2
2.4	$[M+4Cu]^+$	1456.3	1456.8	62.5
3-mer (GHHPH)$_3$G				
3.0	$[M+H]^+$	1772.8	1772.5	0
3.1	$[M+Cu]^+$	1835.3	1835.0	61.5
3.2	$[M+2Cu]^+$	1897.8	1897.3	62.3
3.3	$[M+3Cu]^+$	1959.3	1959.5	62.2
3.4	$[M+4Cu]^+$	2021.8	2022.4	62.9

[a] The simplified representation of molecular ion species does not reflect the probable loss of one proton (H^+) for each additional bound Cu(II) ion.

[b] The increase in peptide (molecular ion) mass associated with the presence of multiple bound Cu(II) ions was calculated using the major Cu isotope (63.0 a.m.u.).
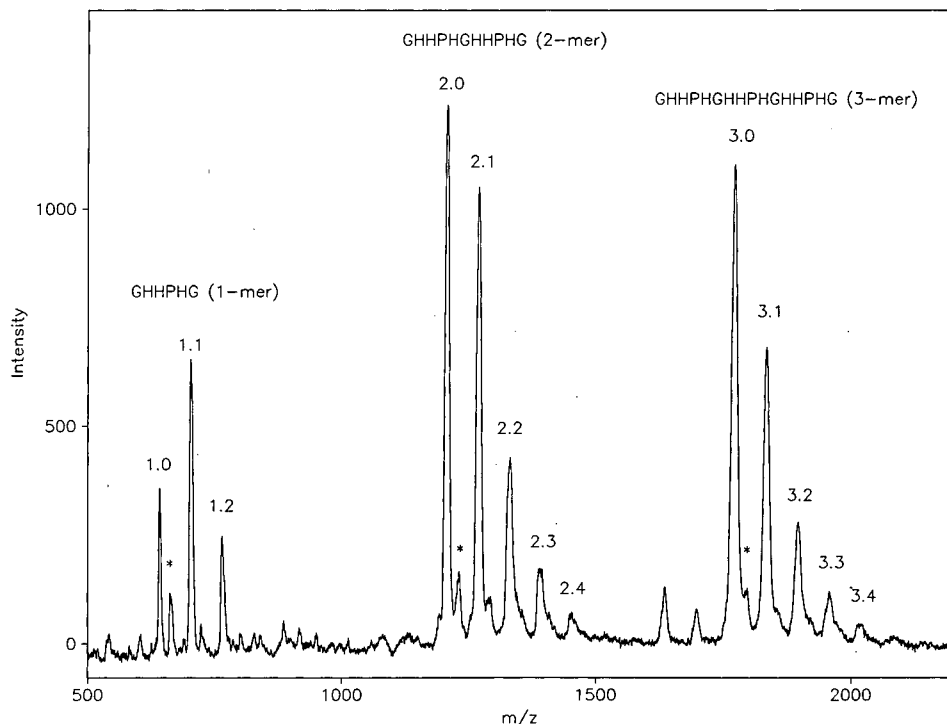
Fig. 4. LDTOF mass spectra of a mixture of all three synthetic HRG peptides (1-mer, 2-mer and 3-mer) after elution from a column of immobilized (GHHPH)$_2$G (2-mer) loaded with Cu(II) ions. The peptide affinity column used for metal ion transfer was prepared by coupling (GHHPH)$_2$G to Affi-10 (Bio-Rad). Cu(II) ions were loaded as described in ref. 20. The column was equilibrated with 20 mM sodium phosphate buffer (pH 7.0) with 0.5 M NaCl. An equimolar mixture of the three different synthetic peptides (free of bound metal ions) was passed through the column unretained. Flow-through fractions were analyzed directly by LDTOF-MS. The peptide sample was applied to the probe tip with 2,5-dihydroxybenzoic acid as the matrix, allowed to air-dry, and analyzed by LDTOF-MS. The metal ion-free HRG peptides (GHHPH)$_1$G (1-mer peak 1.0), (GHHPH)$_2$G (2-mer peak 2.0), and (GHHPH)$_3$G (3-mer peak 3.0) are observed along with peptides with 1 or more bound Cu(II) ions. The small peaks marked by an asterisk indicate the presence of a quasi-molecular sodium ion. A detailed description of the peaks observed in this spectrum is provided in the text.

more recent work, published after the initial presentation of this paper (see Note added in proof) we now know that LDTOF-MS presents the opportunity to investigate several biopolymer–metal ion interaction parameters, such as stoichiometric distributions of bound metal ions [14,15,17], metal ion-dependent molecular recognition events, metal ion transfer, and the detection and mapping of metal ion-binding peptides in samples derived from enzymatic digestion [16].

ACKNOWLEDGEMENTS

NOTE ADDED IN PROOF

Since the original presentation of results outlined in this paper, several additional manuscripts have been published (see refs. 14–17). More recently, specific peptide–metal ion interaction chemistries in-

volving both N and S ligands have been investigated by electrospray ionization mass spectrometry [22,23].

REFERENCES

1 N. Heimburger, H. Haupt, T. Kranz and S. Baudner, *Hoppe-Seyler's Z. Physiol. Chem.*, 353 (1972) 1133–1140.
2 W. T. Morgan, *Biochim. Biophys. Acta*, 533 (1978) 319–333.
3 H. R. Lijnen, M. Hoylaerts and D. Collen, *J. Biol. Chem.*, 255 (1980) 10214–10222.
4 T. Koide, S. Odani and T. Ono, *FEBS Lett.*, 141 (1982) 222–224.
5 W. T. Morgan, *Biochemistry*, 24 (1985) 1496–1501.
6 T. Koide, D. Foster, S. Yoshitake, E. W. Davie, *Biochemistry*, 25 (1986) 2220–2225.
7 T.-T. Yip and T. W. Hutchens, *Protein Expression Purif.*, 2 (1991) 355–362.
8 M. Karas and F. Hillenkamp, *Anal. Chem.*, 60 (1988) 2299–2301.
9 R. C. Beavis and B. T. Chait, *Rapid. Commun. Mass Spectrom.*, 3 (1989) 436–439.
10 R. C. Beavis and B. T. Chait, *Anal. Chem.*, 62 (1990) 1836–1840.
11 R. C. Beavis and B. T. Chait, *Proc. Natl. Acad. Sci. U.S.A.*, 87 (1990) 6873–6877.
12 M. Karas and U. Bahr, *Trends Anal. Chem.*, 9 (1990) 321–325.
13 I. K. Perera, E. Uzcategui, P. Hakansson, G. Brinkmalm, G. Petterson, G. Johansson and B. U. R. Sundqvist, *Rapid. Comm. Mass Spectrom.*, 4 (1990) 285–289.
14 T. W. Hutchens, R. W. Nelson and T.-T. Yip, *J. Mol. Recog.*, 4 (1991) 151–153.
15 R. W. Nelson and T. W. Hutchens, *Rapid Commun. Mass Spectrom.*, 6 (1992) 4–8.
16 T. W. Hutchens, R. W. Nelson and T.-T. Yip, *FEBS Lett.*, 296 (1992) 99–102.
17 T. W. Hutchens, R. W. Nelson, M. H. Allen, C. M. Li and T.-T. Yip, *Biol. Mass Spectrom.*, 21 (1992) 151–159.
18 P. Edman and A. Henschen, in S. B. Needleman (Editor), *Protein Sequence Determination*, Spinger, New York, 1975, pp. 232–279.
19 B. Sunqvist, A. Hedin, P. I. Hakansson, M. Kamensky, M. Salehpour and G. Sawe, *Int. J. Mass Spectrom. Ion Proc.*, 65 (1985) 69–89.
20 T. W. Hutchens and T.-T. Yip, *J. Chromatogr.*, 604 (1992) 133.
21 B. T. Chait, in C. J. McNeal (Editor), *The Analysis of Peptides and Proteins by Mass Spectrometry*, Wiley, Chichester, 1988, pp. 21–39.
22 M. H. Allen and T. W. Hutchens, *Rapid Commun. Mass Spectrom.*, 6 (1992) 308–312.
23 T. W. Hutchens and M. H. Allen, *Rapid Commun. Mass Spectrom.*, 6 (1992) in press.

Synthetic metal-binding protein surface domains for metal ion-dependent interaction chromatography

II. Immobilization of synthetic metal-binding peptides from metal ion transport proteins as model bioactive protein surface domains

T. William Hutchens and Tai-Tung Yip

US Department of Agriculture/Agricultural Research Service, Children's Nutrition Research Center, Department of Pediatrics, Baylor College of Medicine and Texas Children's Hospital, Houston, TX 77030 (USA)

ABSTRACT

This preliminary investigation tests the premise that biologically relevant (1) peptide–metal ion interactions, and (2) metal ion-dependent macromolecular recognition events (*e.g.*, peptide–peptide interactions) may be modeled by biomimetic affinity chromatography. Divinylsulfone-activated agarose (6%) was used to immobilize three different synthetic peptides representing metal-binding protein surface domains from the human plasma metal transport protein histidine-rich glycoprotein (HRG). The synthetic peptides represented 1–3 multiple repeat units of the 5-residue sequence (Gly–His–His–Pro–His) found in the C-terminal of HRG. By frontal analyses, immobilized HRG peptides of the type $(GHHPH)_nG$, where $n = 1$–3, were each found to have a similar binding capacity for both Cu(II) ions and Zn(II) ions (31–38 μmol/ml gel). The metal ion-dependent interaction of a variety of model peptides with each of the immobilized HRG peptide affinity columns demonstrated differences in selectivity despite the similar internal sequence homology and metal ion binding capacity. The immobilized 11-residue HRG peptide was loaded with Cu(II) ions and used to demonstrate selective adsorption and isolation of proteins from human plasma. These results suggest that immobilized metal-binding peptides selected from known solvent-exposed protein surface metal-binding domains may be useful model systems to evaluate the specificity of biologically relevant metal ion-dependent interaction and transfer events *in vitro*.

INTRODUCTION

Despite remarkable increases in the number of solutions to various biopolymer structures, the surface chemistry of biospecific macromolecular interactions remains elusive in the majority of cases. Development of stationary phase surfaces with immobilized ligands of predetermined biochemical specificity and affinity for specific peptides and protein

surface structures may provide useful *in vitro* models to investigate a variety of macromolecular recognition events.

Metal ion-dependent protein–protein and protein–DNA interactions occur frequently in nature and are now being recognized as events of major regulatory significance in biology (*e.g.*, refs. 1 and 2). The interactions of peptides and proteins with surface-immobilized transition metal ions *in vitro* may present an important opportunity to investigate and model the subtleties of metal ion-dependent macromolecular recognition motifs. Proteins with well-defined surface structures have been used

Correspondence to: Dr. T. William Hutchens, Department of Pediatrics (CNRC), Baylor College of Medicine, 1100 Bates, Houston, TX 77030, USA.

to explore differences in the predicted and observed interactions of these proteins with immobilized transition metal ions under a variety of experimental conditions [3–6]. We propose that this approach may be especially informative if the model surface of stationary metal ions is comprised of synthetic peptides which represent naturally occurring metal-binding domains identified from the surface of known metal transport proteins.

The human plasma protein referred to as histidine-rich glycoprotein (HRG) is a 75 000-dalton Zn(II)- and Cu(II)-binding protein rich in His (11–13 mol%) and Pro (14–16 mol%) [7–13]. A 5-residue sequence (GHHPH) in the His-rich C-terminal region of HRG has been identified tentatively as the Zn(II)- and heme-binding motif in this protein [14–17]. This 5-residue primary sequence is found in tandem repeats of up to 25 residues in length. We have synthesized (GHHPH)$_n$G for $n = 1$–3 to investigate the affinity of this protein surface metal-binding domain for free metal ions (see also refs. 18–21, added in proof) and to evaluate metal ion-dependent macromolecular recognition of this peptide.

The purpose of this communication is to discuss concepts, outline problems and present preliminary data which may serve as examples to increase the interest in using a biologically directed approach to the design and investigation of metal ion-dependent biomolecular interactions.

EXPERIMENTAL

Synthesis of HRG metal-binding peptides (GHHPHG tandem repeats)

The 6-residue HRG peptide (GHHPH)$_1$G (1-mer), the 11-residue HRG peptide (GHHPH)$_2$G (2-mer), and the 16-residue HRG peptide (GHHPH)$_3$G (3-mer) were synthesized on an Applied Biosystems Model 430A automated peptide synthesizer using 9-fluorenylmethyloxylcarbonyl (Fmoc) chemistry. Peptide purity was verified by reversed-phase high-performance liquid chromatography. Peptide sequences were verified by sequential Edman degradation (see ref. 22) with an Applied Biosystems Model 473A automated peptide sequence analyzer. Determination of synthetic peptide mass was performed with a Vestec UV laser desorption time-of-flight mass spectrometer [18–21,23].

TABLE I

IMMOBILIZED METAL-BINDING HRG PEPTIDES

Bound transition metal ions: Cu(II), Zn(II)

Immobilized GHHPHG
Immobilized GHHPHGHHPHG
Immobilized GHHPHGHHPHGHHPHG

Immobilization of synthetic HRG peptides

Sepharose 6B (Pharmacia) was activated with divinylsulfone (DVS) as described earlier by Porath and Axen [24]. Equivalent molar quantities of each of the HRG peptides were coupled (10 μmol/g gel) in 0.5 M sodium bicarbonate at pH 8–9 for 20 h at 23–25°C. Remaining vinyl groups were blocked by incubation overnight with 10% glycine in 0.5 M sodium carbonate at pH 9.4. Control preparations included DVS-activated agarose gel treated in an identical manner except for the addition of HRG peptide. Metal binding capacities were confirmed by frontal analyses with copper sulfate (0.8 mM) or zinc sulfate (1.0 mM) in 25 mM 4-(2-hydroxyethyl)-1-piperazinethanesulfonic acid (HEPES) buffer (pH 6.0–6.5). The void (dead) volumes were determined by pumping the same metal ion solutions into control columns of DVS-cross-linked agarose of the same dimension and bed volumes but prepared without immobilized peptides (i.e., glycine inactivated).

Interaction of model peptides with immobilized HRG peptide–Zn(II) and Cu(II) ions

Affinity columns (2.3 cm × 1.0 cm I.D.) of the three different immobilized HRG peptides were loaded with a 0.8 mM solution of Cu(II) ions or a 1.0 mM solution of Zn(II) ions in 25 mM HEPES buffer (pH 6.0–6.5). This is an important distinction from the metal ion loading procedures described previously for work with immobilized iminodiacetate (IDA) or tris(carboxymethyl)ethylenediamine (TED) metal chelate columns where metal ions were loaded in water [13,25–27]. Metal-free peptide samples were added (50–100 μl) to immobilized HRG peptide–Cu(II) or immobilized HRG peptide–Zn(II) equilibrated with 20 mM sodium phosphate buffer (pH 7.0) containing 0.5 M NaCl. Unbound peptides were removed by elution with column equilibration buffer. Bound peptides were eluted

with a pH gradient from pH 7.0 (20 mM sodium phosphate, 0.5 M NaCl) to pH 3.8 (50 mM sodium phosphate, 0.5 M NaCl) unless stated otherwise. The ionic strength of both the column equilibration buffer and the pH gradient elution buffers was elevated by inclusion of 0.5 M NaCl to eliminate nonspecific electrostatic interactions otherwise observed with immobilized metal ion affinity chromatography [25,26]. The absorbance at 220 nm and/or 280 nm and pH were monitored in each fraction (1 ml).

Interaction of human plasma proteins with immobilized HRG peptide-Cu(II) ions

An affinity column (2.3 × 1 cm) of the 11-residue HRG peptide (2-mer) was loaded with Cu(II) ions and equilibrated with 20 mM sodium phosphate buffer (pH 7.0) containing 0.5 M NaCl. An aliquot of human plasma (0.5 ml, dialyzed against 50 mM EDTA, then column equilibration buffer) was injected into the column and washed extensively (over 250 column volumes) until the absorbance at 280 nm had reached baseline. The bound proteins were then eluted with a pH gradient from pH 7 to 3.8 and finally with 50 mM EDTA in 20 mM sodium phosphate pH 7.0.

Sodium dodecyl sulfate (SDS)-polyacrylamide gradient gel electrophoresis (PAGGE)

Samples were heated with 2 to 5 volumes of solubilization buffer (2% SDS, 3% mercaptoethanol, 50 mM Tris–HCl, pH 6–8, and 10% glycerol) at 95°C for 2 min and then separated on a 8–12% polyacrylamide gradient gel according to Laemmli [28]. Silver staining was according to Morrisey [29].

RESULTS

Fig. 1 shows the frontal analyses of Cu(II) ion interaction with the immobilized 6-residue HRG peptide (GHHPH)$_1$G, the immobilized 11-residue HRG peptide (GHHPH)$_2$G (2-mer), and the immobilized 16-residue HRG peptide (GHHPH)$_3$G (3-mer) (Table I). Frontal analyses were performed on two different sets of each immobilized peptide column. Despite differences in the number of internally homologous repeat units, there were no significant differences in the total Cu(II) ion binding capacity (31 μmol/ml gel) among the three different immobi-

Fig. 1. Frontal analyses of Cu(II) ion interaction with the immobilized 6-residue HRG peptide (GHHPH)$_1$G (1-mer; □), the immobilized 11-residue HRG peptide (GHHPH)$_2$G (2-mer; ▽) and the immobilized 16-residue HRG peptide (GHHPH)$_3$G (3-mer; ○). The columns (2.3 cm × 1.0 cm I.D.) were equilibrated in 25 mM HEPES buffer pH 6.0. A solution of CuSO$_4$ (800 $\mu$$M$) in 25 m$M$ HEPES (pH 6.0) was pumped continuously into the columns. Copper elution was monitored by absorbance at 280 nm.

lized HRG peptide affinity columns. Nonetheless, these same columns differed appreciably in their affinity for a given set of model peptide ligates.

Fig. 2 illustrates the Cu(II) ion-dependent interaction of angiotensin I with separate columns of immobilized 6-residue HRG peptide GHHPHG (1-mer), the immobilized 11-residue HRG peptide (GHHPH)$_2$G, and the immobilized 16-residue HRG peptide (GHHPH)$_3$G. In no case was any portion of the applied angiotensin I ever observed to elute unbound in the column flow-through fractions (*i.e.*, equilibration buffer). When elution of bound angiotensin I from each of the three different immobilized HRG peptide–Cu(II) columns was initiated with an identical gradient of descending pH (from pH 7 to pH 4), significant differences in angiotensin I elution were apparent (Fig. 2); differences in angiotensin I elution from these columns were also observed by stepwise pH elution (data not
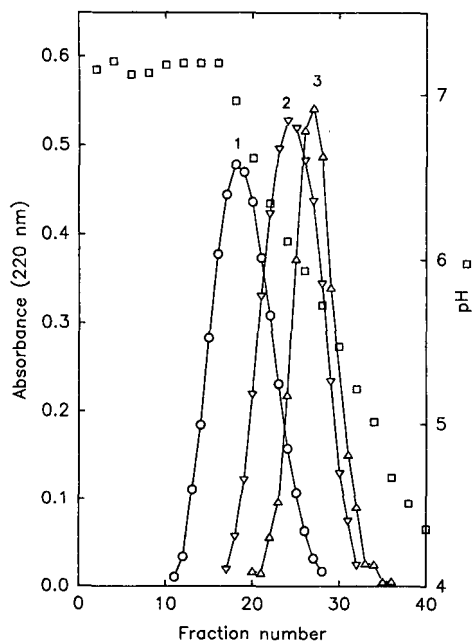
Fig. 2. Cu(II) ion-dependent interaction of angiotensin I with immobilized 1-mer (peak 1; ○), 2-mer (peak 2; ▽) and 3-mer (peak 3, △). After loading with Cu(II) ions as described in Fig. 1, the columns (2.3 cm × 1.0 cm I.D.) were equilibrated with 20 mM sodium phosphate (pH 7.0) containing 0.5 M NaCl. Elution of bound peptide was initiated with a descending pH gradient from pH 7 to pH 4 (□). Fractions of 1.0 ml each were collected. Peptide elution was monitored by absorbance at 220 nm.

Fig. 3. Cu(II) ion-dependent interaction of several different metal-binding peptides with the immobilized 11-residue HRG peptide (GHHPH)$_2$G (2-mer). A 1.8-ml column (2.3 cm × 1 cm I.D.) of the immobilized (GHHPH)$_2$G was loaded with Cu(II) ions and equilibrated with 20 mM sodium phosphate buffer (pH 7.0) containing 0.5 M NaCl. The various peptides to be analyzed were loaded onto the immobilized (GHHPH)$_2$G–Cu(II) ion column separately (50–100 μl). After removing unbound and loosely retained peptides by washing with 22 fractions (1 ml each) of column equilibration buffer, bound peptides were eluted with a discontinuous pH gradient (□) from pH 7.0 to pH 5.8 (20 mM sodium phosphate, 0.5 M NaCl) and from pH 5.8 to pH 3.8 (50 mM sodium phosphate, 0.5 M NaCl). Absorbance at 220 nm or 280 nm in each fraction was monitored as a function of measured elution pH. The numbered peaks indicate the elution positions of (1) bovine gastric inhibitory peptide, (2) angiotensin II, (3) the HRG peptide (GHHPH)$_4$G, (4) angiotensin I, (5) parathyroid hormone 1–34, (6) human gastric inhibitory peptide and (7) the HRG peptide (GHHPH)$_2$G.

shown). Therefore, a larger series of different model peptides were evaluated for indications of selectivity for immobilized HRG peptide–Cu(II).

Results shown in Fig. 3 illustrate further the Cu(II) ion-dependent interaction of several different peptides with only the immobilized 11-residue HRG peptide (GHHPH)$_2$G. The column of immobilized HRG metal-binding peptide (GHHPH)$_2$G was loaded with Cu(II) ions and equilibrated with 20 mM sodium phosphate buffer (pH 7.0) containing 0.5 M NaCl. The separate numbered elution peaks shown in Fig. 3 reflect the ability of the immobilized (GHHPH)$_2$G, only in the presence of bound Cu(II) ions, to resolve bovine gastric inhibitory peptide, angiotensin II, the 6-residue HRG peptide (GHHPH)$_1$G, angiotensin I, parathyroid hormone 1–34 and human gastric inhibitory peptide. When the 11-residue HRG peptide (GHHPH)$_2$G was added as free peptide to the column of immobilized (GHHPH)$_2$G it was tightly

bound and, upon elution at low pH, was only barely distinguished from human gastric inhibitory peptide. None of the peptides were retained on the column of immobilized (GHHPH)$_2$G in the absence of metal ions (data not shown). We next investigated the affinity of each HRG peptide affinity column to bind Zn(II) ions.

Frontal analyses of Zn(II) ion interaction with the immobilized 6-residue HRG peptide (GHHPH)$_1$G, the immobilized 11-residue HRG peptide (GHHPH)$_2$G, and the immobilized 16-res-
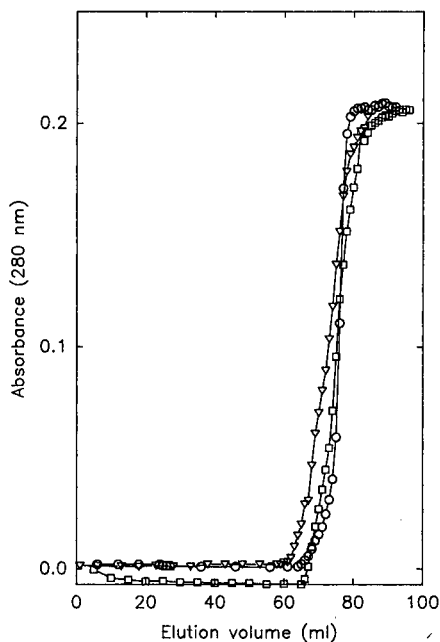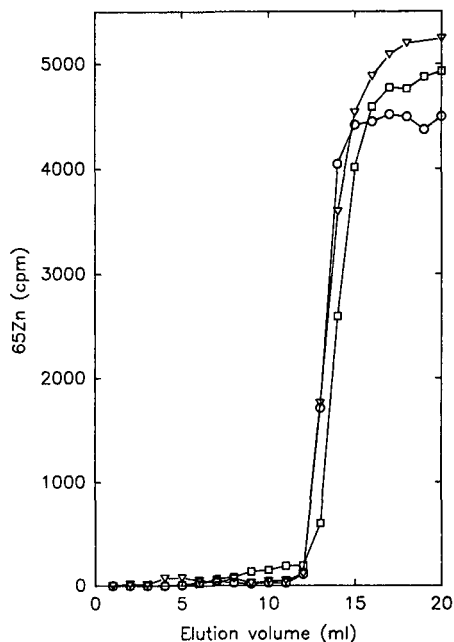
Fig. 4. Frontal analyses of Zn(II) ion interaction with the immobilized 6-residue HRG peptide (GHHPH)₁G (1-mer; ○), the immobilized 11-residue HRG peptide (GHHPH)₂G (2-mer; ▽) and the immobilized 16-residue HRG peptide (GHHPH)₃G (3-mer; □). The columns (2.5 cm × 1.0 cm I.D.) were equilibrated in 25 mM HEPES buffer pH 6.5. A solution of ZnSO₄ (1 mM; labeled with ^{65}ZnSO₄) in 25 M HEPES (pH 6.5) was pumped continuously into the column. Fractions of eluate (1.0 ml each) were monitored for radioactivity to quantitate eluted Zn(II).

idue HRG peptide (GHHPH)₃G is shown in Fig. 4. As in the case of Cu(II) ions, despite a three-fold difference in the number of homologous repeat units, there were no significant difference in the Zn (II)ion binding capacity (38 μmol/ml gel) among the three different immobilized HRG peptides. The immobilized HRG peptide–Zn(II) columns did, however, demonstrate a systematic variation in their affinity for several different model peptides.

Fig. 5 reveals variations in the Zn(II) ion-dependent interaction of three different peptides with columns of the immobilized (GHHPH)₁G (Fig. 5A), the immobilized (GHHPH)₂G (Fig. 5B), and the immobilized (GHHPH)₃G (Fig. 5C). The 16-residue HRG peptide (GHHPH)₃G was bound most tightly to the immobilized 16-residue HRG peptide (GHHPH)₃G and was clearly resolved from angiotensin I and the 11-residue HRG peptide (GHHPH)₂G. This resolution was not observed, or

was less well defined, in the case of chromatography on the immobilized 6-residue peptide (GHHPH)₁G, or the immobilized 11-residue peptide (GHHPH)₂G.

Finally, the immobilized 11-residue HRG peptide–Cu(II) column was investigated for its ability to interact selectivity with proteins present in unfractionated human plasma. Fresh human plasma was dialyzed in column equilibration buffer and loaded onto a column of HRG peptide–Cu(II) affinity column. An estimated 85–90% (based on absorbance at 280 nm) of the applied plasma proteins did not bind to the column and were eluted directly in the flow-through fractions. The column was then washed overnight (approx. 250 column volumes) with equilibration buffer to remove all low-affinity proteins. Introduction of a descending pH gradient resulted in the elution of several plasma proteins (Fig. 6). Subsequent introduction of 50 mM EDTA eluted another set of bound proteins. The composition of the proteins in each of these pools was investigated by SDS–polyacrylamide gradient gel electrophoresis (Fig. 7). The immobilized HRG peptide–Cu(II) column was able to selectivity absorb specific plasma proteins. These proteins are different from some of the plasma proteins adsorbed to other types of immobilized metal ion affinity columns [25,26]. The identity of the adsorbed proteins awaits amino acid sequence and/or immunoblot analyses. The plasma protein adsorption selectivity was metal ion-dependent; more than 98% of the plasma proteins were recovered in the flow-through fractions when applied to an identical column of immobilized peptide in the absence of bound Cu(II) ions (not shown). A detailed comparison of differences in plasma protein adsorption selectivity by the six different types of immobilized HRG peptide–metal ion columns (i.e., HRG 1-mer, 2-mer, 3-mer with bound Cu or Zn) presented here is in progress.

DISCUSSION

Each of the immobilized HRG peptides evaluated in this investigation has a metal binding capacity comparable to the commercially available immobilized chelating groups (IDA). The Pharmacia chelating Sepharose Fast Flow material consists of immobilized IDA groups and has a capacity for Cu(II)
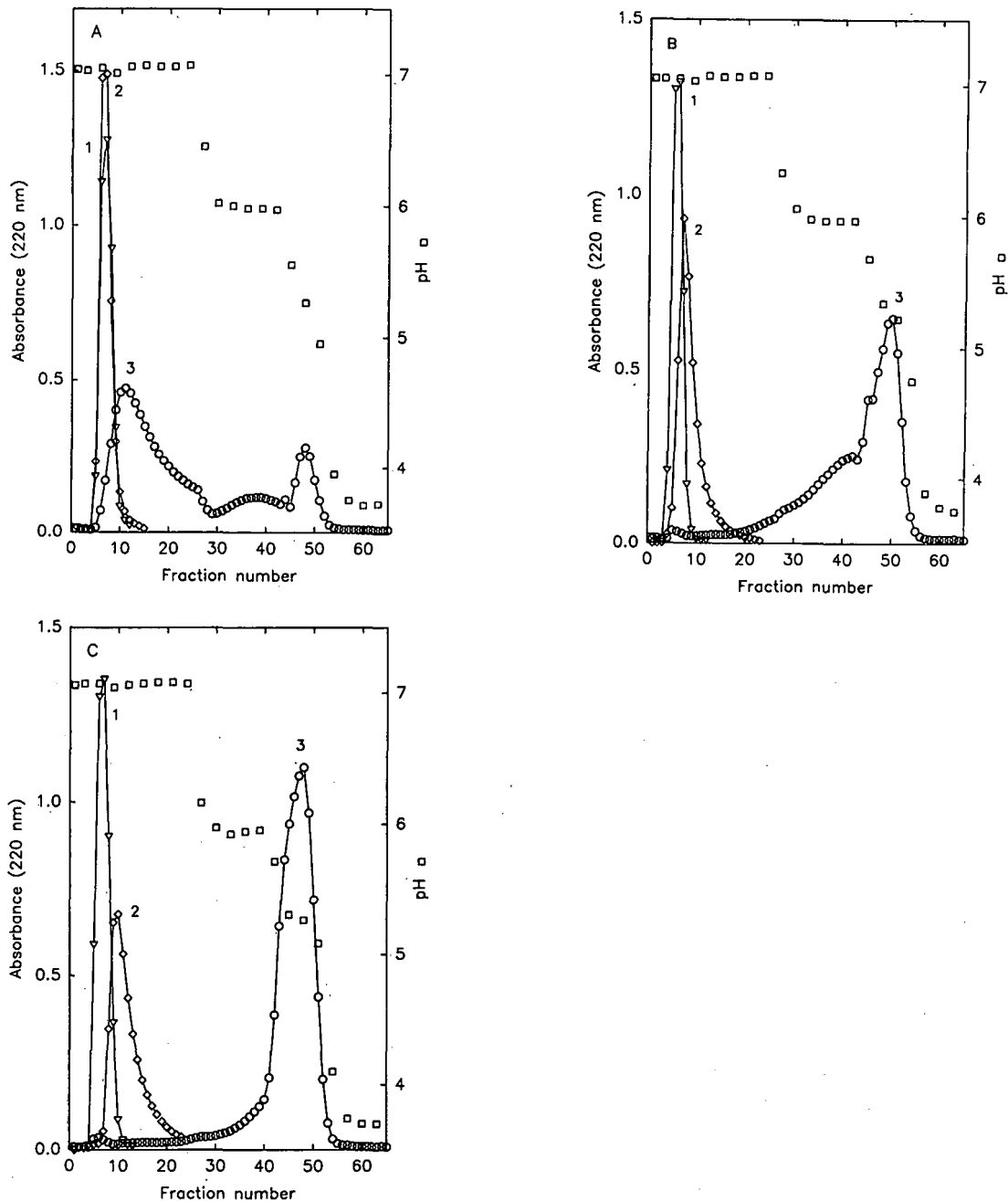
Fig. 5. Zn(II) ion-dependent interaction of angiotensin I (peak 1; ▽), the 11-residue HRG peptide $(GHHPH)_2G$ (peak 2; ◇) and the 16-residue HRG peptide $(GHHPH)_3G$ (peak 3; ○) on columns of the immobilized 6-residue HRG peptide $(GHHPH)_1G$ (A), the immobilized 11-residue HRG peptide $(GHHPH)_2G$ (B) and the immobilized 16-residue HRG peptide $(GHHPH)_3G$ (C). Separate 2.0-ml columns (2.5 cm × 1 cm I.D.) of the immobilized HRG peptide $(GHHPH)_nG$ were loaded with Zn(II) ions and equilibrated with 20 mM sodium phosphate buffer (pH 7.0) containing 0.5 M NaCl. The peptides were loaded onto the immobilized $(GHHPH)_nG$–Zn(II) ion columns separately (50–100 μl). Unbound and loosely retained peptides were removed by washing with 22 fractions (1 ml each) of column equilibration buffer. Bound peptides were eluted with a discontinuous pH gradient (squares) from pH 7.0 to pH 5.8 (20 mM sodium phosphate, 0.5 M NaCl) and from pH 5.8 to pH 3.8 (50 mM sodium phosphate, 0.5 M NaCl). Absorbance at 220 nm in each fraction was monitored as a function of measured elution pH.
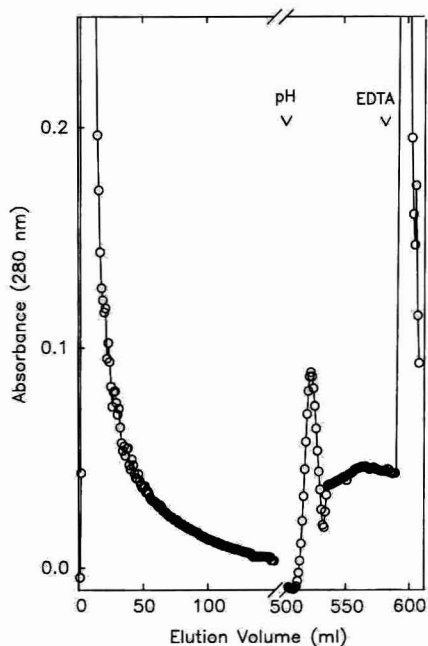
Fig. 6. Cu(II)-dependent interaction of human plasma proteins with the immobilized 11-residue HRG peptide $(GHHPH)_2G$ (2-mer). A 1.8-ml column (2.3 cm × 1 cm I.D.) of the immobilized HRG metal-binding peptide $(GHHPH)_2G$ was loaded with Cu(II) ions and equilibrated with 20 mM sodium phosphate buffer (pH 7.0) containing 0.5 M NaCl. Human plasma was dialyzed against 50 mM EDTA, 20 mM sodium phosphate (pH 7) and then dialyzed against with 20 mM sodium phosphate, 0.5 M NaCl (pH 7). The dialyzed sample (0.5 ml) was applied and the column was washed extensively (overnight) with column equilibration buffer (250 column volumes) until a stable baseline was reached. Bound proteins were eluted with a continuous pH gradient from pH 7–4. Finally, the column was washed with 50 mM EDTA, 20 mM sodium phosphate (pH 7.0). Fractions of 1 ml each were collected for measurement of absorbance (280 nm) and pH.

Fig. 7. SDS–polyacrylamide gel electrophoresis of eluted plasma proteins from the immobilized HRG peptide–Cu(II) affinity column. Peak fractions (5–50 μl) were boiled in SDS solubilization buffer with reducing agent, separated on an 8–12% acrylamide gradient SDS gel, and silver stained. Lanes: 1 = molecular mass markers (kDa = kilodalton); 2 = unretained (flow-through) fraction of plasma protein; 3 = trailing end of unretained peak; 4 = pH gradient eluted peak; 5 = EDTA peak.

and Zn(II) ions which is approximately 30 μmol/ml of gel. The Pharmacia chelating Superose FPLC matrix (IDA) has a metal binding capacity which is reportedly between 20 and 30 μmol metal ion/ml gel. The TSK chelate-5PW high-performance metal chelate (IDA) column (ToyoSoda, Japan) has a Cu(II) binding capacity of 23 μmol/ml of gel. Other types of immobilized chelating groups described in the literature bind transition metal ions with a capacity near that described here for the immobilized HRG peptides. For example, the TED–agarose column described by Porath and Olin [26] was reported to have a metal binding capacity of 47 μmol/ml

of gel. The TED–agarose metal affinity gels synthesized in our laboratory have a somewhat higher capacity, approximately 50 to 65 μmol/ml of gel.

Despite the difference in the number of histidyl residues in the three different immobilized HRG peptides (1–3 internally homologous repeat units), they were nearly indistinguishable in their capacity to bind a given metal ion. Further, the immobilized HRG 1-mer, 2-mer, and 3-mer columns were equivalent in their binding capacity for Cu(II) ions (Fig. 1) and Zn(II) ions (Fig. 4). Although the binding capacity and sequence homology of the three different immobilized HRG peptides were similar, the immobilized peptides displayed differences in both selectivity and affinity for other peptides. Further, the immobilized HRG peptide–Cu(II) ions were found to be a "stronger" interacting affinity ligand

than the equivalent Zn(II) adduct. For example, angiotensin I was retained on each of the HRG peptide–Cu(II) columns but not on the immobilized HRG peptide–Zn(II) columns. This result is consistent with the behavior of peptides and proteins on other immobilized metal ion affinity columns (e.g., IDA and TED).

The selective interaction of model peptides with immobilized HRG peptide–Cu(II) affinity columns was similar to that observed for immobilized iminodiacetate–Cu(II) ions. For example, the elution order (1) bovine gastric inhibitory peptide (1 His/42 residues), (2) angiotensin II (1 His/8 residues), (3) HRG 1-mer (3 His/6 residues), (4) angiotensin I (2 His/10 residues), (5) parathyroid hormone 1–34 (3 His/34 residues), (6) human gastric inhibitory peptide (2 His/42 residues) and (7) HRG 2-mer (6 His/11 residues) is generally similar to that observed for these peptides from immobilized IDA–Cu(II) ions, except for the stronger retention of bovine gastric inhibitory peptide by immobilized IDA–Cu(II) ions [30].

It should be noted that the immobilized HRG peptide columns loaded with Cu(II) were stable to elution with up to 100 mM imidazole. The affinity elution of peptides and proteins from these columns with imidazole is under further investigation. However, even 100 mM imidazole could not elute the tightly bound plasma protein from the immobilized 2-mer–Cu(II) column (data not shown).

The immobilized HRG peptide affinity for Zn(II) ions was significantly less than that of Cu(II) ions. However, the ^{65}Zn(II) ions were not transferred from the immobilized HRG peptide to any of the model peptides that were added to the column and eluted in the flow-through fraction. ^{65}Zn(II) ions were, however, released when the column pH levels were reduced below pH 6.

The selectivity of the immobilized HRG peptide–Cu(II) ion affinity column for proteins in a complex biological fluid such as plasma was quite different from that observed for the immobilized synthetic organic ligand–metal ion affinity column [e.g., TED–Zn(II)] (unpublished data) and demonstrates the need to investigate further the biologically relevant presentation of metal ions to protein surfaces. The use of immobilized biopolymers, especially peptides derived from known metal transport proteins, to investigate biospecific metal ion transfer

events is under further investigation. Preliminary data (unpublished) suggest that alternative chemical methods of peptide immobilization will permit a detailed evaluation of metal ion transfer, one important aspect of understanding metal ion bioavailability. With the discovery of HRG in human colostrum and milk [31] and bovine milk (unpublished), the physiological significance of metal ion transfer from proteins like HRG is evident.

We now have the possibility of designing and building artificial biomimetic surfaces with biologically active protein surface domain structures. We have demonstrated here that the acitivity of these surface immobilized peptides is effectively modulated by bound metal ions. We have now demonstrated several other models of metal ion-dependent protein dimerization (e.g., estrogen receptor subunit protein recognition of the immobilized 53-residue helical dimerization domain) and metal ion-dependent protein recognition of nucleic acids (e.g., estrogen response element interaction with the immobilized 71-residue DNA-binding domain) (submitted).

REFERENCES

1 J. M. Berg, J. Biol. Chem., 265 (1990) 6513–6516.
2 J. M. Berg, Ann. Rev. Biophys. Chem., 19 (1990) 405–421.
3 T. W. Hutchens and T.-T. Yip, J. Chromatogr., 500 (1990) 531–542.
4 T. W. Hutchens and T.-T. Yip, Anal. Biochem., 191 (1990) 160–168.
5 T. W. Hutchens and T.-T. Yip, J. Chromatogr., 536 (1991) 1–15.
6 T. W. Hutchens and T.-T. Yip, J. Inorg. Biochem., 42 (1991) 105–118.

7 N. Heimburger, H. Haupt, T. Kranz and S. Baudner, *Hoppe-Seyler's Z. Physiol. Chem.*, 353 (1972) 1133–1140.

8 W. T. Morgan, *Biochim. Biophys. Acta*, 533 (1978) 319–333.

9 H. R. Lijnen, M. Hoylaerts and D. Collen, *J. Biol. Chem.*, 255 (1980) 10214–10222.

10 T. Koide, S. Odani and T. Ono, *FEBS Lett.* 141 (1982) 222–224.

11 W. T. Morgan, *Biochemistry*, 24 (1985) 1496–1501.

12 T. Koide, D. Foster, S. Yoshitake and E. W. Davie, *Biochemistry*, 25 (1986) 2220–2225.

13 T.-T. Yip and T. W. Hutchens, *Protein Expression Purif.*, 2 (1991) 355–362.

14 W. T. Morgan, *Biochemistry*, 20 (1981) 1054–1061.

15 S. L. Guthans and W. T. Morgan, *Arch. Biochem. Biophys.*, 218 (1982) 320–328.

16 M. N. Blackburn, M. K. Burch and W. T. Morgan, *Biochemistry*, 26 (1987) 7477–7482.

17 M. Katagiri, K. Tsutsui, T. Yamano, Y. Shiminishi and F. Ishiibashi, *Biochem. Biophys. Res. Commun.*, 149 (1987) 1070–1076.

18 T. W. Hutchens, R. W. Nelson and T.-T. Yip, *J. Mol. Recog.*, 4 (1991) 151–153.

19 R. W. Nelson and T. W. Hutchens, *Rapid Commun. Mass Spectrom.*, 6 (1992) 4–8.

20 T. W. Hutchens, R. W. Nelson and T.-T. Yip, *FEBS Lett.*, 296 (1992) 99–102.

21 T. W. Hutchens, R. W. Nelson, M. H. Allen, C. M. Li and T.-T. Yip, *Biol. Mass Spectrom.*, 21 (1992) 151–159.

22 P. Edman and A. Henschen, in S. B. Needleman (Editor), *Protein Sequence Determination*, Springer, New York, 1975, pp. 232–279.

23 T. W. Hutchens, R. W. Nelson, C. M. Li and T.-T. Yip, *J. Chromatogr.*, 604 (1992) 125.

24 J. Porath and R. Axen, *Methods Enzymol.*, 44 (1976) 19.

25 J. Porath, J. Carlsson, I. Disson and G. Belfrage, *Nature (London)*, 258 (1975) 598–599.

26 J. Porath and B. Olin, *Biochemistry*, 22 (1983) 1621–1630.

27 T. W. Hutchens, T.-T. Yip and J. Porath, *Anal. Biochem.*, 170 (1988) 168–182.

28 U. K. Laemmli, *Nature (London)*, 227 (1970) 680–685.

29 J. M. Morrissey, *Anal. Biochem.*, 117 (1981) 307–310.

30 T.-T. Yip, Y. Nakagawa and J. Porath, *Anal. Biochem.*, 183 (1989) 159–171.

31 T. W. Hutchens, T.-T. Yip and W. T. Morgan, *Pediatr. Res.*, 31 (1992) 239–246.

CHROM. 24 063

Production, purification and characterization of recombinant human interferon γ

Z. Zhang

Institute of Virology, Chinese Academy of Preventive Medicine, 100 Ying Xin Jie, Beijing 100052 (China)

K.-T. Tong

Shanghai Institute of Biological Products, Ministry of Public Health, R & D Centre for r-DNA Biological Products, 1262 Yan An Road (West), Shanghai (China)

M. Belew, T. Pettersson and J.-C. Janson

Process Separation Division, Pharmacia LKB Biotechnology AB, S-751 82 Uppsala (Sweden)

ABSTRACT

An essentially three-step chromatographic purification procedure, *i.e.*, ion-exchange, immobilized metal ion affinity and size-exclusion chromatography, is described for the purification to homogeneity of recombinant human interferon-γ (rhIFN-γ) from the inclusion bodies produced in genetically transformed *Escherichia coli* cells. Batchwise adsorption of the cloudy solution of renatured rhIFN-γ obviated the need for high-speed centrifugation to clarify the suspension. This step effectively removed about 70% of extraneous protein impurities. The established purification process is reproducible and leads to a total recovery of 32%. Pilot-scale processing of *E. coli* cells grown in a 30-l fermentor gave about 70 mg of a homogeneous preparation of rhIFN-γ. The specific biological activity of purified rhIFN-γ is *ca.* $3.4 \cdot 10^7$ I.U./mg protein, which is comparable to that of its natural counterpart. It is basic protein (p*I* > pH 9) with a monomer relative molecular mass of 15 000. It behaves, however, as a dimer on size-exclusion chromatography. Its partial NH$_2$-terminal sequence is identical with that established for the rhIFN-γ. However, its amino acid composition and its relative molecular mass (15 067 as determined by electrospray mass spectrometry) indicate that the purified protein is a truncated form lacking fifteen amino acid residues from its carboxyl-terminal side. This modification does not seem to have any adverse effect on its biological potency. The levels of DNA, bacterial endotoxins and Ni(II) ions in the final product were determined.

INTRODUCTION

The human interferons (hIFNs) are a family of proteins the initial discovery of which was based on their ability to inhibit viral growth in target cells [1]. Their biological effects *in vivo* include antiviral activity, cell growth inhibition and immunomodulatory activity [2]. Based on major antigenic differences, they are grouped into three main classes, *viz.*, hIFN-α (leucocyte), hIFN-β (fibroblast) and

hIFN-γ (immune) [3–5]. Few, if any, of the natural hIFN-α sub-classes are glycosylated whereas hIFN-β and hIFN-γ are produced in their glycosylated form. hIFN-α and hIFN-β are otherwise similar in many respects, *e.g.*, both maintain their activity after exposure to sodium dodecylsulphate (SDS) or pH 2 and have relative molecular masses (M_r) in the range 20 000–26 000 [6,7]; each is composed of a single polypeptide chain of about 166 amino acid residues cross-linked by one or more disulphide bridges; they also share about 30% amino acid sequence homology [8].

hIFN-γ is different from hIFN-α or -β in several

Correspondence to: Dr. M. Belew, Process Separation Division, Pharmacia LKB Biotechnology AB, S-751 82 Uppsala, Sweden.

respects. It is inactivated on exposure to pH 2 or SDS [9]. Its cell surface receptors are different from those of hIFN-α or hIFN-β [10]. Its virus and cell specificities and the antiviral mechanism it induces are also distinct [11]. It is more potent than the other two hIFNs in its immunomodulatory activities and the antiproliferative effects it elicits in transformed cells [11,12], making it a potentially useful drug against cancer. Some clinical trials indicate that recombinant hIFN-γ (rhIFN-γ) has therapeutic efficacy on kidney cell carcinoma, leukaemia, melanoma, pulmonary cell carcinoma, colon cancer and rheumatoid arthritis [13–18].

Natural hIFN-γ is composed of 143 amino acid residues with a calculated formula mass of 16 775 [19]. It is glycosylated and does not contain any Cys residues [19]. It is a basic protein with an isoelectric point above pH 9. Its reported relative molecular mass is variable ranging from 15 500 to as much as 70 000 [9,12,19–22], which is apparently due to its tendency to exist in several aggregated forms [9,22–23]. Its cDNA has been successfully cloned and expressed at high levels in *Escherichia coli* [24,25], which made possible the production of rhIFN-γ in relatively large amounts. Several methods have subsequently been published describing its purification to apparent homogeneity [23,26–28]. Its availability in large amounts has made possible some detailed structure–function analysis on the purified protein [29] and its use in diverse clinical trials.

The rhIFN-γ (produced in *E. coli*) is not glycosylated and has Met as its NH_2-terminal residue instead of pyroglytamic acid. Its amino acid sequence is otherwise identical with that of its natural counterpart without any internal insertions or deletions [19]. The observed differences in its primary structure do not seem, however, to have any adverse effect on its biological activities. It is also worth mentioning that the soluble form of hIFN-γ receptor, expressed in *E. coli*, has recently been purified and characterized [30], which is expected to simplify the rational search for agonists and antagonists of hIFN-γ activities and thereby the development of newer and more effective drugs.

This paper describes an optimized downstream purification procedure for rhIFN-γ expressed intracellularly in *E. coli* as inclusion bodies. The adopted procedure is reproducible and well suited for process-scale operations. Sufficient data are presented to show the purity of the final product and its identity with its natural counterpart. Structural analyses of the purified rhIFN-γ indicate that it is in its truncated form, lacking fifteen amino acid residues from its carboxyl-terminal end relative to its natural counterpart.

EXPERIMENTAL

Unless stated otherwise, all experiments were performed at room temperature (20°C). Chromatographic columns, gel media, electrophoretic apparatus and the BioPilot chromatographic system were products of Pharmacia LKB Biotechnology (Uppsala, Sweden). Guanidine hydrochloride (Gu · HCl) (95%) was obtained from Aldrich Chemie. During the developmental phase of the downstream purification procedure, XK16, XK26 and K50 columns were used. For large-scale applications, Bio-Process glass columns (BPG 100/500 and BPG 100/950) were used. Relevant details will be outlined in appropriate sections.

The following buffers were used for extraction, solubilization and renaturation of the inclusion bodies and the chromatographic experiments. They will be referred to in abbreviated form throughout.

(A) 20 m*M* sodium phosphate buffer–0.125 *M* NaCl–5 m*M* EDTA (disodium salt) (pH 7.2).

(B) 20 m*M* sodium phosphate buffer–0.125 *M* NaCl–0.5 *M* urea–1 m*M* EDTA (disodium salt) (pH 7.0).

(C) 7 *M* Gu · HCl dissolved in 50 m*M* boric acid and the pH adjusted to 7.2 with 0.1 *M* NaOH.

(D) 20 m*M* sodium phosphate buffer–0.125 *M* NaCl–1 m*M* EDTA (disodium salt)–5% (w/v) sucrose (pH 7.2).

(E) 20 m*M* sodium phosphate buffer–0.125 *M* NaCl–1 m*M* EDTA (disodium salt)–5% (w/v) sucrose–2 *M* Gu · HCl (pH 7.2).

(F) 20 m*M* sodium phosphate buffer (pH 7.0) (conductivity = 3 mS/cm at 21°C).

(G) 20 m*M* sodium phosphate buffer–0.3 *M* NaCl (pH 7.0) (conductivity = 25 mS/cm at 21°C).

(H) 20 m*M* sodium phosphate buffer–0.6 *M* NaCl (pH 7.0) (conductivity = 45 mS/cm at 21°C).

(I) 20 m*M* sodium phosphate buffer–0.3 *M* NaCl (pH 7.5).

(J) 20 m*M* sodium phosphate buffer–9 m*M* imidazole–0.5 *M* NaCl (pH 7.5).

(K) 50 mM Na_2HPO_4–0.5 M NaCl, pH adjusted to 4.0 with dilute phosphoric acid solution.

Production of rhIFN-γ

E. coli strain DH5α was transformed by plasmid pBV220/IFN-γ, which contains hIFN-γ cDNA inserted downstream of P_RP_L promoter and CIts857 regulator gene. The expression of hIFN-γ by the cultured E. coli cells was induced by raising the temperature of the cell culture from 30 to 42°C within about 15 min [31,32]. About 600 ml of an overnight cell culture in LB medium was seeded in a 30-l fermenter containing 25 l of modified M 9 medium and the fermentation was performed essentially as described by Song and Tong [33]. After about 14 h of continuous culturing, the temperature was raised to 42°C and the fermentation allowed to continue for a further 4 h. The cells were then harvested by centrifugation at 3000 g at 4°C for 10 min using a Heraeus Cryofuge 1000 fitted with a model 6606 rotor.

Preparation of crude rhIFN-γ extract

One part by weight of E. coli cells were suspended in ten volumes of buffer A at 4°C and dispersed using an Ultra Turrax (IKA-Werk, Germany). The homogenized suspension was passed through an APV Gaulin press for a total of three passages, maintaining the pressure at 500 bar during the milling process. The press was cooled by a circulating water bath maintained at 4°C throughout the entire operation. The suspension of disintegrated cells was centrifuged at 1000 g for 30 min at 4°C. The pellet was resuspended in buffer A, homogenized using the Ultra Turrax and centrifuged as above. The resulting pellet was resuspended in buffer B followed by homogenization and centrifugation.

The washed pellet, containing highly purified inclusion bodies, was suspended in 3 ml of buffer C per gram of wet pellet and solubilized by homogenization for about 5 min using the Ultra Turrax. This was followed by centrifugation at 17 000 g and 4°C to remove insoluble material and residual cell debris. The supernatant, containing solubilized but denatured proteins of the inclusion bodies, was stored at 4°C until further use. It will be referred to as the "crude extract" throughout.

The crude extract was renatured by diluting it about 70-fold with buffer D followed by buffer E to obtain a final protein concentration of 0.1–0.2 mg/ml in 0.2 M Gu · HCl. This was stored overnight at 4°C for optimum renaturation of the proteins. The product obtained is a cloudy suspension, probably owing to the presence of partially renatured and/or aggregated proteins.

Ion-exchange chromatography (IEC)

The renatured rhIFN-γ suspension (1.4 l, corresponding to 20 ml of crude extract) was clarified by centrifugation at 17 000 g for 30 min at 4°C. The supernatant was applied to a K50 column (bed height = 5 cm; bed volume = 98 ml) of S-Sepharose FF equilibrated with buffer F followed by washing with 2 bed volumes of the equilibration buffer to elute unbound proteins. The column was then washed with 4.5–5 bed volumes of buffer G to elute weakly bound impurities and finally with 2.5–3 bed volumes of buffer H to elute the strongly bound rhIFN-γ fraction. The column was regenerated by washing it with 2–3 bed volumes of 1 M NaCl dissolved in buffer F and equilibrated for the next run by washing it with about 3 bed volumes of buffer F. This procedure was used during the developmental stages of the downstream purification process.

For large-scale operations, batch adsorption was adopted. To 1.4 l of the cloudy suspension of renatured rhIFN-γ were added 80 g of suction-dried S-Sepharose FF (corresponding to 100 ml of packed gel) that had previously been equilibrated with buffer F. The mixture was stirred intermittently for 1 h at 20°C and then filtered through a No. G2 glass filter, which allows the passage of the fine precipitates through its pores. The suctioned gel was then washed with 200-ml portions of buffer F until the filtrate was no longer cloudy (a total of about 600 ml of the buffer was required). The gel was then packed in a column and the bound proteins were eluted according to the procedure outlined above.

Immobilized metal ion affinity chromatography (IMAC) on Ni(II)–chelating Sepharose Fast Flow

The chelating Sepharose Fast Flow gel (CS FF) was packed in an XK 16 column (bed height = 15 cm; bed volume = 30 ml) and washed with about 2 bed volumes of distilled water. It was then charged with Ni(II) ions (8 ml of 0.2 M $NiSO_4$ solution, pH 4.7) followed by washing with about 2 bed volumes of deionized water to elute the excess of metal ions.

The column was then washed with 2 bed volumes of buffer K, to elute loosely bound metal ions, followed by 6 bed volumes of buffer I for equilibration.

The partially purified rhIFN-γ fraction obtained from the ion-exchange step was applied to the column followed by washing with about 3 bed volumes of buffer I to elute unbound impurities. The column was then washed with about 7 bed volumes of buffer J to elute the adsorbed rhIFN-γ fraction and finally with about 3 bed volumes of buffer K to elute the strongly bound impurities and also to regenerate the column. The column was then re-equilibrated with buffer I and can be used again for at least ten consecutive runs without any detectable deterioration in its capacity or selectivity.

Size-exclusion chromatography (SEC)

The active fraction obtained from the Ni(II)–CS FF column was applied to a prepacked Superdex 75 column (60 × 6 cm I.D.; bed volume = 1696 ml) equilibrated with buffer I. The volume of sample applied corresponded to *ca.* 6% of the total bed volume. The flow-rate was maintained at 15–20 cm/h. For laboratory-scale operations, fractions corresponding to 1% of the total bed volume were collected. For large-scale operations, fractions were pooled directly on the basis of the continuous chart recording of the effluent.

From the various pooled fractions obtained after each chromatographic step, aliquots of 1 ml were saved for electrophoretic analysis and for determining their biological activity and protein content. Samples used for biological assay contained 1% (w/v) human serum albumin (HSA) to prevent the loss of interferon by adsorption to surfaces.

Analytical methods

The distribution of proteins in the column effluents was determined by continuous on-line measurement of the absorbance at 280 nm (A_{280}) and direct recording. Proteins were determined according to the Lowry procedure using a Sigma protein assay kit. The concentration of purified rhIFN-γ in solution was determined using the factor $A_{280}^{1\%} = 8.62$. This was calculated from the quantitative amino acid composition analysis of the purified rhIFN-γ and its UV absorption spectrum. Its amino

acid composition was determined after hydrolysis in 6 *M* HCl for 24 and 72 h at 110°C. The hydrolysates were analysed on a Model 4151 Alpha Plus amino acid analyser (Pharmacia LKB Biotechnology).

The NH$_2$-terminal sequence of purified rhIFN-γ was determined using the Edman degradation method on an Applied Biosystems Model 477A sequencer. The resulting phenylthiohydantoin (PTH)-amino acid derivatives were identified using an Applied Biosystems Model 120A PTH analyser.

Determination of biological activity

This was a standard microtitre assay [34] based on the reduction of the cytopathic effect (CPE). The assay was performed by incubating a fixed count of WISH cells with a serially diluted rhIFN-γ sample followed by challenging the cells with difined plaque-forming units of vesicular stomatitis virus (VSV), all according to a standardized procedure [34]. The interferon activity was calculated as the reciprocal of the dilution in the well of the titre plate where 50% of the WISH cell monolayer is protected from the CPE of the challenging virus.

SDS–polyacrylamide gel electrophoresis (SDS-PAGE)

This was performed routinely to assess the progress achieved at each stage of the downstream purification process and to examine the electrophoretic homogeneity of purified rhIFN-γ preparations. The Pharmacia LKB PhastSystem electrophoresis apparatus and 20% homogeneous or 8–25% gradient PhastGel media were used following the recommended procedures of the manufacturer. Molecular mass marker proteins were also run simultaneously.

Approximately 20–30 μg of each sample were applied to the gel for electrophoresis. The separated protein bands were stained using either the Coomassie Brilliant Blue or silver staining techniques according to the detailed procedure outlined in the PhastSystem manual. The molecular mass of the purified rhIFN-γ was calculated relative to the migration distance of standard calibration proteins run simultaneously. This was performed accurately and conveniently using the Pharmacia LKB PhastImage gel scanner.

Reversed-phase high-performance liquid chromatography (RP-HPLC)

RP-HPLC was used to check the homogeneity of the purified rhIFN-γ preparation. The column (250 × 4 mm I.D. packed with Pep-S, C_2–C_{18} gel of 5-μm average particle diameter) was equilibrated with 5% acetonitrile in 0.05% trifluoroacetic acid (TFA) and developed with a linear gradient of acetonitrile (from 5 to 80%) in 0.05% TFA at a flow-rate of 1 ml/min in a total gradient time of 66 min. The effluent was monitored continuously at 226 nm.

Analytical ultracentrifugation

Analytical equilibrium sedimentation analysis was performed in an MSA Centriscan ultracentrifuge fitted with a six-place analytical rotor and a photoelectric UV scanner. The sample was centrifuged at 26 000 g for 48 h at 20°C. The concentration of the purified rhIFN-γ was 0.49 mg/ml dissolved in buffer G.

Mass spectrometry

The purified rhIFN-γ was subjected to electrospray mass spectrometric (ES-MS) analysis [35,36] to determine its molecular mass accurately and also to characterize the size of the fragments generated on digesting it with a *Staphylococcus aureus* V8 protease (Glu-C endoproteinase, obtained from Boehringer, Mannheim, Germany).

Quality control

Contaminating residual DNA was determined using the Threshold total DNA detection system [37]. The content and concentration of bacterial endotoxin were determined using a standard Limulus test [38]. Trace amounts of Ni(II) ions were determined by atomic emission spectrometry using a JY 70 Plus inductively coupled plasma atomic emission spectrometer (Jobin Yvon, Longjumeau, France).

The possible presence of viruses was assayed by determining any CPE produced in MDBK cells (from bovine kidney) co-cultured with a sample of purified rhIFN-γ at 37°C for 7 days in a 5% carbon dioxide atmosphere. The cells were frozen and thawed three times to release any viruses and the supernatant was poured off to a new MDBK cell culture and incubated as above. This procedure was repeated one more time and the cells were examined for any CPE produced during the above process.

RESULTS AND DISCUSSION

During the explorative stages of this investigation, a variety of hydrophobic and metal chelate adsorbents were tried for the initial purification of the renatured rhIFN-γ. Their selectivities and adsorption capacities were low, however. The most promising results were obtained using S-Sepharose FF as the initial adsorbent for the renatured rhIFN-γ from the cloudy suspension without the necessity for dialysis or high-speed centrifugation. The results so obtained and the subsequent purification steps used for obtaining a homogeneous rhIFN-γ preparation are described below. The reproducibility of the adopted downstream purification procedure shown in Talbe I was checked by at least fifteen independent runs with satisfactory results.

Step 1: ion-exchange chromatography

A typical elution profile obtained after this initial purification step is shown in Fig. 1. In batch adsorption experiments, fraction 1A is not seen on the elution diagram as it is washed out prior to packing of the gel to elute the bound fractions 1B and 1C. Fraction 1A contains about 60–70% of the proteins and 5–20% of the activity in the renatured rhIFN-γ sample applied to the column. The corresponding figures for fraction 1B are 1–2% of the proteins and 2–7% of the activity and for fraction 1C 25–35% of the proteins and about 85% of the activity (see Table II). This step is therefore very effective in removing most of the impurities and also leads to the simultaneous concentration of the active fraction 1C, which is eluted in a volume that corresponds to approximately one tenth of the volume of the renatured sample applied to the column.

Batch adsorption is adopted as the preferred method as it is simple, fast and can easily be scaled up for large-scale operations. The cloudy solution of renatured rhIFN-γ need not be clarified by centrifugation prior to the adsorption step. The recovery of activity was, in most instances, more than 100%. This is probably due to the further solubilization of active rhIFN-γ from the precipitate found in the renatured sample as it comes into contact with the S-Sepharose FF gel beads [39].

The apparent capacity of the S-Sepharose FF adsorbent was low, amounting to *ca.* 2 mg of proteins

TABLE I

PILOT-SCALE PURIFICATION SCHEME FOR rhIFN-γ

Step	Separation principle	Downstream process	

```
                    ┌─────────────────┐
                    │  E. Coli cells  │
        Extraction  └────────┬────────┘────────►  Cells, cell debris,
                             │                     DNA etc.
                             ▼
                    ┌─────────────────┐
                    │ Inclusion bodies│
 Solubilization     └────────┬────────┘────────►  Insoluble particles,
 (7 M Gu · HCl)              │                     cell debris
                             ▼
                    ┌─────────────────┐
                    │  Crude extract  │
 Renaturation.      └────────┬────────┘
 (70 × dilution)             │
                             ▼
                    ┌─────────────────┐
                    │ Renatured rhIFN-γ│         (Cloudy solution)
                    └────────┬────────┘
                             │
                             ▼
  I    Ion exchange  ┌─────────────────┐
                     │ S-Sepharose FF  │
                     └───────┬─────────┘───────►  Ca. 70% unbound
                        (Fraction 1C)             impurities
                             │                    (Fractions 1A & 1B)
                             ▼
  II   IMAC           ┌─────────────────┐
                      │  Ni(II) - CS FF │
                      └──────┬──────────┘──────►  Ca. 20% impurities
                        (Fraction 2B)            (Fractions 2A & 2C)
                             │
                             ▼
  III  Size exclusion ┌──────────────────────┐
                      │ Superdex 75 prep grade│
                      │  (Sephacryl S-100)    │
                      └──────────┬───────────┘
                                 │
                                 ▼
                      ┌──────────────────────┐
                      │  Purified   rhIFN-γ   │
                      │   (Fraction 3A)       │
                      └──────────────────────┘
```

(in 14 ml of the renatured rhIFN-γ) per millilitre of the ion exchanger. This is due to the presence of high concentrations of competing ions ($0.2\ M$ Gu · HCl, $0.125\ M$ NaCl) in the renatured sample. The removal of these ions in order to increase the adsorption capacity of the ion exchanger implies the use of time-consuming procedures such as desalting or dialysis, which are inconvenient for use in large-scale operations.

Step 2: IMAC on Ni(II)–Chelating Sepharose FF

Fig. 2 shows the elution profile obtained after chromatography of pooled fraction 1C on a column of Ni(II)–CS FF. The pH or salt concentration of the sample was not adjusted prior to its chromatography, a consideration which is very advantageous in large-scale operations. The unbound fraction 2A contains about 6–12% of the proteins and at most 4–5% of the activity, while fraction 2B contains about 70–80% of the proteins and more than 70% of the activity applied to the column (see Table II). Fraction 2C contains about 6–10% of the proteins and is virtually inactive.

It takes about 7 column volumes of the desorption buffer J to elute fraction 2B completely in a total of about 2–3 bed volumes. Usually, this fraction was eluted without dilution relative to the volume of sample applied to the column. The results
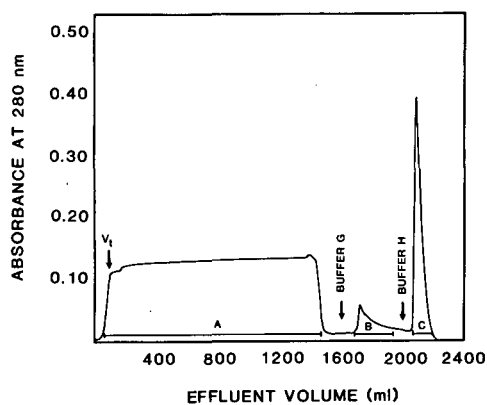
Fig. 1. IEC of 1400 ml of renatured crude extract on a K50/20 laboratory column (5 × 5 cm I.D.; bed volume = 98 ml) of S-Sepharose FF. The sample was centrifuged at 17 000 g to remove the suspension of finely divided precipitate prior to its application to the column. The flow-rate was maintained at 60 cm/h throughout and fractions were pooled as they were eluted from the column on the basis of the continuous chart tracing. For further experimental details, see text. Pooled fractions are indicated by the horizontal bars. Approximately 85% of the eluted IFN-γ activity was found in the strongly bound fraction 1C.

indicate that the column needs to be saturated with the competing ion (i.e., imidazole) before this fraction is eluted. The process could be speeded up by using a higher concentration of imidazole in the eluent buffer, but this led to the co-elution of some
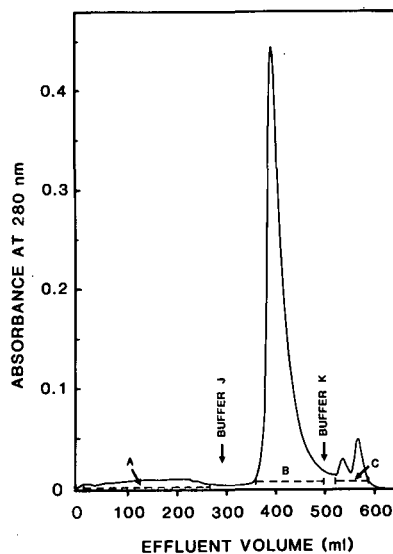
Fig. 2. IMAC of pooled fraction 1C (see Fig. 1) on an XK26/20 laboratory column (6 × 2.6 cm I.D.; bed volume = 32 ml) of Ni(II)–Chelating Sepharose FF. A flow-rate of 60 cm/h was used throughout. Bound fractions were desorbed by stepwise change of the elution conditions and were pooled directly as shown by the horizontal bars. For further experimental details, see text. The IFN-γ activity was localized in fraction 2B.

strongly bound contaminants. Lowering the pH of the eluent buffer to 6.8 paradoxically led to a broadening of the peak. In normal IMAC procedures

TABLE II

RECOVERY OF rhIFN-γ ACTIVITY AFTER EACH CHROMATOGRAPHIC SEPARATION STEP USED FOR ITS PURIFICATION FROM THE INCLUSION BODIES OF TRANSFORMED E. COLI CELLS

The values obtained are averages of four independent experiments performed on 1400 ml of renatured rhIFN-γ samples prepared from 20 ml of the same batch of crude extract (7 M Gu · HCl-solubilized inclusion bodies). The recovery and purification factors are calculated relative to the total activity in 1400 ml of the renatured sample. Details of the pooled fractions referred to here are shown in Figs. 1–3. The numbers in parentheses are ranges of values obtained for the recovery of activity.

Step	Sample	Total protein (mg)	Total activity ($\times 10^7$ I.U.)	Specific activity ($\times 10^7$ I.U./mg)	Recovery (%)	Purification factor (-fold)
–	Renatured rhIFN-γ	118.9	146.7	1.2	100	1
I (IEC)	Pool 1C	31.7	126.0	4.0	85.8 (54–115)	3.2
II (IMAC)	Pool 2B	27.2	94.5	3.5	64.4 (37–73)	2.8
III (SEC)	Pool 3A	13.7	46.8	3.4	31.9 (21–47)	2.8

[40], a lower pH should have facilitated the desorption of the bound proteins. We have also observed that the concentration of NaCl in the equilibration buffer, ranging from 0.1 to 1.0 M, did not have any influence on the adsorption–desorption kinetics, contrary to what one would expect for such a basic protein [41].

The bound rhIFN-γ fraction could also be eluted by decreasing the pH of the desorption buffer to 4.5 or lower [26]. However, there was a marked decrease in activity of the eluted fraction, apparently due to the instability of this rhIFN-γ in an acidic medium.

IMAC was found to be a necessary step for the efficient purification and high recovery of the rhIFN-γ activity. Some orienting experiments were performed in which this step was omitted and the partially purified fraction 1C was further fractionated on a column of Superdex 75 Prep Grade. The purified fraction so obtained still contained some protein impurities, as judged by SDS-PAGE, and

Fig. 3. SEC of pooled fraction 2B on a BioPilot 60/600 column (bed volume = 1700 ml) packed with Superdex 75 Prep Grade. Usually, the pooled fraction 2B from the previous step was applied to the column without further concentration as it is eluted from the IMAC column in a sufficiently concentrated form. The column was equilibrated and eluted with buffer I at a flow-rate of 15 cm/h. The volume of the applied sample corresponded to about 6% of the total bed volume of the packed Superdex 75 Prep Grade column. Fractions were pooled directly as shown by the horizontal bars. More than 96% of the eluted IFN-γ activity is localized in the major fraction 3A. The calculated relative elution volume (V_e/V_t) for fraction 3A was 0.54.

its overall recovery was low. The results clearly showed that IMAC on Ni(II)–CS FF effectively removes some low-molecular-mass impurities in fraction 1C, thereby facilitating its further purification to homogeneity by a subsequent SEC step.

Step 3: Size-exclusion chromatography

Some minor impurities present in fraction 2B (see Fig. 4) were effectively removed by SEC on a column of Superdex 75 Prep Grade or Sephacryl S-100 (Fig. 3). The main fraction 3A contained the interferon activity whereas the minor fraction 3B was inactive. The recovery of activity in fraction 3A was *ca.* 50% relative to the activity applied to the column and *ca.* 32% relative to the total activity in the renatured sample (Table II). The significant decrease in activity after this step is surprising and might be due to unspecific adsorption of the already highly purified fraction 2B on the gel surfaces. The addition of various "stabilizers" (*e.g.*, 5%´ sucrose, 0.5% SDS or 1% Dextran T40) to the elution buffer, or of 1% purified HSA to the pooled fraction 3A soon after its elution from the column, did not prevent the observed loss of interferon activity. Despite this loss, however, about 14 mg of highly purified rhIFN-γ were obtained (Table II) after processing 1400 ml of the renatured sample according to the adopted downstream purification scheme shown in Table I.

The Superdex 75 Prep Grade column was run at a flow-rate of 15 cm/h and a sample volume corresponding to 4–6% of the total bed volume. A flowrate of 25 cm/h also gave satisfactory results. According to Kågedal *et al.* [42], Superdex 75 Prep Grade retains its high resolving power for some model proteins at flow-rates in excess of 60 cm/h. It is therefore possible to optimize further the flowrate and sample load for use in the future that would consistently lead to a homogeneous rhIFN-γ preparation with a minimum of processing time.

As shown in Fig. 4, the purified rhIFN-γ was homogeneous by SDS-PAGE with a calculated molecular mass of 16 000. We have, on different occasions, also observed the presence of a minor band that migrated as a an M 31 000 protein. On desitometric analysis of two different gels using the Phast-Image gel scanner, this band represented about 1–10% of the proteins in the purified rhIFN-γ. At first, we thought that it was an impurity and several
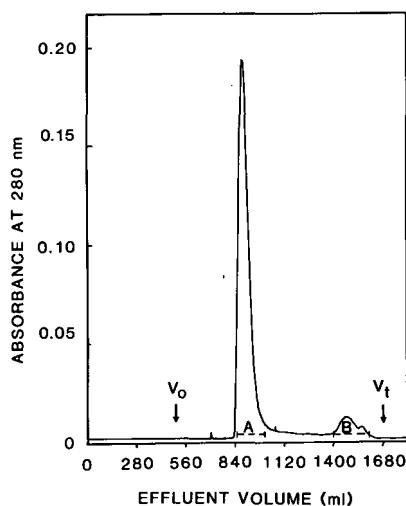
Fig. 4. PhastGel homogeneous (20%) SDS-PAGE patterns of the various fractions obtained during the three-step chromatographic purification process of rhIFN-γ. The gels were stained with PhastGel Blue R (plate A) or by the silver staining technique (plate B). About 25 μg of each sample, in 2 μl of solution, were applied to plate A and about half of this amount to plate B. 1 = Crude extract (in 7 M Gu · HCl); 2 = renatured crude extract; 3 and 4 = unbound and buffer H-desorbed fractions, respectively, from an S-Sepharose FF column; 5 and 6 = unbound and buffer J-desorbed fractions, respectively, from a Ni(II)–chelating Sepharose FF column; 7 = major fraction that was eluted from a Superdex 75 Prep Grade column (purified rhIFN-γ); 8 = molecular mass marker proteins with indicated M_r on the right (kDa = kilodalton).

separation methods (including modifications to the procedures we had adopted) were used in an attempt to remove it. None of these approaches gave the desired outcome. We later observed that the native molecular mass of the purified rhIFN-γ is about 31 000 as determined by analytical SEC on a calibrated column of Superdex 75 HR or Sephacryl S-100 HR. The results suggested that this minor electrophoretic band is the dimeric form of the purified rhIFN-γ which was not denatured by SDS. On heating the purified sample in 5% SDS at 100°C for about 2–3 times the recommended time, a single band of M_r 16 000 was obtained.

Criteria of purity

On SDS-PAGE in gradient (8–25%) or homogeneous (20%) gels, the purified rhIFN-γ showed a single band with an apparent M_r of 16 000 (Fig. 4A and B). Considering that the silver staining technique (performed according to the PhastSystem development method) can detect impurities as low as 1 ng/μl of sample, it is concluded that the level of

trace impurities, if any, in 12 μg of the purified rhIFN-γ is less than 1 ng.

Analysis of the purified rhIFN-γ on an analytical SEC column gave a single symmetrical peak. Further analysis on an Ni(II)–CS FF column (25 × 10 mm I.D.) developed with a linear gradient of imidazole from 1 to 10 mM in buffer I also gave a single peak. On chromatography of the purified protein (*ca.* 1 mg) on a Mono S HR 5/5 fast protein liquid chromatography column and gradient elution (from 0–1.0 M NaCl in buffer F) of the bound protein, no material was desorbed. Further elution with 2 M NaCl in buffer F also gave the same result. The highly purified rhIFN-γ has thus been irreversibly adsorbed on the ion exchanger.

Further analysis of the purified protein on an analytical RP-HPLC column also gave a single symmetrical peak (Fig. 5). During an orienting experiment, a small peak eluted at the end of the gradient. Checking the system by running a blank experiment showed, however, that this minor peak was due to reagent artifacts and not to a contaminating protein.
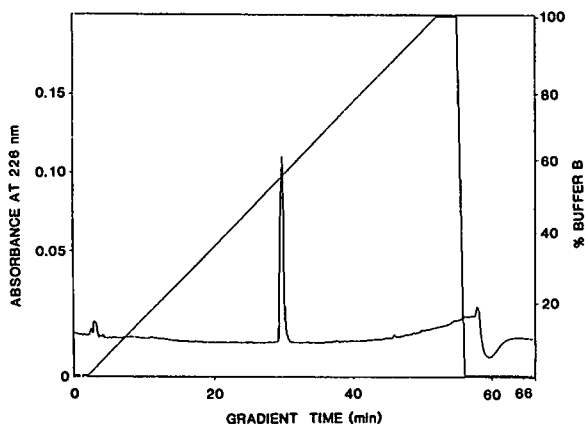
Fig. 5. RP-HPLC of purified rhIFN-γ (pool 3A in Fig. 3) on a column (250 × 4 mm I.D.) of Pep-S, C_2–C_{18} gel of 5-μm particle diameter. The chromatogram was developed with a linear gradient of acetonitrile (from 5 to 80%) in 0.05% TFA at a flow-rate of 1 ml/min in a total gradient time of 66 min.

The purified r-HuIFN-γ sedimented as a single, monodisperse protein when subjected to analytical equilibrium sedimentation analysis. Isoelectric focusing on IEF 3–9 PhastGel media also indicated that the purified rhIFN-γ migrated as an essentially homogeneous band. However, as the pI of this protein is above pH 9, the band seen on the gel migrated beyond the separation range of the IEF 3–9 gel.

Biological potency

The specific biological activity of the purified rhIFN-γ is about $3.4 \cdot 10^7$ I.U./mg protein (Table II), which is equal to or better than that reported by other investigators for the *E. coli*-derived rhIFN-γ or its natural counterpart [12,23,28]. It also remained constant after the IEC step indicating that the biological assay is not sensitive enough to respond to the minor impurities which are clearly revealed by SDS-PAGE.

Molecular size and structure

Data concerning the amino acid composition, partial amino-terminal sequence and molecular mass of the purified rhIFN-γ are presented in Tables III, IV and V, respectively. Its partial NH_2-terminal sequence (Table 4) is identical with that reported for the rhIFN-γ [28]. Its amino acid composition data (Table III) show, however, that it lacks fifteen amino acid residues compared with

that established for the recombinant protein [19,28]. The calculated residue molecular mass of the rhIFN-γ we purified, based on its amino acid composition, is 15 046, which agrees very well with that obtained by ES-MS (15 067; see Table V). The latter method has an accuracy of 0.01% for proteins with molecular mass up to 30 000 [36]. These results suggest that the purified rhIFN-γ is in its truncated form.

According to Rinderknecht *et al.* [19], the *E. coli*-derived rhIFN-γ has the same primary structure as its natural counterpart without any internal insertions or deletions. The only difference is that the recombinant protein has Met as its amino-terminal residue instead of pyroglutamic acid [23]. The missing fifteen amino acid residues must therefore have

TABLE III

AMINO ACID COMPOSITION OF PURIFIED rhIFN-γ

The numbers of amino acid residues per molecule are averages of the values calculated from the analyses performed on a 24- and 72-h hydrolysed sample. They represent the nearest integers obtained from the normalized values for each amino acid so obtained. Its content of Trp was not determined but is taken to be 1 residue per mole based on the sequence established for its natural counterpart [19] or the recombinant protein [29]. The values obtained for Met are based on analysis of the sample hydrolysed for 24 h and are lower than expected owing to its partial oxidation during acid hydrolysis.

Amino acid	Notation	Relative No. of residues	Residues per mole
Lysine	K	18.7	19
Histidine	H	2.0	2
Arginine	R	3.3	3
Half-cystine	C		
Aspartic acid	D	19.7	20
Threonine	T	4.8	5
Serine	S	9.2	9
Glutamic acid	E	16.3	16
Proline	P	2.1	2
Glycine	G	4.0	4
Alanine	A	7.2	7
Valine	V	7.9	8
Methionine	M	3.2	(4)
Isoleucine	I	6.8	7
Leucine	L	9.3	9
Tyrosine	Y	3.9	4
Phenylalanine	F	9.0	9
Tryptophan	W	(1)	(1)
Total		128.4	129

TABLE IV

AMINO-TERMINAL SEQUENCE OF RESIDUES 1–15 OF PURIFIED rhIFN-γ

The sequence is generated from data obtained after analysis of a purified sample of rhIFN-γ on an Applied Biosystems Model 477A automatic micro-sequencing apparatus according to standardized procedures.

1	5	10	15 · · · · · · · · · · · · · 129
H$_2$N · Met–Gln–Asp–Pro–Tyr–Val–Lys–Glu–Ala–Glu–Asn–Leu–Lys–Lys Tyr---------------------COOH			

TABLE V

RELATIVE MOLECULAR MASS OF PURIFIED rhIFN-γ AS DETERMINED BY VARIOUS METHODS

Method	M_r
SDS-PAGE	16 000
Ultracentrifugation	14 000
Analytical SEC	31 000
ES-MS	15 067

been situated at its carboxyl-terminal side and are cleaved off from the parent molecule owing to post-translational processes either during or after its secretion. Identical results were obtained by Kung et al. [27], who also showed that the truncated rhIFN-γ has a comparable specific activity to the natural hIFN-γ, leading them to conclude that the

last fifteen COOH-terminal amino acids are not essential for full biological activity. On the basis of the known primary structure of the intact rhIFN-γ [19,28] and the results obtained here, it is concluded that the truncated form arises by proteolytic cleavage between Lys$_{128}$–Arg$_{129}$ of the native molecule.

The reliable molecular mass of the purified rhIFN-γ is 15 000 as determined by three independent analytical methods (Table V). It behaves, however, as a protein with M_r 31 000 on analytical SEC (Table V), indicating that, under physiological conditions, the purified protein exists as a dimer. This result is consistent with the conclusions of other investigators [12,19,23,43–45]. However, for reasons which are not apparent to us, this molecule sediments as a monomer (Table V) on anlytical equilibrium sedimentation analysis.

TABLE VI

LEVELS OF SOME EXTRANEOUS COMPONENTS IN RELEVANT CHROMATOGRAPHIC FRACTIONS OBTAINED DURING THE PURIFICATION OF rhIFN-γ

The analyses were performed on samples purified on the BioPilot system using sterilized buffers, gel media and connecting tubes for the chromatographic columns. The results serve as guidelines in assessing the efficiency of removal of these components by the gel media used during the entire purification process. For identification of the samples referred to here, see Figs. 1–3. Blank: 20 mM sodium phosphate–0.3 M NaCl (pH 7.5) (buffer I).

Sample	Protein concentration (mg/ml)	DNA[a] (ng/ml)	Endotoxin[a] (I.U./ml)	Viruses
Renatured rhIFN-γ	0.24	194	745	nd[b]
Fraction 1A	0.13	nd	45	nd
Fraction 1C	0.85	3.9	5.2	nd
Fraction 2B	0.75	2.3	3.6	nd
Fraction 3A	0.35	1.6	1.2	Negative
Buffer blank	0	< 10 pg/ml	<0.3	nd

[a] Assuming that one dose of purified rhIFN-γ corresponds to ca. 29 μg of protein, the amount of DNA per injection in the final product is ca. 133 pg. According to the WHO Study Group on Biologicals [46], the probability of risk associated with heterogeneous contaminating DNA is negligible when the amount of such DNA is 100 pg or less in a single dose administered parenterally. The level of bacterial endotoxin in the final product is as low as 0.1 I.U. per dose.

[b] nd = Not determined.

TABLE VII

CONCENTRATION OF Ni(II) IONS IN rhIFN-γ SAMPLES OBTAINED AFTER CHROMATOGRAPHY ON AN Ni(II)–CHELATING SEPHAROSE FF COLUMN FOLLOWED BY SEC ON A SUPERDEX 75 PREP GRADE COLUMN

The samples were analysed by atomatic emission spectrometry using a JY 70 Plus inductively coupled plasma atomic emission spectrometer. The limit of detection of Ni(II) ions by this method is 2.7 μg/l. Blank = equilibration buffer (buffer I) for the Superdex 75 Prep Grade column. In the purified rhIFN-γ sample obtained from the final gel filtration step, the level of Ni(II) ions is as low as that in the column equilibration buffer. The total amount of Ni(II) ions that are stripped off the Ni(II)–CS FF column (V_t = 30 ml) is also very low. About 1000 μmol of Ni(II) ions are immobilized on the column, corresponding to ca. 58.7 mg of Ni(II) ions. The column is washed with ca. 210 ml (i.e., 7 · V_t of the column) of the desorption buffer. Hence, only 0.04 mg of Ni(II) ions were washed out during the elution of the adsorbed rhIFN-γ from the IMAC column.

Sample	Column	Protein concentration (mg/ml)	Concentration of Ni(II) ions (mg/l)
Fraction 2B	Ni(II)–CS FF	0.24	0.21
Fraction 3A	Superdex 75 Prep Grade	0.22	<0.01
Blank		0	<0.01

Quality control

Recombinant proteins expressed in genetically transformed cells must accurately represent the natural molecules that they are intended to replace or complement. They should also fulfil the minimum requirements for biological efficacy, safety and quality criteria as do other preparations intended for pharmaceutical use. The results presented here give ample evidence for the identity of the purified rhIFN-γ with its natural counterpart to the extent that it can be used in its place for clinical trails. Additional data are presented in Tables VI & VII regarding the level of biological active components and chemical substances derived from those used during its purification.

The DNA content in the final product (1.6 ng/ml; see Table VI) corresponds to about 133 pg per dose, which is about 50% higher than the recommended level for such a product (see ref. 46 and footnote to Table VI). It is possible to decrease its concentration further by using an anion-exchange column, such as Q Sepharose FF, to bind the remaining traces of DNA. The level of bacterial endotoxins is very low, indicating its efficient removal during the downstream purification process.

The same applies to the amount of Ni(II) ions (Table VII), whose concentration in the final product is reduced to that in the blank buffer. The leakage of Ni(II) ions from the IMAC column after each chromatographic run is extremely low and corresponds to about 0.07% of the total amount of Ni(II) ions immobilized on the chelating Sepharose FF column. The column can therefore be used for several cycles of adsorption–desorption experiments without regeneration.

REFERENCES

1 A. Isaacs and J. Lindenmann, *Proc. Soc. London, Ser. B*, 147 (1957) 258.

2 W. E. Stewart, II, *The Interferon System*, Springer, New York, 1979.

3 W. E. Stewart, II, J. E. Blalock, D. C. Burke, C. Chany, J. K. Dunnick, E. Falcoff, R. M. Friedman, G. J. Galasso, W. K. Joklik, J. T. Vilcek, J. S. Youngner and K. C. Zoon, *Nature (London)*, 286 (1980) 110.

4 S. Pestka and S. Baron, *Methods Enzymol.*, 78 (1981) 3.

5 E. A. Havell, B. Berman, C. Ogburn, K. Berg, K. Paucker and J. Vilcek, *Proc. Natl. Acad. Sci. USA*, 72 (1975) 2185.

6 T. Taniguchi, S. Ohno, Y. Fujii-Kuriyama and M. Muramatsu, *Gene*, 10 (1980) 11.

7 S. Pestka, *Arch. Biochem. Biophys.*, 221 (1983) 1.

8 T. Taniguchi, N. Mantei, M. Schwarzstein, S. Nagata, M. Muramatsu and C. Weissman, *Nature (London)*, 285 (1980) 547.

9 Y. K. Yip, B. S. Barrowclough, C. Urban and J. Vilcek, *Science*, 215 (1982) 411.

10 M. Revel and J. Cherbath, *Trends Biochem. Sci.*, 11 (1986) 166.

11 B. Y. Rubin and S. L. Gupta, *Proc. Natl. Acad. Sci. U.S.A.*, 77 (1980) 5928.

12 S. Pestka, J. A. Langer, K. C. Zoon and C. E. Samuel, *Annu. Rev. Biochem.*, 56 (1987) 727.

13 J. H. Edmonson, H. J. Long, E. T. Creagan, S. Frytka, S. A. Sherwin and M. N. Chang, *Cancer Treat. Rep.*, 71 (1987) 211.

14 S. E. Krown, *Interferon*, 7 (1986) 185.

15 K. Tamura, S. Makino, Y. Araki, T. Imamura and M. Seita, *Cancer*, 59 (1987) 1059.

16 P. Shah, P. H. Meide, T. Borman, N. Schroeder, J. M. Bliss and R. C. Coombes, *Br. J. Cancer*, 59 (1989) 206.

17 K. Gohji, S.-I. Murao, S. Maeda, T. Sugiyama and S. Kamidono, *Cancer Res.*, 46 (1986) 6264.

18 K. Gohji, S. Maeda, T. Sugiyama, J. Ishigami and S. Kamidono, *J. Urol.*, 137 (1987) 539.

19 E. Rinderknecht, B. H. O'Connor and H. Rodriguez, *J. Biol. Chem.*, 259 (1984) 6790.

20 M. P. Langford, J. A. Georgiades, G. J. Stanton, F. Dianzani and H. M. Johnson, *Infect. Immunol.*, 26 (1979) 36.

21 I. A. Braude, *Biochemistry*, 23 (1984) 5603.

22 S. Pestka, B. Kelder, P. C. Familletti, J. A. Moschera, R. Crowl and E. S. Kempner, *J. Biol. Chem.*, 258 (1983) 9706.

23 T. Arakawa, N. K. Alton and Y. R. Hsu, *J. Biol. Chem.*, 260 (1985) 14435.

24 P. W. Gray, D. W. Leung, D. Pennica, E. Yelverton, R. Najarian, C. C. Simonsen, R. Derynck, P. J. Sherwood, D. M. Wallace, S. L. Berger, A. D. Levinson and D. V. Goeddel, *Nature (London)*, 295 (1982) 503.

25 R. Devos, H. Cheroutre, Y. Taya, W. Degrave, H. van Heuverswen and W. Fiers, *Nucleic Acids Res.*, 10 (1982) 2487.

26 D. H. Coppenhaver, *Methods Enzymol.*, 119 (1986) 199.

27 H.-F. Kung, Y.-C.E. Pan, J. Moschera, K. Tsai, E. Bekesi, M. Chang, H. Sugino and S. Honda, *Methods Enzymol.*, 119 (1986) 204.

28 L. Perez, J. Vega, C. Chuay, A. Mendez, R. Ubieta, M. Montero, G. Padron, A. Silva, C. Santizo, V. Besada and L. Herrera, *Appl. Microbiol. Biotechnol.*, 33 (1990) 429.

29 S.K.-S. Luk, E. Jay and F. T. Jay, *J. Biol. Chem.*, 265 (1990) 13314.

30 M. Fountoulakis, J.-F. Juranville, D. Stuber, E. K. Weibel and G. Garotta, *J. Biol. Chem.*, 265 (1990) 1326831.

31 Z. Q. Zhang, Y.-D. Hou, Y. Y. Li, X. X. Zhao, Y. Zhou, S. M. Duan and L. H. Yao, *Chin. J. Virol.*, 4 (1988) 97.

32 Z. Q. Zhang, L. H. Yao, and Y.-D. Hou, *Chin. J. Virol.*, 6 (1990) 111.

33 Y. M. Song and K. T. Tong, *Sel. Pap. Shanghai Inst. Biol. Prod.*, (1990) 23.

34 P. C. Familletti, S. Rubinstein and S. Pestka, *Methods Enzymol.*, 78 (1981) 387.

35 J. B. Fenn, M. Mann, C. K. Meng, S. F. Wong and C. M. Whitehouse, *Science*, 246 (1989) 64.

36 B. Monegier, F. F. Clerc, A. V. Dorsselaer, M. Vuilhorgne, B. Green and T. Cartwright, *Pharma. Technol. Int.*, Nov. (1990) 19.

37 S. McKnabb, R. Rupp and J. L. Tedesco, *Biotechnology*, 7 (1989) 343.

38 P. Friberger, in J. W. Cate, H. Büller, A. Sturk and J. Levin (Editors), *Bacterial Endotoxins: Structure, Biomedical Significance and Detection With the Limulus Amoebocyte Lysate Test*, Alan R. Liss, New York, 1985, p. 139.

39 A. Hoess, A. K. Arthur, G. Wanner and E. Fanning, *Biotechnology*, 6 (1988) 1214.

40 M. Belew and J. Porath, *J. Chromatogr.*, 516 (1990) 333.

41 E. Sulkowski, in R. Burgess (Editor), *Protein Purification: Micro to Macro*, Alan R. Liss, New York, 1987, p. 149.

42 L. Kågedal, B. Engström, H. Ellegren, A.-K. Lieber, H. Lundström, A. Sköld and M. Schenning, *J. Chromatogr.*, 537 (1991) 17.

43 H. V. Le, C. A. Mays, R. Syto, T. L. Nagabhushan and P. P. Trotta, in W. E. Stewart, II, and H. Schellekens (Editors), *The Biology of the Interferon System*, Elsevier, Amsterdam, 1986, p. 73.

44 Y. K. Yip, R. H. L. Pang, C. Urban, and J. Vilcek, *Proc. Natl. Acad. Sci. USA*, 78 (1981) 1601.

45 R. Falcoff, *J. Gen. Virol.*, 16 (1972) 251.

46 *WHO Tech. Rep. Ser.*, No. 745 (1987) Annex 3.

CHROM. 24 071

Purification, characterization and crystallization of recombinant HIV-1 reverse transcriptase

Ramagauri Bhikhabhai, Thorleif Joelson, Torsten Unge, Bror Strandberg, Thomas Carlsson and Seved Lövgren

Department of Molecular Biology, Uppsala University, Box 590, S-751 24 Uppsala (Sweden)

ABSTRACT

The pol I gene from HIV-1 encoding the protease, reverse transcriptase (RT) and endonuclease has been expressed in *Escherichia coli*. By modifying the fermentation conditions and developing a new purification scheme, the yield of purified RT has been increased substantially compared with that obtained in an earlier procedure. The expressed RT was purified to homogeneity by ammonium sulphate fractionation followed by chromatography on DEAE Sepharose, Heparin Sepharose, S Sepharose and Poly(A)-Sepharose. The purified HIV-RT is a heterodimer (p66/p51) with an isoelectric point close to 8 and with a tendency to aggregate. The proteolytic product (p51), corresponding to the N-terminal end of the RT molecule, was isolated and identified, as were also some bacterial polypeptides that co-elute with HIV-RT during the early stages of the purification. The heterodimer was crystallized in several morphological forms using the vapour-diffusion hanging drop technique. To concentrate the protein and to change the buffer for crystallization, reverse-salt-gradient chromatography and micropreparative columns were used. The best crystals diffracted to 9 Å resolution. The best crystals of native RT diffracted to 9 Å resolution and in complex with nucleic acids to 4.5 Å resolution (using a rotating anode X-ray source).

INTRODUCTION

Reverse transcriptase (RT) is an RNA-dependent DNA polymerase (E.C. 2.7.7.49) [1]. This enzyme is a potential target for drugs designed to block retroviral infections, notably human immunodeficiency virus (HIV), which causes acquired immunodeficiency syndrome (AIDS) (for reviews, see refs. 2–4). RT is present in a few copies per retrovirus particle. Because of the small amount of protein and for security reasons, RT has been cloned and expressed in different organisms: *Escherichia coli* [5–7], *Bacillus subtilis* [8], yeast [9] and vaccinia virus [10]. The recombinant proteins have been shown to be identical or nearly identical with the viral RT with respect to size, composition and activity [11].

The HIV-RT is stable as a heterodimer. The two polypeptides have calculated molecular weights of 64 346 (p66) and 51 229 (p51), respectively. The p66 and p51 polypeptides have identical N-terminal sequences and p51 is the product of a cleavage of p66 into p51 and a small peptide p15, with the RNaseH activity [12,13]. The detailed three-dimensional (3-D) structure of the RNaseH polypeptide has been determined [14]. The interaction between p51 and p66 is much stronger than that between the two polypeptides of the homodimers [15]. The homodimer p51/p51 has polymerase activity but it is lower than those of the heterodimer and the homodimer p66/p66 [16]. This fact, along with site-directed mutagenesis data [3,4,17], localizes the polymerase activity to the N-terminal part of the RT molecule.

HIV contains single-stranded RNA as the genomic material. On infection, RT copies the RNA into a complementary DNA strand, using $tRNA_3^{Lys}$ as a primer [18]. The viral RNA is then degraded by the RNaseH domain of RT. The RT also has a DNA-dependent DNA polymerase activity, which

---

Correspondence to: Dr. R. Bhikhabhai, Department of Molecular Biology, Uppsala University, Box 590, S-751 24 Uppsala, Sweden.

is used to make a complementary strand to the single-stranded DNA [1].

To date, only one 3-D structure of a polymerase is known at high resolution, namely, that of the Klenow fragment [19], which is *E. coli* DNA polymerase I without the domain responsible for the 5'–3' exonuclease activity. A low-resolution 3-D structure, nominally at about 4 Å resolution, is available for phage T7 RNA polymerase [20]. HIV-RT and DNA polymerase I belong to different polymerase families with very low sequence homology. However, sequence alignments of a great number of polymerases from different families [21] have revealed a few conserved amino acids. On the basis of other experiments, some of these amino acids have turned out to be residues of vital importance for the catalytic acitivity. This is the case for the dNTP-binding amino acid residues LYS 758 and TYR 766 and for the probable metal-ion-binding residues ASP 705 and ASP 882 of the Klenow fragment [22]. These amino acids must therefore have nearly the same topological and 3-D positions in the Klenow fragment and in the HIV-RT. This could hardly happen without an appreciable similarity in tertiary structure between these parts of the two polymerase molecules.

Despite these similarities, we still need a detailed 3-D structural model of HIV-RT in order to design HIV-RT inhibitors with optimum binding and specificity. The necessary prerequisite for a good 3-D model is the availability of high-quality crystals of the enzyme. Lowe *et al.* [23] and Lloyd *et al.* [24] have reported morphologically different forms of HIV-RT crystals which diffract to 7–9 Å resolution. In our laboratory we have expressed the pol I gene in *E. coli* (the pol I polypeptide is processed to protease, RT and endonucleoase; RT is further processed to the heterodimer p66/p51) and we have reported earlier the expression, purification and crystallization of the heterodimer [25].

With the aim of producing larger amounts of RT and crystals of improved quality, we have substantially modified the fermentation conditions and the purification scheme, resulting in a reasonably high yield and very high purity. The isoelectric point has been estimated by chromatofocusing. The chromatographic properties of RT seem to change on association with other polypeptides or itself. Micropreparative columns were used to concentrate the protein and to carry out buffer exchanges for the crystallization experiments. We describe here numerous crystallization experiments and many different morphological forms of RT crystals. So far, these crystals diffract to about the same resolution as those reported earlier [23–25].

EXPERIMENTAL

Equipment

Fast Protein Liquid Chromatography (FPLC®) System, SMART System and PhastSystem™ were obtained from Pharmacia LKB Biotechnology (Uppsala, Sweden).

Materials

All chromatographic and electrophoretic gel media were obtained from Pharmacia LKB Biotechnology. Electrophoresis gels were PhastGel gel media. Chromatographic gels were DEAE-Sepharose Fast Flow, Heparin Sepharose CL-6B, Sepharose 4B and Poly(A)-Sepharose 4B.

The following prepacked columns were used: HiLoad 26/10 S Sepharose HP, Mono Q HR 5/5, Phenyl Superose HR 5/5, HiTrap heparin (1 ml), Superdex 75 HR 10/30, HiLoad 16/10, Phenyl Sepharose HP, Mono S HR 5/5, Mono P HR 5/20 and Superose 12 HR 10/30. The micropreparative columns used were Phenyl Superose PC 1.6/5 and Mono S PC 1.6/5.

Microconcentrators were purchased from Amicon. Chemicals were obtained from Sigma and Merck and were of analytical-reagent grade.

Expression of RT in E. coli

RT was expressed in *E. coli* strain N4830-1 essentially as reported earlier [25], with a few modifications. A 1.4-kilobase DNA fragment containing a kanamycin resistance gene [26] was inserted into the Pst I site of the β-lactamase gene of pN10E-15. With the resulting plasmid pN10EK, N4830-1 was grown with 50 mg l⁻¹ of kanamycin in a 100-l fermenter. The richer media, 2 × YT, was used instead of Luria broth (LB) [27].

Amino acid analysis

Before amino acid analysis, the sample was dialysed thoroughly against water and a spectrum was recorded over the range 230–340 nm. The RT was

hydrolysed for 24 h at 110°C in 6 M HCl containing 2 mg ml^{-1} of phenol. The hydrolysates were analysed using an LKB Alpha Plus amino acid analyser.

The amino acid sequence obtained from the DNA sequence was used to calculate the number of tryptophan and tyrosine residues. Tryptophan was also determined by determining the molar absorptivity of the protein in connection with the amino acid analyses and using the molar absorptivities of tyrosine and tryptophan at neutral pH. This was done to compare the experimental and calculated molar absorptivities.

Determination of protein concentration

Protein concentrations were determined either by the Bradford assay technique (Bio-Rad Labs.) or spectrophotometrically at 280 nm. The calculated molar absorptivity at 280 nm is 2.52 · 10^5 1 mol^{-1} cm^{-1}.

Analysis by electrophoresis

Sodium dodecyl sulphate–polyacrylamide gel electrophoresis (SDS-PAGE), native PAGE and isoelectric focusing (IEF) were performed with the PhastSystem using the appropriate PhastGel gel media. PAGE with acidic buffer and 6 M urea was carried out using the reversed polarity electrode assembly. Two-dimensional electrophoresis was run using either IEF or native PAGE in the first dimension and SDS-PAGE in the second dimension. The protein bands were revealed by the silver staining method with the following modification: 20% trichloroacetic acid was used as the first step for fixation with all kinds of gel media; and washing steps with 10% ethanol and 5% acetic acid were omitted. All PAGE experiments and staining were otherwise done as recommended in the instruction manual for the PhastSystem.

Other analytical methods

Protein sequencing, western blotting using antibodies directed toward RT and assay of RT activity were performed as described by Unge et al. [25]. GENEPRO, a sequence data base (Riverside Scientific Enterprises), was used to identify N-terminally sequenced polypeptides.

Analytical chromatography

Gel filtration. The molecular weight of RT was determined by gel filtration on Superose 12 (30 × 1 cm I.D.) and Superdex 75 columns (30 × 1 cm I.D.) in 50 mM Tris–HCl (pH 8.0)–0.15 M NaCl–1 mM dithiothreitol (DTT). Blue Dextran, thyroglobulin, albumin, ovalbumin, trypsin inhibitor and lysozyme were used as molecular weight markers.

Chromatofocusing. The purified RT [after Poly (A)-Sepharose chromatography] was dialysed against 25 mM ethanolamine–10% glycerol (pH 9.4) and applied to a Mono P column (20 × 0.5 cm I.D.) which was then eluted with 30 ml of 10% Polybuffer 96 (pH 6.0). A partially purified sample of RT [before Poly(A)-Sepharose chromatography] was also chromatofocused using similar elution conditions. The experiments were done at room temperature.

Chromatography on Mono Q. The Mono Q column was equilibrated with buffer D, pH 9.5 (10 mM ethanolamine–10% glycerol–20 mM KSCN–5 mM DTT) and was eluted with a linear gradient from 0 to 0.5 M NaCl in buffer D.

Purification procedure

All chromatographic experiments were performed using the FPLC system at 4°C. The purification scheme was optimized on small columns and the production was done on larger columns as described below. During the early stages of optimization, the enzyme activity assay was used to detect RT in different chromatographic steps. When pure RT was assayed, there was a linear increase in the amount of DNA, measured in terms of radioactive incorporation of ^{3}H dTTP for 24 h. When the activity assay was done on the fractions from the crude extract and from the previous purification steps, the impurities present interfered with the activity measurement. Therefore, it was not possible to evaluate the purification of RT in different steps in terms of specific acitivity. SDS-PAGE was used to detect RT in each chromatographic step. Purified heterodimer of RT was used as the marker to identify fractions containing RT.

Preliminary steps. The bacterial cells from the fermenter were harvested by centrifugation, washed twice with 20 mM Tris–HCl–75 mM NaCl–1 mM EDTA (pH 8.2) and then suspended in the lysis buffer (pH 8.2) [20 mM Tris–HCl–75 mM NaCl–5

mM EDTA–5 mM DTT–1 mM phenylmethylsulphonyl fluoride (PMSF)–2 mM benzamidine–1 mM MgSO$_4$–DNase–RNase]. After disruption of the cells using a French pressure cell, the lysate was centrifuged at 23 000 g for 10 min to remove cell debris. The supernatant was subjected to ammonium sulphate fractionation. Saturated ammonium sulphate solution adjusted to pH 8 with NaOH was used. The protein that precipitated with ammonium sulphate in the interval 30–70% saturation was dissolved in buffer A (pH 8.2) (20 mM Tris–HCl–1 mM EDTA–1 mM DTT–2% glycerol) and dialysed for at least 1 h against the same buffer.

Anion-exchange and affinity chromatography in tandem. After dialysis, the conductivity of the solution was adjusted to 1.5 mS by dilution with buffer A. A solution corresponding to 100 g of bacteria was then applied to a column of DEAE Sepharose which was connected in tandem to a column of Heparin Sepharose. After application of the solution the columns were washed with buffer A, the DEAE Sepharose column was disconnected and the Heparin Sepharose column was eluted stepwise with buffer A (pH 7.9) containing 0.15 M NaCl in the first step and 0.35 M NaCl in the second step. The RT-containing fractions eluted in 0.35 M NaCl and were pooled.

Cation-exchange chromatography. The RT pool from the Heparin Sepharose column was diluted and adjusted to pH 6.5 by addition of a solution of 2-morpholinoethanesulphonic acid (MES) and applied to an S Sepharose column pre-equilibrated with buffer B (pH 6.5) (20 mM MES–1 mM DTT–1 mM EDTA–2% glycerol). The column was eluted with a linear gradient from 0 to 0.3 M NaCl in buffer B (total volume = 12 × bed volume). RT elutes at about 0.18 M NaCl.

Affinity chromatography on Poly(A)-Sepharose 4B. The fractions containing the heterodimer RT from the previous step were pooled and dialysed against buffer C, pH 8.2 (20 mM Tris–HCl–10% glycerol–1 mM DTT–1 mM EDTA) and applied to a column of Poly(A)-Sepharose 4B equilibrated with buffer C. Elution was carried out with a linear gradient from 0 to 0.2 M NaCl in buffer C (total volume = 6 × bed volume).

Hydrophobic interaction chromatography. The fractions containing RT from the step above were pooled and the concentration of ammonium sul-

phate was adjusted to 1.5 M and applied to a Phenyl Sepharose HP column equilibrated with 1.5 M ammonium sulphate–50 mM HEPES (pH 7.8)–1 mM DTT–10 mM MgCl$_2$. RT was eluted with a linear gradient from 1.5 to 0 M ammonium sulphate in three column volumes of buffer.

Concentration of RT using different chromatographic methods

The following steps were performed to concentrate the protein further and for buffer exchange. The SMART System, a micropreparative chromatography system, was used for concentration of RT on Phenyl Superose and Mono S. The small size of the the columns (100 μl) and the collection of fractions in small volumes are the most important features of the SMART system. The FPLC System was used for the other columns mentioned below to concentrate the protein.

Phenyl Superose. A Phenyl Superose column (100 μl) was equilibrated with 1 M ammonium sulphate at the desired pH. RT was applied to the column and was eluted directly with a buffer of low ionic strength which contained the appropriate additives for crystallization. RT eluted in small volumes and at the concentrations required for crystallization. When crystallization were performed in the presence of mercury(II) salts or sodium sulphite (in these instances the presence of DTT is not desired), the following steps were carried out to remove DTT while keeping the RT reduced: the sample applied was completely reduced by adding 10 mM DTT; the washing and eluting buffers (without DTT) were made oxygen free by passing nitrogen through the solution. The eluted fractions were used for the hanging drop crystallization experiments.

Heparin Sepharose or Mono S. The pure RT was applied to either a Hitrap Heparin Sepharose column (1 ml) or a Mono S column (100 μl). RT was eluted in the required buffer with a high salt concentration. The peak fractions contained the optimum concentrations of protein and salt and were used directly for crystallization. For example, RT was eluted in 0.75 M ammonium sulphate when 1.5 M ammonium sulphate was used as the precipitant.

Reverse salt gradient chromatography on Sepharose 4B [28]. In this instance the protein was precipitated on Sepharose 4B packed into an HR 5/5 column (1 ml) which was equilibrated with 1.5 M

ammonium sulphate. RT was eluted with a linear gradient of six column volumes from 1.5 to 0 M ammonium sulphate. The saturated solution of RT was used directly for crystallization. Similar reverse salt gradients were used to obtain the proper concentrations of other precipitants for the crystallization experiments.

Crystallization

RT was concentrated to 10 mg ml^{-1} either in a Centricon microconcentrator with a molecular weight cut-off of 10 000 or by the chromatographic techniques described above. Crystallization was done by the hanging drop vapour diffusion technique [29]. In a typical experiment, a 5 μl drop of RT was mixed with an equal volume containing 1.5 M ammonium sulphate, buffer and various additives such as DTT, MgCl$_2$ and methylmercury acetate. The drop was equilibrated against 1.5 M ammonium sulphate (10 ml) containing the same buffer, in a plastic Petri dish (9 cm diameter) sealed with parafilm. The time for crystallization varied from 2 days to 2 weeks.

X-Ray diffraction

X-Ray diffraction photographs were taken both with rotating anode and synchrotron X-ray sources. In both instances Enraf–Nonius Arndt–Wonacott oscillation cameras were used. The rotating anode generator was an Elliot GX-6 instrument operating at 35 kV and 50 mA. In this instance, the wavelength (λ) was 1.54 Å (Cu Kα), the crystal–film distance 100 mm, the oscillation angle 0.25° and the oscillation time 120 000 seconds per degree (total exposure time *ca.* 8.3 h). The conditions when using the synchrotron X-ray source at the SERC Synchrotron Radiation source (Daresbury, UK) were λ = 0.895 Å, crystal–film distance 145 mm, oscillation angle 1.0° and oscillation time 1000 seconds per degree (total exposure time *ca.* 16.7 min).

RESULTS AND DICUSSION

The expression and purification of recombinant HIV-RT have been reported by several laboratories [6–9, 18, 25, 30–32]. RT is expressed in fairly small amounts when the whole HIV-pol I gene is used to express the authentic RT, protease and endonuclease. The low yield might be due to the proteases

TABLE I

VOLUME, CONCENTRATION, YIELD AND PURIFICATION FACTOR OF RT (FROM 250 g WET CELL WEIGHT) AT DIFFERENT STAGES OF PURIFICATION

Purification step	Volume (ml)	Total protein (mg)	Purification factor	
			A[a]	B[b]
Lysate after centrifugation	600	30 000		
Ammonium sulphate precipitate[c]	5500	16 000	2	0.18
Heparin Sepharose	410	410	39	7
S Sepharose	70	37	11	75
Poly(A)-Sepharose	40	28	1.3	100

[a] A = Purification factor of protein between the two steps.

[b] B = Percentage of RT in each step calculated by using the final yield of RT in relation to the amount of total protein after each step.

[c] 30–70% ammonium sulphate precipitate dissolved and diluted.

in *E. coli* [33] and/or a reduction in translational efficiency due to, for example, secondary structural elements and short half-life of the mRNA [34]. In order to achieve the high homogeneity which is required to obtain well diffracting protein crystals, the purification scheme used earlier in our laboratory [25] was modified. To increase the yield of RT, we also modified the expression plasmid and the medium used in the fermenter as described under Experimental. Using the new protocol, 25–35 mg of RT, purified to homogeneity, were obtained from 200–250 g of cells. The purification scheme consists of salt fractionation and the following chromatographic principles: anion-exchange, affinity and cation-exchange chromatography. The purified RT was concentrated by hydrophobic interaction chromatography.

We have been using this scheme for more than one year and many interesting observations concerning the properties of RT have been made. RT has a strong tendency to aggregate and to associate with small polypeptides which seem to change the chromatographic properties of the protein.

Chromatofocusing was performed for the determination of the isoelectric point of p66/p51. For
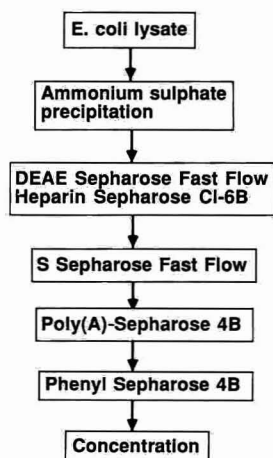
Fig. 1. Flow diagram for the purification and concentration of HIV-reverse transcriptase.

crystallization of the heterodimer in various buffers, salts and precipitants, micropreparative columns (100 μl) were used both for concentration of the protein and for change of buffers.

Purification of the heterodimer RT (p66/p51)

The details of the purification are described under Experimental. The purifications scheme is summarized in Table I and Fig. 1.

To obtain a high yield and high homogeneity of RT, it is essential to wash the cells thoroughly and to start the ammonium sulphate fractionation immediately after lysis and centrifugation of the cells. If this procedure is not followed, RT seems to become degraded, resulting in a lower yield and a less homogeneous enzyme. This might be attributed to the activity of bacterial proteases or to the HIV-1 protease, which is co-expressed with RT. Many proteins in *E. coli*, being acidic, bind to DEAE Sepharose, whereas the basic RT molecules are recovered in non-adsorbed fractions from DEAE Sepharose. RT binds to Heparin Sepharose at the pH and ionic strength used to run the DEAE Sepharose column. The columns of DEAE and Heparin Sepharose were coupled in tandem in order to reduce the purification time. Approximately 90% of the host contaminant proteins bound to DEAE Sepharose. About 1–2% of the total soluble protein in the lysate was eluted with 0.35 *M* NaCl from the Hepa-
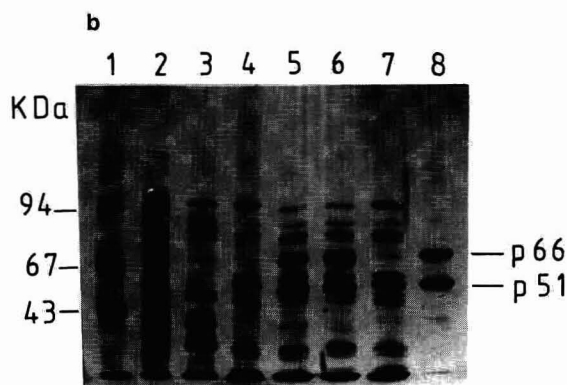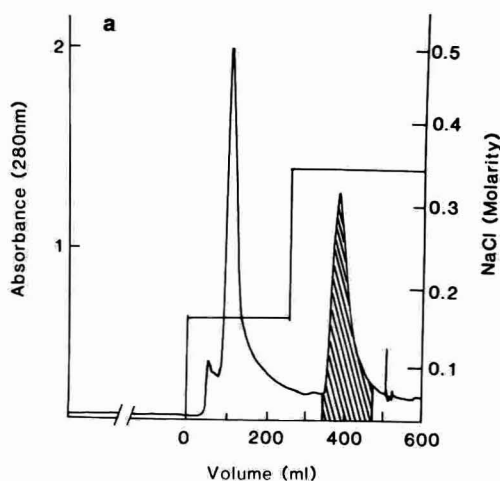
Fig. 2. (a) Affinity chromatography using Heparin Sepharose. Stepwise elution were done at 0.15 *M* NaCl and 0.35 *M* NaCl in buffer A (pH 7.9) (20 m*M* Tris–HCl–2% glycerol–1 m*M* EDTA–1 m*M* DTT). The shaded peak shows the fractions containing RT. Column size: 5 × 5 cm I.D. (b) SDS-PAGE (7.5%) analysis on PhastGel homogeneous 7.5. Samples are: lane 1 = molecular weight marker in kilodalton, (KDa); 2 = starting material applied on DEAE and Heparin Sepharose; 3 = flow-through fraction of Heparin Sepharose; 4 = 0.15 *M* NaCl pool; 5 and 6 = 0.35 *M* NaCl pool; 7 = 1.0 *M* NaCl pool; 8 = RT as a marker.

rin Sepharose column (Fig. 2a and b). As shown in Fig. 3a and b, RT eluted from the S Sepharose column in a symmetrical peak. In this step, RT was concentrated about 100-fold.

The chromatogram from the Poly(A)-Sepharose column is presented in Fig. 4a. The purified RT from this step had a very high specific acitvity [35,36]. The Poly(A)-Sepharose column could be
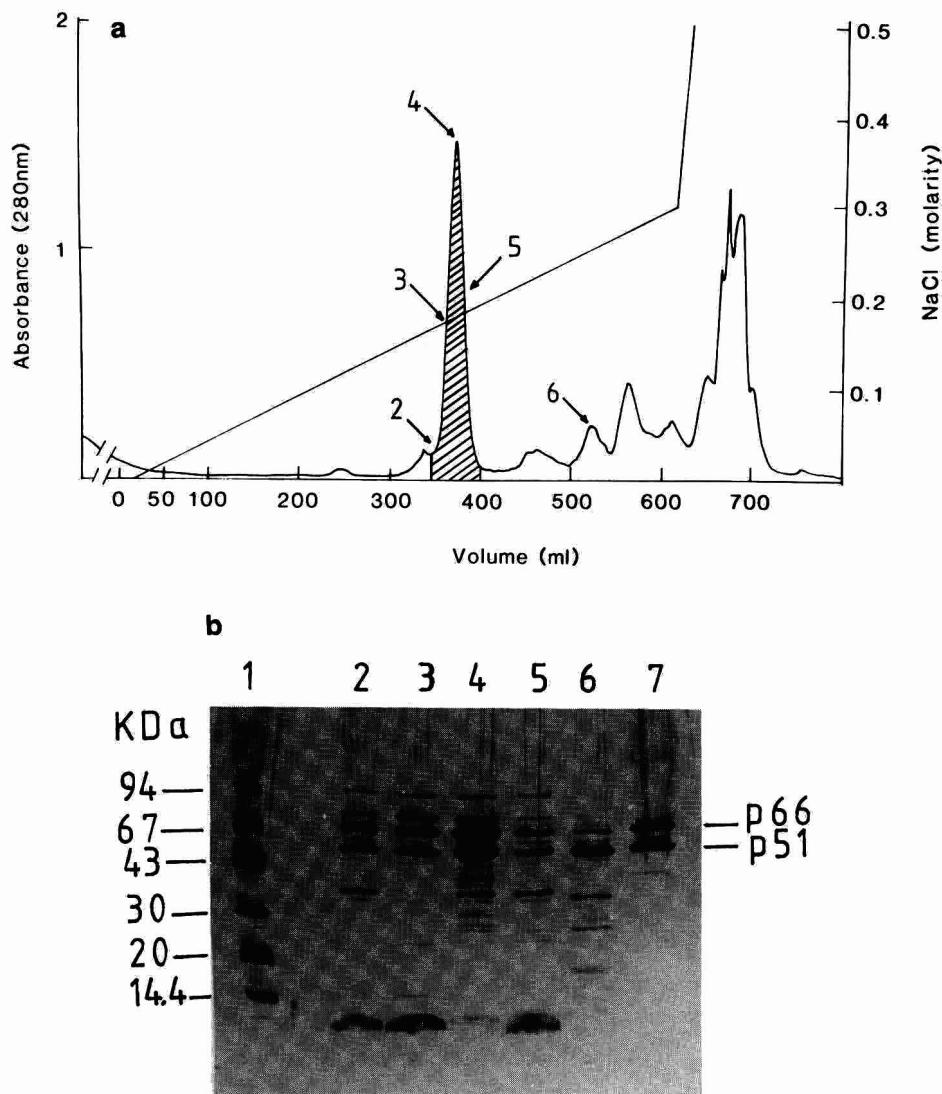
Fig. 3. (a) Cation-exchange chromatography using HiLoad 26/10 S Sepharose HP. Sample, 0.35 M pool from Heparin Sepharose; column size, 26 × 10 cm I.D.; fraction volume, 10 ml. Elution was performed with a linear gradient (600 ml) of 0 to 0.3 M NaCl in buffer B, pH 6.5 (20 mM MES–2% glycerol–1 mM EDTA–1 mM DTT). The shaded peak shows the fractions containing the heterodimer RT. (b) SDS-PAGE (8–25%) analysis on PhastGel gradient 8–25. Samples are: lane 1 = molecular weight markers; 2–6 = fractions indicated by arrows 2–6, respectively, in Fig. 3a; 7 = RT as a marker.

used for four or five runs. The reduced binding capacity might be due to hydrolysis of the poly r(A). For further concentration of the protein a Phenyl Sepaharose column was used. SDS-PAGE of purified RT from the peak fraction revealed a few faint bands of molecular weights between 40 000 and 50 000 in the silver-stained gel (Fig. 4b). When the

samples were diluted 10-, 50- and 100-fold these contaminating bands disappeared. We calculate that the protein must be at least 99% pure. Analysis of purified RT, by PAGE in acidic buffer and 6 M urea, revealed two sharp bands. As seen from the dilution series of RT on SDS-PAGE, the ratio between p66 and p51 is very close to unity.
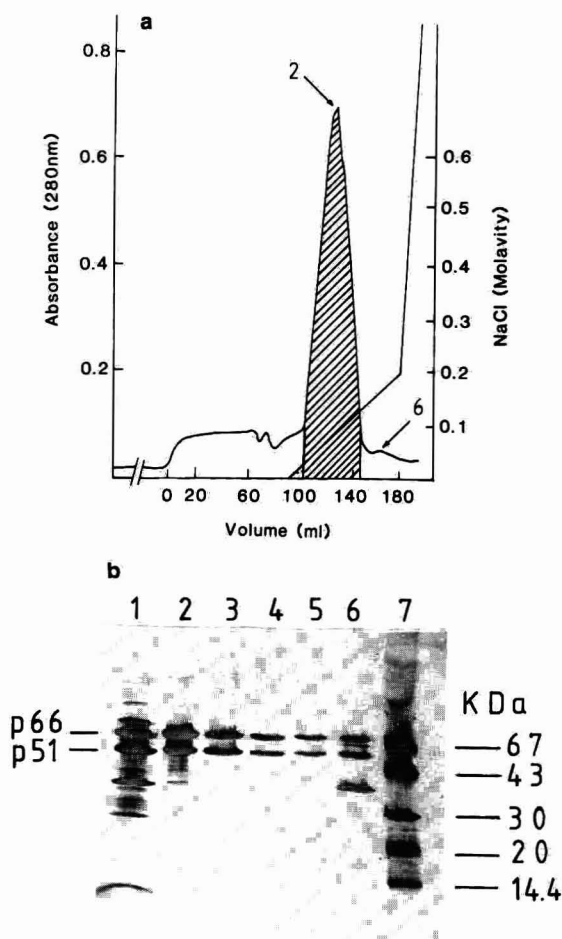
Fig. 4. (a) Elution profile from Poly(A)-Sepharose. Sample, dialysed RT fractions from S Sepharose; column size, 10 × 1.6 cm I.D.; fraction volume, 5 ml. Elution was performed with a linear gradient (six bed volumes) from 0 to 0.2 M NaCl in buffer C (pH 8.2): 20 mM Tris–HCl–10% glycerol–1 mM EDTA–1 mM DTT. The peak containing RT is shaded. (b) SDS-PAGE (8–25%) analysis on Phastgel gradient 8–25. Samples in lane 1 = starting material; 2 = peak fraction indicated by arrow 2 in the chromatogram; 3, 4 and 5 = 10 ×, 50 × and 100 × dilutions of the peak fraction, respectively; 6 = fraction indicated by arrow 6 in the chromatogram; 7 = molecular weight marker.

Further analysis of polypeptide p51

The heterodimer RT eluted in a symmetrical peak from the S Sepharose column. The other peak fractions from S Sepharose were analysed on SDS-PAGE (Fig. 2b). The p51 polypeptide, along with other small polypeptides, were spread out over the

chromatogram. The chromatographic pattern on S Sepharose reflected the degree of proteolytic degradation. The relative heights of the peaks containing p51 increased when (i) instead of direct lysis after the cell harvest, the bacterial cells were frozen before the purification, and (ii) the time taken to reach this purification step happened to be unusually long. The p51 band was identified as part of RT as it reacted positively in western blot analysis using antibodies raised against a synthetic peptide with the N-terminal sequence of RT. The N-terminal sequence analysis of p51 confirmed its identity as the N-terminal part of p66. An attempt to purify p51 further either by anion-exchange chromatography on Mono Q or by gel filtration on Superdex 75 resulted in fractions containing the p51 band co-eluting with a few small polypeptides. The p51 polypeptide bound strongly to Phenyl Superose and could only be eluted with 6 M urea. This indicates that p51, in comparison with the heterodimer, displays new hydrophobic surfaces.

Characterization of RT

There are no disulphide bridges between p66 and p51, as SDS-PAGE under non-reducing conditions resulted in two distinct bands. The aparent molecular weight of the heterodimer is 110 000 as determined by gel filtration experiments. The N-terminal amino acid sequences of p66 and p51 are identical, as shown by N-terminal sequence determination. The amino acid composition of the purified heterodimer corresponds to the sum of those of p66 (1–560) and p51 (1–440) and to that reported by Mizrahi et al. [6]. The molar absorptivity (ε) obtained from the experimental data agreed with the calculated value ($\varepsilon = 2.52 \times 10^5 \, \mathrm{l \, mol^{-1} \, cm^{-1}}$).

Isoelectric point of RT

Although the purification of recombinant RT has been reported by several groups, none has determined the isoelectric point. The isoelectric point of the protein was calculated from the pK_a values of the amino acids contributing to the charge. For both p66 and p51, the calculated isoelectric point is 9.1. To determine the pI experimentally, pure RT was analysed on a IEF gel in the pH range 3–9. The protein did not focus in a sharp band but gave a smear in the pH range 6.5–8. The same result was obtained in the presence of 6 M urea. The partially
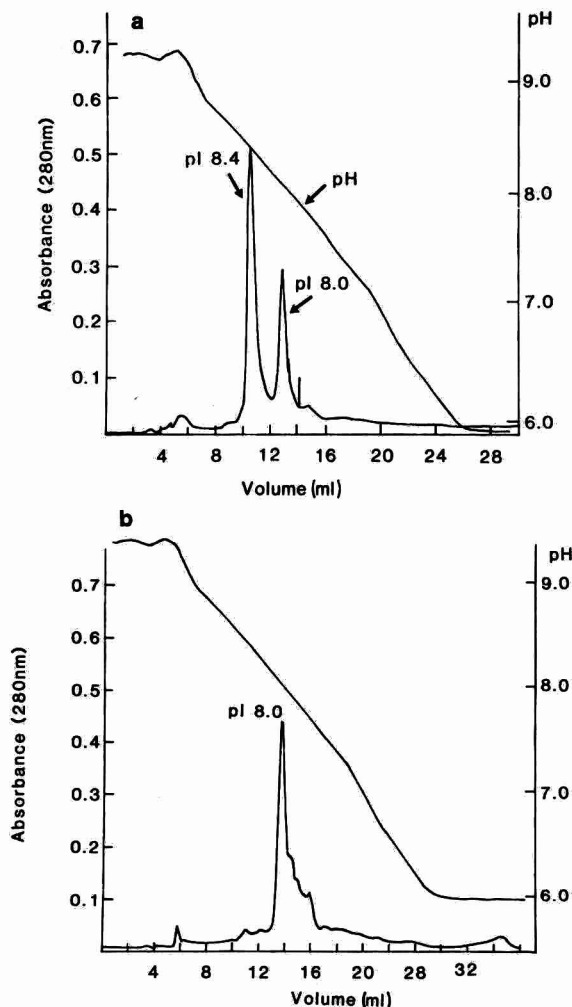
Fig. 5. Chromatofocusing on Mono P 5/20. The column was equilibrated with 25 mM ethanolamine–10% glycerol (pH 9.4). A pH gradient from 9.4 to 6.0 was created by eluting the column with 10% Polybuffer 96 (pH 6.0). (a) Sample: purified RT [after Poly(A)-Sepharose chromatography]. (b) Sample: partially purified RT [before Poly(A)-Sepharose chromatography].

purified RT was analysed by two-dimensional electrophoresis. In the first dimension on IEF gels, a patch and a number of bands between pH 5 and 9 were seen. The second dimension using SDS-PAGE revealed that the heterodimer was present in all of the bands.

As the results from IEF could not be interpreted,

chromatofocusing was attempted on a Mono P column to determine the exact pI. Purified RT showed a tendency to elute in a broad pH range as in isoelectric focusing gels. When DTT was added to the sample solution, two sharp peaks at pH 8.0 and 8.4 were observed (Fig. 5a) with some trailing of RT in the pH range 7.0–8.5. Several chromatofocusing runs with different concentrations of RT were performed using identical elution conditions. These experiments showed that the smearing of the protein was not due to overloading. The ratio between the two peaks, which appeared in all runs at pH 8.0 and 8.4, varied among the experiments. When these peaks were re-run on the chromatofocusing column under similar conditions, RT was found to be evenly distributed over a broad pH range. Dynamic light scattering investigations of these fractions showed aggregates of different sizes (results not shown). It was not feasible to perform chromatofocusing in 6 M urea because RT precipitated in 6 M urea at pH 9.4, the starting pH of the column. When partially purified RT (the fractions containing RT from the S Sepharose chromatographic step) was chromatofocused, a distinct peak eluted at pH 8.0 and very little protein was found elsewhere in the chromatogram (Fig. 5b). Furthermore, the elution of RT from the ion-exchange column in a single symmetrical peak precludes charge heterogeneity. The data above indicate that the true isoelectric point is close to 8. It seems likely that the broadening of the peak in chromatofocusing of the pure RT is caused by aggregation.

Polyacrylamide gel electrophoresis

The electrophoretic mobility of RT heterodimers in native PAGE at pH 8.8 was very high compared with that of many other proteins of similar size. This is surprising, as PAGE was performed at a pH close to the isoelectric point. Two diffuse bands or smears appeared when the gel was stained. Two-dimensional electrophoresis with native PAGE in one dimension and SDS-PAGE in the second dimension revealed that both bands contained the heterodimer, p66/p51. This behaviour of RT in both IEF and native electrophoresis gels is probably due to aggregation. PAGE in acidic buffer containing 6 M urea resulted in two sharp bands as in SDS-PAGE.

TABLE II

N-TERMINAL AMINO ACID SEQUENCES OF THE POLYPEPTIDES (1–5) WHICH CO-ELUTED WITH RT IN THE FIRST THREE CHROMATOGRAPHIC STEPS AND WERE ISOLATED ON POLY(A)-SEPHAROSE

The approximate sizes of the polypeptides were estimated from SDS-PAGE.

No.	Contaminating peptides
1	MW 20 000
	[56]Lys–Ala–Asn–Arg–Val–Thr–Lys–Pro–Glu–Ala–Gly–X–Phe...
	Ribosomal protein L3 *E. Coli*
2	MW 16 000
	[3]Lys–Lys–Asp–Ile–His–Pro–Lys–Tyr–Glu...
	Ribosomal protein L31 *E. coli*
3	MW 42 000
	Ala–Glu–Glu–Met–Leu–Arg–Lys–Ala–Val–Gly–Lys–X–Ala–Tyr–Gly...
	Unidentified
4	MW 23 000
	Phe–Ser–Ile–Asp–Asp–Val–Ala–Lys–Gln–Ala...
	Unidentified
5	MW 14 000
	Met–X–Pro–Met–Leu–Asn–Ile–Ala–Val...
	Unidentified
6	MW 12 000
	Met–Asn–Lys–Thr–Gln–Leu–Ile–Asp–Val–Ile...
	DNA-binding protein NS2 *E. coli*

Investigation of contaminating polypeptides

During optimization of the conditions for the Poly(A)-Sepharose chromatography, wherein RT was eluted with a linear gradient (ten column volumes) from 0 to 0.5 M NaCl, polypeptides of low molecular weight were eluted together with the heterodimer RT. Often, one of the contaminating polypeptides was dominant (Fig. 4b, lane 6), but the molecular weight of the contaminant varied between 12 000 and 45 000 in different preparations. In no case were the polypeptides degradation products of RT, as shown by western blot analysis. To eliminate the contaminating polypeptides, the elution on the Poly(A)-Sepharose column was done using a shallow gradient as described under Experimental. Under these conditions the polypeptide eluted immediately after the heterodimer RT. The N-terminal amino acid sequences of these polypeptides from a few preparations (Table II, 1–5) were determined. Two of these polypeptides were identified as parts of the ribosomal proteins L3 and L31, whereas for the others no homologous sequences were found in the data base. These ribosomal proteins L3 [37] and L31 [38] are basic and L3, at least, binds to the ribosomal RNA. The calculated iso-

electric points of these proteins are similar to that of RT. This may explain the co-elution of these polypeptides in all the purification steps.

The fractions containing the heterodimer RT from the S Sepharose chromatography were analyzed further on a Mono Q column. All of the fractions were analysed by SDS-PAGE under non-reducing conditions. Most of the heterodimer RT adsorbed to the column at pH 9.5. However, the nonbound fractions showed three bands on the PAGE gel, two of which coincided with the heterodimeric marker (p66 and p51). The third polypeptide was identified by the N-terminal amino acid sequence determination as the DNA binding protein NS2 from *E. coli*. When SDS-PAGE was run without boiling the samples, two bands occurred very close to each other at a position around MW 66 000 and the small peptide was not observed. One explanation for this observation might be that the association of the NS2 protein with RT might prevent the binding of RT to Mono Q at pH 9.5.

Crystallization

Several groups have attempted to crystallize RT but so far none has reported crystals diffracting to
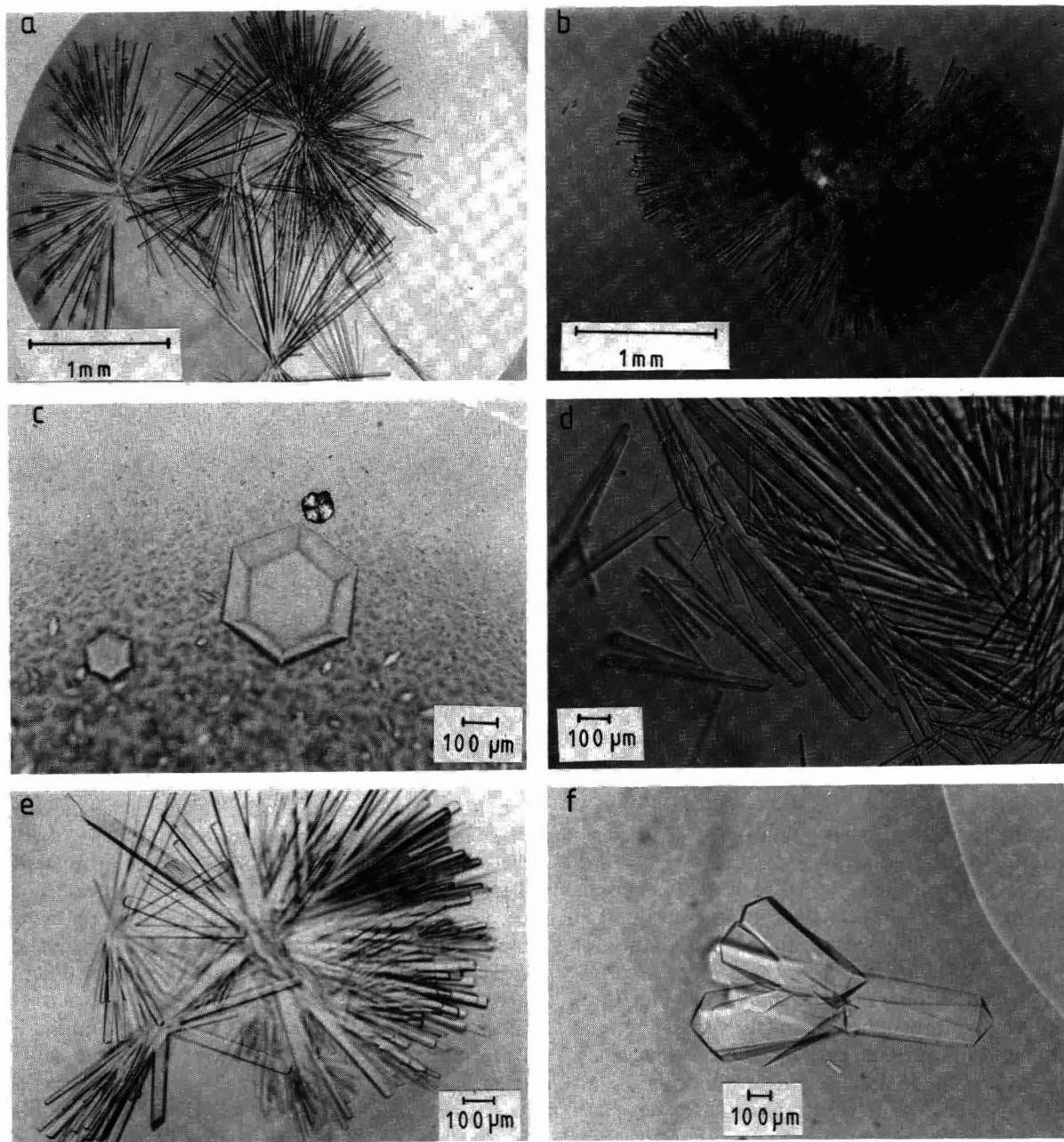
Fig. 6. Photographs showing different morphological forms of some of the crystals obtained in the laboratory. Crystallization was done by the hanging-drop vapour diffusion method with 1.5 M ammonium sulphate–50 mM 4-(2-hydroxyethyl)-1-piperazineethanesulphonic acid (HEPES)–10 mM MgCl$_2$–1 mM DTT–50 mM NaCl (pH 7.8) as precipitant at 4°C and with protein concentration of 10 mg ml^{-1}. Size calibration is given by bars in each photograph. (a) Needles and rods. These are typical crystals which appeared within 3–5 days. The material was obtained directly from those experiments where small columns were used for concentration and buffer exchange. (b) Crystals forming sea urchins were obtained under similar conditions as in (a). (c) Truncated hexagonal pyramid crystals grown with 100 mM mercaptoethanol instead of 1 mM DTT in the buffer. Spindle-shaped crystals appeared first. Some of them were transformed into hexagonal pyramids. (d) Rod-shaped crystals obtained with the addition of 50 mM sodium pyrophosphate. Similar crystals could be obtained by the addition of phosphate, guanidine sulphate, spermidine and spermine (10–100 mM). (e) Crystals obtained in the presence of a synthetic deoxyoligonucleotide (TGC AGG GCA CGT). In this instance the rods had more defined ends. (f) Crystals obtained in the presence of 1 mM p-chloromercuribenzenesulphonic acid.

Fig. 7. X-ray diffraction pattern from a crystal of heterodimer RT. The X-ray photograph was obtained by the use of Enraf–Nonius Arndt–Wonacott camera and an X-Ray synchrotron source (at the SERC Synchrotron Radiation source, Daresbury, UK) with the following conditions: wavelength (λ), 0.895 Å; crystal–film distance, 145 mm; oscillation angle, 1.0°C; and oscillation time, 1000 s per degree (total exposure time ca. 16.7 min). The diffraction limit is about 9 Å resolution and the X-ray reflections are well suited for intensity measurements.
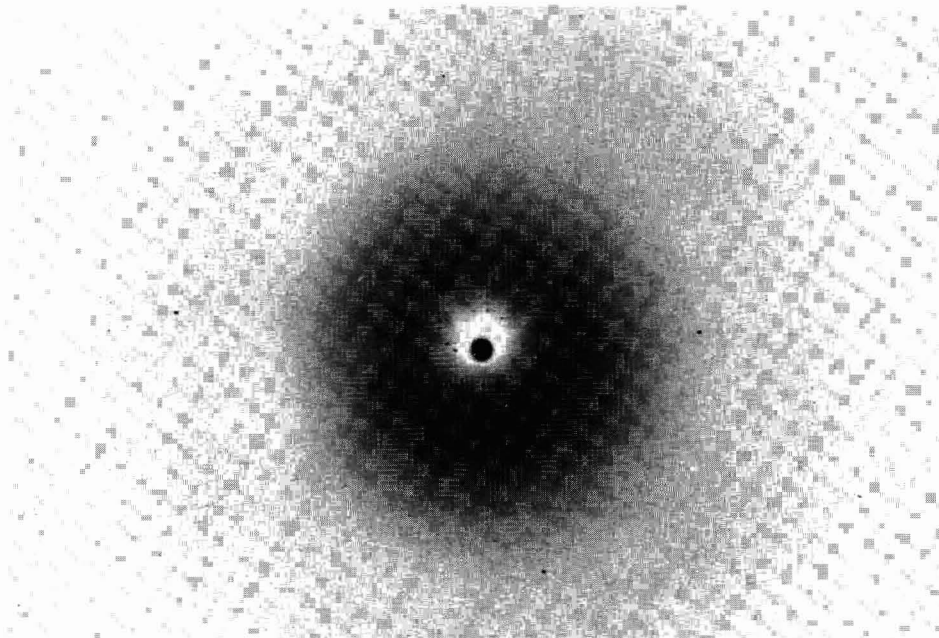
better than about 7 Å resolution [23–25]. We investigated a variety of crystallization conditions, e.g., different pH, ionic strength and temperature, and also stabilization with synthetic deoxyoligonucleotides and inhibitors. Attempts to co-crystallize RT with some of the polypeptides listed in Table II did not lead to better crystals. Further, we used micropreparative columns to exchange buffers and increase the RT concentrations at the same time. The reverse salt gradient chromatographic technique on Sepharose 4B [28] was used to produce saturated solutions of RT for crystallization. The reverse salt gradient method, when performed using different precipitants, not only gave a saturated solution of the protein but also enabled us to determine the appropriate concentration of the precipitant in the reservoir. The crystals appeared within two days when ammonium sulphate was used as the precipitant.

Fig. 6 shows a number of different morphological forms of RT crystals grown in our laboratory. The growth conditions are described in the legend. In most instances the crystals started to grow as needles or rods. The growth of the crystals terminated after some time. Instead, more needles appeared or needles started to branch off, resulting in feathery fans or sea urchin structures. In some instances the crystals had the shape of well defined truncated hexagonal pyramids. These hexagonal crystals sometimes disappeared and needles were formed instead. Both crystal forms could also occur in the same drop.

The best heterodimer crystals (Fig. 6e and f) diffracted to about 9 Å resolution, with both rotating anode and synchrotron X-ray sources (Fig. 7).

NOTE ADDED IN PROOF

Recently we have obtained crystals of heterodimer RT in complex with nucleic acid which diffract to 4.5 Å resolution (using a rotating anode X-ray source).

SUMMARY

The HIV-1 pol I gene proteins (protease, reverse transcriptase and endonuclease) expressed in *E. coli* by the use of an inducible expression vector have been reported by Unge *et al.* [25]. Authentic reverse transcriptase (HIV-RT) was purified in a stable heterodimeric form (p66/p51) exhibiting a high degree of purity and high activity. By modifying the fermentation conditions and developing a new purification scheme, the yield of purified RT has been substantially increased compared with that obtained in our earlier procedure [25]. The purification procedure consists of ammonium sulphate fractionation followed by chromatography on DEAE Sepharose, Heparin Sepharose, Poly(A)-Sepharose and Penyl Sepharose.

The heterodimer has an isoelectric point close to 8 (as determined by the chromatofocusing technique) and shows a tendency to aggregate (as indicated by dynamic light scattering).

Some bacterial polypeptides, *e.g.*, the ribosomal proteins L3 and L31 and the DNA binding protein NS2, co-eluted with HIV-RT during the early stages of purification, indicating similar properties (L3 and L31) and, in the case of NS2, association with the heterodimer.

A proteolytic product of the heterodimer was separated and identified as the protein p51 (the N-terminal end of the p66), which appears to be more hydrophobic than the heterodimer.

The HIV-RT has been crystallized in different morphological forms using the hanging drop vapour diffusion technique. The use of reverse salt gradient chromatography and micropreparative columns resulted in increased control of the crystallization process.

With the aim of obtaining crystals of higher quality, we are devoting considerable efforts towards improving the expression systems, modifying the RT molecule, achieving complex formation between RT and Fab fragments of monoclonal antibodies and other measures.

REFERENCES

1 H. Varmus and R. Swanstrom, in R. A. Weiss, N. M. Teich, H. E. Varmus and J. M. Coffin (Editors), *Molecular Biology of Tumor Viruses: RNA Tumor Viruses*, Cold Spring Harbor Laboratory, Cold Spring Harbor, NY, 1982, pp. 381–384.
2 L. A. Evans and J. A. Levy, *Biochim. Biophys. Acta*, 989 (1989) 237–254.
3 S. H. Hughes, A. L. Ferris and A. Hizi, in W. G. Laver and G. M. Air (Editors), *Use of X-Ray Crystallography in the Design of Antiviral Agents*, Academic Press, New York, 1990, pp. 297–307.
4 D. K. Stammers, K. L. Powell, B. A. Larder, G. Darby, D. J. M. Purifoy, M. Tisdale, D. M. Lowe, D. I. Stuart, E. Y. Jones, G. L. Taylor, E. F. Garman, R. Griest and D. C. Phillips, in W. G. Laver and G. M. Air (Editors) *Use of X-Ray Crystallography in the Design of Antiviral Agents*, Academic Press, New York, 1990, pp. 309–317.
5 B. Müller, T. Restle, S. Weiss, M. Gautel, G. Sczakiel and R. S. Goody, *J. Biol. Chem.*, 264 (1989) 13975–13978.
6 V. Mizrahi, G. M. Lazarus, L. M. Miles, C. A. Meyers and C. Debouck, *Arch. Biochem. Biophys.*, 273 (1989) 347–358.
7 M. R. Deibel Jr., T. J. McQuade, D. P. Brunner and W. G. Tarpley, *AIDS Res. Hum. Retrovirus*, 6 (1990) 329–340.
8 S. F. J. Le Grice, V. Beuck and J. Mous, *Gene*, 55 (1987) 95–103.
9 I. C. Bathurst, L. K. Moen, M. A. Lujan, H. L. Gibson, P. H. Feucht, S. Pichuantes, C. S. Craik, D. V. Santi and P. J. Barr, *Biochem. Biophys. Res. Commun.*, 171 (1990) 589–595.
10 V. Karacostas, K. Nagashima, M. A. Gonda and B. Moss, *Proc. Natl. Acad. Sci. U.S.A.*, 86 (1989) 8964–8971.
11 W. G. Farmerie, D. D. Loeb, N. C. Casavant, C. A. Hutchison, III, M. H. Edgell and R. Swanstrom, *Science*, 236 (1987) 305–308.
12 J. Hansen, T. Schulze, W. Mellert and K. Moelling, *EMBO J.*, 7 (1988) 239–243.
13 M. C. Graves, M. C. Meidel, P. E. Yu-Ching, M. Manneberg, H.-W. Lahn and F. Gruninger-Leitch, *Biochem. Biophys. Res. Commun.*, 168 (1990) 30–36.
14 J. F. Davies, II, Z. Hostomska, Z. Hostomsky, S. R. Jordan and D. A. Matthews, *Science*, 252 (1991) 88–90.
15 T. Restle, B. Müller and R. Goody, *J. Biol. Chem.*, 265 (1990) 8986–8988.

16 V. R. Prasad and S. P. Goff, *Proc. Natl. Acad. Sci. U.S.A.*, 86 (1989) 3104–3108.

17 D. M. Lowe, V. Parmar, S. D. Kemp and B. A. Larder, *FEBS Lett.*, 282 (1991) 231–234.

18 M.-L. Sallafranque-Andreola, D. Robert, P. J. Barr, M. Fournier, S. Litvak, L. Sarih-Cottin and L. Tarrago-Litvak, *Eur. J. Biochem.*, 184 (1989) 367–374.

19 D. L. Ollis, P. Brick, R. Hamlin, N. G. Xuong and T. A. Steitz, *Nature (London)*, 313 (1985) 762–766.

20 Y. J. Chung, R. Sousa, J. P. Rose, E. Lafer and B. C. Wang, in F. Y.-H. Wu and C.-W. Wu (Editors), *Structure and Function of Nucleic Acid and Proteins*, Raven Press, New York, 1990, pp. 55–59.

21 M. Delarque, O. Poch, N. Tordo, D. Moras and P. Argos, *Protein Eng.*, 3 (1990) 461–467.

22 C. M. Joyce, *Curr. Opinion Struct. Biol.*, 1 (1991) 123–129.

23 D. M. Lowe, A. Aitken, C. Bradley, G. K. Darby, B. A. Larder, K. L. Powell, D. J. M. Purifoy, M. Tisdale and D. K. Stammers, *Biochemistry*, 27 (1988) 8884–8889.

24 L. F. Lloyd, P. Brick, L. Mei-Zhen, N. E. Chayen and D. M. Blow, *J. Mol. Biol.*, 217 (1990) 19–22.

25 T. Unge, H. Ahola, R. Bhikhabhai, K. Bäckbro, S. Lövgreen, E. M. Fenyö, A. Honigman, A. Panet, G. S. Gronowitz and B. Strandberg, *AIDS Res. Hum. Retrovirus*, 6 (1990) 1297–1303.

26 J. Vieira and J. Messing, *Gene*, 19 (1982) 259–268.

27 T. Maniatis, E. F. Fritsch and J. Sambrook, *Molecular Cloning: a Laboratory Manual*, Cold Spring Harbor Laboratory, Cold Spring Harbor, NY, 3rd ed., 1989.

28 K. Gulewicz, D. Adamiak and M. Sprinzl, *FEBS Lett.*, 189 (1985) 179–182.

29 A. J. McPherson, *Methods Biochem. Anal.*, 23 (1979) 249–345.

30 A. Hizi, C. McGill and S. H. Hughes, *Proc. Natl. Acad. Sci. U.S.A.*, 85 (1988) 1218–1222.

31 B. Larder, D. Purifoy, K. Powell and G. Darby, *EMBO J.*, 6 (1987) 10 3133–3137.

32 S. F. J. Le-Grice and F. Grüninger-Leitch, *Eur. J. Biochem*, 187 (1990) 307–314.

33 D. E. Danley, K. F. Geoghegan, K. G. Scheld, S. E. Lee, J. R. Merson, S. J. Hawrylik, G. A. Rickett, M. J. Ammirati and P. M. Hobart, *Biochem. Biophys. Res. Commun.*, 165 (1989) 1043–1050.

34 P. Balbas and F. Bolivar, *Methods Enzymol.*, 185 (1990) 14–37.

35 J. S. Gronowitz, M. Neümuller, J. Lennerstrand, R. Bhikhabhai, T. Unge, H. Weltman and C.. F. R. Källander, *Biotechnol. Appl. Biochem.*, 13 (1991) 127–142.

36 M. Neumüller, A. Karlström, C. Källander and S. Gronowitz, *Appl. Biochem.*, 12 (1989) 34–56.

37 P. O. Ollins and M. Nomura, *Cell*, 26 (1981) 205–211.

38 J. Brosius, *Biochemistry*, 17 (1978) 501–507.

Affinity chromatographic separation of gonadotropic hormone agonist and antagonist antibodies

Implications for structure, immunological and biological properties of glycoproteins

M. R. Sairam and L. G. Jiang

Reproduction Research Laboratory, Clinical Research Institute of Montreal, 110 Pine Avenue West, Montreal, Quebec H2W 1R7 (Canada)

ABSTRACT

Gonadotropic hormones which have lost peripheral sugar residues in their oligosaccharide chains display antagonistic properties and produce antibodies that fail to recognize the fully glycosylated hormone (agonist form). These polyclonal antibodies were separated by successive affinity chromatography on divinylsulfonyl-Sepharose coupled agonist and antagonist columns. The immunoglobulin G fraction from the agonist affinity columns recognizes both free agonist and antagonist in solution radioimmunoassays and also when these hormone forms are bound to receptors on gonadal cells. However, antagonist-specific antibodies recognize only the free antagonist in solution but not when it is receptor bound, implying that the conformation of the receptor-bound antagonist is different from that of the agonist. Affinity-purified antibodies against the different forms are useful in analyzing immunological and biological properties of the hormones. The studies with these glycosylated hormones serve as a useful model for other glycoproteins of pharmaceutical value.

INTRODUCTION

Receptor–ligand interactions are widely used to design compounds with desired pharmacological properties with either cellular activation (agonistic) or inhibitory (antagonistic) characteristics. For simple ligands such as amino acid derivatives, steroids or even peptides of moderate length, to indicate only a few, the task of designing structural variants is now explored in a systematic manner. This is facilitated by advances in organic synthesis and computer modeling so that appropriate conformations can be selected beforehand for detailed study. For complicated structures such as larger peptides, simple

protein hormones and even more complex glycoprotein hormones such as the gonadotropins, the usual and classical methods of structure–function study and careful analysis in various assays have been the established avenues of choice and are likely to remain so for some time. More and more revelations of the crystal structure of pharmacologically active compounds such as hormones, enzymes and receptors and site-directed mutagenesis approaches offer exciting avenues for rapid exploration in this direction.

Among hormones are many examples in which selected deletions of amino acids by either natural occurrence or deliberate design have produced molecules with altered biological properties. Some examples of these are corticotropin inhibitory peptide and analogues of ACTH and β-endorphin [1,2], recombinant growth hormones [3–5], different forms

----

Correspondence to: Dr. M. R. Sairam, Reproduction Research Laboratory, Clinical Research Institute of Montreal, 110 Pine Avenue West, Montreal, Quebec H2W 1R7, Canada.

of thyrotropin in tumor extracts, sera and pituitary extracts [6] and recombinant [7,8] and chemically modified gonadotropins [9,10].

Extensive studies have been conducted in our laboratory emphasizing the hormonal antagonistic properties of deglycosylated gonadotropins [9,11]. Together with reports from other laboratories [10,12–14], these studies have shown that the deglycosylated gonadotropins bind to the cell membrane receptors on target cells but fail to convey the message into the interior of the cell. Post-receptor events, such as second messenger production (viz., cyclic AMP) or end responses such as steroid accumulation in gonadal cells are greatly compromised. Because of their discordant behavior, these variants have displayed antagonistic properties under various experimental conditions. Many biophysical investigations [9,10] have provided suggestive evidence but not proof of significant changes in hormone conformation following loss of peripheral sugars. Immunological analyses of hydrofluoride treated gonadotropins in which the only documented change is the reduction in peripheral sugars with an intact quaternary structure have offered the best evidence of alteration in conformation [15–20]. In this regard, affinity chromatographic separation of agonist and antagonist-specific antibodies from polyclonal antisera have been very valuable in exploring the differences in receptor–ligand interactions and events leading to biological response. These results are highlighted here with selected examples.

EXPERIMENTAL

Highly purified gonadotropin preparations, human choriogonadotropin (hCG), ovine luteinizing hormone (oLH) and ovine follicle-stimulating hormone (oFSH), prepared in our laboratory were subjected to one-step chemical deglycosylation with anhydrous HF treatment and further purified by exclusion chromatography on concanavalin A-Sepharose and gel filtration [21]. These steps remove traces of remaining glycosylated hormone. All three deglycosylated hormones (DG-hCG, DG-oLH and DG-oFSH) were used for immunization of male mice, rats and rabbits [17–19]. Radioimmunoassays using the respective ^{125}I-labeled agonist and antagonist variety of hormones revealed differences in

immunological cross-reactivities, which showed the presence of two classes of antibodies in all three species [17–19]. This then led to experiments designed to separate the two sets of antibodies. Affinity chromatography was performed using ligands immobilized on divinylsulfonyl (DVS)-Sepharose according to methods which we have used on previous occasions [22]. This involved coupling the agonist and antagonist forms of each hormone (except for DG-oFSH) to the affinity matrix at pH 9.3. Excellent coupling (80–90%) was achieved within 2–4 h as determined by measuring the absorbance at 280 nm. The columns were extensively washed with 0.025 M Tris–HCl buffer (pH 7.5). Rabbit antisera (5 ml per run) were diluted and fractionated batchwise first on DVS–hormone (agonist) columns and then on DVS–hormone (antagonist) columns. In each instance after eliminating non-volatile buffer salts with 0.05 M ammonium hydrogencarbonate bound immunoglobulin Gs (IgGs) were eluted with 0.1 M ammonia solution at room temperature. The eluted fractions were diluted and lyophilized for storage in powder form at 4°C. Whenever needed, they were weighed accurately on an electrobalance and dissolved in appropriate buffers for immunoassay, bioassays or radiolabeling to examine post-receptor binding phenomena (see Results and Discussion).

RESULTS AND DISCUSSION

Because of their availability, rabbit antisera to DG-hCG and DG-oLH have been studied extensively to obtain the two kinds of antibodies of different specificity. According to the scheme depicted in Fig. 1, two successive affinity chromatographies produced IgG populations designated B and A2. A quantitative evaluation performed using the respective ligands and fractionated antibodies (Table I) reveals a clear separation. In general, the B fraction in each instance could react to the same extent with labeled agonist and antagonists, but the A2 fraction was clearly more discriminatory, showing preferential binding of labeled antagonists.

The antibodies were highly purified, as revealed by protein staining (not shown), and specific when examined by Western blot analysis (Fig. 2). For comparison, in lanes 1 and 2 are shown two oLH antibodies (1 μg) derived from animals immunized

```
                    Polyclonal rabbit antiserum
                    to DG-oLH, DG-oFSH, DG-hCG
                              |
                              |    First chromatography
                              |    DVS-Sepharose coupled
                              |    oLH, oFSH or hCG
                              |
         +--------------------+------------------------------+
         |                                                   |
         v                                                   v
    Unadsorbed A                             Adsorbed and eluted by NH3
Second chromatography    |                         Fraction B
DVS-Sepharose coupled    |                      Agonist/Antagonist
DG-LH or DG-hCG          |
         +---------------+
         |                                   |
         v                                   v
    Unadsorbed                     Adsorbed and eluted by NH3
    Discard                              Fraction A2
                                         DG-LH specific or
                                         DG-hCG specific
```
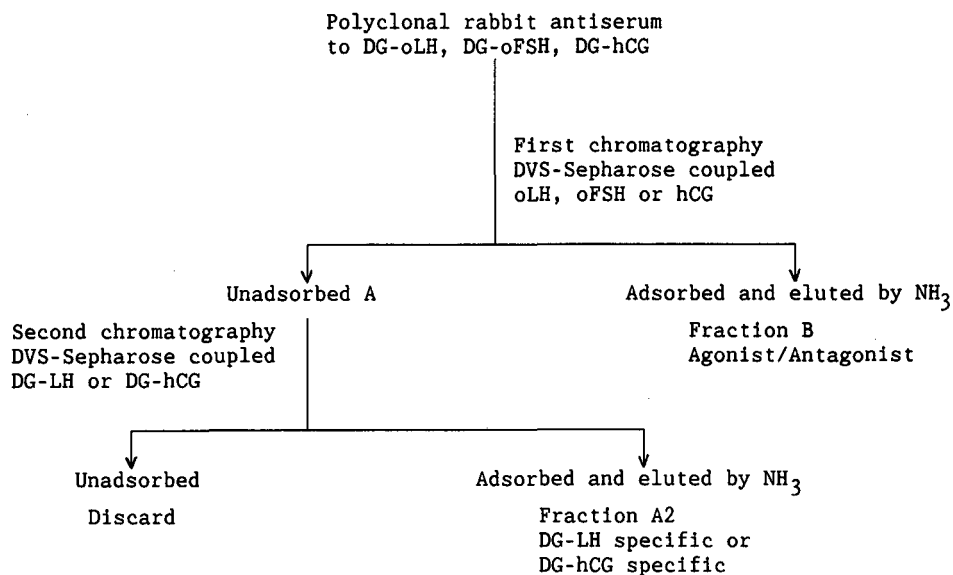
Fig. 1. Affinity chromatographic separation of agonist and antagonist gonadotropin antibodies by successive fractionation of DG-hormone polyclonal antisera on DVS-linked columns of native or DG-hormone. For DG-oFSH antiserum, the IgG in fraction A was processed by ammonium sulfate precipitation. In each example antibody in fraction B shows binding to both [^{125}I]native or -DG-hormone, but antibody in fraction A2 shows preferential binding of [^{125}I]DG-hormone.

TABLE I

BINDING OF LABELED GONADOTROPIN AGONISTS (oLH, oFSH AND hCG) AND ANTAGONISTS (DG-oLH, DG-oFSH, DG-hCG) TO AFFINITY-PURIFIED ANTIBODIES

For determination of binding 100 ng of purified lyophilized antibody (except in experiment 2, where the asterisk denotes the ammonium sulfate fraction) were incubated with the appropriate labeled ligand. In the three experiments the antisera fractionated were of DG-oLH, DG-oFSH and DG-hCG, respectively.

Experiment No.	Fraction	Binding (%)	
		[^{125}I]oLH	[^{125}I]DG-oLH
1	Fraction B	56	36
	Fraction A2	4	36
	Ratio (A2/B)	1:0.07	1:1
		[^{125}I]oFSH	[^{125}I]DG-oFSH
2	Fraction B	34	38
	Fraction A*	2	46
	Ratio (A/B)	1:0.06	1:1.2
		[^{125}I]hCG	[^{125}I]DG-hCG
3	Fraction B	40	41
	Fraction A2	5	50
	Ratio (A2/B)	1:0.125	1:1.2

with oLH. In lanes 3 and 4, containing 1 μg of fractions B and A2, the latter representing DG-oLH antibody reacted very weakly with [^{125}I]oLH compared with the intense reaction in the other lanes. Similar results were obtained with fractions derived from DG-hCG antiserum.

Thus, successive affinity chromatographic steps effected the separation of antibodies that could differentiate between agonist (oLH, hCG and oFSH) and antagonistic forms (DG-LH, DG-hCG and DG-oFSH) of the three hormones. Based on detailed competitive displacement studies we could calculate the percentage cross-reactivities using labeled agonist and antagonists and the respective purified antibodies (e.g., oLH–DG-oLH) (Table II). As similar results were obtained with hCG–DG-hCG and their antibodies also, we are able to generalize that sites in the protein core of the subunits in the quaternary structure of the hormones play a major role in contributing to the distinctive epitopes. We can also conclude that some new epitopes must have arisen after removal of antennary sugars in the N-glycosylation sites of the hormones. This conclusion is reasonable because there has been no documented evidence of nicks in polypeptide structure [15,21] of the two subunits in the hormones. Based on other detailed studies with deglycosylated
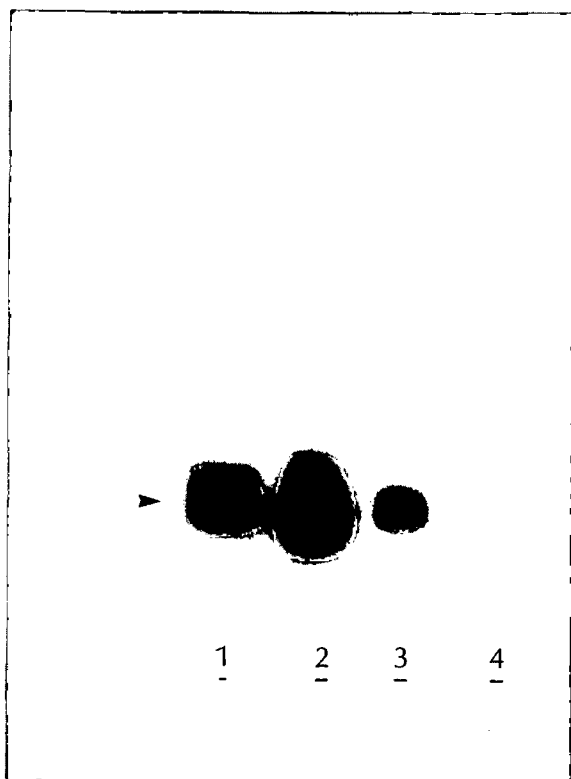
Fig. 2. Western blotting of affinity-purified oLH and DG-oLH antibodies. A 1-μg amount of the lyophilized IgG fraction was subjected to 5–15% gradient sodium dodecyl sulfate–polyacrylamide gel electrophoresis and transferred to nitrocellulose sheets. Following saturation with 1% skim milk powder, the sheet was allowed to react with $2 \cdot 10^6$ cpm of [^{125}I]oLH in 25 ml of phosphate-buffered saline (pH 7.5) for 16 h. The sheet was then washed and exposed to Kodak X-ray film for 72 h. Lanes 1 and 2 contain affinity-purified oLH IgG, lane 3 IgG of fraction B from DG-LH antiserum (Fig. 1) and lane 4 IgG of fraction A2 of DG-LH antiserum (Fig. 1). Densitometric analysis (with lane 1 as 100%) showed 181% for lane 2, 60% for lane 3 and 5% for lane 4. Arrows show migration of M_r 150 000.

subunits and preferential recombinant hormones [18], we have argued against the direct participation of peripheral sugars in generating new determinants. However, their absence has had the net effect of generating new determinants not previously present in the mature fully glycosylated hormone.

Affinity-purified antibodies are valuable in probing differences in the manner in which agonists and antagonists react with the same receptor. A striking example of such differences is shown in Table III, where we examined antigenic sites that may be available for reaction once the agonist or antagonist has already reacted with the receptor. Rat testicular membranes containing receptors for hCG/LH were first incubated with the unlabeled hormone (100 ng of hCG or DG-hCG) in separate tubes. After removal of the free hormone by centrifugation and washing, the washed H–R complex was incubated a second time with excess of purified antibodies (B or A2 in Fig. 1). A third incubation with ^{125}I-labeled protein A facilitates detection of the bound IgG in the form of an R–H–Ab–protein A* complex. In the example shown, antibody to native hCG (B) reacts with receptor-bound hCG or DG-hCG; however, DG-hCG antibodies (fraction A2) fail to recognize receptor-bound DG-hCG. We interpret these data to mean that occupation of receptor by native hormone (agonist) leaves antigenic sites available to be recognized by B-type antibodies, but when antagonist binds these same antigenic sites are still available but others, which can be recognized by antagonist antibodies, are all masked. Hence, there are distinct differences in agonist–receptor and antagonist–receptor interactions and this may be one of the underlying causes of the loss of signal transduction.

TABLE II

IMMUNOLOGICAL CROSS-REACTIVITY OF AGONISTS AND ANTAGONISTS USING AFFINITY PURIFIED IgGs

These % cross-reactivity calculations are derived from competitive displacement analyses and calculating concentration required for 50% displacement and compared to agonist or antagonist. Purified antibodies were used at 50 ng per tube.

Hormone	Assay type and % cross-reaction			
	[^{125}I]DG-LH/fraction A2	[^{125}I]DG-FSH/fraction A	[^{125}I]LH/fraction B	[^{125}I]oFSH/fraction B
oLH	0		100	
DG-LH	100		100	
oFSH		7.1		100
DG-oFSH		100		82

TABLE III

REACTION OF AFFINITY-PURIFIED ANTIBODIES WITH RECEPTOR-BOUND AGONIST OR ANTAGONIST

This experiment using rat testicular membranes as receptor (R) was performed in three parts. In the first incubation, hormone (H) binding occurs for 16 h at 22°C. During the second incubation, available antigenic sites of the receptor bound hormone react with added antibody (Ab) (10 μg) to form an R–H–Ab complex. In the third incubation, the added ^{125}I-labeled protein A detects the complex via its liaison with Ab to form R–H–Ab–protein A*. For each set, the net radioactivity found in the presence of the native hormone Ab (fraction B) was set as 100% for comparison. The experiment shows that antigenic sites of antagonist are not available (for reaction with fraction A2) once it has reacted with the receptor. (Adapted from ref. 11.)

First incubation, 16 h, 22°C	Second incubation + antibody, 2 h, 22°C	Third incubation, [125I]protein A (cpm ± S.E.M.)[a]	%
R + 100 ng hCG	Fraction B	9955 ± 694	100
R + 100 ng hCG	Fraction A2	–	0
R + 100 ng DG-hCG	Fraction B	10 753 ± 792	100
R + 100 ng DG-hCG	Fraction A2	189 ± 20	1.8

[a] S.E.M. = standard error of the mean (n = 3).

We used the fractionated antibodies in additional studies to show that only B-type IgGs are able to revive signal transduction in DG-hormones bound to cells (Table IV). In these experiments done with mouse Leydig tumor cells, progesterone production is indicative of hormone response. As in Table III, these also include multiple incubations, but in a different format. Following agonist or antagonist binding, the respective antibodies are included in the incubation and after allowing time for interaction at 4°C metabolic activity is resumed at 37°C, a temperature at which steroidogenesis will proceed. As seen in Table IV, only agonist antibodies are able to restore full steroidogenic response in DG-hCG exposed cells. It should be noted that cells incubated with DG-hCG alone or those with added

TABLE IV

ABILITY OF AFFINITY-PURIFIED ANTIBODIES TO REVIVE CELLULAR RESPONSE BY HORMONE ANTAGONIST

These experiments were done in mouse Leydig tumor cells (MA-10) growing in 24-well plates [11] with 10^5 cells per well. As in Table III, the incubations were performed in three parts. In the first the added hormone (agonist or antagonist) binds to cell membrane receptor for 1 h at 37°C. In the second incubation, the added IgG (normal or affinity-purified fraction, 10 μg each, see Fig. 1) from DG-hCG antiserum reacts for 2 h at 4°C. After a third incubation at 37°C for 2 h (total 5 h), the amount of progesterone accumulated in the medium is determined and represents a measure of response. Note that DG-hCG by itself is inactive (only 3%), but in the presence of fraction B antibody almost complete revival occurs. In treatment 5, when hCG has already initiated action, the addition of fraction B has no diminishing effect. (Adapted from ref. 11.)

Control	Progesterone per well in 5 h (ng)[a]	Response (%) (revival)
(1) Basal (no hormone)	0.15 ± 0.02	
(2) Antibody fraction	0.20 ± 0.03	
(3) 10 ng hCG + 10 μg normal IgG	134.50 ± 4.1	100
(4) 10 ng DG-hCG + 10 μg normal IgG	4.5 ± 0.20	3
(5) 10 ng hCG + fraction B IgG	110.4 ± 3.30	82
(6) 10 ng DG-hCG + fraction B IgG	111.40 ± 4.10	(83)
(7) 10 ng DG-hCG + fraction A2 IgG	2.30 ± 0.30	(1.7)

[a] Mean values ± S.E.M. (n = 3).

normal non-immune IgG also do not cause progesterone accumulation in the medium. We infer that the anchoring of agonist antibodies on the receptor-bound antagonist (DG-hCG) has substituted for the loss of antennary sugars and that this in turn altered the orientation of the hormone–receptor complex for productive coupling to the effector system inside the cell [11]. Others also have made similar if not identical observations [16,23].

In conclusion, the exercise of separating gonadotropin agonist and antagonist antibodies by affinity chromatography has shown that peripheral glycosylation has an effect on the conformation of biologically active proteins. As many substances of therapeutic value produced by biotechnology are glycosylated, due consideration must be given to the extent of glycosylation of the product produced in different cellular systems. For example, a chosen mammalian cell for the production of a therapeutically active substance such as erythropoietin produced molecules which differed in their antennary oligosaccharides with biological activity being proportional to the ratios of the different structures [24]. Because the presence or absence of peripheral sugar residues could also alter the antigenicity of the protein, it is best to choose a system which yields antennary carbohydrates as close as possible to the natural product. Even in normal physiology, as shown in the example of glycoprotein hormones, glycosylation patterns could vary, reflecting differences in biological potency [11,25].

REFERENCES

1 C. H. Li, D. Chung, D. Yamashiro and C. Y. Lee, *Proc. Natl. Acad. Sci. U.S.A.*, 75 (1978) 4306.
2 C. Y. Lee, M. McPherson, V. Licko and J. Ramachandran, *Arch. Biochem. Biophys.*, 201 (1980) 411.
3 A. Gertler, A. Shamay, N. Cohen, A. Ashkenazi, H. G. Friesen, A. Levanon, M. Gorecki, H. Aviv, D. Hadary and T. Vogel, *Endocrinology*, 118 (1986) 720.
4 A. Ashkenazi, T. Vogel, I. Barash, D. Hadari, A. Levanon, M. Gorecki and A. Gertler, *Endocrinology*, 121 (1987) 414.
5 U. J. Lewis, L. J. Lewis, M. A. M. Salem, N. R. Stalen, S. S. Galosy and G. G. Krivi, *Mol. Cell. Endocrinol.*, 78 (1991) 45.
6 L. Joshi and B. D. Weintraub, *Endocrinology*, 113 (1983) 2145.
7 M. Matzuk and I. Boime, *Biol. Reprod.*, 40 (1989) 48.
8 R. K. Campbell, D. M. Dean-Emig and W. R. Moyle, *Proc. Natl. Acad. Sci. U.S.A.*, 88 (1991) 760.
9 M. R. Sairam, in C. H. Li (Editor), *Hormonal Proteins and Peptides*, Vol. 11, Academic Press, New York, 1983, p. 1.
10 R. J. Ryan, M. C. Charlesworth, D. J. McGormick, R. P. Milius and H. T. Keutmann, *FASEB J.*, 2 (1988) 2661.
11 M. R. Sairam, *FASEB J.*, 3 (1989) 1915.
12 N. K. Kalyan and O. P. Bahl, *J. Biol. Chem.*, 258 (1983) 67.
13 M. Matzuk, J. L. Keene and I. Boime, *J. Biol. Chem.*, 264 (1989) 2409.
14 W. K. Liu, J. D. Young and D. N. Ward, *Mol. Cell. Endocrinol.*, 37 (1984) 29.
15 H. T. Keutmann, L. Johnson and R. J. Ryan, *FEBS Lett.*, 185 (1985) 333.
16 R. V. Rebois and M. T. Liss, *J. Biol. Chem.*, 262 (1987) 3891.
17 M. R. Sairam, J. Linggen and G. N. Bhargavi, *Biosci. Rep.*, 8 (1988) 271.
18 M. R. Sairam, J. Linggen, J. Sairam and G. N. Bhargavi, *Biochem. Cell. Biol.*, 68 (1990) 889.
19 L. Lamarre and M. R. Sairam, *Mol. Cell. Endocrinol.*, 66 (1989) 181.
20 M. J. Papandreou, I. Sergi, G. Medri, C. L. Jullie, J. M. Braun, C. Canonne and C. Ronin, *Mol. Cell. Endocrinol.*, 78 (1991) 137.
21 P. Manjunath and M. R. Sairam, *Methods Enzymol.*, 109 (1985) 725.
22 M. R. Sairam and J. Porath, *Biochem, Biophys. Res. Commun.*, 69 (1976) 190.
23 M. Hattori, T. Hachisu, Y. Shimohigashi and K. Wakabayashi, *Mol. Cell. Endocrinol.*, 57 (1988) 17.
24 A. Kobata, in *15th International Congress of Biochemistry, Jerusalem, 1991*, p. 307.
25 C. A. Wilson, A. J. Leigh and A. J. Chapman, *J. Endocrinol.*, 125 (1990) 3.

Isolation and characterization of catalase from *Penicillium chrysogenum*

Grigory S. Chaga☆, Anders S. Medin, Simeon G. Chaga☆ and Jerker O. Porath

Institute of Biochemistry, Uppsala University, Box 576, S-751 23 Uppsala; and Biochemical Separation Centre, Uppsala University, Box 577, S-751 23 Uppsala (Sweden)

ABSTRACT

Catalase from a crude preparation of *Penicillium chrysogenum* was isolated in a single chromatographic step by immobilized metal ion affinity chromatography (IMAC) on Cu(II)–Chelating Sepharose Fast Flow. A chromatographically and electrophoretically homogeneous enzyme was obtained in 89% yield. IMAC was found to be superior to ion-exchange, hydrophobic interaction, size-exclusion and concanavalin A affinity chromatography. Analytical and preparative chromatography gave essentially the same chromatograms. Isoelectric point, molecular weight (by ultracentrifugation), amino acid composition, carbohydrate content and subunit organization were determined. The apparent Michaelis–Menten constant, K_M, and the azide competitor constant, K_i, were calculated and found to be 59 μM and 6.1 μM, respectively.

INTRODUCTION

Catalase is a key enzyme in all aerobic cells and the enzyme from various sources is widely used in biochemical and bioindustrial processes. Cultural liquid from *Penicillium chrysogenum* is reported to be a suitable source for industrial production of catalase combining the high output of biosynthesis, up to 8000 U/ml cultural liquid or 400 U/mg protein, with excretion of the enzyme into the medium. Chaga *et al.* [1–3] investigated the biosynthesis and the partial purification of this catalase, but little has been published on its purification and characterization.

In a previous paper [4], we showed that immobilized metal ion affinity chromatography (IMAC) can be used as a simple, yet highly efficient, method for the purification of animal enzymes. On an industrial scale, however, microbial sources of enzymes are preferable to animal sources, so purification techniques with a high capacity and selectivity for enzymes from bacteria, yeasts and moulds are required. With this in mind, we investigated the purification of catalase from *P. chrysogenum*.

EXPERIMENTAL

Starting material

The crude enzyme was prepared according to the methods of Chaga [2,3]. Ultrafiltration of the culture liquid was followed by "negative adsorption" using a complex of $CuSO_4$ and $K_4Fe(CN)_6$ and the crude enzyme was precipitated with $(NH_4)_2SO_4$ and isopropanol. The final precipitate was desalted and lyophilized.

Preliminary studies

Preliminary studies involving chromatography of the catalase on ion-exchange chromatographic (IEC), hydrophobic interaction chromatographic (HIC), size-exclusion chromatographic (SEC), IMAC and biospecific concanavalin A (Con A)–Sepharose columns. Only IMAC showed promise for one-step purification.

Correspondence to: Dr. J. O. Porath, Biochemical Separation Centre, Uppsala University, Box 577, S-751 23 Uppsala, Sweden.
☆ Permanent address: Institute for Bioproducts, Plovdiv, Bulgaria.

Purification procedure

Columns for IMAC (analytical, 1.6 × 0.9 cm I.D., and preparative, 5 × 3.2 cm I.D.) were prepared by pouring in degassed slurries in deionized water of Chelating Sepharose Fast Flow (Pharmacia–LKB Biotechnology, Uppsala, Sweden) and the gel beds were settled by opening of the outlets. The gels were charged with four bed volumes of 20 mM CuSO$_4$ solution. Excess copper ions were removed by washing with deionized water. The columns were equilibrated with ten bed volumes of 50 mM sodium phosphate buffer (pH 7.3) containing 1 M NaCl. For the analytical protocol 25 mg of lyophilized crude enzyme were dissolved in 5 ml of the equilibration buffer and for the preparative protocol 1 g of the crude enzyme was dissolved in 100 ml of the buffer. The samples were applied to the columns and the non-adsorbed material was removed by washing with the equilibration buffer. The columns were washed with 50 mM sodium phosphate–0.5 M NaCl (pH 6.0), then the catalase eluted with 20 mM sodium acetate (pH 5.5). Finally, the columns were washed with 50 mM sodium phosphate–1.0 M NaCl (pH 7.3) containing 0.2 M imidazole. Flow-rates of 0.5 and 8 ml/min, respectively, were kept constant throughout the analytical and preparative procedures.

The relative protein concentration was monitored by detection of the absorbance at 280 nm utilizing a Model 2238 Uvicord SII and recorded on a Model 2210 recorder (Pharmacia–LKB Biotechnology). During the analytical run 2-ml fractions were collected.

Assay for catalase activity

The catalase activity was determined according to the method described by Beers and Sizer [5]. The method is based on the determination of the rate of disappearance of H$_2$O$_2$, as measured at 240 nm. Both a Pye Unicam Model 8700 UV–VIS and an LKB Ultrospec II spectrophotometer were used for these assays.

Purity index

A purity index, R_z, the ratio of the absorbances at 405 and 280 nm ($R_z = A_{405}/A_{280}$), was used as an indicator of the purity of the enzyme in solution [6,7].

Tests for homogeneity

Chromatography. The purified enzyme was analysed for homogeneity by IEC on a Mono Q HR5/5 column and by SEC on a Superose 6 column (Pharmacia–LKB Biotechnology).

Electrophoresis. Electrophoretic assays were performed with Phast System (Pharmacia–LKB Biotechnology on Phast Gel gradient 8–25 using Phast Gel sodium dodecyl sulphate (SDS) and native buffer strips according to the manufacturer's instructions.

Characterization of the enzyme properties

Amino acid analysis. The amino acid composition and content of glucosamine were determined after hydrolysis in 6 M HCl for 24 and 68 h. Cysteic acid was determined after oxidation with performic acid.

N-Terminal sequence analysis. The N-terminal sequence analysis was performed according to Edman [8] on a solid-phase sequenator.

Carbohydrate analysis. The total neutral sugar content was determined by the phenol–sulphuric acid method [9] using D-mannose as a standard. The composition of the neutral sugars was determined according to Theander and Westerlund [10]. The hydrolysis with trichloroacetic acid was performed at 121°C for 90 min instead of 90°C for 16 h.

Molecular weight determination. The molecular weight of the enzyme was determined by a sedimentation experiment in an MSE ultracentrifuge, analytical model, at 7500 rpm in equilibrium medium, 0.2 M sodium acetate–0.04 M acetic acid, for 72 h.

Inhibition of catalase with sodium azide. The azide competitor constant, K_i, of NaN$_3$ as an inhibitor of the *P. Chrysogenum* catalase was determined spectrophotometrically by the method of Dixon and Webb [11].

Determination of isoelectric point. The isoelectric point of the enzyme was determined by isoelectric focusing (IEF) and by chromatofocusing. IEF was performed with Phast System using Phast Gel IEF 3–9, according to manufacturer's instructions. The chromatofocusing was performed on PBE 94 gel (Pharmacia–LKB Biotechnology). A 6.5 × 0.5 cm I.D. column filled with PBE 94 was equilibrated with 25 mM piperazine–HCl (pH 5.5). A sample of *ca.* 0.5 mg of enzyme in 0.5 ml of the equilibration buffer was loaded on to the column. After washing with three column volumes of the equilibration

buffer, a pH gradient was formed with Polybuffer 74 (Pharmacia–LKB Biotechnology) diluted tenfold at a flow-rate of 9 ml/h.

RESULTS AND DISCUSSION

Purification

In previous studies elaborate schemes were used for the purification of this enzyme. Eriksson *et al.* [12] used high-performance methods including high-performance IEC on diethylaminohydroxypropyl–agarose gel [13] and high-performance HIC on pentyl–agarose gel [14]. The final recovery was 72%; the purity factor was not reported.

In order to develop a purification procedure feasible for large-scale isolation, preliminary investiga-

tions on SEC, IEC, HIC and affinity chromatography on Con A–Sepharose were carried out. In contrast to IMAC on Cu^{2+}–Chelating Sepharose Fast Flow these methods could not achieve a one-step isolation of the enzyme, nor could they improve the purification of catalase after IMAC. Chromatography of the enzyme on Cu^{2+}–Chelating Sepharose Fast Flow (Fig. 1a and b) was promising from the initial studies and by optimizing the conditions a protocol which gave a high-purity catalase in good yields was obtained.

In Cu(II)–IMAC, imidazole is frequently used for desorption of proteins [15] but in this instance proved to be unsatisfactory, giving a purity index of less than 0.6. This did not increase after desalting or dialysis against deionized water, indicating some kind of interaction between the enzyme and imidazole. It is known that protein adsorption to chelated metal ions, such as Cu^{2+}, Zn^{2+} and Ni^{2+}, is quantitatively dependent on the type of salt and concentration [16] and also the pH, and in this instance both the salt concentration and pH were changed simultaneously. High purity was achieved only with a stepwise decrease in these parameters.

The purification of the *P. chrysogenum* catalase is presented in Fig. 1. Much of the protein from the crude preparation was eluted in the equilibration buffer, but washing with 50 m*M* sodium phosphate–0.5 *M* sodium chloride (pH 6.0) was necessary to remove the contaminants. When applied in this buffer, however the catalase was only adsorbed in low amounts. The catalase-containing fraction was desorbed from the column by lowering the pH and ionic strength simultaneously to 20 m*M* sodium acetate (pH 5.5). The Cu(II) adsorbent was regenerated by washing with 50 m*M* sodium phosphate–1.0 *M* sodium chloride (pH 7.3) containing 0.2 *M* imidazole, which removed impurities and remaining catalase. Finally, the adsorbent was depleted of Cu^{2+} ions by washing with 0.2 *M* EDTA solution (pH 7.0). This protocol was used for both the analytical and the preparative runs (Fig. 1a and b). The catalase specific activity was determined and similar results were obtained for both runs (Table I).

The purity index of the enzyme in water was calculated to be 1.04 and the homogeneity of the material in peak III (Fig. 1a and b) was analysed by IEC on Mono Q and SEC on Superose 6 (Fig. 2a and b).
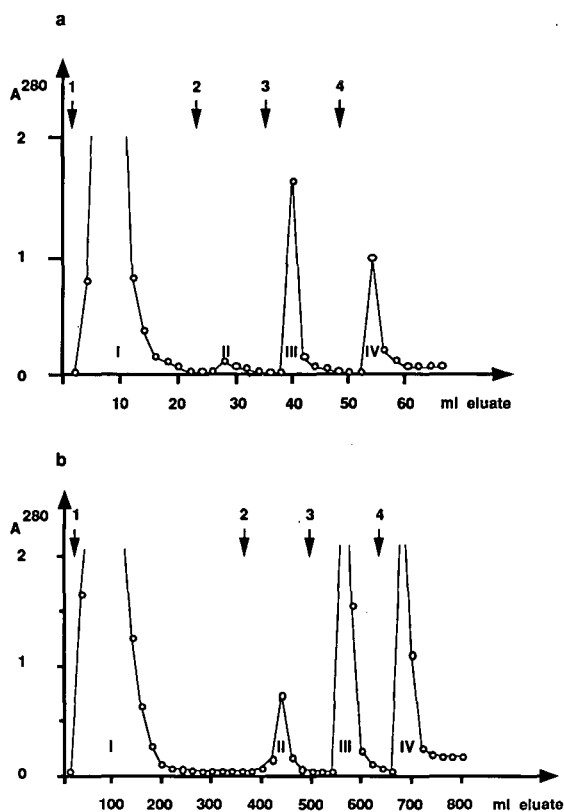

Fig. 1. Chromatography of crude preparation of catalase from *Penicillium chrysogenum* on Chelating Sepharose Fast Flow–Cu^{2+}. 1 = 50 m*M* $NaPO_4$–1 *M* NaCl (pH 7.3); 2 = 50 m*M* $NaPO_4$–0.5 *M* NaCl (pH 6.0); 3 = 20 m*M* sodium acetate (pH 5.5); 4 = 50 m*M* sodium phosphate–1 *M* NaCl–0.2 *M* imidazole (pH 7.3). (a) Analytical run; (b) preparative run.

TABLE I

RECOVERY OF CATALASE ACTIVITIES IN ANALYTICAL AND PREPARATIVE CHROMATOGRAPHY EXPRESSED AS A PERCENTAGE OF APPLIED ACTIVITY

Peak No.	Analytical run	Preparative run
I	0	0
II	1.5	1
III	93	89
IV	4	7

Gel electrophoresis was performed with the Phast System and showed a single band. The molecular weight was calculated to be 280 000 (Fig. 3).

The capacity of Cu^{2+}–Chelating Sepharose Fast Flow to adsorb catalase from the crude preparation was determined by frontal analysis according to ref. 17. The crude enzyme in equilibration buffer was fed into the column and the eluate was analysed for catalase activity. The dynamic binding capacity is given by $C(V_M - V_0)$, where C is the concentration of enzyme, 1.5 mg/ml, in the crude mixture, 7–8 mg protein/ml, and V_M and V_0 are the breakthrough
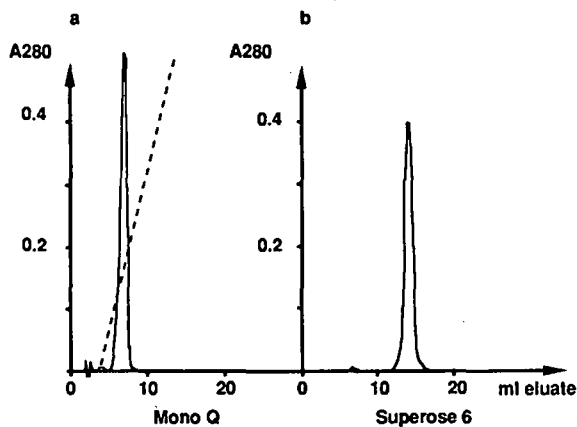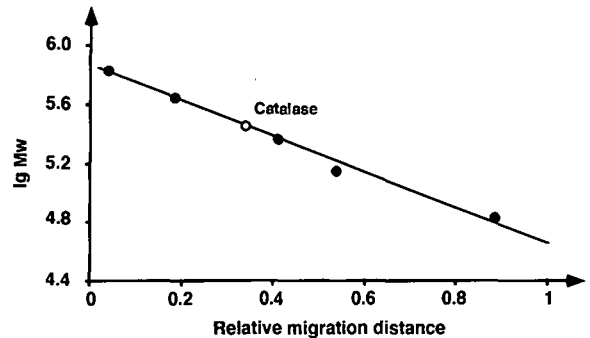

Fig. 3. Electrophoresis of the purified native catalase on Phast Gel gradient 8–25. Filled circles, represent calibration proteins, HMW-kit (Pharmacia-LKB Biotechnology). lg Mw = log molecular weight.

elution volumes of the enzyme in the presence and absence of metal ions, respectively. The capacity for binding of catalase from P. chrysogenum in a crude preparation was calculated to be 7.0 mg per ml of Cu^{2+}–Chelating Sepharose Fast Flow.

The catalase from P. chrysogenum was purified in a single step from crude material with a specific activity of 6500 U/mg protein to an electrophoretically homogeneous preparation with a specific activity of 35 000 U/mg. The recovery was higher than 85% (Table I), which demonstrates the high capacity and resolution of IMAC.

Characterization

The amino acid and carbohydrate compositions of P. chrysogenum catalase in comparison with two other fungal catalases are presented in Table II. The amino acid composition of the enzyme differs significantly from these reported for Aspergillus niger and Penicillium vitale catalases [6,18,19] (Table II). P. chrysogenum catalase contains a smaller number of the neutral amino acids glycine and alanine but more of the aromatic amino acids phenylalanine and tryptophan. There is also a considerable difference in carbohydrate composition between these catalases. Thus catalase from A. niger is reported to have a total carbohydrate content of 10.2% (w/w) [6], the enzyme from P. vitale to have 8.2% (w/w) [19] whereas the content of the P. chrysogenum enzyme was determined to be 8.5% (w/w). The carbohydrate composition differs qualitatively in that A. niger is lacking galactose and P. vitale lacks glucose residues, but P. chrysogenum catalase contains both

Fig. 2. (a) Chromatography of catalase (peak III from Fig. 1) on Mono Q HR 5/5. A 500-μl sample (ca. 1 mg of enzyme) in 20 mM Tris-HCl (pH 7.5) was applied to the column. The enzyme was eluted in a linear gradient of NaCl from 0 to 0.8 M at a flow-rate of 1.0 ml/min. (b) Chromatography of catalase (peak III from Fig. 1) on Superose 6, HR 10/30. A 200-μl sample (ca. 0.7 mg of enzyme) in 20 mM Tris-HCl–0.1 M NaCl (pH 7.5) was applied to the column. The enzyme was chromatographed at a flow-rate of 0.2 ml/min.

TABLE II

AMINO ACID AND CARBOHYDRATE COMPOSITIONS
OF CATALASES FROM DIFFERENT FUNGI

Component	Percentage of MW		
	Penicillium chrysogenum	*Penicillium vitale* [18]	*Aspergillus niger* [5,17][c]
Residue			
Aspartic acid	11.0	11.9	9.87
Glutamic acid	11.5	11.6	7.63
Proline	3.8	–	5.84
Glycine	4.1	10.0	6.65
Alanine	5.8	9.30	7.99
Valine	5.3	5.25	5.39
Methionine	1.3	1.14	1.62
Isoleucine	3.5	3.76	3.23
Leucine	7.1	7.65	5.66
Tyrosine	2.2	1.78	3.23
Phenylalanine	8.6	8.16	5.39
Lysine	4.8	4.48	5.03
Histidine	2.6	2.15	2.16
Arginine	6.5	5.31	3.95
Cysteine	0.14		1.53
Threonine	5.4	7.07	6.29
Serine	5.5	5.68	8.26
Tryptophan	2.2[a]	–[b]	–
Carbohydrate			
Mannose	6.8	+	8.1
Galactose	0.9	+	
Glucose	0.2	–	0.2
Glycosamine	0.6	+	1.9

[a] Calculated.
[b] – indicates the absence of this monosaccharide residue in the glycoprotein; + indicates the presence of this monosaccharide.
[c] Calculated from data given in ref. 17, using an MW of 385 000 [5].

glucose and galactose. The sequence of the last twenty amino acid residues at the N-terminus of the enzyme was determined and is reported in comparison with the N-terminal sequence of catalase from *P. vitale* in Table III [20].

TABLE III

AMINO ACID SEQUENCES OF CATALASES FROM *P. CHRYSOGENUM* AND *P. VITALE*

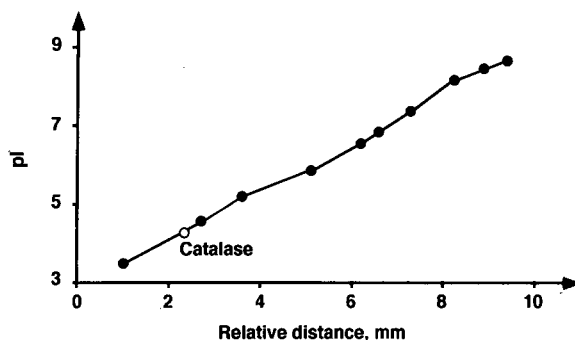| Source	Amino acid sequence (N-terminal)
P. chrysogenum	TEEFLS Q FYL NDQDVYLTS D
P. vitale	AAAQRRQNDS S VFLA IMVAA

Fig. 4. Isoelectric focusing of the purified catalase on Phast Gel IEF 3–9. Filled circles represent calibration proteins, p*I* markers (Pharmacia-LKB Biotechnology).

Gel electrophoresis performed on Phast Gel gradient 8–25 revealed only one band with silver staining. The molecular weight was found to be 280 000 (Fig. 3). For a more precise determination of the molecular weight a sedimentation equilibrium experiment in the ultracentrifuge was performed. The partial specific volume was calculated according to ref. 21 to be 0.718 and the molecular weight for the enzyme was calculated to be 280 000, confirming the value found by gel electrophoresis.

The determination of the isoelectric point for this catalase was performed by IEF on the Phast System and chromatofocusing and showed good agreement, with p*I* values of 4.3 and 4.2, respectively (Figs. 4 and 5).
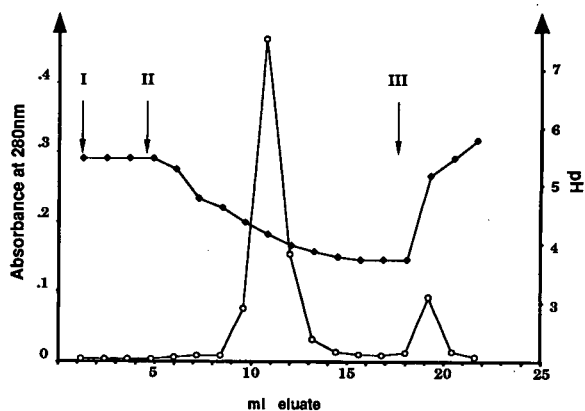

Fig. 5. Chromatofocusing of the purified catalase on PBE 94 with Polybuffer 74. I = 25 m*M* piperazine–HCl (pH 5.5); II = Polybuffer–HCl diluted tenfold (pH 4.0); III = 25 m*M* piperazine–HCl (pH 5.5) containing 1 *M* NaCl.
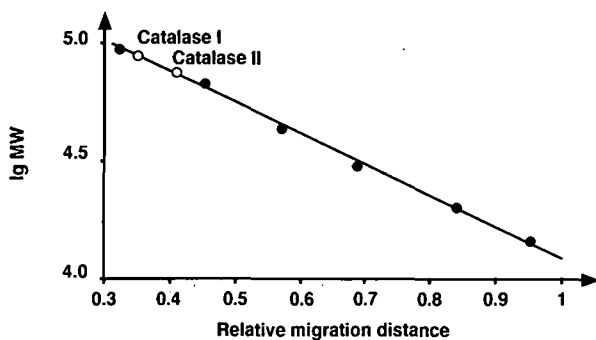
Fig. 6. SDS electrophoresis of the purified catalase on Phast Gel gradient 8–25 and SDS buffer strips. Lanes: 1 = LMW-kit (Pharmacia–LKB Biotechnology); 2 = purified enzyme. Filled circles represent calibration proteins, LMW-kit (Pharmacia–LKB Biotechnology).

The subunit organization of the enzyme was investigated by SDS electrophoresis with Phast System on Phast Gel gradient 8–25. The results confirmed those published in ref. 12 (Fig. 6). The presence of two different subunits (Fig. 6) is an interesting phenomenon also reported for a catalase from the bacterium *Vitreoscilla* [22]. This is distinctly different from *A. niger* and *P. vitale* catalases, which consists of four identical subunits [18,19]. This could be interpreted as an impure enzyme preparation, but all attempts to increase the purity of the enzyme did not improve the result as judged from electrophoresis of the native enzyme (electrophoresis run with sample overloading). Moreover, when the enzyme was studied for its stability against denaturation as in the pretreatment of samples for
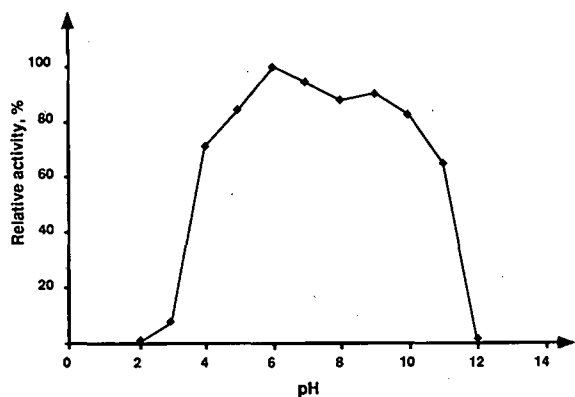

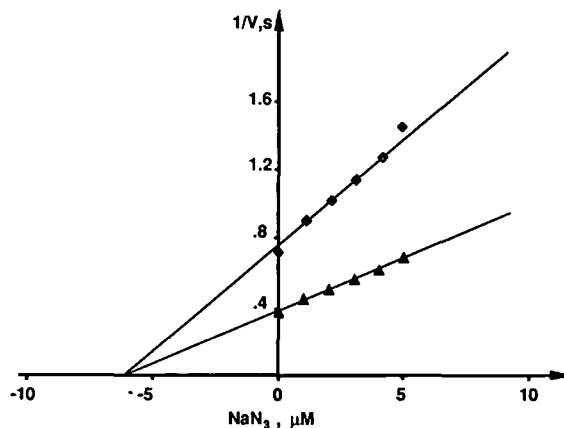Fig. 8. Dixon plot of the inhibition of catalase from *P. chrysogenum* with NaN_3 performed in 0.1 M sodium phosphate buffer, pH 6.5, at substrate concentrations: ◆ = 10 mM H_2O_2; ▲ = 20 mM H_2O_2.

SDS electrophoresis, the enzyme was found to remain in its native state even after treatment at 60°C in a solution containing 1% of SDS and 2.5% of 2-mercaptoethanol (not shown).

The apparent Michaelis–Menten constant, K_M, of the enzyme was calculated to be 59 mM H_2O_2. The enzyme was found to be active in a broad range of pH from 3.5 to 11.0 with an optimum of 6.0 (Fig. 7). The specific activity of the *P. chrysogenum* catalase was calculated to be 35 000 U/mg protein at an H_2O_2 concentration of 18 mM. The inhibition effect of sodium azide as investigated according to Dixon and Webb [11] for two different concentrations of substrate (Fig. 8) indicates that the azide is a non-competitive inhibitor of *P. chrysogenum* catalase with K_i = 6.1 mM. UV–VIS spectra were run and showed a typical high-spin iron(III) haeme spectrum with absorption maxima at 405 nm. The
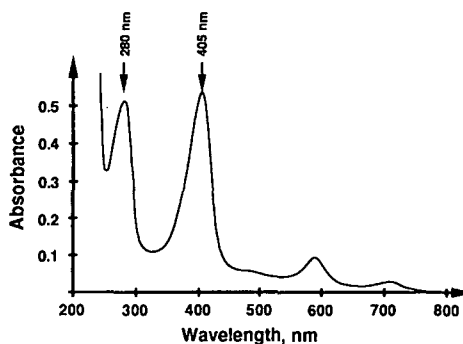

Fig. 7. pH optimum of catalase. Relative activity (% of maximum activity) *versus* pH.

Fig. 9. UV–VIS spectrum of catalase from *Penicillium chrysogenum*.

TABLE IV

COMPARISON OF PROPERTIES OF CATALASES FROM DIFFERENT FUNGI

Species	pI	MW	Subunit composition	R_z	K_M, H_2O_2 (mM)	K_i, NaN$_3$ (mM)	Specific activity (U/mg)
Penicillium chrysogenum	4.3	280 000	$\alpha_2\beta_2$	1.05	59	6.1	35000
Aspergillus niger [6,17]	6.5	385 000	α_4	0.8	280	475	8500[a]
Cilindrocarpon didymum [24]	5.5	215 000	–	–	–	–	1500

[a] Data from Merck.

purity factor, R_z (UV–VIS spectrum in Fig. 9), being the relationship between absorbances at 405 nm (haeme group) and 280 nm (mainly tryptophan), was found to be 1.04.

A comparison of the properties of catalases from bacteria, fungi, plants and animals showed that the molecular size and subunit organization are similar. The catalases are large enzymes with molecular weights ranging from 200 000 to 400 000 and containing four subunits, with the exceptions of an enzyme from *Klebsiella pneumoniae* [23], with two subunits, and from porcine erythrocytes [7], reported to be a dimeric form of the enzyme with eight subunits. The efficiencies of the enzymes differ so that the specific activities vary from 1500 U/mg for the fungus *Cilindrocarpon didymum* enzyme [24] 68 100 U/mg for the enzyme from *Bacillus subtilis* [25,26]. Also the K_M and K_i (NaN$_3$) values vary considerably. *P. chrysogenum* catalase is in the middle of the range for most of the variables investigated. It is, however, the most acidic enzyme of the reported catalases (pI = 4.3). A comparison of the properties of catalases from fungi is given in Table IV.

We conclude that *P. chrysogenum* culture liquid is an excellent source for the production of catalase. This enzyme has a higher specific activity than other commercially available catalases from bovine liver or *A. niger* culture medium. The isolation procedure reported here gives stable enzyme preparations with purity >99%.

REFERENCES

1 S. Chaga, T. Sapundzieva and A. Kraevska, *Khranit. Promst. Nauka*, 3 (1987) 75–78.
2 S. Chaga, *Tr. Nauchno-Issled. Inst. Konserv. Prom. Plovdiv*, 8 (1971) 105–113.
3 S. Chaga, personal communication, 1975.
4 G. Chaga, L. Andersson, B. Ersson and J. Porath, *J. Biotechnol. Appl. Biochem.*, 11 (1989) 424–431.
5 R. F. Beers and I. W. Sizer, *J. Biol. Chem.*, 195 (1952) 133–140.
6 K. Kikushi-Torii, S. Hayashi, H. Nanamoto and S. Nakamura, *J. Biochem.*, 92 (1982) 1449–1456.
7 A. Takeda and T. Samejma, *J. Biochem.*, 82 (1977) 1025–1033.
8 P. Edman and G. Begg, *Eur. J. Biochem.*, 1 (1967) 80–91.
9 M. Dubois, K. A. Gilles, J. K. Hamilton, P. A. Reber and F. Smith, *Anal. Biochem.*, 28 (1956) 350–356.
10 O. Theander and E. Westerlund, *J. Agric. Food Chem.*, 34 (1986) 133–140.
11 M. Dixon and E. Webb, in *Enzymes*, Academic Press, New York, 3rd ed., 1979.
12 K.-O. Eriksson, I. Kourtera, K. Yao, J.-L. Liao, F. Kilár, S. Hjertén and G. Chaga, *J. Chromatogr.*, 397 (1987) 239–249.
13 K. Yao and S. Hjertén, *J. Chromatogr.*, 385 (1987) 87.
14 S. Hjertén, K. Yao, K.-O. Eriksson and B. Johansson, *J. Chromatogr.*, 359 (1986) 99.
15 L. Andersson, E. Sulkowsky and J. Porath, *Bioseparation*, 2 (1991) 15–22.
16 J. Porath and B. Olin, *Biochemistry*, 22 (1983) 1621–1630.
17 N. Ramadan and J. Porath, *J. Biochem.*, 321 (1985) 93–104.
18 A. Gruft, R. Ruan and J. Traunor, *Can. J. Biochem.*, 56 (1978) 916–919.
19 L. V. Gudkova, M. F. Guliy, R. T. Degtjar and O. V. Pisarevich, *Ukr. Biokhim. Zh.*, 57 (1985) 29.
20 B. K. Vainshtein, W. R. Melik-Adamyan, V. V. Barynin, K. S. Bartels, I. Fita and M. G. Rossmann, *J. Mol. Biol.*, 188 (1986) 49–61.
21 E. Cohen and J. Edsall (Editors), *Amino Acids and Peptides as Ions and Dipolar Ions*, Rheinold, New York, 1943.
22 J. J. Abrams and D. A. Webster, *Arch. Biochem. Biophys.*, 279 (1990) 54–59.
23 I. Goldberg and A. Hochman, *Biochim. Biophys. Acta*, 991 (1989) 330–336.
24 S. Lartillot, P. Kedziora and A. Athias, *Prep. Biochem.*, 18 (1988) 241–246.
25 P. C. Loewen and J. Switala, *Biochem. Cell Biol.*, 65 (1987) 939–947.
26 P. C. Loewen and J. Switala, *Biochem. Cell Biol.*, 66 (1988) 707–714.

END OF SPECIAL ISSUE

NEWS SECTION

SYMPOSIUM PROGRAMME

BIOCHEMICAL SEPARATION TECHNOL-
OGY (PAPERS PRESENTED AT THE HONOR-
ARY SYMPOSIUM ON THE OCCASION OF
THE 70TH BIRTHDAY OF JERKER O. POR-
ATH, UPPSALA, JUNE 16–19, 1991)

Sunday, June 16, 1991

Welcome and Information (J.-C. Janson, Uppsala,
Sweden)

Unified in separation — A tribute to Jerker Porath
and the Uppsala School of Biochemistry (K.D.
Caldwell, Salt Lake City, UT, USA)

Separated or united — What are the social responsi-
bilities of scientists (B. von Hofsten, Uppsala,
Sweden)

Monday, June 17, 1991

*Session 1: Separation technologies (Chairman:
T. Takagi)*

New polymer gels for separation (P. Flodin, Gothen-
burg, Sweden)

Displacement chromatography: concepts, tools and
impediments (Cs. Horváth, New Haven, CT,
USA)

New separation techniques: molecular imprinting
and bio-imprinting (K. Mosbach, Lund, Sweden)

*Session 2: Separation technologies (continued)
(Chairman: P. Flodin)*

High-performance electrophoretic light scattering:
towards the development of a modern version of
the Tiselius apparatus (T. Takagi, Osaka, Japan)

A general mathematical approach to study phenome-
na which can be described by a special class of
functions, exemplified by applications in chroma-
tography and electrophoresis (S. Hjertén, Uppsa-
la, Sweden)

Studies of plant organelles using partition in aqueous
two-phase systems (B. Andersson, Stockholm,
Sweden)

Poster session

*Session 3: Separation technologies (continued)
(Chairman: K. Mosbach)*

The evolution of stationary phase design: chemical or
natural selections (T.W. Hutchens, Houston, TX,
USA)

Water-soluble biospecific polymers for new affinity
purification techniques (P. Hubert, Nancy,
France)

Flow field-flow fractionation in hollow fibers (J.-Å.
Jönsson, Lund, Sweden)

High-performance hydroxyapatite chromatography
of proteins in complex with sodium dodecyl sul-
phate (P. Lundahl, Uppsala, Sweden)

Poster session

Session 4: Separation and purification (Chairman: S. Hjertén)

Chiral separations on cellulose in aqueous solvents (M. Lederer, Lausanne, Switzerland)

Immobilized haemoglobin in the purification of haemoglobin-based blood substitutes (E. Chiancone, Rome, Italy)

Interactions of immobilized histidine with human immunoglobulin G; mechanistic and kinetic aspects (M.A. Vijayalakshmi (Compiegne, France)

RNA polymerase B — General transcription factors: purification, cloning, expression (J.-M. Egly, Strasbourg, France)

Tuesday, June 18, 1991

Session 5: Protein structure-function (Chairman: M.R. Sairam)

Avidin–biotin: structure–function (M. Wilchek, Rehovot, Israel)

Structure–function relationships in human carbonic anhydrase II as studied by site-specific mutagenesis (S. Lindskog, Umeå, Sweden)

Lipopolysaccharide-binding proteins (H. Bennich, Uppsala, Sweden)

Protein interactions with colloidal substrates as viewed by field-flow fractionation (K.D. Caldwell, Salt Lake City, UT, USA)

Poster Session

Session 6: Protein structure–function (continued) (Chairman: M. Wilchek)

The structural and functional organization of gonadotropic hormones and their receptors (M.R. Sairam, Montreal, Canada)

POMC ConYertaseS for ACTH and β-endorphin (M. Chretien, Montreal, Canada)

Protein Engineering of glutathion transferase (B. Mannervik, Uppsala, Sweden)

How does one tRNA-modifying enzyme recognize a specific subset of tRNA species (K. Stråby, Umeå, Sweden)

Session 7: Miscellaneous (Chairman: H. Bennich)

Run away — Replication plasmids as tools to produce large quantities of proteins from cloned genes (K. Nordström, Uppsala, Sweden)

Cytochrome c oxidase as a redox-driven proton pump (B. Malmström, Gothenburg, Sweden)

Mass spectrometry studies of C_{60} (B. Sundquist, Uppsala, Sweden)

The complexity of protein evolution (L. Ryden, Uppsala, Sweden)

Wednesday, June 19, 1991

Session 8: IMAC — Technologies and applications (Chairman: J. Porath)

IMAC of proteins, an update (E. Sulkowski, Buffalo, USA)

Chelated ferric ions: prospects, limitations (G. Muszynska, Warsaw, Poland)

IMAC and the ferric ion — a hard one (L. Andersson, Uppsala, Sweden)

IMAC purification of synthetic peptides (G. Lindeberg, Uppsala, Sweden)

Poster session

Session 9: Industrial applications etc. (Chairman: Cs. Horváth)

Sophisticated separation science — a prerequisite for high-quality protein pharmaceuticals (L. Fryklund, Stockholm, Sweden)

Affinity chromatography in plasma protein fractionation (R. Eketorp, Stockholm, Sweden)

Purification of recombinant human interferon-γ from the inclusion bodies of transformed *E. coli* cells (M. Belew, Uppsala, Sweden)

Thiophilic interaction chromatography of sweet potato β-amylase (F. Batista-Viera, Montevideo, Uruquay)

Poster session

Session 10: Separation and purification (continued) (Chairman: M. Lederer)

Recycling isoelectric focusing: use of simple buffers (M. Bier, Tucson, AZ, USA)

The purification of an anti-ageing enzyme (J.-L. Ochoa, La Pas, Mexico)

Coupling of chelating agents to proteins: synthesis and characterization of insulin–diethylenetriaminepentaacetic acid conjugates (F. Maisano, Milan, Italy)

Purification of recombinant HIV-l reversed transcriptase (R. Bikhabhai, Uppsala, Sweden)

Closing remarks

POSTERS

Optimization of chiral separations on cellulase (CBH 1) silica (I. Marle, S. Jönsson, C. Pettersson, P. Erlandsson, L. Hansson, R. Isaksson and G. Pettersson, Uppsala and Lund, Sweden)

Capillary electroseparations of peptides (D. Westerlund, I. Beijersten and C. Pettersson, Uppsala, Sweden)

Isolation of the perisinusoidal vitamin A-storing cells from rat liver on Ca^{2+}-immobilized glass surfaces (T. Mantovaara, J. Alston-Smith and H. Pertoft, Uppsala, Sweden)

Presentation of the Biochemical Separation Centre (B. Ersson, M. Berg, L. Dahlberg and L.-B. Wahlberg, Uppsala, Sweden)

Activities at the pilot plant for fermentation of the Biomedical Centre (T. Illeni, Uppsala, Sweden)

Thiophilic adsorption — a diagnostic approach (S. Oscarsson, G. Chaga and J. Porath, Uppsala, Sweden)

Purification of catalase from penicillium chrysogenum (G. Chaga, A. Medin, S. Chaga and J. Porath, Uppsala, Sweden)

Studies on aqueous polymer 2-phase systems containing agarose (A.S. Medin and J.-C. Janson, Uppsala, Sweden)

Chemical stability of two gel filtration media: Superdex 75 pg and Superdex 200 pg (1. Drevin, B.-L. Johansson and L. Kågedal, Uppsala, Sweden)

SMART assistant — an integrated knowledge-based support tool for a new micropurification system (B. Österlund, H. Shayn and G. Sahlberg, Uppsala, Sweden)

PICTURES MADE DURING THE SYMPOSIUM

Fig. 1. From left to right: Dr. Francisco Batista-Viera and Professor Jerker Porath.

Fig. 2. From left to right: Professors Jerker Porath, Torvard Laurent and Klaus Mosbach.
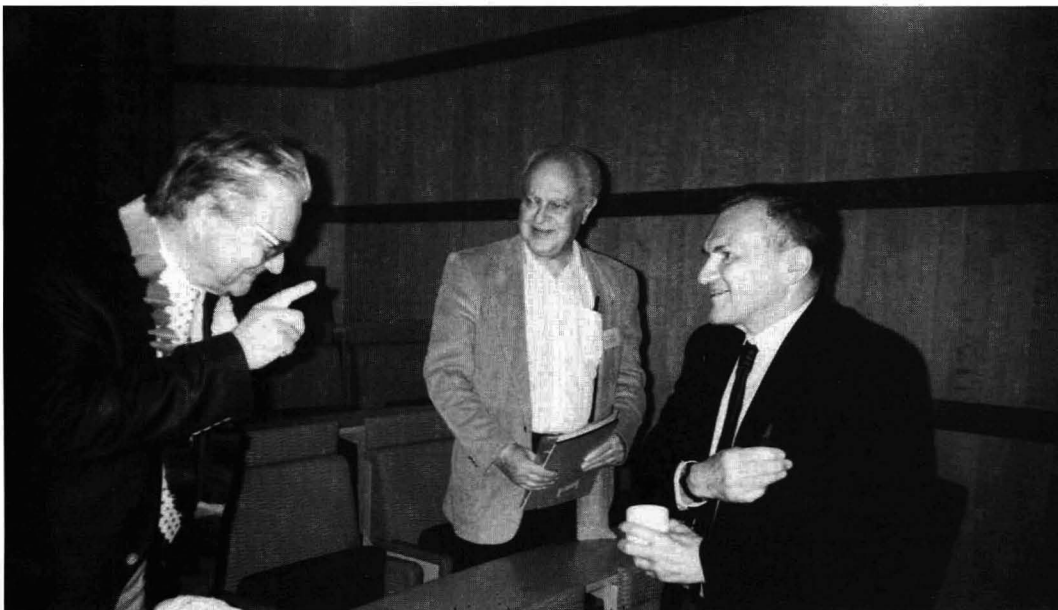

Fig. 3. From left to right: Professors Jerker Porath, Milan Bier and Michael Lederer.

Fig. 4. From left to right: Professors Klaus Mosbach, Grazyna Muzynska and Meir Wilchek.

Fig. 5. From left to right: Professor Jan-Christer Janson, Mrs. Inga Johansson, Prpfessor Jerker Porath, Professor Karin Caldwell and Dr. Jan Carlsson.

Fig. 6. Professors Takagi and Jerker Porath.

New Developments in Ion Exchange

Materials, Fundamentals and Applications

Proceedings of the International Conference on Ion Exchange, ICIE '91, Tokyo, Japan, October 2-4, 1991

edited by **M. Abe**, Tokyo Institute of Technology, Tokyo, Japan, **T. Kataoka**, University of Osaka Prefecture, Osaka, Japan and **T. Suzuki**, Yamanashi University, Yamanashi, Japan

This volume contains the papers presented at the International Conference on Ion Exchange (ICIE '91). Included are reviews and original papers reflecting recent progress in new branches of science and technology based on novel ion-exchange materials and ion-exchange theory.

Topics covered include: Fundamentals (Ion exchange theory and process), Synthesis of New Materials, Chromatography (Ion and liquid chromatography, and associated techniques), Water Purification, Environmental, Membranes, Hydrometallurgy, Separation Science and Technology (Food, pharmaceutical, biological and others).

Contents:
Fundamentals.
(21 papers).

Synthesis of New Materials.
(24 papers).

Chromatography.
(8 papers).

Water Purification.
(7 papers).

Environmental.
(12 papers).

Membranes.
(14 papers).

Hydrometallurgy.
(8 papers).

Separation Science and Technology.
(14 papers).

1991 xlii + 636 pages
Price: US $ 218.00 / Dfl. 425.00
ISBN 0-444-98688-X

Co-edition with and distributed in Japan by Kodansha Scientific Ltd.

Stationary Phases in Gas Chromatography

by **H. Rotzsche**, *VEB Chemiewerk, Nünchritz, Radebeul, Germany*

Journal of Chromatography Library Volume 48

The primary aim of this volume is to make the chemist familiar with the numerous stationary phases and column types, with their advantages and disadvantages, to help in the selection of the most suitable phase for the type of analytes under study. The book also provides detailed information on the chemical structure, physico-chemical behaviour, experimental applicability, physical data of liquid and solid stationary phases and solid supports. Such data were previously scattered throughout the literature. To understand the processes occurring in the separation column and to offer a manual both to the beginner and to the experienced chromatographer, one chapter is devoted to the basic theoretical aspects. Further, as the effectiveness of the stationary phase can only be considered in relation to the column type, a chapter on different column types and the arrangement of the stationary phase within the column is included.

The secondary aim of this book is to stimulate the development of new and improved standardized stationary phases and columns, in order to improve the reproducibility of separations, as well as the range of applications.

Contents: **1. Introduction. 2. Basic Concepts.** Basic components of a gas chromatographic system. Raw data measured from the chromatogram. Derived basic chromatographic parameters. Flow of gases in a gas chromatographic column and formation of bands. Thermodynamic bases of gas chromatography. The quality of chromatographic separation. The time of analysis. Definition of symbols used and list of essential relationships. **3. The Chromatographic Column.** Packed columns. Micro-packed columns. Open-tubular columns. Properties and comparison of the main column types. **4. Characterization of Stationary Phases.** Intermolecular forces. Quantities for the description of interactions. **5. Solid Stationary Phases.** Classification of adsorbents. Carbon adsorbents. Boron nitride and molybdenum disulphide. Adsorbents with hydroxylated and dehydroxylated surfaces. Porous organic polymers. Substances forming inclusion compounds. Modified adsorbents. **6. Chemically Bonded Stationary Phases.** Adsorbents for bonding reactions. Bonding reactions. Properties and characterization of chemically bonded phases. Outlook and prospects for chemically bonded phases. **7. The Solid Support.** The particle size and shape. The surface area. Activity of the original and of the coated solid support. Diatomite supports. Synthetic silica-based supports (Volaspher and quartz). Silica gel. Micro glass beads and porous layer beads. Fluorocarbon supports. Other support materials. **8. Liquid Stationary Phases.** General properties of liquid stationary phases. Hydrocarbons. Silicones. Alcohols, ethers and carbohydrates. Esters. Nitriles and nitrile ethers. Nitro compounds. Amines. Amides. Heterocyclics. Sulphur compounds. Fluorine compounds. Fatty acids and their salts. Salts. Chiral stationary phases. Liquid crystals. Mixed stationary phases. **9. Selection of Stationary Phases.** General recommendations for choosing a suitable stationary phase. Choosing stationary phases for special separation problems with regard to the desired selectivity. Preferred stationary phases. Approaches to stationary phase selection. **Literature. Indexes.**

PUBLICATION SCHEDULE FOR 1992

Journal of Chromatography and *Journal of Chromatography, Biomedical Applications*

MONTH	O 1991–F 1992	M	A	M	J	J	
Journal of Chromatography	Vols. 585–593	594/1 + 2 595/1 + 2	596/1 596/2 597/1 + 2	598/1 598/2 599/1 + 2 600/1 600/2	602/1 + 2 603/1 + 2 604/1	604/2 605/1 605/2 606/1	The publication schedule for further issues will be published later.
Cumulative Indexes, Vols. 551–600					*a*		
Bibliography Section		610/1			610/2		
Biomedical Applications	Vols. 573 and 574	575/1 575/2	576/1	576/2 577/1	577/2	578/1 578/2	

a Cumulative Indexes will be Vol. 601, to appear early 1993.

INFORMATION FOR AUTHORS

(Detailed *Instructions to Authors* were published in Vol. 558, pp. 469–472. A free reprint can be obtained by application to the publisher, Elsevier Science Publishers B.V., P.O. Box 330, 1000 AH Amsterdam, The Netherlands.)

Types of Contributions. The following types of papers are published in the *Journal of Chromatography* and the section on *Biomedical Applications:* Regular research papers (Full-length papers), Review articles and Short Communications. Short Communications are usually descriptions of short investigations, or they can report minor technical improvements of previously published procedures; they reflect the same quality of research as Full-length papers, but should preferably not exceed five printed pages. For Review articles, see inside front cover under Submission of Papers.

Submission. Every paper must be accompanied by a letter from the senior author, stating that he/she is submitting the paper for publication in the *Journal of Chromatography*.

Manuscripts. Manuscripts should be typed in double spacing on consecutively numbered pages of uniform size. The manuscript should be preceded by a sheet of manuscript paper carrying the title of the paper and the name and full postal address of the person to whom the proofs are to be sent. As a rule, papers should be divided into sections, headed by a caption (*e.g.,* Abstract, Introduction, Experimental, Results, Discussion, etc.). All illustrations, photographs, tables, etc., should be on separate sheets.

Introduction. Every paper must have a concise introduction mentioning what has been done before on the topic described, and stating clearly what is new in the paper now submitted.

Abstract. All articles should have an abstract of 50–100 words which clearly and briefly indicates what is new, different and significant.

Illustrations. The figures should be submitted in a form suitable for reproduction, drawn in Indian ink on drawing or tracing paper. Each illustration should have a legend, all the *legends* being typed (with double spacing) together on a *separate sheet*. If structures are given in the text, the original drawings should be supplied. Coloured illustrations are reproduced at the author's expense, the cost being determined by the number of pages and by the number of colours needed. The written permission of the author and publisher must be obtained for the use of any figure already published. Its source must be indicated in the legend.

References. References should be numbered in the order in which they are cited in the text, and listed in numerical sequence on a separate sheet at the end of the article. Please check a recent issue for the layout of the reference list. Abbreviations for the titles of journals should follow the system used by *Chemical Abstracts*. Articles not yet published should be given as "in press" (journal should be specified), "submitted for publication" (journal should be specified), "in preparation" or "personal communication".
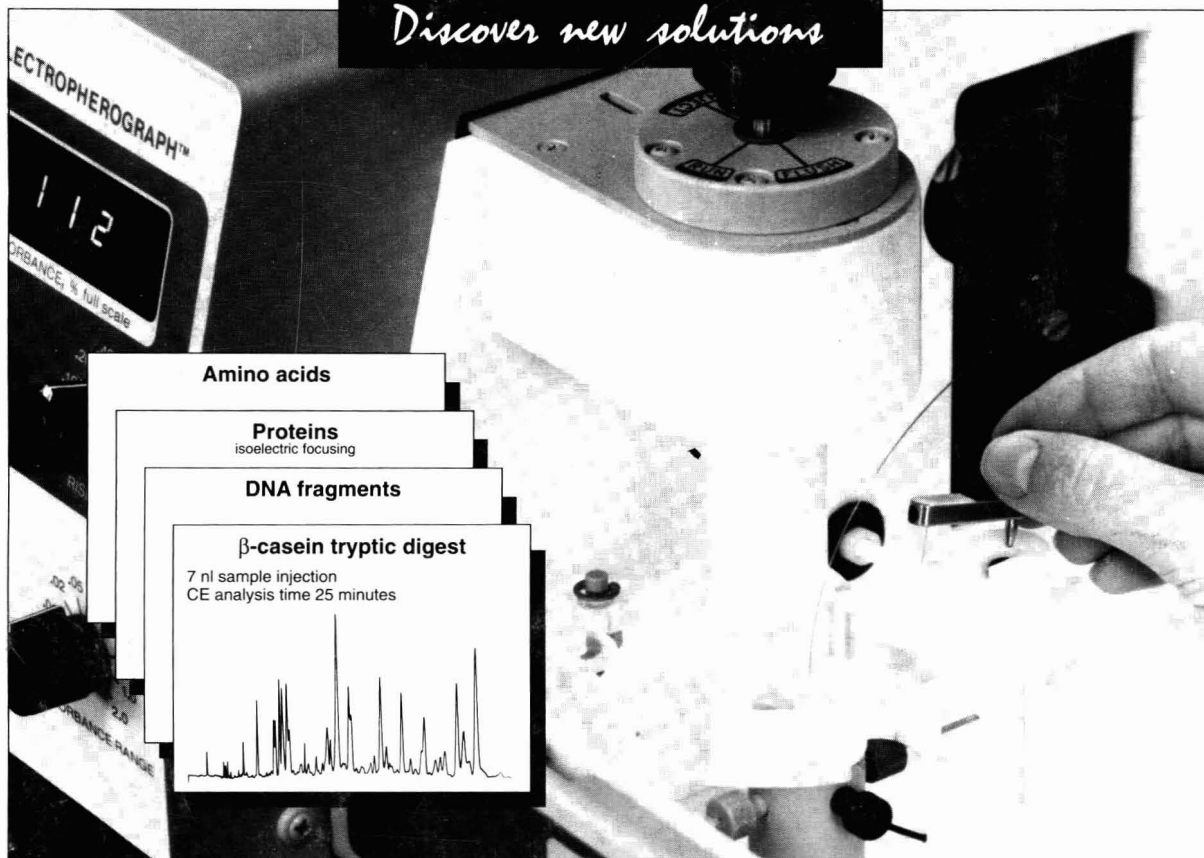
Dispatch. Before sending the manuscript to the Editor please check that the envelope contains four copies of the paper complete with references, legends and figures. One of the sets of figures must be the originals suitable for direct reproduction. Please also ensure that permission to publish has been obtained from your institute.

Proofs. One set of proofs will be sent to the author to be carefully checked for printer's errors. Corrections must be restricted to instances in which the proof is at variance with the manuscript. "Extra corrections" will be inserted at the author's expense.

Reprints. Fifty reprints of Full-length papers and Short Communications will be supplied free of charge. Additional reprints can be ordered by the authors. An order form containing price quotations will be sent to the authors together with the proofs of their article.

Advertisements. The Editors of the journal accept no responsibility for the contents of the advertisements. Advertisement rates are available on request. Advertising orders and enquiries can be sent to the Advertising Manager, Elsevier Science Publishers B.V., Advertising Department, P.O. Box 211, 1000 AE Amsterdam, Netherlands; courier shipments to: Van de Sande Bakhuyzenstraat 4, 1061 AG Amsterdam, Netherlands; Tel. (+31-20) 515 3220/515 3222, Telefax (+31-20) 6833 041, Telex 16479 els vi nl. *UK*: T. G. Scott & Son Ltd., Tim Blake, Portland House, 21 Narborough Road, Cosby, Leics. LE9 5TA, UK; Tel. (+44-533) 753 333, Telefax (+44-533) 750 522. *USA and Canada*: Weston Media Associates, Daniel S. Lipner, P.O. Box 1110, Greens Farms, CT 06436-1110, USA; Tel. (+1-203) 261 2500, Telefax (+1-203) 261 0101.

Discover new solutions

Amino acids

Proteins
isoelectric focusing

DNA fragments

β-casein tryptic digest
7 nl sample injection
CE analysis time 25 minutes

This personal CE makes your bioseparations faster and easier

Capillary electrophoresis is the most significant new bioseparation tool in 20 years. Peptides, proteins, amino acid derivatives, nucleic acids, DNA fragments – even viruses and bacteria – all have been resolved by CE with unprecedented speed and efficiency. And now there's a complete, compact "personal CE " system – Isco's Model 3850 Electropherograph™ – that gives you affordable access to this powerful technology.

New multi-mode sample introduction
offers unbiased, highly reproducible
vacuum injection; fast split-flow
injection for CE-MS interfacing;
and electromigration for gel-
filled columns.

Dual-polarity power supply
delivers up to 30 kV and 300 μA
for any CE separation method.

Variable UV detection gives excellent sensitivity over a wide range of samples.

Quick-change capillary holder lets you install any coated, uncoated, or gel-filled capillary in under two minutes.

Find out how you can get faster, easier, bioseparations at less-than-HPLC prices. Contact us today for complete details.
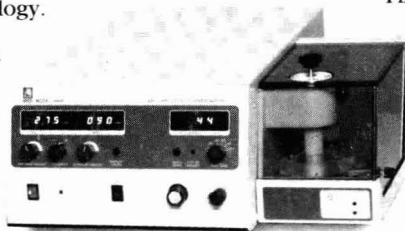
Isco, Inc., P.O. Box 5347
Lincoln NE 68505, U.S.A.
Phone **(800)228-4250**
Isco Europe AG, Brüschstr. 17
CH8708 Männedorf, Switzerland
Fax **(41-1)920 62 08** **ISCO**